PHARMACOLOGICAL MANIPULATION OF MICROGLIA TO SUPPRESS NEUROINFLAMMATION AND PROTECT NEURONS

By

Alexander P. Young

Submitted in partial fulfilment of the requirements
for the degree of Doctor of Philosophy

at

Dalhousie University
Halifax, Nova Scotia
August 2023

Table of Contents

List of Tables

List of Figures

Abstract

Microglia are the resident immune cells of the brain that survey the microenvironment, provide trophic support to neurons, and clear debris to maintain homeostasis and healthy brain function. Microglia are also drivers of neuroinflammation in several neurodegenerative diseases. Excessive pro-inflammatory activity by microglia involves the release of soluble factors that can impair neuronal function. In this thesis, I tested the hypothesis that pro-inflammatory microglia could induce secondary damage to neurons and explored multiple pharmacological strategies to prevent this process. I found that stimulation of cultured microglia with bacterial lipopolysaccharide (LPS) and interferon-gamma (IFNγ) elicited a pro-inflammatory response that was strong enough to directly kill cultured neurons and that pre-treatment of microglia with synthetic cannabinoids targeting cannabinoid type 1 (CB_1) and type 2 (CB_2) receptors could reduce the inflammatory response enough to reduce neuronal death (Chapter 1). I then further explored the effects of LPS and IFNγ on the capacity of microglia to synthesize, degrade, and respond to cannabinoid receptor agonists. LPS and IFNγ each stimulated the upregulation of mRNA for *Cnr2* and *DAGLB* in a biphasic manner (Chapter 2). The use of synthetic CB_2 agonists (HU-308 and HU-433) were then used to further probe the mechanism of the anti-inflammatory effects of CB_2 receptor activation on microglia. Activation of microglial CB_2 receptors suppressed the canonical signaling of toll-like receptor 4 (TLR4) and directly inhibited the release of nitric oxide (NO) and tumour necrosis factor (TNF) (Chapter 4). An in-depth examination of the effects of LPS and IFNγ on microglia revealed that these stimuli act in a synergistic manner that is dependent on Janus kinase (JAK)1/2 as suppression of JAK1/2 prevented the microglial response to both molecules (Chapter 5). Finally, I explored the mechanisms by which the neurons were killed by microglia. Microglial-secreted factors induced apoptosis and necroptosis in neuronal cells which could be completely prevented by neutralization of TNF (Chapter 6). These findings suggest that direct suppression of microglia is sufficient to reduce secondary neurotoxicity and highlight some potential opportunities for the treatment of neuroinflammation.

List of Abbreviations and Symbols Used

2-AG	2-arachidonoylglycerol
5xFAD	Five familial AD
A_{2A}	Adenosine type 2A
ACEA	Arachidonyl-2'-chloroethylamide
AD	Alzheimer's disease
ADP	Adenosine diphosphate
AEA	N-arachidonoylethanolamine (anandamide)
ALS	Amyotrophic lateral sclerosis
AMPA	α-amino-3-hydroxyl-5-methyl-4-isoxazole-propionate
AMPK	AMP-activated protein kinase
ATP	Adenosine triphosphate
AUC	Area under the curve
Aβ	Amyloid-beta
BBB	Blood-brain barrier
C1q	Complement component 1q
cAMP	Cyclic adenosine monophosphate
CB_1	Cannabinoid type 1
CB_2	Cannabinoid type 2
CCL	Chemokine ligand
cDNA	Complementary DNA
CNS	Central nervous system
COX2	Cyclooxygenase 2
CREB	cAMP response element-binding protein
CSF	Cerebrospinal fluid
CSF1	Colony stimulating factor 1
CX3CL	C-X3-C motif ligand
CXCL	C-X-C motif chemokine ligand
CXCR	C-X-C motif receptor
D_2	Dopamine type 2
DAGL	Diacylglycerol lipase
dCq	delta Cq
DMEM	Dulbecco's modified eagle's medium
DMSO	Dimethyl sulfoxide
ECS	Endocannabinoid system
ERK	Extracellular signal-regulated kinase
FAAH	Fatty acid amide hydrolase
GABA	γ-aminobutyric-acid
GPCR	G protein-coupled receptor
HD	Huntington's disease
HEK	Human embryonic kidney

HTT/HTT	Huntingtin (gene/protein)
IFN	Interferon
IFNGR	Interferon-gamma receptor
IL	Interleukin
iNOS	Inducible nitric oxide synthase
iPSCs	Inducible pluripotent stem cells
JAK	Janus kinase
JNK	c-Jun N-terminal kinase
LPS	Lipopolysaccharide
mAb	Monoclonal antibody
MAGL	Monoacylglycerol lipase
MAPK	Mitogen-activated protein kinase
mHTT	Mutant huntingtin
mRNA	Messenger ribonucleic acid
MS	Multiple sclerosis
MSN	Medium-spiny neuron
mTOR	Mammalian target of rapamycin
NAPE-PLD	N-acyl phosphatidylethanolamine-specific phospholipase D
Nec-1	Necrostatin-1
NF-κB	Nuclear factor kappa-light-chain-enhancer of activated B cells
NMDA	N-methyl-D-aspartate
NO	Nitric oxide
NSAID	Non-steroidal anti-inflammatory drug
P2Y6	P2Y purinoceptor 6
pAb	Polyclonal antibody
PBS	Phosphate buffered saline
PD	Parkinson's disease
RIP3	Receptor interacting protein kinase 3
SIM	Spontaneously immortalized microglia
STAT	Signal transducer and activator of transcription
TBS	Tris buffered saline
TDP-43	TAR DNA-binding protein 43
TGFβ	Transforming growth factor beta
THC	Δ9-tetrahydrocannabinol
TLR2	Toll-like receptor 2
TLR4	Toll-like receptor 4
TNF	Tumour necrosis factor
UDP	Uracil diphosphate
wt	Wild type
α-syn	α-synuclein

Acknowledgements

First and foremost, I must thank Dr. Eileen Denovan-Wright for her efforts to support my development as a scientist. Eileen has encouraged my independence, supported every crazy idea that I had, and provided me with every opportunity to succeed. Her guidance and dedication allowed me to progress smoothly in the face of adversity, including the COVID-19 pandemic. I greatly appreciate her and everything she has given me.

I would like to thank my advisory committee members, Dr. Jim Fawcett and Dr. Jason McDougall, as well as Dr. Melanie Kelly and the rest of the Department of Pharmacology. The department offered guidance, advice, and collaboration which meant that I never felt alone when I wanted to learn something new, when an experiment failed, or when an incubator 'exploded'.

Thank you to Bowtie and Snakebite for your friendship and comradery. Having people to laugh with during every success and especially after each failure made this journey a lot easier. I will always fondly remember our thoughtful scientific discussions that were seamlessly mixed with highly compelling business ideas and philosophical musings.

Finally, I would like to thank my friends and family, including my wife Lauren and daughter Aubrey for their love, patience, and support.

This work was supported by the Natural Sciences and Engineering Research Council of Canada and Mitacs in addition to provincial and institutional support.

Chapter 1: Introduction

Neurodegenerative diseases are among the most threatening to an ageing population. Such diseases involve the progressive loss of neuronal function and primarily occur in the later stages of life. Advancements in other areas of medicine such as oncology, immunology, and cardiology have allowed for small but gradual increases in life expectancy and healthspan over the past century (Griffin 2008; Crimmins 2015; Chambers-Richards et al. 2022). However, this has correlated with an increased incidence of some age-related neurodegenerative diseases as larger numbers of individuals enter the higher-risk age brackets (Erkkinen et al. 2018; Li et al. 2022). Dementia and other symptoms of neurodegeneration will place an increasingly massive societal and economic burden on most developed countries (Leicht et al. 2013; Alzheimer Society of Canada 2016; Nandi et al. 2022). More tragically, an increasing number of individuals will be robbed of their ability to think, move, play, make new memories, and participate in activities that make longer lives worth living. The purpose of this thesis is to make a small contribution to our greater understanding of neurodegeneration in the hope that effective treatments for these devastating diseases will eventually emerge.

Although neurons are not the most abundant cells of the brain, neurons facilitate the key functions of the brain, and the loss of neuronal function or viability is a defining feature of neurodegeneration. Neurodegeneration generally follows an unfavourable change in the neuronal microenvironment which can manifest differently based on the specific disease. Once thought to be immune privileged and thus spared from peripherally mediated damage, it is now understood that systemic inflammation can penetrate the brain (Sankowski et al. 2015). A common feature of neurodegenerative disease is a pro-inflammatory environment within the brain (DiSabato et al. 2016). Microglia are the resident immune cells of the brain that regulate both pro- and anti-inflammatory processes to maintain homeostasis, and microglia are the primary cells that produce disease-associated alterations in the inflammatory state of the brain (Perry et al. 2010). These alterations can be caused by intrinsic microglial defects as well as in response to peripheral inflammatory stimuli. This series of observations has initiated a widespread effort to control inflammation as a method to preserve brain health.

1.1 The immune system influences the brain

It was long believed that the brain was separated from the immune system to prevent the entry of pathogens or collateral damage from the inflammation associated with the clearance of such pathogens. This concept arose from early reports of tissue transplantation which identified that tumours would fail to grow when transplanted into the subcutaneous tissue of rats, but would grow rapidly when inoculated into the brain (Shirai 1921; Murphy and Sturm 1923). Later experiments by Medawar demonstrated that if skin was first grafted peripherally, then skin from the same donor would later be destroyed when grafted into the brain (Medawar 1948). These initial findings indicated that the brain was unlikely to mount an immune response but was sensitive to the activity of the peripheral immune system (Widner and Brundin 1988). The blood-brain barrier (BBB) is a set of protective structures that prevents the passive entry of peripheral cells as well as many proteins and small molecules, but it has become clear that there is incomplete separation of the peripheral immune system and the central nervous system (CNS)(Fig. 1. 1A). Indeed, these systems are in close communication and the interactions can be beneficial as well as detrimental depending on the context.

Under certain pathological conditions, the peripheral immune system can provide benefits and offer protection to the CNS. In the healthy adult CNS, T cells exist in the meninges and may secrete interleukin (IL)-4 and IL-13 which can promote the resolution of inflammation and facilitate learning and memory (Derecki et al. 2010; Brombacher et al. 2017; Mamuladze and Kipnis 2023). Mice subjected to experimental stroke exhibit infiltration of macrophages into the brain parenchyma to clear dead cells and debris which promotes resolution of inflammation and subsequent tissue repair (Zhang et al. 2019c). The infiltration of T cells and macrophages also limits secondary damage and promotes neuronal recovery following optic nerve crush injury (Moalem et al. 1999). Conversely, amyotrophic lateral sclerosis (ALS) mice bred to lack functional T cells exhibit accelerated motoneuron degeneration (Beers et al. 2008). Interferon-gamma (IFNγ) in the brain can stimulate the entry of macrophages which assist with the phagocytosis and clearance of amyloid-beta (Aβ), resulting in improved cognitive

performance (Baruch et al. 2016). Thus, an insult to the brain can prompt peripheral immune cells to enter the brain and promote recovery.

Although the peripheral immune system can protect the brain, there is also an apparent link between immune system dysfunction and neurodegeneration. Human Alzheimer's disease (AD) patients exhibit elevated quantities of cytotoxic T cells in the cerebrospinal fluid that are negatively associated with cognitive performance (Gate et al. 2020). Similar infiltration of cytotoxic T cells into the brain is correlated with neuronal loss in AD mice (Chen et al. 2023). In ageing humans with cognitive impairment, monocyte-derived C-X-C motif chemokine ligand 16 (CXCL16) is upregulated in the cerebrospinal fluid (CSF) which engages CXC receptor 6 (CXCR6) on T cells and promote entry into the brain (Piehl et al. 2022). T cells in the dural sinuses can also recognize CNS antigens that have been captured by dendritic cells from the CSF and subsequently engage in pro-inflammatory activity within the meninges (Rustenhoven et al. 2021). Thus, brains in the process of degeneration actively recruit immune cells from the blood stream or CSF into the parenchyma. Although T cells can suppress inflammation and promote tissue repair, excessive recruitment of $CD8^+$ cytotoxic T cells to the brain is associated with secondary tissue damage (Walsh et al. 2014; Kaya et al. 2022).

The connection between the immune system and the CNS is not limited to the entry of immune cells. Chronic low-grade neuroinflammation is characterized by elevated quantities of pro-inflammatory cytokines in the brain without the infiltration of cells. Although glia can produce cytokines, those generated in the periphery can penetrate the BBB which allows systemic inflammation to modify the progression of neurodegenerative diseases (Bettcher et al. 2021). Elevated plasma concentrations of pro-inflammatory cytokines such as IL-6 and tumour necrosis factor (TNF) in otherwise healthy patients are associated with an increased risk to develop all-cause dementia, including AD (Engelhart et al. 2004; Tan et al. 2007; Holmes et al. 2009; Swardfager et al. 2010; Koyama et al. 2013). The increased quantities of cytokines are typically secreted by peripheral blood mononuclear cells and may be associated with chronic inflammatory diseases or infection. Patients that are hospitalized with bacterial or viral

infections also have an increased risk to develop dementia later in life (Sipilä et al. 2021). The greatest risk is seen with CNS infections but even peripheral infections increase the risk of dementia decades into the future (Sipilä et al. 2021). Mice that are challenged by simulated viral or bacterial infections exhibit long-term cognitive deficits and neuronal loss that mimics neurodegeneration in humans (Qin et al. 2007; Krstic et al. 2012; Zhao et al. 2019). Even in the absence of infection, AD patients exhibit marked differences in the gut microbiome that include increased quantities of pro-inflammatory genera such as *Escherichia* and *Shigella*, and reduced quantities of beneficial genera such as *Eubacterium* and *Bacillota* (Cattaneo et al. 2017; Vogt et al. 2017). Several recent meta-analyses have revealed that dysregulation of the gut microbiome is also observed in other neurodegenerative disorders and psychiatric conditions (Boddy et al. 2021; Romano et al. 2021; Zhang et al. 2022a). This growing body of evidence supports the concept that the brain is sensitive to systemic inflammation, and that chronic inflammation throughout the body increases the risk of neurodegeneration.

1.2 Microglia as effectors of neuroinflammation

Microglia are specialized macrophages that reside in the brain parenchyma and are the primary responders to pro-inflammatory stimuli that penetrate the BBB (Fig. 1. 1B). As the resident immune cells of the brain, the ontogenesis of microglia is distinct from other cell types in the CNS. Microglia arise from early erythro-myeloid progenitors in the extraembryonic yolk sac which become yolk sac macrophages during primitive hematopoiesis (Ginhoux et al. 2010; Masuda and Prinz 2016). These yolk sac macrophages invade the developing CNS and become permanently compartmentalized from peripheral tissues following closure of the BBB (Hoeffel and Ginhoux 2015). Development into mature microglia and subsequent persistence in the central nervous system is dependent on specific proteins including IL-34 and transforming growth factor beta (TGFβ) (Masuda and Prinz 2016). At maturity, microglia comprise roughly 10% of cells in the brain and turn over at a relatively slow rate, with some cells surviving up to 20 years in humans (Lawson et al. 1992; Réu et al. 2017).

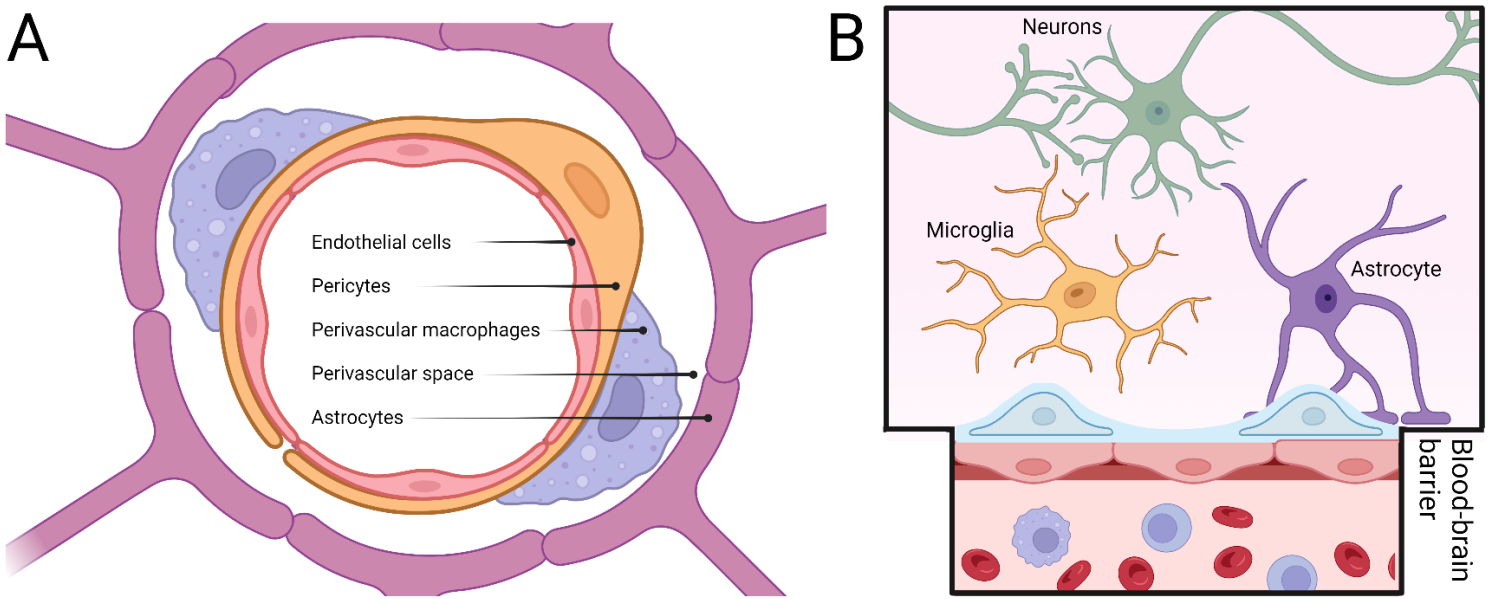

Figure 1. 1. Schematic of the blood-brain barrier (BBB). A Cross-sectional view of the specialized vessels of the BBB. **B** Longitudinal view of the BBB and the parenchyma which contains microglia and neurons.

Microglia perform a broad variety of critical functions in the healthy CNS during postnatal development. Like macrophages, microglia are phagocytes and use this ability to shape the formation of the CNS. During development, microglia engulf and digest synapses in a complement-dependent manner (Stevens et al. 2007). This synaptic pruning is regulated by neuronal activity which facilitates maintenance of active synapses and removal of underused synapses (Schafer et al. 2012). In addition to individual synapses, microglia also clear dead and superfluous cells which is necessary for the spatial patterning of the developing brain (Vaux and Korsmeyer 1999; Schafer and Stevens 2015). These functions of microglia are indispensable during initial wiring of the CNS and ultimately impact the molecular architecture of the brain.

In the adult brain, microglia primarily monitor the microenvironment and use scavenger receptors to detect disruptions in homeostasis and react appropriately (Nimmerjahn et al. 2005). Microglia survey the influx of blood-borne molecules and are highly sensitive to pro-inflammatory cytokines or pathogen-associated molecular patterns (Kettenmann et al. 2011). Circulating cytokines such as IFNγ or IL-6 may infiltrate the BBB and interact with microglial receptors to engage Janus kinase (JAK) and signal transducers and activators of transcription (STAT) signaling cascades (Jain et al. 2021). JAK-STAT signaling is a critical component of the innate immune response and facilitates intracellular signaling of immune cells, including microglia, to an array of molecules including interleukins, chemokines, and interferons (Nicolas et al. 2013; Yan et al. 2018). Upon interaction with such stimuli, microglia utilize JAK-mediated signaling in addition to several parallel signaling pathways to initiate a pro-inflammatory reaction. In a pro-inflammatory state, microglia shift from a ramified to amoeboid morphology and upregulate their phagocytic capacity to clear debris, dying cells, or microbes from the site of insult. Under persistent pro-inflammatory conditions, microglia release chemokines to attract peripheral immune cells and engulf astrocytic end-feet and endothelial cells to facilitate entry of immune cells through the BBB (Haruwaka et al. 2019; Pan et al. 2021). Following resolution of inflammation in the brain, microglia also deposit and sculpt the extracellular matrix and promote angiogenesis to restore homeostasis and provide an

optimal microenvironment for neural function (Dudvarski Stankovic et al. 2016; Dudiki et al. 2020; Nguyen et al. 2020; Crapser et al. 2021).

Although microglia serve many important functions to maintain healthy brain function, microglial dysfunction is implicated in the progression of neurodegeneration (Perry et al. 2010; Hickman et al. 2018). In AD patients, disease progression and cognitive decline is more correlated with the abundance of pro-inflammatory microglia than the quantity of Aβ plaques (Edison et al. 2008). In pre-symptomatic Huntington's disease (HD) patients, the accumulation of activated microglia is observed several years prior to the expected age of onset based on the degree of expansion of the *huntingtin* (*HTT*) gene (Pavese et al. 2006; Tai et al. 2007). Activated microglia in the substantia nigra and putamen are elevated in post-mortem brain tissue from Parkinson's disease (PD) patients relative to healthy controls and the degree of microglial activation correlates with the degree of neuronal loss (McGeer et al. 1988; Imamura et al. 2003). In multiple sclerosis (MS), the prototypical neuroinflammatory disease, increased quantities of activated microglia are observed in the white matter of MS patients compared to healthy controls (Zrzavy et al. 2017). Specifically, microglia are found in active lesions during the early stages of demyelination. In animal models, exaggerated phagocytic activity of microglia is involved in the synaptic loss that occurs in AD, HD, and ageing (Hong et al. 2016; Wilton et al. 2021; Dundee et al. 2023).

To survive in the CNS, microglia require constitutive activation of colony stimulating factor 1 (CSF1) receptors through the endogenous ligands, CSF1 and IL-34 (Lin et al. 2008; Ginhoux et al. 2010; Erblich et al. 2011; Nandi et al. 2012). Brain-penetrant antagonists of CSF1 receptors deplete microglia from living animals and have provided insight into the functional roles of microglia during health and disease (Elmore et al. 2014). In 10-month-old mice with five familial AD (5xFAD) mutations, elimination of microglia had no effect on existing Aβ plaques, however, there was an overall rescue of the loss of dendritic spines and a general reduction in neurodegeneration (Spangenberg et al. 2016). This would suggest that microglia are required to induce neurodegeneration, potentially in response to Aβ. A follow-up study examined the effects of chronic microglial depletion in 6-week-old mice, prior to the onset of Aβ plaques (Spangenberg

et al. 2019). Early elimination of microglia reduced the formation of Aβ plaques in the parenchyma which suggests that microglia are active contributors to plaque formation in the early phases of AD. Given that many of the genes known to influence AD risk are specific to microglia, it is certainly possible that microglia would contribute to plaque formation in 5xFAD mice and humans with specific alleles (Efthymiou and Goate 2017). Depletion of microglia from the R6/2 mouse model of HD resulted in fewer motor deficits and improved cognitive performance (Crapser et al. 2020). Similar results were shown in mouse models of PD, whereby microglial depletion ameliorated both behavioral deficits and markers of neuroinflammation (Oh et al. 2020; Zhang et al. 2021a). This body of microglial depletion experiments suggests that activation of microglia is a common factor in mouse models of neurodegeneration and that removal of microglia generally improves outcomes.

1.3 Behavioural and cellular consequences of neuroinflammation

The symptoms of chronic low-grade neuroinflammation include changes in behavior and cognitive performance. Acute encephalitis, most commonly caused by a viral or bacterial infection in the CNS, involves more severe symptoms such as memory loss, seizures, aggression, and psychosis in addition to fever and other traditional symptoms of infection (Ellul and Solomon 2018; Kumar 2020). Even during peripheral infections which do not penetrate the CNS, the upregulated production of IL-1β and TNF by peripheral immune cells induces fatigue and regulates sleep through interaction with serotonergic neurons in the brain stem (Imeri and Opp 2009). These symptoms resolve upon clearance of the infection which indicates these cognitive deficits and behavioral changes are directly linked to high levels of inflammation in the brain. Peripheral injection with bacterial-derived lipopolysaccharides (LPS) is sufficient to induce neuroinflammation characterized by glial activation and neuronal loss in mice (Batista et al. 2019). The neuroinflammation and subsequent cognitive impairment induced by LPS can be blocked by toll-like receptor 4 (TLR4)-specific peptides which indicates that LPS penetrates the BBB to elicit inflammatory responses that are specific to the brain (Zhao et al. 2019). Activation of microglial TLR2 and TLR4 in the mouse prefrontal cortex has

also been shown to underlie stress-induced social avoidance via secretion of IL-1α and TNF (Nie et al. 2018). Overall, neuroinflammation influences cognition in humans as well as rodents. Importantly, these changes can be observed even in the absence of immune cell infiltration into the CNS.

In line with the known effects of neuroinflammation on cognition and behaviour, inflammation has also been identified as a component of several psychiatric illnesses including depression, anxiety, and addiction. Elevated markers of inflammation and microglial activation are observed in several brain regions of humans during major depressive episodes, and the degree of inflammation correlates with the severity of the episodes (Setiawan et al. 2015; Richards et al. 2018). Post-mortem tissue samples from the white matter of patients with major depressive disorder also exhibit increased markers of microglial priming and inflammation as well as infiltration of peripheral immune cells including macrophages (Torres-Platas et al. 2014). Suicide among patients with depression has also been correlated with an increased abundance of reactive microglia in several brain regions including the dorsolateral prefrontal cortex, anterior cingulate cortex, and mediodorsal thalamus (Steiner et al. 2008). Exposure of neonatal rat pups to LPS has been demonstrated to affect anxiety-like behaviour and induce memory impairments that last into adulthood (Sominsky et al. 2012; Wang et al. 2013). Mice injected with LPS have also been shown to exhibit anxiety- and depressive-like behaviors due to enhanced excitability of projection neurons in the basolateral amygdala (Zheng et al. 2021). With respect to the addictive behaviour of animals, direct inhibition of TLR4-mediated signaling reduces the drug-seeking behaviour of rodents in response to both opioids as well as cocaine (Hutchinson et al. 2012; Brown et al. 2023). These data suggest that microglia-mediated inflammation is a component in several aspects of neuropsychiatric conditions.

Within the CNS, cytokine receptors are expressed on neurons and glia, and the presence of specific cytokines can affect the functional properties of individual neurons and neuronal circuits. IL-1β and TNF increase neuronal excitability *in vitro* and *in vivo* by enhancing glutamate-mediated signaling through N-methyl-D-aspartate (NMDA) and α-amino-3-hydroxyl-5-methyl-4-isoxazole-propionate (AMPA) receptors (Hagan et al.

1996; Viviani et al. 2003; Pickering et al. 2005; He et al. 2012). Although these effects have been associated with enhanced synaptic plasticity and scaling, excessive quantities of these cytokines are also associated with excitotoxicity (Beattie et al. 2002; Stellwagen and Malenka 2006; Jara et al. 2007). Excessive production of TNF by microglia induces circuit instability and susceptibility to lethal seizures in mice (Feinberg et al. 2022). Elevated TNF in the CNS of rats can also upregulate $Na_v1.3$ and $Na_v1.8$ which are important contributors to neuropathic pain (He et al. 2010). In contrast with IL-1β and TNF, IL-6 is known to dampen neuronal activity through regulation of adenosine receptors and $Ca_v1.2$ (Biber et al. 2008; Ma et al. 2012). Inhibitory GABAergic (γ-aminobutyric-acid) neurons are particularly sensitive to IFNγ which can impact inhibitory tone and affect learning and memory as well as stress-related cognitive impairment (Brynskikh et al. 2008; Filiano et al. 2016; Monteiro et al. 2017). Cytokines play important roles in the functions of neuronal circuits but can create dysfunction when not maintained within specific concentrations which highlights the importance of regulating inflammation in the brain.

It is likely that the transient behavioural correlates of neuroinflammation can be caused by the effects of inflammation on neural activity, however, more long-term cognitive changes can also occur when chronic inflammation facilitates the permanent loss of synapses or the death of neurons. Mice in recovery from viral infection exhibit increased release of IFNγ from T cells which stimulates microglia and mediates deficits in learning as well as synapse elimination and neuronal apoptosis in the hippocampus (Garber et al. 2019). These effects are regulated by complement-dependent microglial phagocytosis of synapses and perikarya as well as astrocyte-derived IL-1β which has been shown to promote learning deficits and inhibit neurogenesis (Garber et al. 2018). In a mouse model of AD, IFNα and IFNβ signaling in microglia is associated with the loss of post-synaptic terminals, however, in neurons, stimulation by interferons is associated with memory loss and increased deposition of Aβ (Roy et al. 2020, 2022). Another characteristic of AD is an overabundance of activated T cells which secrete IFNγ that coincides with the activation of both microglia and astrocytes in the CNS and loss of synapses and viable neurons (Town et al. 2005; Dai and Shen 2021).

1.4 Neuroinflammation as a therapeutic target

Neuroinflammation is a common characteristic of virtually all brain ailments, however, inflammation in the brain is highly heterogeneous and can be initiated by a wide variety of different factors depending on the disease or injury (Ransohoff 2016b). Four primary neurodegenerative diseases are AD, PD, ALS, and HD, of which the initial signs and symptoms of pathology are directly related to neuronal dysfunction. This is in contrast with MS where neuronal damage occurs secondarily to the initial autoimmune response against myelin. AD, PD, ALS, and HD each feature defects in distinct proteins that either initiate or contribute to the progression of the disease. These proteins include Aβ and hyperphosphorylated-tau in AD, α-synuclein (α-syn) in PD, TAR DNA-binding protein 43 (TDP-43) in ALS, and mutant HTT (mHTT) in HD. Each of these proteins have a propensity to form extracellular or cytoplasmic aggregates. These protein aggregates may subsequently induce neuroinflammation or elicit direct cytotoxicity through the formation of intracellular oligomers or fibrils (Reish and Standaert 2015; Crotti and Glass 2015; Selkoe and Hardy 2016; Bright et al. 2021). For example, microglia respond directly to Aβ and α-syn with a storm of pro-inflammatory cytokines including TNF, IL-6, and IL-1β which can initiate neuronal loss *in vivo* (Wang et al. 2015; De et al. 2019; Hughes et al. 2020; Choi et al. 2020; Xie et al. 2020). Ongoing treatment strategies for these primary neurodegenerative diseases have focused on the direct removal of these protein aggregates. This includes the use of neutralizing antibodies raised against Aβ to prevent aggregation and promote clearance, or the use of antisense oligonucleotides to reduce the translation of m*HTT* (van Dyck 2018; Rook and Southwell 2022). However, there is growing interest in the common roles of inflammation in these diseases and exploring neuroinflammation as a source of therapeutic targets.

As neuroinflammation is often associated with systemic inflammation, an obvious treatment option would be the use of global anti-inflammatory agents to suppress inflammation in both the brain and periphery. An early prospective, population-based cohort study using patient records of nearly 7,000 subjects found that there was a reduced

risk of AD with long-term non-steroidal anti-inflammatory drug (NSAID) usage (in t' Veld et al. 2001). A follow-up meta-analysis of over 600 studies contradicted these findings and demonstrated that there was no reduced risk of AD associated with the use of NSAIDs or steroidal anti-inflammatory drugs (Jaturapatporn et al. 2012). More recent evidence has also failed to identify a link between NSAID usage and PD or ALS (Fondell et al. 2012; Brakedal et al. 2021). Given the additional adverse effects associated with chronic use of various NSAIDs or steroidal anti-inflammatories, the opportunities to use these drugs for the treatment of neurodegenerative diseases appear to be limited.

Current efforts in neuroinflammation treatment are focused on the suppression of pro-inflammatory glial activity through indirect inhibition of processes that lead to microglial activation or direct action on microglia. NP001 is a proprietary formulation of sodium chlorite which was developed by Neuvivo for the treatment of ALS. NP001 targets macrophages to divert activation from a pro-inflammatory phenotype toward an anti-inflammatory phenotype and has shown benefits to select subsets of patients with respect to clinical disease progression, respiratory function, serum pro-inflammatory markers, and microbial translocation from the intestine to the bloodstream (Miller et al. 2014, 2015, 2022; Zhang et al. 2022c; McGrath et al. 2023). NP001 was slated for a phase 1 trial (ClinicalTrials.gov identifier: NCT03179501) in AD patients but this was terminated due to insufficient recruitment. Xpro™, developed by Inmune Bio, Inc., is a next-generation TNF inhibitor which comprises an engineered recombinant human TNF protein that forms trimers with native soluble TNF but cannot bind the type 1 TNF receptor (TNFR1). Xpro™ has recently completed a phase 1 trial in February, 2022 (ClinicalTrials.gov identifier: NCT03943264) to determine safety and efficacy in AD patients. The company has reported a marked reduction in hyperphosphorylated tau in the cerebrospinal fluid (CSF). Phase 2 trials for Xpro™ in patients with mild AD and cognitive impairment with elevated biomarkers of inflammation are currently in the recruitment phase and will include neuroimaging as well as cognitive testing (ClinicalTrials.gov identifiers: NCT05318976 and NCT05321498). ACZ885, developed by Novartis, is a monoclonal antibody designed to neutralize circulating IL-1β. ACZ885 was successful in phase 1 safety trials (ClinicalTrials.gov identifiers: NCT00619905 and

NCT00421226) and is currently recruiting for a phase 2 trial in patients with mild cognitive impairment or AD (ClinicalTrials.gov identifier: NCT04795466). These early successes suggest that the peripheral immune system can be targeted to improve outcomes in neurodegenerative disease through the reduction of pro-inflammatory myeloid cells and circulating cytokines such as TNF or IL-1β.

One of the first compounds used in AD clinical trials to specifically target microglia is GC021109, developed by GliaCure Inc. GC021109 is a prodrug that is metabolized into an agonist of microglial P2Y purinoceptor 6 ($P2Y_6$) receptors. Adenosine diphosphate (ADP) and uracil diphosphate (UDP) are the endogenous ligands of $P2Y_6$ receptors and are released by pro-inflammatory astrocytes as well as injured neurons (Guthrie et al. 1999; Davalos et al. 2005; Koizumi et al. 2007). Activation of $P2Y_6$ stimulates microglial phagocytosis and reduces cytokine release, and the rationale for this compound was to induce microglial uptake and clearance of Aβ with simultaneous reduction of neuroinflammation (Li et al. 2013). The phase 1b trial to evaluate safety and pharmacokinetics in AD patients was completed in February, 2016 (ClinicalTrials.gov identifier: NCT02386306), however, the results have not been published. Stimulation of microglial $P2Y_6$ receptors has more recently been shown to induce phagocytic uptake of stressed but viable neurons *in vitro* and *in vivo* which would contradict the use of a $P2Y_6$ receptor agonist for therapeutic purposes (Puigdellívol et al. 2021). AL003, developed by Alector Inc., and Lu AG22515, developed by H. Lundbeck A/S, are two more compounds that target the microglial receptors, CD33 and CD40, respectively. CD33 and CD40 have each been associated with microglial inflammatory and phagocytic activity (Gerritse et al. 1996; Ponomarev et al. 2006; Estus et al. 2019; Bhattacherjee et al. 2021). AL003 recently completed a phase 1 safety trial in AD patients (ClinicalTrials.gov identifier: NCT03822208) and a phase 1 safety trial with Lu AG22515 is currently in progress as of June, 2023 (ClinicalTrials.gov identifier: NCT05136053).

There are currently no approved drugs to specifically treat the neuroinflammation that precedes the onset of virtually all neurodegenerative diseases. Although current clinical efforts skew heavily toward AD, the results of ongoing trials

will provide insight into the value of neuroinflammation as a therapeutic target. As neuroinflammation is a unifying process in neurodegenerative disease, there is hope that progress made toward the treatment of AD will be transferrable to other diseases, including HD, PD, ALS, and more. Furthermore, the ability to pharmacologically modulate chronic low-grade neuroinflammation could also be useful to improve or preserve brain function in healthy ageing individuals.

1.5 Objectives of this research

Although there is a clear link between systemic inflammation, neuroinflammation, and impairment of neuronal function, the sequences of events are difficult to confirm. It is unclear whether peripheral inflammation induces glia activation and subsequent neuronal loss, or if inflammation can directly induce neuronal loss which promotes glial activation. *In vivo* models of neurodegenerative disease are useful to build our understanding of the broad relationship between neuroinflammation and neurodegeneration. However, *in vitro* models allow for a more mechanistic investigation into the relationships between microglia, neurons, and individual cytokines.

The purpose of this research is to investigate the mechanisms by which microglia respond to common pro-inflammatory stimuli as well as the mechanisms by which activated microglia can negatively affect neurons. The core questions are whether the pro-inflammatory activities of microglia will directly impair neuronal function and survival, and if so, whether pharmacological manipulation of microglial activity can prevent these negative effects. As microglia are innate immune cells, I focus on the use of immune-modulating drugs to either control the activity of microglia in response to pro-inflammatory stimuli to reduce the release of cytokines before they interact with neuronal cytokine receptors. The group of pharmacological agents explored in this thesis is broad and includes experimental signaling inhibitors, synthetic cannabinoid receptor agonists as well as endocannabinoids, JAK inhibitors, and anti-cytokine biologics. Ultimately, the goal of this thesis is to improve our mechanistic understanding of how microglia can damage neurons and provide some evidence to support whether traditional immunomodulatory drugs hold promise for the treatment of neuroinflammation.

Chapter 2: Synthetic cannabinoids reduce the inflammatory activity of microglia and subsequently improve neuronal survival *in vitro*

Copyright statement

Contribution statement

All experiments were performed, and data were collected by myself. Analysis and interpretation of the data were performed in consultation Dr. Eileen Denovan-Wright. Preparation of the manuscript was done by me with support from Dr. Eileen Denovan-Wright.

Preface

Chronologically, the experiments contained within this chapter were performed before the experiments contained in other chapters. The primary purposes of this chapter were to establish the conditioned media model and determine whether cultured microglial cells would induce secondary damage to cultured neuronal cells. The secondary purpose was to assess the potential anti-inflammatory properties of different classes of cannabinoids on the microglia. This chapter provides a jumping-off point for the remainder of the thesis as each subsequent chapter expands on a specific component of this chapter.

2.1 Abstract

Microglia are resident immune cells of the brain that survey the microenvironment, provide trophic support to neurons, and clear debris to maintain homeostasis and healthy brain function. Microglia are also drivers of neuroinflammation in several neurodegenerative diseases. Microglia produce endocannabinoids and express both cannabinoid receptor subtypes suggesting that this system is a target to suppress neuroinflammation. We tested whether cannabinoid type 1 (CB_1) or type 2 (CB_2) receptors could be targeted selectively or in combination to dampen the pro-inflammatory behavior of microglia, and whether this would have functional relevance to decrease secondary neuronal damage. We determined that components of the endocannabinoid system were altered when microglia are treated with lipopolysaccharide and interferon-gamma and shift to a pro-inflammatory phenotype. Furthermore, pro-inflammatory microglia released cytotoxic factors that induced cell death in cultured ST*Hdh*$^{Q7/Q7}$ neurons. Treatment with synthetic cannabinoids that were selective for CB_1 receptors (ACEA) or CB_2 receptors (HU-308) dampened the release of nitric oxide (NO) and pro-inflammatory cytokines and decreased levels of mRNA for several pro-inflammatory markers. A nonselective agonist (CP 55,940) exhibited similar influence over NO release but to a lesser extent relative to ACEA or HU-308. All three classes of synthetic cannabinoids ultimately reduced the secondary damage to the cultured neurons. The mechanism for the observed neuroprotective effects appeared to be related to cannabinoid-mediated suppression of MAPK signaling in microglia. Taken together, the data indicate that activation of CB_1 or CB_2 receptors interfered with the pro-inflammatory activity of microglia in a manner that also reduced secondary damage to neurons.

2.2 Introduction

Neuroinflammation is a hallmark of damage to the brain that occurs with chronic neurodegenerative diseases as well as acute conditions such as traumatic brain injury or septic encephalopathy (Guzman-Martinez et al. 2019; Li et al. 2020; Witcher et al. 2021). Microglia are recognized as resident immune cells of the brain and have been identified as active propagators of neuroinflammation (Perry et al. 2010). At rest, unreactive microglia survey the microenvironment using scavenger receptors, clear debris, and provide trophic support to neurons to maintain homeostasis and healthy brain function (Nimmerjahn et al. 2005; Cherry et al. 2014). Microglia may detect soluble factors released by damaged neurons or infiltrating peripheral immune cells and transition to an activated pro-inflammatory phenotype to mediate host defense via release of pro-inflammatory cytokines such as interleukin (IL)-1β and tumor necrosis factor alpha (TNFα) (Chhor et al. 2013). Sufficient concentrations of these cytokines trigger neuronal signaling cascades that lead to cellular impairment or apoptosis (Neumann et al. 2002; Brown and Vilalta 2015; Bachiller et al. 2018). Thus, the sustained pro-inflammatory activity of these microglia promotes chronic neuroinflammation which induces secondary neuronal damage and impairs global cognitive function (d'Avila et al. 2018; Zhao et al. 2019).

The endocannabinoid system functions at the interface between the nervous system and the immune system and has been proposed as a source of targets to treat inflammation and neurodegeneration (Pacher et al. 2006). The endocannabinoid system comprises synthetic and degradative enzymes for the endocannabinoids, anandamide (AEA) and 2-arachidonoylglycerol (2-AG), as well as the cognate G protein-coupled receptors (GPCRs), which are the cannabinoid type 1 (CB_1) and type 2 (CB_2) receptors (Howlett 2002). CB_1 receptors are abundant in neurons in the central nervous system and typically inhibit the release of neurotransmitters when activated (Howlett et al. 2002). Conversely, CB_2 receptors are primarily found in macrophage and other immune cells, including microglia (Galiègue et al., 1995; Howlett et al., 2002; Stella, 2009). CB_1 receptors are primarily responsible for the psychoactive effects of Δ^9-tetrahydrocannabinol (THC), whereas CB_2 receptors typically mediate the anti-

inflammatory effects of specific cannabinoids (Galiègue et al. 1995; Marsicano and Lutz 1999; Maresz et al. 2005).

Treatment with nonselective cannabinoids, including endocannabinoids and synthetic molecules, has been shown to reduce pro-inflammatory markers in rodent models of neuroinflammation and dampen the pro-inflammatory behavior of microglia (Ehrhart et al. 2005; Eljaschewitsch et al. 2006; Panikashvili et al. 2006; Fernández-López et al. 2006; Tanaka et al. 2020; Komorowska-Müller and Schmöle 2020). Microglia express both CB_1 and CB_2 receptors, and cross-talk can occur at the signaling level when both receptors are targeted simultaneously (Stella 2010; Callén et al. 2012; Navarro et al. 2018a; Young et al. 2022). However, the pharmacological contributions of CB_1 and CB_2 receptors to the pro-inflammatory activity of microglia have not been clearly delineated using selective agonists and antagonists. Furthermore, the biological relevance of these effects has not been determined with respect to secondary damage to neurons.

In this work, we aimed to determine the effects of synthetic cannabinoids on pro-inflammatory microglia using drugs that selectively activate either CB_1 or CB_2 receptors, or nonselectively activate both receptors. We used a strategy that involved conditioned media to assess the effects of secreted microglial factors on downstream neuronal viability (Chhor et al. 2013; Janefjord et al. 2014; Dai et al. 2015; Wang et al. 2017; García et al. 2018 p.; Liu et al. 2019). We present evidence that each class of cannabinoid receptor agonists dampen the pro-inflammatory activity of microglia, and that selective activation of cannabinoid receptors may be more beneficial than dual activation in this context. Moreover, these effects translated to subsequent improvements in neuronal survival the model of microglial-driven neurotoxicity. Taken together, these data support that the microglial endocannabinoid system is a promising target to dampen microglia-mediated neuroinflammation and prevent subsequent neuronal damage.

2.3 Results

2.3.1. LPS and IFNγ stimulated microglia to release pro-inflammatory factors

SIM-A9 microglia were treated with a combination treatment of LPS (1000 ng/mL) and IFNγ (20 ng/mL) to elicit a pro-inflammatory response (Fig. 2. 1A). The treatment stimulated the release of NO, TNFα, IL-1β and IL-6 into the culture medium with distinct temporal profiles. NO release was significantly elevated within 16 h and continued to increase up to 72 h (Fig. 2. 1B). NO release retained an upward trajectory throughout all time points and reached 279 ± 9 pmol per microgram of protein at the endpoint of 72 h. TNFα peaked at 16,555 ± 2,548 pg/mL at 16 h and was elevated in the media between 16 and 24 h following stimulation but returned to baseline by 48 h (Fig. 2. 1C). IL-1β release peaked at 113 ± 31 pg/mL 24 h following stimulation, but the peak concentration at this time point was not statistically different from baseline (Fig. 2. 1D). IL-6 peaked at 832 ± 135 pg/mL within 8 h and remained significantly elevated until 16 h but returned nearly to baseline by 48 h (Fig. 2. 1E).

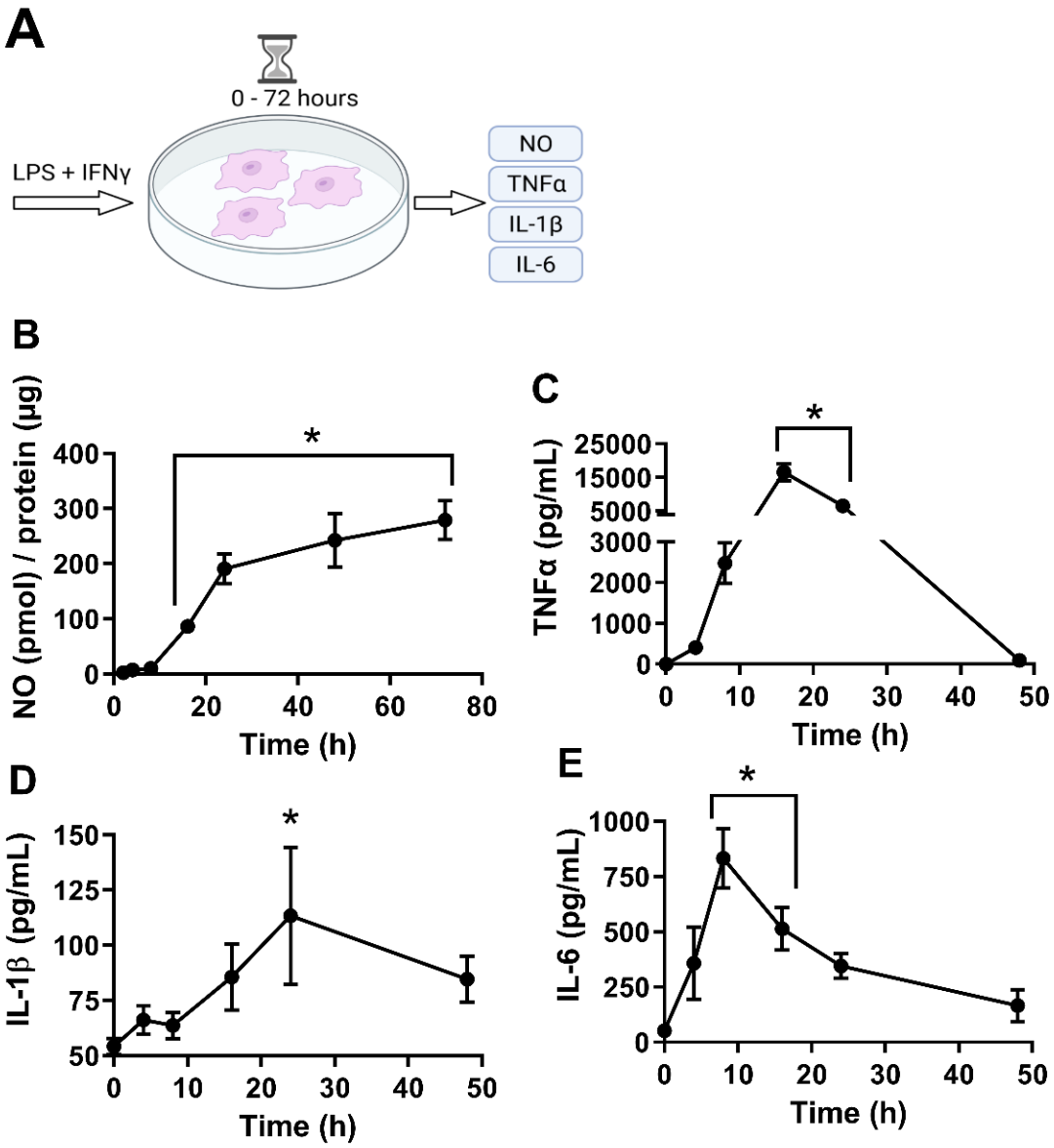

Figure 2. 1. Soluble factors released following pro-inflammatory treatment. A SIM-A9 microglia were treated with LPS and IFNγ and the release of the soluble pro-inflammatory factors NO, TNFα, IL-1β, IL-6 was monitored for up to 48 or 72 h. **B** NO was monitored in the cell supernatant via Griess assay for up to 72 hours following treatment (n = 8). **C** TNFα (n = 4), **D** IL-1β (n = 4), and **E** IL-6 (n = 4) were monitored for up to 48 hours following treatment using specific enzyme-linked immunosorbent assays. Data is presented as mean ± standard error of the mean. Significance was determined using the non-parametric Kruskal-Wallis test with Dunn's post-hoc test; * $p < 0.05$ vs. 0-hour time-point. Panel A was prepared using BioRender.

In subsequent experiments, conditioned media from SIM-A9 microglia was applied to cultured neurons. For these experiments, microglia were stimulated with LPS and IFNγ for 16 h before the media was harvested. This time point was chosen as the media harvested at this time point included elevated quantities of NO, TNFα, and IL-6 compared to baseline. Thus, this conditioned media contained 86.5 ± 1.9 pmol NO per microgram of protein, 16,555 ± 2,548 pg/mL TNFα, 85.6 ± 15.0 pg/mL IL-1β, and 512.9 ± 96.4 pg/mL IL-6 in addition to the pro-inflammatory factors that were not specifically quantified in this study.

2.3.2. The microglial endocannabinoid system was altered under pro-inflammatory conditions

Given the roles that the endocannabinoid system may play in neuroinflammation, we measured gene expression of several components of the endocannabinoid system in microglia upon treatment with LPS and IFNγ. Under the pro-inflammatory conditions, there was a decrease in the mRNA abundance of *Cnr1* (CB_1; 3.22-fold, $p = 0.0022$, Fig. 2. 2A) and *Cnr2* (CB_2; 17.82-fold, $p = 0.0022$, Fig. 2. 2B) relative to microglia that did not receive the pro-inflammatory stimuli. There was no change in *NAPEPLD* (NAPE-PLD; Fig. 2. 2C) but there was an increase in mRNA abundance for *FAAH* (FAAH; 26.07-fold, $p = 0.0022$, Fig. 2. 2D). Conversely, there was an increase in *DAGLA* (DAGLα; 1.60-fold, $p = 0.0022$, Fig. 2. 2E) but no change in *MGLL* (MAGL; Fig. 2. 2F).

As the abundance of *Cnr1* and *Cnr2* mRNA was diminished upon treatment with the pro-inflammatory stimuli, immunofluorescence staining of CB_1 and CB_2 receptors was used to determine whether the pro-inflammatory microglia expressed cannabinoid receptors at the cell surface. Qualitative immunofluorescence staining revealed both CB_1- and CB_2 receptor-like immunoreactivity in the unreactive and pro-inflammatory states which indicated that the microglia expressed both receptor proteins following treatment with LPS and IFNγ (Fig. 2. 2G-H). Control samples were prepared using a blocking peptide for the anti-CB_2 receptor antibody which ablated CB_2-like immunoreactivity as determined qualitatively in all samples regardless of treatment (Fig. 2. S1).

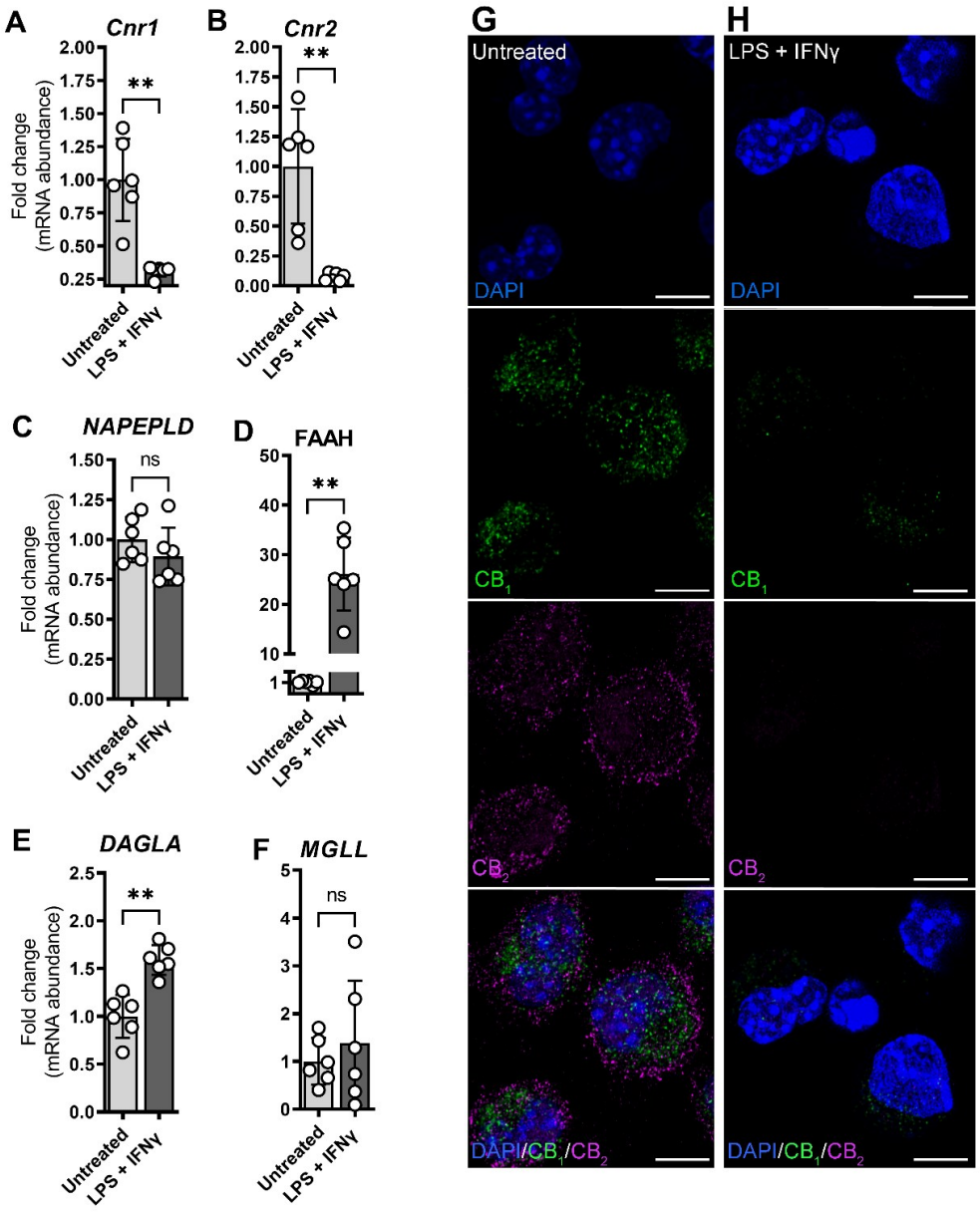

Figure 2. 2. Components of the endocannabinoid system were dysregulated in microglia exposed to pro-inflammatory stimuli. A-F Reverse transcription quantitative PCR analysis of mRNA abundance of **A** *Cnr1* (CB_1 receptors), **B** *Cnr2* (CB_2 receptors), **C** *NAPEPLD* (NAPE-PLD), **D** *FAAH* (FAAH), **E** *DAGLA* (DAGLα), and **F** *MGLL* (MAGL) following 24 h treatment with vehicle or LPS and IFNγ. Statistical significance was determined using the non-parametric Mann-Whitney test; ** $p < 0.01$. **G-H** Immunofluorescence labeling of CB_1 (green) and CB_2 (magenta) receptors in SIM-A9 microglia treated with **G** vehicle or **H** LPS and IFNγ. Scale bar; 10 μm for all panels.

2.3.3. Conditioned media from pro-inflammatory microglia was neurotoxic

To determine if the media from pro-inflammatory microglia was cytotoxic, SIM-A9 microglia were stimulated with LPS and IFNγ for 16 h, and the conditioned media was applied to cultured ST*Hdh*$^{Q7/Q7}$ neurons for 24 h. To identify a potential dose-response relationship between the conditioned media treatment and subsequent neuronal survival, the conditioned media was diluted in serum-free DMEM:F12 media so that treatment groups would receive as little as 60% of the conditioned media or up to 100% conditioned media (Fig. 2. 3A).

The neurons were cultured in the conditioned media for 24 h and cell viability was measured. Compared to media taken from unstimulated microglia, the pro-inflammatory conditioned media was observed to be neurotoxic to ST*Hdh*$^{Q7/Q7}$ neurons at a concentration of 85% or higher (Fig. 2. 3B). In these neurons, 100% conditioned media induced death in up to 64.4 ± 4.4% of cells whereas the undiluted media from unstimulated microglia induced death in only 30.9 ± 1.7% of cells. Cultured HEK 293T cells were subjected to the same treatments for comparison to determine if the pro-inflammatory media may be selectively neurotoxic. The conditioned media did not induce more cell death in HEK 293T cells compared to media from unstimulated microglia at any given dilution (Fig. 2. 3C). HEK 293T cells that received 100% conditioned media from pro-inflammatory microglia exhibited 19.3 ± 1.3% cell death whereas the proportion of cell death was 17.2 ± 4.1% in cells that received media from unstimulated microglia.

As a corroborating measure of cell viability, the concentration of ATP was measured in ST*Hdh*$^{Q7/Q7}$ neurons and HEK 293T following exposure to pro-inflammatory conditioned media. The ST*Hdh*$^{Q7/Q7}$ neurons exhibited a significant reduction in ATP concentration upon exposure to a concentration of 70% or greater conditioned media (Fig. 2. 3D). In HEK 293T cells, the pro-inflammatory conditioned media had no effect on the concentration of ATP.

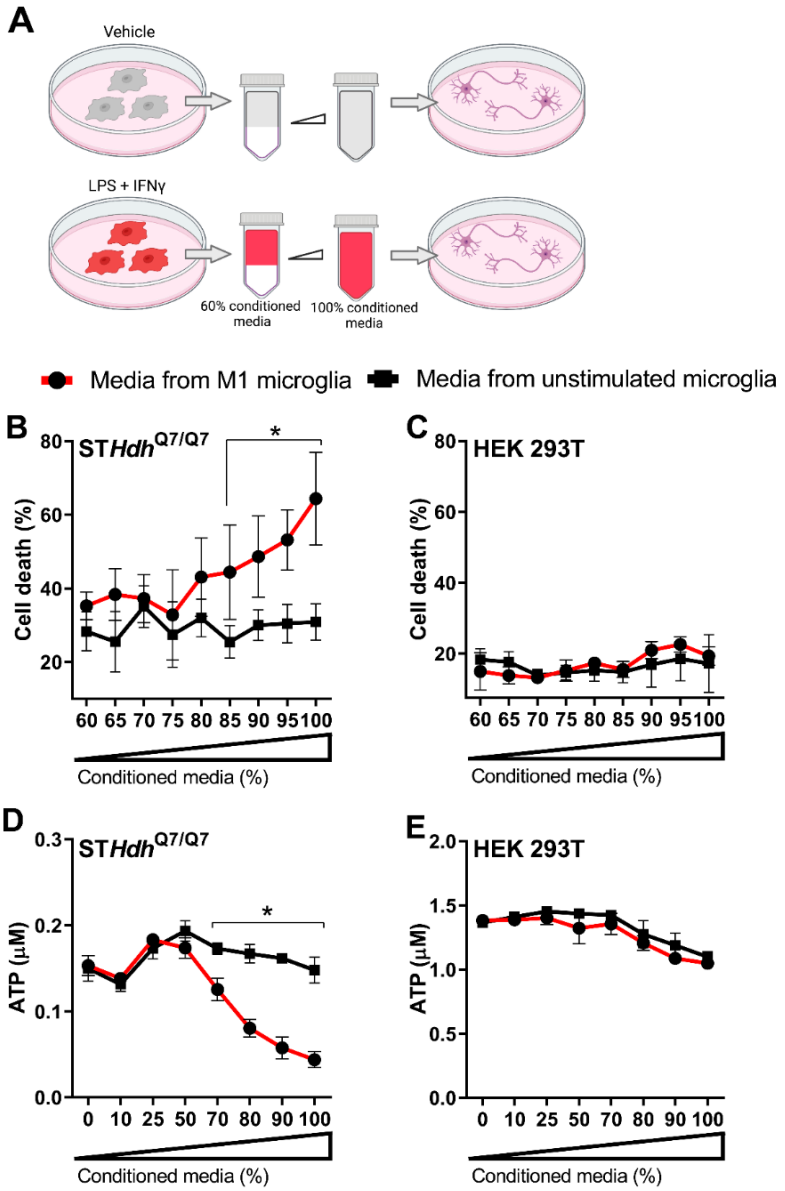

Figure 2. 3. Conditioned media from pro-inflammatory microglia was toxic to STHdh$^{Q7/Q7}$ neurons and not HEK 293T cells. A Media was harvested from pro-inflammatory microglia, diluted in serum-free media, and applied to STHdh$^{Q7/Q7}$ neurons or HEK 293T cells in the ratios indicated (60-100% conditioned media). Cell viability was measured in **B** STHdh$^{Q7/Q7}$ neurons (n = 8) and **C** HEK 293T cells (n = 4) following exposure to conditioned media for 24 hours. The concentration of ATP was also determined in **D** STHdh$^{Q7/Q7}$ neurons (n = 8) and **E** HEK 293T cells (n = 4) as a measure of overall cell viability. Data is presented as the mean ± standard deviation. Statistical significance was determined using two-way ANOVA with Sidak correction for multiple comparisons; * $p < 0.001$. Panel A was prepared using BioRender.

2.3.4. Cannabinoid treatments dampened the microglial pro-inflammatory response

Cannabinoid receptor agonists have been repeatedly shown to have anti-inflammatory effects in different models of neurodegenerative disease (Price et al. 2009; Fakhfouri et al. 2012; Aso et al. 2013; Javed et al. 2016; Chung et al. 2016; Cassano et al. 2017). We aimed to determine whether stimulation of CB_1 or CB_2 receptors by selective or nonselective synthetic agonists would influence the pro-inflammatory behavior of SIM-A9 microglia. Microglia were treated with ACEA (>1400-fold selectivity for CB_1 over CB_2), HU-308 (>440-fold selectivity for CB_2 over CB_1), or CP 55,940 (relatively non-selective) and the effect on NO release following stimulation with LPS and IFNγ was determined (Pertwee 1997; Hillard et al. 1999; Hanus et al. 1999). Co-treatment with ACEA produced a dose-dependent decrease in NO release, to 53.22 ± 14.09% relative to control samples with an EC_{50} of 677.64 nM (Fig. 2. 4A). HU-308 suppressed NO release to 72.43 ± 6.13% with an EC_{50} of 692.04 nM and CP 55,940 suppressed NO release to 81.26 ± 6.97% with an EC_{50} of 564.94 nM.

To corroborate the effects of cannabinoids on NO release, the experiments were repeated using the EC_{90} dose of ACEA (1.2 μM), HU-308 (2.5 μM), or CP 55,940 (1.8 μM) and/or AM251 (2 μM) or AM630 (1 μM). Microglia treated with ACEA exhibited suppressed NO release to 136.8 ± 41.0 nmol per μg total protein compared to 190.9 ± 27.0 in the cells that received only LPS ± IFNγ ($F(3, 52) = 70.38$, $p < 0.0001$) (Fig. 2. 4B). The effect of ACEA was also blocked by the selective antagonist AM251 ($p = 0.0121$) which indicated the effect was mediated by CB_1 receptors. Treatment with HU-308 reduced NO release to 148.0 ± 19.7 nmol per μg total protein ($F(3, 52) = 114.8$, $p < 0.0001$) and the effect was blocked the the CB_2 receptor antagonist, AM630 ($p = 0.0185$) (Fig. 2. 4C). This indicated that the effect of HU-308 on NO release was mediated by CB_2 receptors. Finally, treatment with CP 55,940 suppressed NO release to 147.1 ± 36.3 nmol per μg total protein ($F(4, 67) = 65.44$, $p = 0.0004$) and the effect was partially blocked by both AM251 ($p = 0.0219$) and AM630 ($p = 0.0303$) which suggested a contribution of both receptors to the effects of CP 55,940 (Fig. 2. 4D). As AM251 and AM630 are known as inverse agonists of CB_1 and CB_2 receptors, respectively, we prepared dose-response curves with these drugs alone to determine whether there was a

dose-dependent potentiation of NO release with the inverse agonism of CB_1 or CB_2 receptors (Fig. 2. S2). We found that there was not a dose-dependent effect of AM251 or AM630 alone on NO release from SIM-A9 microglia. This indicated that either these ligands behaved as neutral antagonists in this assay, or that inverse agonism of the cannabinoid receptors did not induce NO release.

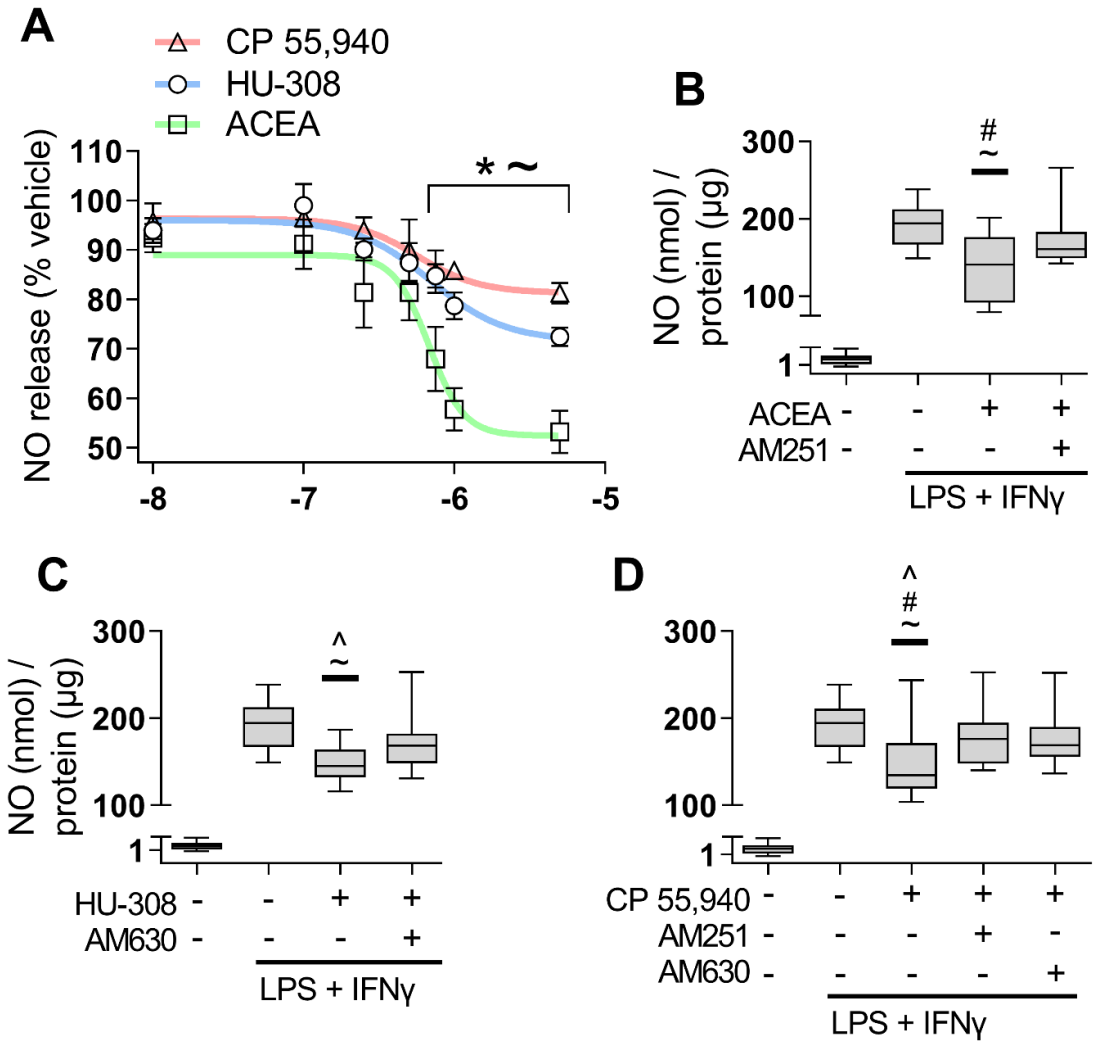

Figure 2. 4. Microglia treated with cannabinoids exhibited reduced NO release and mRNA of pro-inflammatory markers. A NO release following treatment with LPS + IFNγ and vehicle, ACEA, HU-308, or CP 55,940 (n = 11). Statistical significance was determined using two-way ANOVA with Sidak correction for multiple comparisons; * $p < 0.05$, ACEA vs. CP 55,940; ~ $p < 0.05$, HU-308 vs. ACEA. **B-D** Cells treated with vehicle or LPS + IFNγ and the EC_{90} dose of **B** ACEA (1.2 µM), **C** HU-308 (2.5 µM), or **D** CP 55,940 (1.8 µM) and/or AM251 (2 µM) or AM630 (1 µM) (n = 16). Statistical significance was determined using the non-parametric Kruskal-Wallis test with Dunn's post-hoc test; ~ $p < 0.05$ vs. LPS + IFNγ; # $p < 0.05$ vs. agonist + AM251; ^ $p < 0.05$ vs. agonist + AM630.

To determine whether the synthetic cannabinoid agonists also had an effect on the abundance of pro-inflammatory markers, mRNA for *Nos2* (iNOS), *Tnf* (TNFα), *Il1b* (IL-1β), and *Il6* (IL-6) were measured following treatment with LPS and IFNγ in the presence of cannabinoids. The CB_1 and CB_2 receptors were targeted individually or in combination using the EC_{90} of ACEA, HU-308 or CP 55,940. For comparison, a combination of ACEA and HU-308 was used at half of the EC_{90}. Treatment with LPS and IFNγ in the presence of ACEA or HU-308 reduced the abundance of mRNA for *Nos2* ($p < 0.0001$; Fig. 2. 5A), *Tnf* ($p < 0.0002$; Fig. 2. 5B), *Il1b* ($p < 0.0001$; Fig. 2. 5C), and *Il6* ($p < 0.0001$; Fig. 2. 5D) relative to LPS and IFNγ alone. Treatment with CP 55,940 did not influence the mRNA abundance of *iNOS* or *IL-6* but reduced the abundance of mRNA for *TNFα* ($p < 0.0001$) and *IL-1β* ($p = 0.0007$). Interestingly, the combination of ACEA and HU-308 was less impactful on the mRNA for pro-inflammatory markers, and only reduced the mRNA abundance for *IL-1β* ($p = 0.0048$).

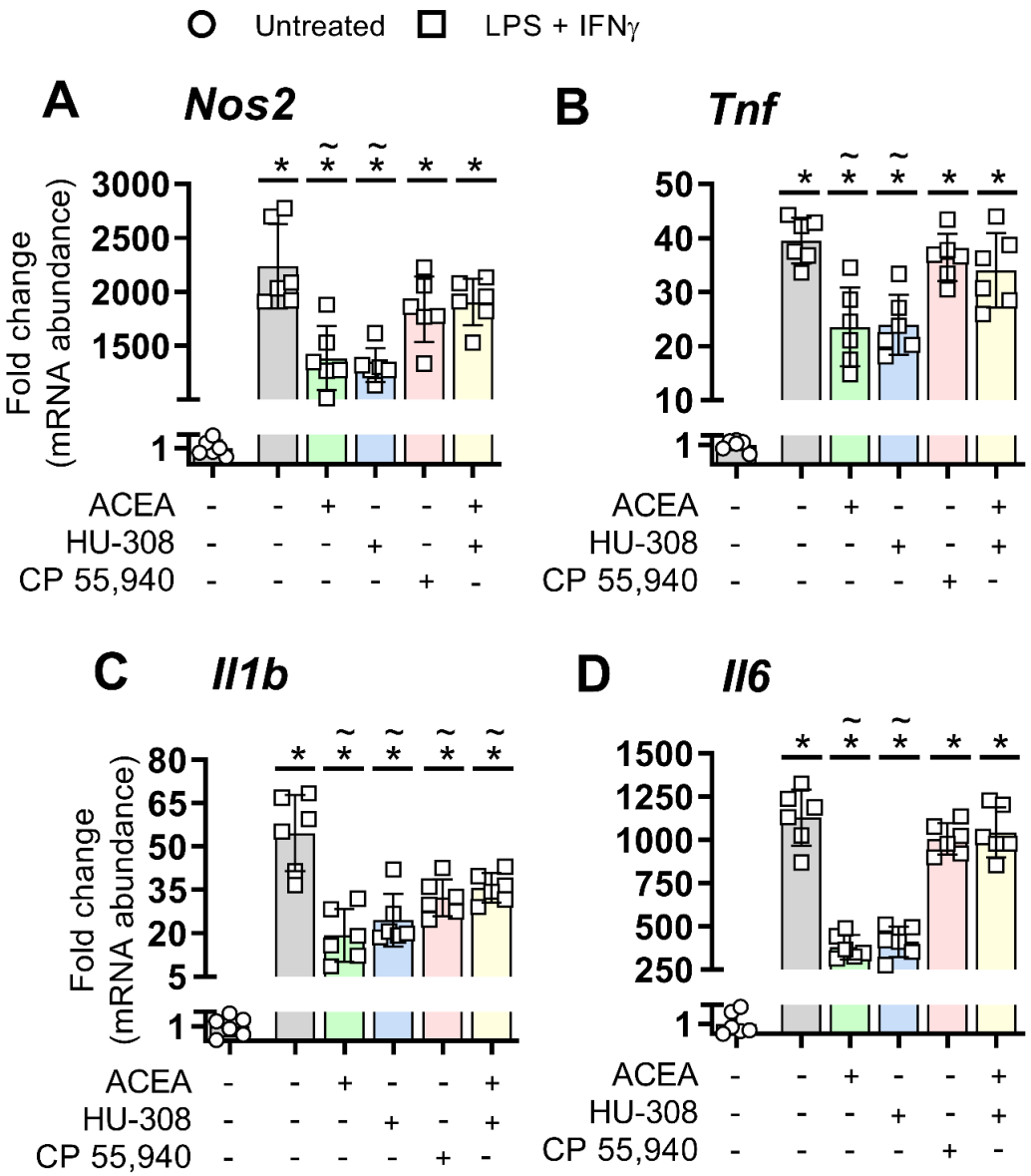

Figure 2. 5. Microglia treated with cannabinoids exhibited reduced mRNA of pro-inflammatory markers. SIM-A9 microglia were treated with LPS + IFNγ in conjunction with ACEA (1.20 μM), HU-308 (2.50 μM), CP 55,940 (1.80 μM), or ACEA (0.60 μM) and HU-308 (1.25 μM). **A-D** Relative quantities of mRNA for pro-inflammatory markers **A** *Nos2*, **B** *Tnf*, **C** *Il1b*, and **D** *Il6* (n = 6). The mRNA abundance is presented as fold change over cells that did not receive the LPS + IFNγ or cannabinoid treatments. Significance was determined via one-way ANOVA with Dunnett's correction for multiple comparisons; * $p < 0.05$ vs. untreated; ~ $p < 0.05$ vs. LPS + IFNγ.

To confirm that the synthetic cannabinoid treatments suppressed the release of TNFα, IL-1β, and IL-6, the microglial culture medium was analyzed following treatment with LPS and IFNγ in combination with ACEA, HU-308, or CP 55,940. Treatment with the pro-inflammatory stimuli induced the release of TNFα which was reduced by co-treatment with ACEA ($p = 0.0341$) or HU-308 alone ($p = 0.0066$) whereas CP 55,940 or the combination of ACEA and HU-308 did not influence the release of TNFα (Fig. 2. 6A). The release of IL-1β was also only dampened by co-treatment with ACEA ($p = 0.0021$) or HU-308 alone ($p = 0.0496$) (Fig. 2. 6B). Similarly, IL-6 release was suppressed only by treatment with ACEA ($p = 0.0024$) or HU-308 ($p = 0.0254$) (Fig. 2. 6C).

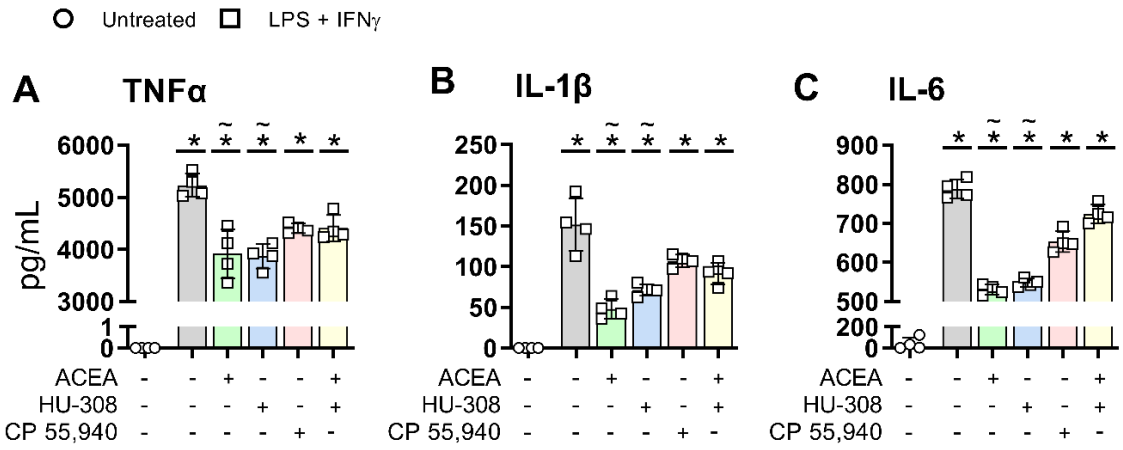

Figure 2. 6. Microglia treated with cannabinoids exhibited reduced release of TNFα, IL-1β, and IL-6. SIM-A9 microglia were treated with LPS + IFNγ in conjunction with ACEA (1.20 μM), HU-308 (2.50 μM), CP 55,940 (1.80 μM), or ACEA (0.60 μM) and HU-308 (1.25 μM). **A-D** Quantities of protein for pro-inflammatory markers **A** TNFα, **B** IL-1β, and **C** IL-6 (n = 4) released by SIM-A9 microglia following treatment with vehicle or LPS + IFNγ in conjunction with ACEA, HU-308, or CP 55,940. Significance was determined using the non-parametric Kruskal-Wallis test with Dunn's post-hoc test; * $p < 0.05$ vs. untreated; ~ $p < 0.05$ vs. LPS + IFNγ.

2.3.5. Microglial cannabinoid treatment reduced neurotoxicity of conditioned media

The stimulation of CB_1 and CB_2 receptors reduced the abundance of mRNA for pro-inflammatory markers and reduced NO release from cultured SIM-A9 microglial cells. To determine whether these effects had biological relevance, the conditioned media was again applied to ST*Hdh*$^{Q7/Q7}$ neurons and HEK 293T cells and cytotoxicity was measured (Fig. 2. 7A). ST*Hdh*$^{Q7/Q7}$ neurons that received the conditioned media exhibited 62.2 ± 7.0% cell death. The proportion of cell death was reduced when the SIM-A9 microglia were pretreated with ACEA (43.3 ± 3.6%; $p < 0.0001$), HU-308 (37.8 ± 4.5%; $p < 0.0001$), or CP 55,940 (49.8 ± 5.2%; $p = 0.0056$) (Fig. 2. 7B). Furthermore, the direct treatment of neurons with the cannabinoid drugs or the pro-inflammatory stimuli had no effect on cell viability (Fig. 2. S3). The effects of ACEA pretreatment were abrogated when the SIM-A9 microglia were also pretreated with AM251 or AM630. Interestingly, the effects of HU-308 and CP 55,940 were blocked only by AM251 pretreatment whereas AM630 had no influence. We also found that although AM630 did not block the neuroprotective effects of HU-308 or CP 55,940, an alternative CB_2 receptor inverse agonist, SR144528, fully blocked the effects of these agonists (Fig. 2. S4). When HEK 293T cells were subjected to the same treatments, there was no effect of the conditioned media, regardless of whether the SIM-A9 microglia had been treated with LPS + IFNγ, ACEA, HU-308, or CP 55,940 (Fig. 2. 7C).

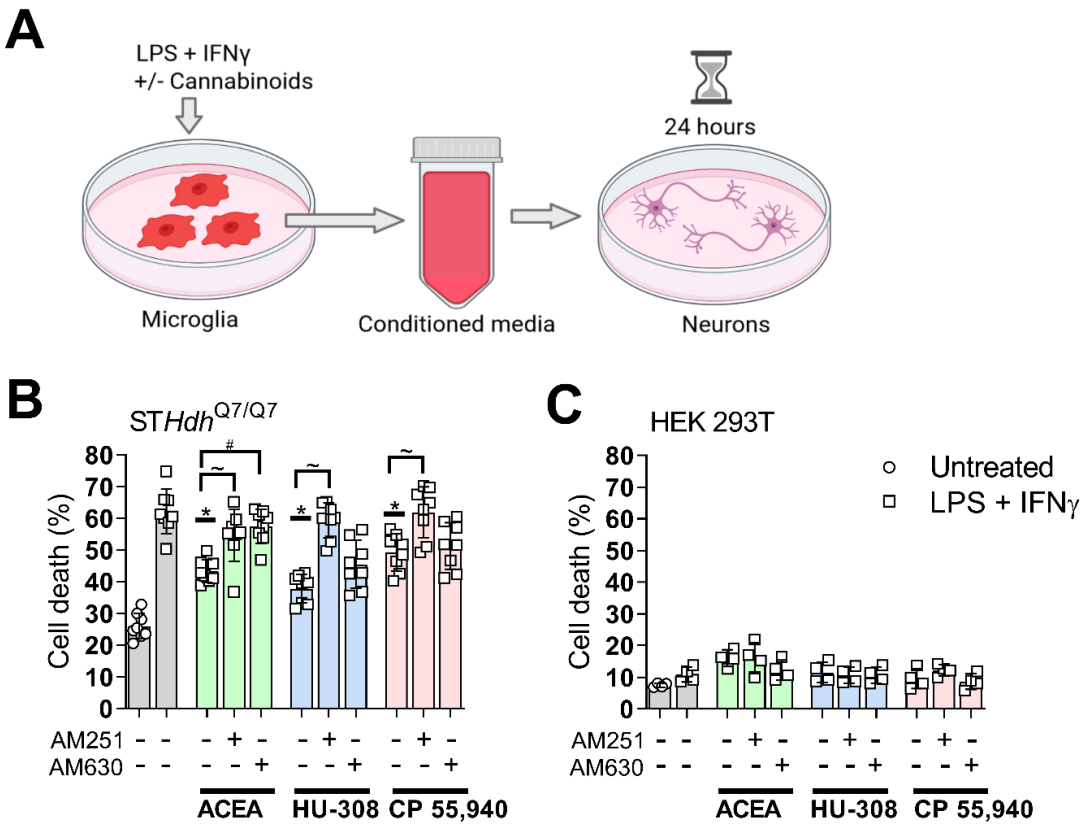

Figure 2. 7. Microglial cannabinoid treatments reduced neurotoxicity of conditioned media. A SIM-A9 microglia were treated with LPS + IFNγ with vehicle, ACEA, HU-308, or CP 55,940 in conjunction with AM251 or AM630. The conditioned media was subsequently applied directly to cultured **B** STHdh$^{Q7/Q7}$ neurons (n = 8) or **C** HEK 293T cells (n = 4) and cell viability was measured after 24 h. * $p < 0.01$ vs. LPS + IFNγ; ~ $p < 0.05$ vs. LPS + IFNγ + agonist + AM251; # $p < 0.05$ vs. LPS + IFNγ + agonist + AM630. Panel A was prepared using BioRender.

We assessed the presence of CB_1 and CB_2 receptors in ST*Hdh*$^{Q7/Q7}$ neurons using immunofluorescence and semi-quantitative RT-PCR and determined that the cells may contain both CB_1 and CB_2 receptors (Fig. 2. S5). We observed strong CB_1-like immunoreactivity but weak CB_2-like immunoreactivity which was abrogated using the blocking peptide for the anti-CB_2 antibody. RT-PCR revealed that ST*Hdh*$^{Q7/Q7}$ neurons possess mRNA for both *Cnr1* and *Cnr2* despite the weak CB_2 receptor staining. Thus, it could not be ruled out that the cannabinoid drugs in the conditioned media could also interact with neuronal CB_1 or CB_2 receptors to contribute to the neuroprotective effects.

2.3.6. Cannabinoid treatments differentially influenced LPS and IFNγ-mediated signaling in microglia

LPS has been previously shown to signal via NF-κB whereas IFNγ has been shown to signal via JAK/STAT1 and phosphoinositide 3-kinase (PI3K)/Akt pathways in microglia (Darnell et al. 1994; Ramana et al. 2002; Ehrhart et al. 2005; Eljaschewitsch et al. 2006; Zhao et al. 2019; Kang et al. 2019). We hypothesized that activation of CB_1 and/or CB_2 receptors would interfere with the phosphorylation of NF-κB p65 or STAT1 at the early (5 min) or late (30 min) stage of signaling. We found that upon treatment with LPS + IFNγ (5 min), NF-κB p65 phosphorylation was elevated to 136.5 ± 11.8% relative to vehicle and this was not influenced by co-incubation with ACEA, HU-308, or CP 55,940 [$F = 3.112$ (3, 11.90)] (Fig. 2. 8A). Similarly, at the 30 min time point, NF-κB p65 phosphorylation was elevated to 126.1 ± 7.9% relative to vehicle and there was no significant effect of cannabinoid co-incubation [$F = 3.302$ (3, 11.08)] (Fig. 2. 8B).

Upon treatment with LPS + IFNγ (5 min), STAT1 phosphorylation was elevated to 134.6 ± 10.5% relative to vehicle and there was no significant effect of ACEA, HU-308, or CP 55,940 [$F = 2.143$ (3, 10.88)] (Fig. 2. 8C). Finally, at the 30 min time point, STAT1 phosphorylation was elevated to 148.3 ± 7.6% relative to vehicle, and this was not affected by cannabinoid co-treatment [$F = 1.522$ (3, 10.77)] (Fig. 2. 8D).

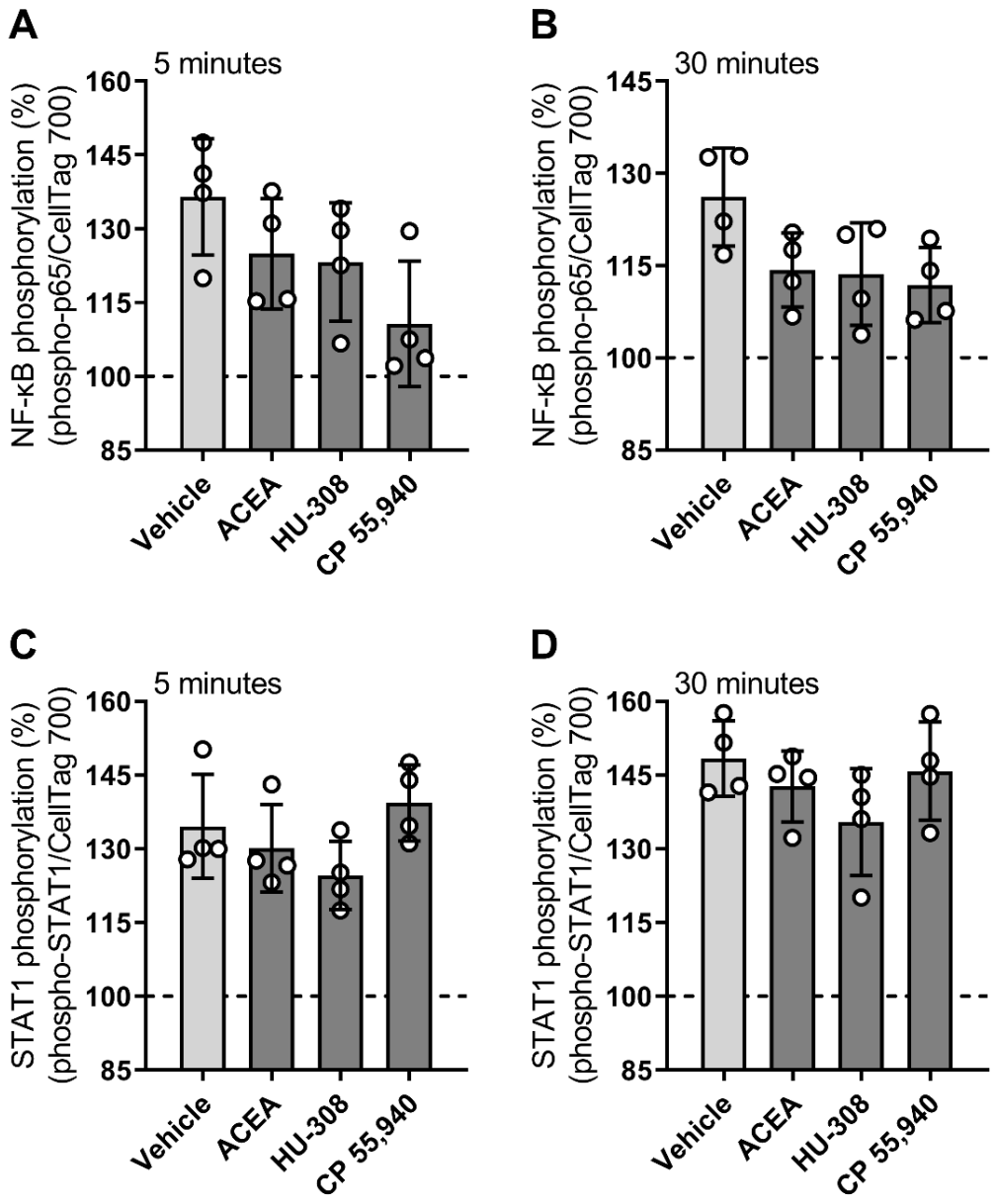

Figure 2. 8. NF-κB and STAT1 phosphorylation was not influenced by ACEA, HU-308, or CP 55,940 treatment in conjunction with LPS + IFNγ. SIM-A9 microglia were treated with LPS + IFNγ in conjunction with either the vehicle, ACEA (1.2 μM), HU-308 (2.5 μM), or CP 55,940 (1.8 μM). Phosphorylation of NF-κB (Ser536) was measured at **A** 5 min and **B** 30 min. Phosphorylation of STAT1 (Tyr701) was measured at **C** 5 min and **D** 30 min. Quantities of phosphorylated proteins were normalized to cell number using CellTag 700. Phosphorylation (%) was normalized to cells that did not receive LPS + IFNγ (constrained to 100%, indicated by dashed line). Statistical significance was assessed using Brown-Forsythe and Welch ANOVA tests with Dunnett correction for multiple comparisons.

Signaling of LPS and IFNγ has also been associated with activation of mitogen-activated protein kinase (MAPK) pathways including extracellular signal-regulated kinases (ERK)1/2, c-Jun N-terminal kinase (JNK), and p38 as well as the PI3K/Akt pathway (Waetzig et al. 2005; Eljaschewitsch et al. 2006; Khatchadourian et al. 2012; Subedi et al. 2017; Ye et al. 2020; Lu et al. 2021). As the cannabinoid treatments dampened the LPS + IFNγ-induced activation of SIM-A9 microglia, we hypothesized that activation of CB_1 and/or CB_2 receptors would interfere with the activation of one or several of these signaling pathways. We found that treatment with ACEA or HU-308 blunted the LPS + IFNγ-induced phosphorylation of ERK1/2 whereas CP 55,940 did not have an effect [$F = 136.4 (3, 5.530)$] (Fig. 2. 9A). HU-308 also dampened the LPS + IFNγ-induced phosphorylation of JNK [$F = 27.86 (3, 6.532)$] (Fig. 2. 9B) and p38 [$F = 7.892 (3, 9.525)$] (Fig. 2. 9C) whereas ACEA and CP 55,940 had no statistically significant effect on these pathways. Finally, all three treatments blunted the LPS + IFNγ-induced phosphorylation of Akt [$F = 38.88 (3, 6.525)$] (Fig. 2. 9D).

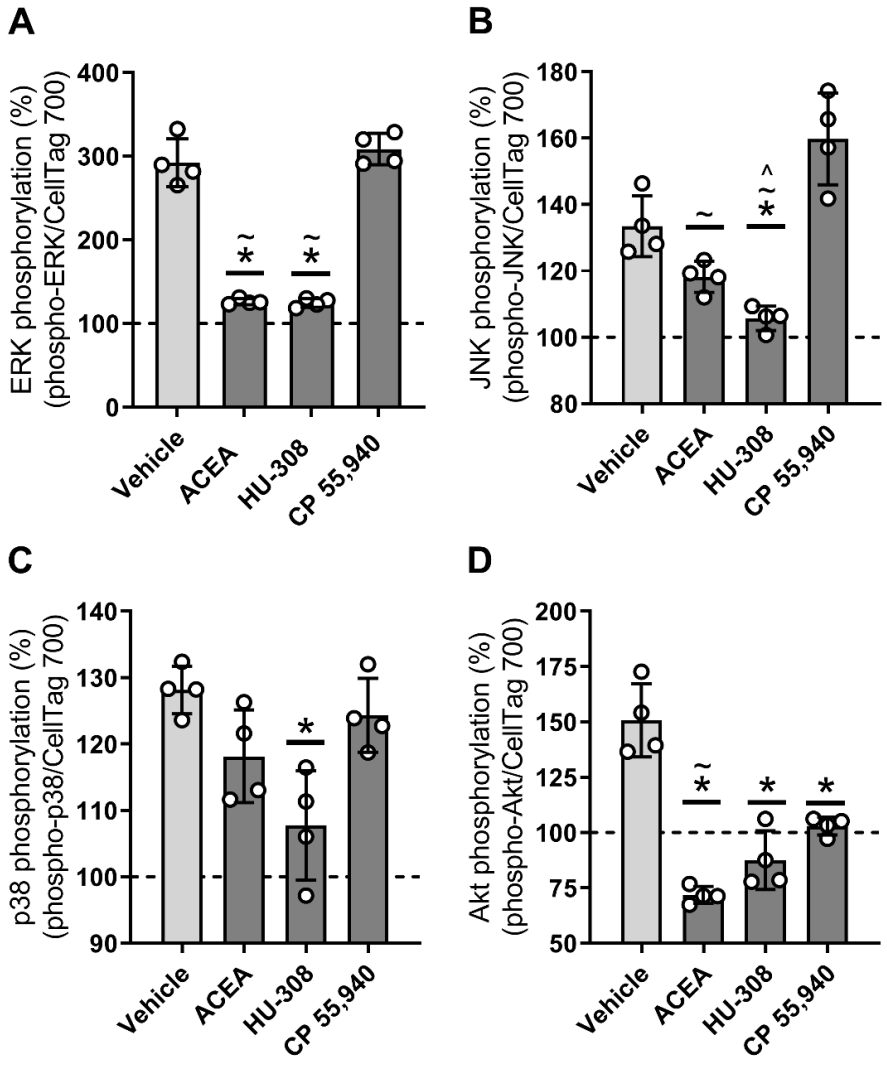

Figure 2. 9. MAPK and PI3K-Akt pathways were differentially influenced by ACEA, HU-308, and CP 55,940 treatment in conjunction with LPS + IFNγ. SIM-A9 microglia were treated with LPS + IFNγ with either the vehicle, ACEA (1.2 μM), HU-308 (2.5 μM), or CP 55,940 (1.8 μM) for 30 min. Phosphorylation of **A** ERK1/2 (Thr202/Tyr204), **B** JNK (Thr183/Tyr185), **C** p38 (Thr180/Tyr182), and **D** Akt (Ser473) was measured and normalized to cell number using CellTag 700. Phosphorylation (%) was normalized to cells that did not receive LPS + IFNγ (constrained to 100%, indicated by dashed line). * $p < 0.05$ vs. LPS + IFNγ + vehicle; ~ $p < 0.05$ vs. LPS + IFNγ + CP 55,940; ^ $p < 0.05$ vs. LPS + IFNγ + ACEA. Statistical significance was determined using Brown-Forsythe and Welch ANOVA tests with Dunnett correction for multiple comparisons.

2.4 Discussion

We have investigated the influence of synthetic cannabinoid drugs to determine the contributions of CB_1 and CB_2 receptor activation on the pro-inflammatory activity of cultured microglia and the downstream effects on cultured neurons. The data suggest that in microglia, activation of CB_1 or CB_2 receptors effectively dampened the release of NO, TNFα, IL-1β, and IL-6 and reduced the abundance of mRNA corresponding to these factors. Co-activation of CB_1 and CB_2 receptors also reduced NO release and mRNA for IL-1β. Ultimately, treatment with ACEA, HU-308, or CP 55,940 reduced the subsequent neurotoxicity of the conditioned media from pro-inflammatory microglia. This indicated that either individual or simultaneous activation of cannabinoid receptors effectively reduced the pro-inflammatory and neurotoxic activity of microglia in a biologically relevant manner.

Microglia exhibit fluctuations in the endocannabinoid system components under pro-inflammatory conditions (Young and Denovan-Wright 2022a). We observed that the components of the microglial endocannabinoid system fluctuated upon treatment with the proinflammatory stimuli, LPS and IFNγ. The cultured microglia exhibited greatly reduced quantities of CB_1 and CB_2 receptor mRNA, similar findings were reported by Maresz et al. (2005) where CB_2 receptor mRNA was suppressed in LPS-treated microglia. CB_2 receptor mRNA was also substantially reduced in primary rat microglia and RAW 264.7 macrophage-like cells upon treatment with LPS alone or LPS and IFNγ (Maresz et al. 2005). Despite the observed reduction in cannabinoid receptor mRNA, the microglia exhibited CB_1 and CB_2 receptor-like immunoreactivity following treatment with LPS and IFNγ. However, antibodies raised against GPCRs and especially CB_2 receptors generally do not exhibit a high degree of specificity (Baker 2015; Zhang et al. 2019b). This prevented direct correlation between immunofluorescence and CB_1 or CB_2 receptor abundance. Ultimately, the microglia were responsive to cannabinoid drugs following treatment with LPS and IFNγ which supported that there were still functional receptors at the cell surface in this pro-inflammatory state. The microglia exhibited changes in mRNA for the endocannabinoid metabolic machinery, including increased DAGLα and FAAH. In primary rat microglial cells, LPS treatment also resulted in

decreased mRNA for FAAH and MAGL but increased mRNA for DAGLα/β (Mecha et al. 2015). Taken together, these data suggest that the pro-inflammatory microglia could have shifted to synthesize relatively more 2-AG and less AEA under the pro-inflammatory conditions. It has been previously observed that activated pro-inflammatory microglia release more 2-AG compared to unreactive microglia via a mechanism controlled by P_2X_7 purinoceptors (Witting et al. 2004, 2006). 2-AG has also been found to enhance recruitment of leukocytes to facilitate a pro-inflammatory response whereas AEA has been found to dampen such a response via cannabinoid receptor activation (Eljaschewitsch et al. 2006; Turcotte et al. 2016). Thus, pro-inflammatory microglia may release 2-AG to facilitate the recruitment of additional immune cells to propagate neuroinflammation.

We observed that conditioned media from the pro-inflammatory SIM-A9 microglia induced cell death in the cultured ST*Hdh*$^{Q7/Q7}$ neurons but not in HEK 293T cells. Furthermore, there was a relationship between neuronal survival and the relative concentration of conditioned media in which the cells were incubated. Microglia can potentially kill neurons via several mechanisms including direct phagocytosis or the release of toxic factors (reviewed in Brown and Vilalta, 2015). As the microglia were not cultured in contact with the neurons, the microglia affected neuronal survival via factors released into the media rather than via direct contact. Similar findings have been reported as conditioned media from pro-inflammatory microglia was shown to induce apoptosis in primary cortical neurons (Chhor et al. 2013). Although it is unclear which molecules specifically induced cell death in the cultured neurons, it appeared that the neurons had receptors to respond to these factors whereas the HEK 293T cells did not. A limitation associated with the use of glial conditioned media is the complete composition of the conditioned media is unknown in most cases. In this work, we performed time-course experiments and monitored the release of four known pro-inflammatory mediators (NO, TNFα, IL-1β, IL-6) to provide multiple reference points for the composition of the conditioned media. Furthermore, although glial conditioned media can be prepared in a reproducible manner, the composition of glial conditioned media does not represent the

concentrations of pro-inflammatory cytokines *in vivo*. This highlights a benefit of animal models in future work.

Previous work has demonstrated that the endocannabinoid system modulates the pro-inflammatory activity of microglia (Eljaschewitsch et al. 2006; Correa et al. 2010; Hernangómez et al. 2012; Malek et al. 2015; Ma et al. 2018; Askari and Shafiee-Nick 2019; Tanaka et al. 2020). Both CB_2 receptor-selective agonists and nonselective agonists have demonstrated the potential to suppress the LPS-mediated induction of pro-inflammatory markers in immortalized and primary microglia (Waksman et al. 1999; Ehrhart et al. 2005; Ma et al. 2015, 2018; Mecha et al. 2015; Askari and Shafiee-Nick 2019). We found that selective activation of CB_1 or CB_2 receptors suppressed NO release in a dose-dependent manner and attenuated the induction of mRNA of *Nos2*, *Tnf*, *Il1b*, and *Il6* as well as TNFα, IL-1β, and IL-6 proteins. However, activation of both receptors by CP 55,940 only affected NO release and mRNA for *Il1b*. This indicated that treatment of microglia with different classes of cannabinoids could produce unique anti-inflammatory responses. As these effects were abrogated by blockade of either CB_1 receptors by AM251 or CB_2 receptors by AM630, it is likely that both cannabinoid receptors contributed to these anti-inflammatory effects. In agreement with these findings, the selective agonists ACEA and JWH-133 also inhibited NO release from N9 microglia treated with LPS and IFNγ (Navarro et al. 2018a).

The effects of cannabinoids on cultured SIM-A9 microglia were biologically relevant in the cell culture model of inflammation-induced neurotoxicity. We found that treatment with either cannabinoid receptor-selective or nonselective agonists reduced the subsequent proportion of cell death when the conditioned media was applied to cultured neurons. The effects of ACEA were blocked by pre-treatment with AM251 or AM630 whereas the effects of HU-308 and CP 55,940 were blocked by AM251 or SR144528. This may be indicative that the antagonists exhibited cross-antagonism which has previously been reported in activated microglia as well as transfected cells (Callén et al. 2012; Navarro et al. 2018a; Young et al. 2022). Microglia possess several additional cannabinoid-sensitive receptors including GPR18 and GPR55 (Walter et al. 2003; McHugh et al. 2010; Stella 2010). It is possible that the high concentrations of ACEA

(1.2 μM), HU-308 (2.5 μM), or CP 55,940 (1.8 μM) also engaged these other receptors, in either an orthosteric or allosteric manner, which contributed to the anti-inflammatory effects in a manner that was not completely abrogated by CB_1 or CB_2 receptor-selective antagonists. Alternatively, CB_1 and CB_2 receptor antagonists alone have previously demonstrated anti-inflammatory properties in microglia which could potentially explain how the effects of HU-308 or CP 55,940 were not blocked by AM630 (Ribeiro et al. 2013). Interestingly, the CB_2 receptor inverse agonist, SR144528, effectively inhibited the protective effects of HU-308 and CP 55,940 where AM630 did not. AM630 has been demonstrated to act as a partial agonist of CB_1 receptors in addition to an inverse agonist at CB_2 receptors whereas SR144528 has been shown to interact only with CB_2 receptors at concentrations up to 10 μM (Rinaldi-Carmona et al. 1998; Ross et al. 1999). Thus, SR144528 may be a superior antagonist in experimental systems that involve both receptors, such as microglia.

In this experimental system, there was no evidence that neuronal cannabinoid receptors contributed to the changes in neuronal viability upon treatment with conditioned media. Direct treatment of the neurons with cannabinoid receptor ligands alone did not influence the viability of the ST*Hdh*$^{Q7/Q7}$ neurons. Janefjord et al. (2014) also found no changes in cell viability upon direct treatment of cultured SH-SY5Y neuronal cells with ACEA or the CB_2 receptor-selective agonist, JWH-015 (Janefjord et al. 2014). However, it cannot be ruled out that a neuronal cannabinoid receptor mechanism could contribute to neuroprotection under pro-inflammatory conditions via cannabinoids that remain in the conditioned media. As ST*Hdh*$^{Q7/Q7}$ neurons contain CB_1 receptors, it is possible that ACEA or CP 55,940 in the conditioned media could interact with the neurons. We found that ST*Hdh*$^{Q7/Q7}$ may also contain CB_2 receptors. Furthermore, there is evidence that neurons may express CB_2 receptors *in vivo* (Chen et al. 2017; Ma et al. 2019). These neuronal CB_2 receptors have also been reported to become upregulated *in vivo* following pathology or drug treatment (Wotherspoon et al. 2005; Jordan and Xi 2019; Grenier et al. 2021). Thus, the contributory role of neuronal cannabinoid receptors in addition to glial cannabinoid receptors should be considered in future work.

We found that cannabinoid treatments differentially influenced intracellular MAPK signaling when co-administered with the pro-inflammatory stimuli. MAPK signaling pathways including ERK1/2, JNK, and p38 have previously been associated with the pro-inflammatory activities of microglia (Kim et al. 2004; Waetzig et al. 2005; Eljaschewitsch et al. 2006; Bachstetter et al. 2011; Li et al. 2019b; Chen et al. 2021). Treatment with AEA dampened the release of pro-inflammatory cytokines IL-12 and IL-23 in a mouse model of multiple sclerosis via the JNK and ERK1/2 pathways (Correa et al. 2011). In this case, AEA treatment induced the phosphorylation of ERK1/2 and JNK which suppressed the release of IL-12 and IL-23 from microglia via CB_2 receptors. However, AEA has also been demonstrated to mediate ERK dephosphorylation which countered the effects of LPS upon co-treatment in immortalized BV-2 mouse microglia (Eljaschewitsch et al. 2006). Other studies have indicated that CB_2 receptor activation interacts with signaling patterns initiated by LPS and IFNγ such as ERK1/2 and p38 in immortalized and primary microglia (Ribeiro et al. 2013; Ma et al. 2015; Reusch et al. 2022). Based on the data from our work in SIM-A9 microglia, it appears that treatment with LPS + IFNγ initiated the phosphorylation of a variety of different signaling pathways including MAPK, PI3K-Akt, NF-κB, and JAK/STAT pathways. Furthermore, co-treatment with selective and non-selective cannabinoid agonists indicated that activation of CB_1 and/or CB_2 receptors differentially interfered with the phosphorylation of the ERK1/2, JNK, p38, and Akt pathways. Although other work has identified a link between cannabinoid receptor activation and the attenuation of NF-κB and JAK/STAT phosphorylation, we did not make the same observations under the specific reported experimental conditions (Ehrhart et al. 2005; Ribeiro et al. 2013). Ultimately, it appears that the effects of cannabinoids are mediated by mechanisms that directly oppose those driven by the pro-inflammatory stimuli that initiate the transition to a pro-inflammatory phenotype. Further research will provide insight into the specific pathways that are linked to the induction of different aspects of pro-inflammatory microglial phenotypes.

We observed a previously identified phenomenon whereby co-activation of CB_1 and CB_2 receptors using a nonselective agonist produced unique effects compared to activation of CB_1 or CB_2 receptors via selective agonists. This phenomenon has been

previously explained by the formation of physically interacting receptor complexes known as heteromers (Callén et al. 2012; Navarro et al. 2018a, 2018b). This has been shown to occur in cell types that express both receptors such as microglia which primarily mediate the anti-inflammatory effects of cannabinoids in the central nervous system (Staiano et al. 2016; Navarro et al. 2018a). Microglia treated with LPS and IFNγ were shown to have an enhanced proportion of CB_1-CB_2 interactions and respond differently to combinations of cannabinoid ligands relative to untreated cells (Navarro et al. 2018a). For example, co-activation of CB_1 and CB_2 receptors with agonists for both receptors resulted in reduced ERK1/2 phosphorylation in microglia and transfected neurons compared to agonism of either receptor individually (Callén et al. 2012; Navarro et al. 2018a). Antagonists for either CB_1 or CB_2 receptors can also diminish signaling from both types of receptors (Callén et al. 2012; Navarro et al. 2018a). Similar patterns of cross-talk have been observed between CB_1 receptors and dopamine D_2 receptors as such interactions caused differential G protein coupling ($G\alpha_{i/o}$ to $G\alpha_s$) which mediated cellular events not observed from activation of CB_1 or D_2 receptors alone (Bagher et al. 2016, 2017, 2020).

Although activation of either CB_1 and/or CB_2 receptors reduced the pro-inflammatory activity of SIM-A9 microglia, these receptors do not necessarily represent equally clinically relevant targets. The prolonged global activation of CB_1 receptors can induce negative side effects such as psychoactivity and fibrosis (Ashton and Glass 2007; Marquart et al. 2010; Volkow et al. 2014; Cinar et al. 2017). Without proper management, these effects would preclude the use of selective CB_1 receptor agonists to treat neuroinflammation in a clinical context. Conversely, drugs that selectively target CB_2 receptors have shown promise with respect to neuroinflammation, without negative side effects associated with nonselective cannabinoids or nonsteroidal anti-inflammatory drugs (Ashton and Glass 2007; Vonkeman and van de Laar 2010). Due to these effects, selective CB_2 receptor agonists have gained traction as potential treatments for both systemic inflammation and neuroinflammation (Komorowska-Müller and Schmöle 2020). Importantly, some aspects of neuroinflammation can also be beneficial and support neuronal survival as well as tissue repair (DiSabato et al. 2016). Thus, it will be

important to consider potential immunosuppression as an adverse effect in future strategies to develop CB_2 receptor-targeted drugs.

There are known differences in microglial behavior among *in vitro* and *in vivo* models. There is a growing body of work that involves the stimulation of microglia to a pro-inflammatory phenotype *in vitro* using LPS and/or IFNγ, or other stimuli such as amyloid-$\beta_{1\text{-}42}$ (Maresz et al. 2005; Ehrhart et al. 2005; Eljaschewitsch et al. 2006; Navarro et al. 2018a). However, populations of microglia do not exhibit strict adherence to such a phenotype *in vivo* which is an inherent limitation of cell culture models (Ransohoff 2016a; Dubbelaar et al. 2018). Transcriptomic studies have revealed that microglia in the mammalian brain appear to exhibit more complex phenotypes that contain aspects of both the pro-inflammatory phenotype and an anti-inflammatory phenotype as well as other transcriptomic profiles that are indicative of additional functions (Hammond et al. 2019; Masuda et al. 2019). Thus, the mechanisms observed in immortalized microglia *in vitro* may only apply to specific subsets of microglia *in vivo* that exhibit similar pro-inflammatory properties under specific conditions. Given these known discrepancies, there is a growing body of evidence that CB_2 receptor-targeted therapies improve markers of inflammation in microglia and neuronal survival in several animal models of neurodegenerative disease (reviewed in Tanaka et al., 2020). Thus, the mechanisms that underlie the beneficial effects of CB_2 receptor activation *in vitro* systems may translate to more complex models of disease.

In conclusion, we have demonstrated that the pro-inflammatory behavior of cultured microglia can be attenuated through the activation of CB_1 or CB_2 receptors using synthetic selective agonists. Co-activation of CB_1 and CB_2 receptors using a nonselective agonist did not produce additive effects but had reduced efficacy compared to the selective agonists. Ultimately, all three types of cannabinoid treatment applied to microglia reduced the subsequent neurotoxicity of the glial conditioned media. Given the psychoactivity associated with global CB_1 receptor activation, this work highlights the potential of selective CB_2 receptor agonists to regulate pro-inflammatory microglial activity in diseases with a neuroinflammatory component.

2.5 Supplementary data

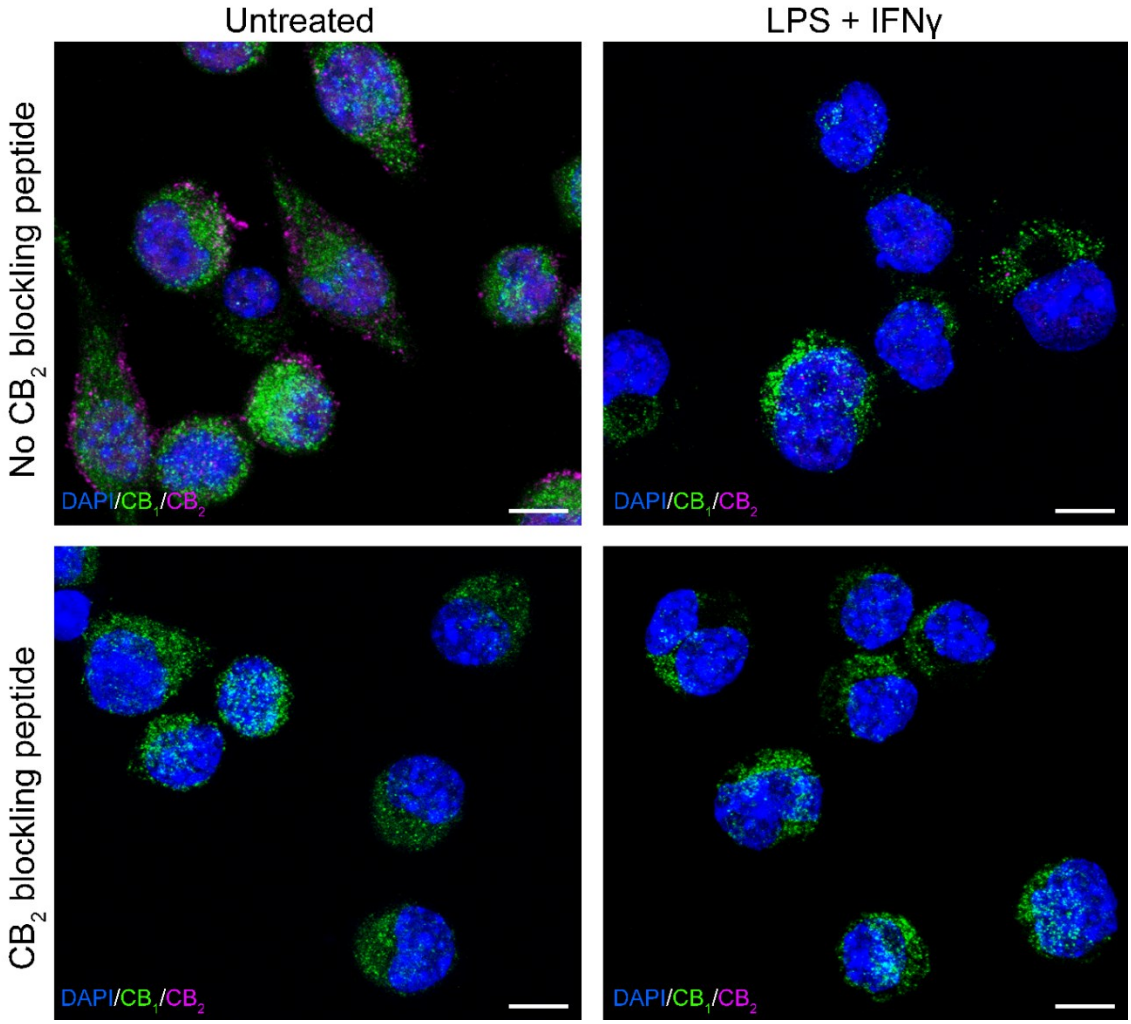

Figure 2. S1. CB_2-like immunoreactivity in SIM-A9 microglia was abolished by pretreatment with an anti-CB_2 receptor blocking peptide. CB_1 receptor (green) and CB_2 receptor (magenta)-like immunoreactivity in SIM-A9 microglia treated with vehicle or LPS and IFNγ in the presence or absence of a blocking peptide to disrupt the binding of the anti-CB_2 receptor antibody. Scale bar; 10 μm for all panels.

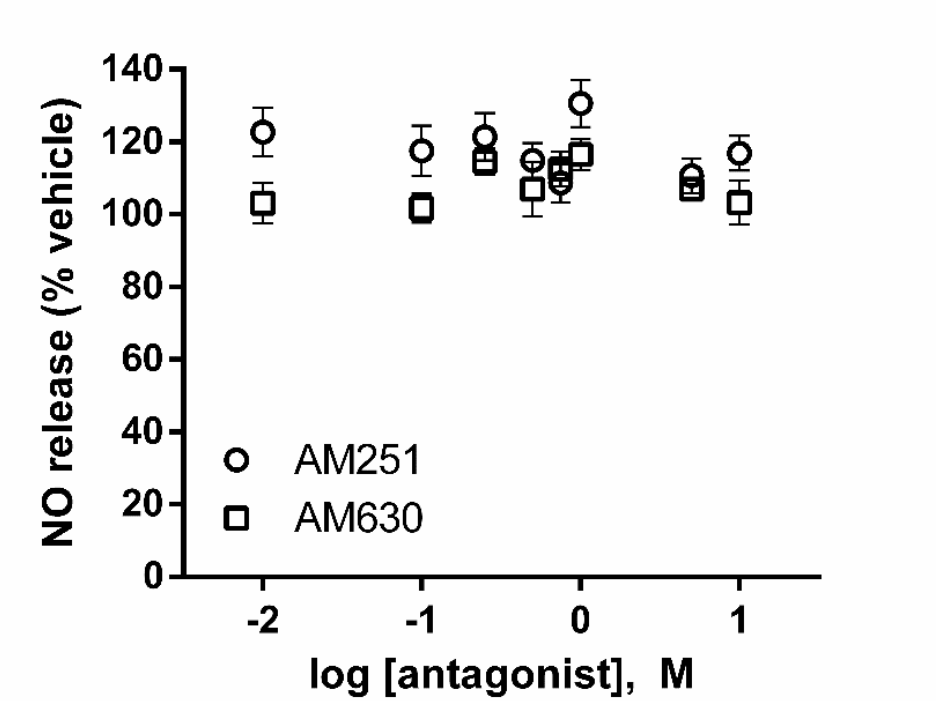

Figure 2. S2. Inverse agonists of CB_1 and CB_2 receptors did not influence NO release in a dose-dependent manner. SIM-A9 microglia were treated with LPS + IFNγ and either vehicle, AM251, or AM630. NO release was measured via the Griess assay and normalized to total protein. NO release was plotted normalized to the vehicle (constrained to 100%).

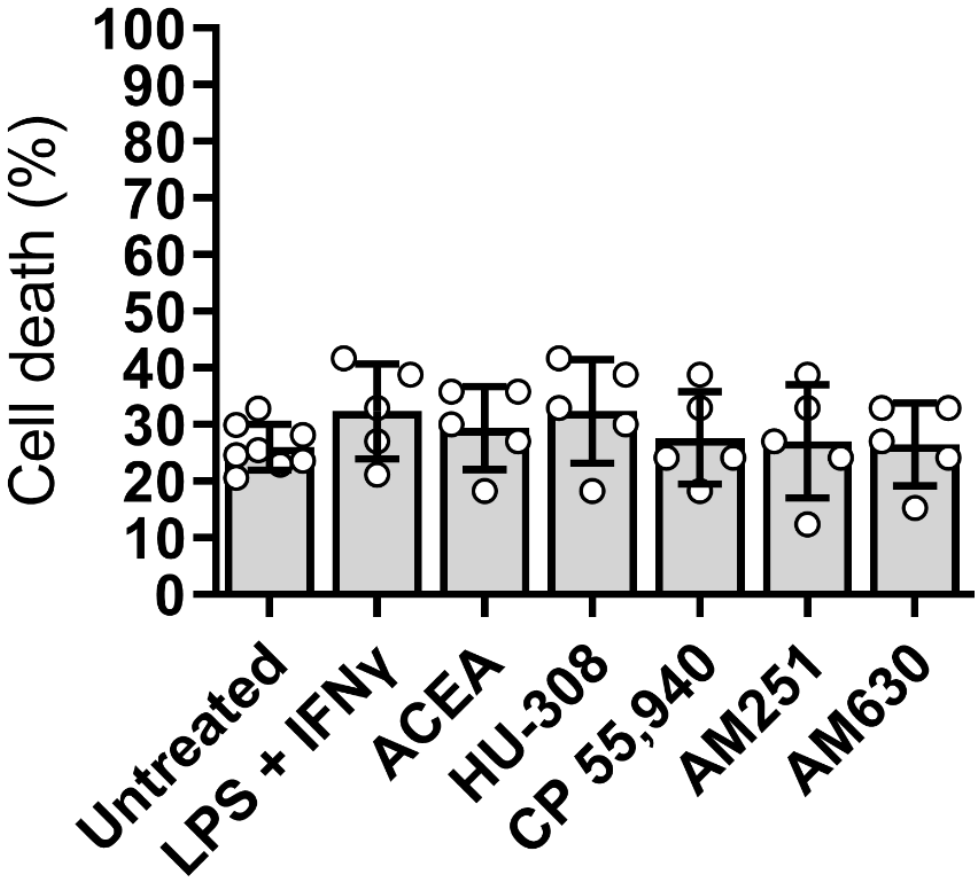

Figure 2. S3. LPS + IFNγ or cannabinoid treatments alone did not influence ST*Hdh*$^{Q7/Q7}$ viability. ST*Hdh*$^{Q7/Q7}$ neurons were treated with LPS + IFNγ, ACEA, HU-308, CP 55,940, AM251, or AM630 (n = 5-8). Neuronal viability was measured following 24 h of treatment.

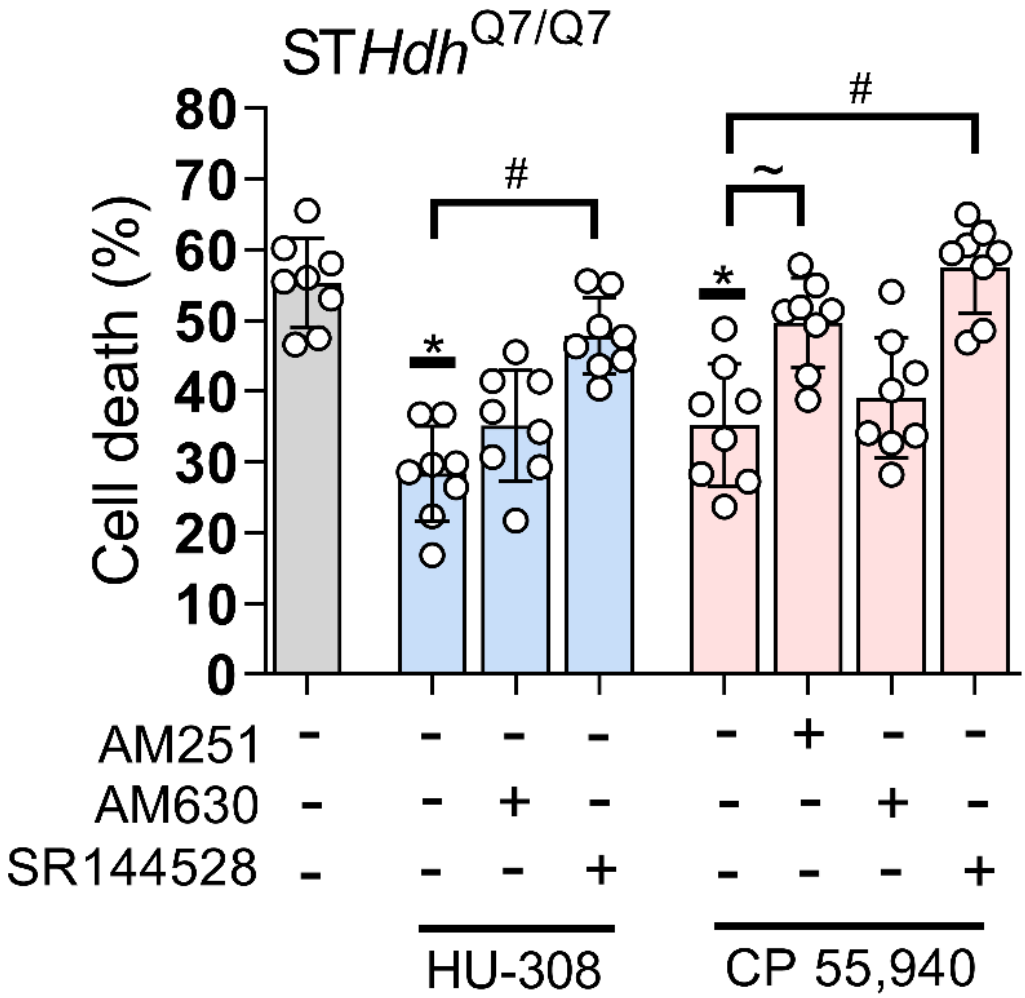

Figure 2. S4. The selective CB_2 receptor inverse agonist SR144528 effectively abrogated the neuroprotective effects of HU-308 and CP 55,940. SIM-A9 microglia were treated with LPS + IFNγ with vehicle, HU-308 (2.5 μM), or CP 55,940 (1.8 μM) in conjunction with AM251 (2 μM), AM630 (1 μM), or SR144528 (2 μM). The conditioned media was subsequently applied directly to cultured $STHdh^{Q7/Q7}$ neurons (n = 8) and cell viability was measured after 24 h. * $p < 0.01$ vs. LPS + IFNγ; ~ $p < 0.05$ vs. LPS + IFNγ + agonist + AM251; # $p < 0.05$ vs. LPS + IFNγ + agonist + SR144528.

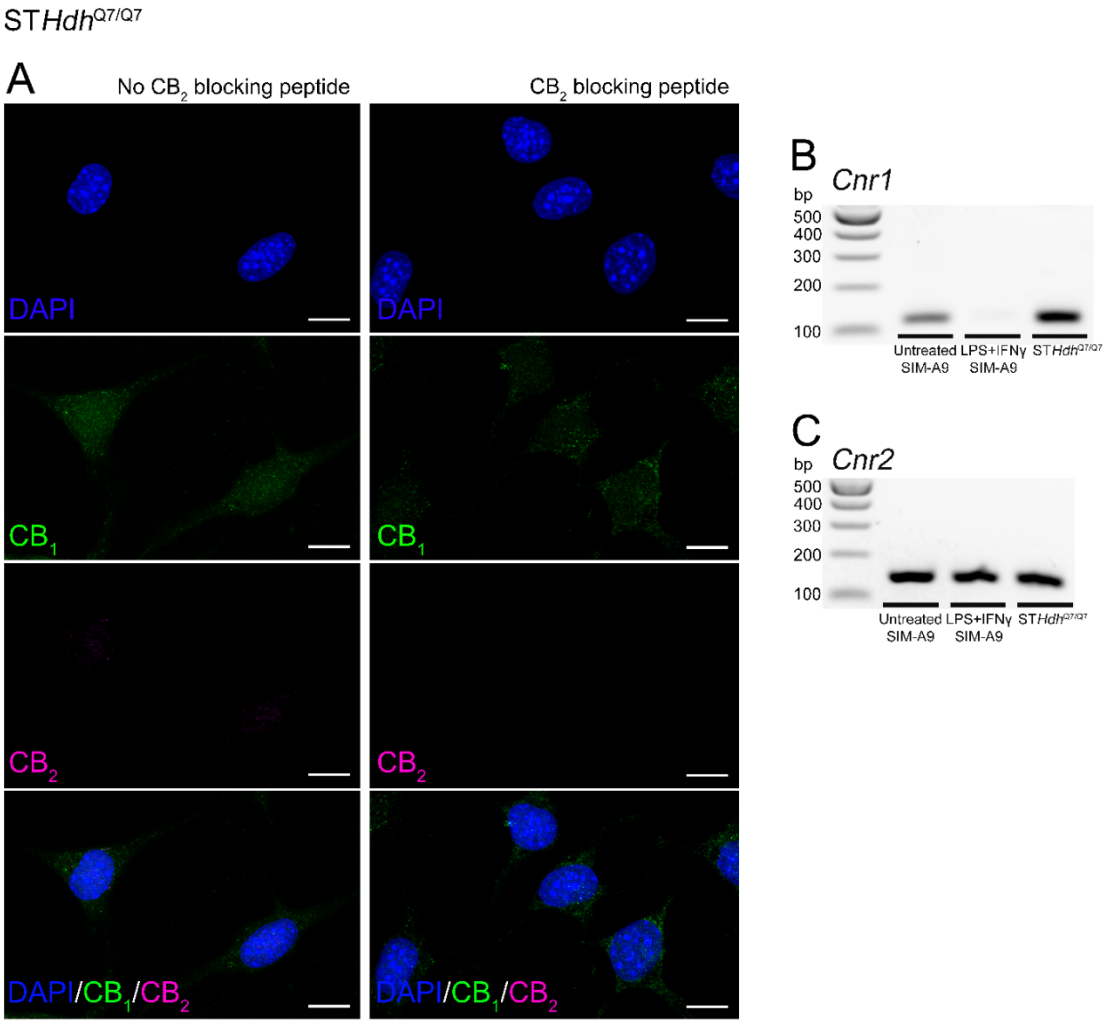

Figure 2. S5. ST*Hdh*$^{Q7/Q7}$ neurons may contain both CB_1 and CB_2 receptors. A ST*Hdh*$^{Q7/Q7}$ neurons were assessed for the presence of CB_1 and CB_2-like immunoreactivity in the presence or absence of a blocking peptide for the anti-CB_2 receptor antibody. Scale bar; 10 µm in all panels. **B-C** Using semi-quantitative RT-PCR with agarose gel electrophoresis, the presence of **B** *Cnr1* and **C** *Cnr2* was assessed in ST*Hdh*$^{Q7/Q7}$ neurons relative to SIM-A9 that were treated with LPS and IFNγ or not. The fragments were amplified with the primers used for qPCR (Table S1). The sizes of the amplicons are indicated in base pairs (bp).

Chapter 3: The microglial endocannabinoid system is dynamically regulated by lipopolysaccharide and interferon gamma

Copyright statement

Contribution statement

All experiments were performed, and data were collected by myself. Analysis and interpretation of the data were performed in consultation Dr. Eileen Denovan-Wright. Preparation of the manuscript was done by me with support from Dr. Eileen Denovan-Wright.

Preface

This chapter expands on the observation that the microglial endocannabinoid system became dysregulated upon treatment with LPS and IFNγ. There had been many conflicting reports of whether inflammatory conditions cause components of the endocannabinoid system to become up- or down-regulated. I aimed to address this question using LPS and IFNγ separately at multiple different concentrations to determine if past discrepancies could be due to stimulus- or concentration-dependent differences.

3.1 Abstract

Perturbation of the endocannabinoid system can have profound effects on immune function and synaptic plasticity. Microglia are one of few cell types with a self-contained endocannabinoid system and are positioned at the interface between the immune system and the central nervous system. Past work has produced conflicting results with respect to the effects of pro-inflammatory conditions on the microglial endocannabinoid system. Thus, we systematically investigated the relationship between the concentration of two distinct pro-inflammatory stimuli, lipopolysaccharide and interferon gamma, on the abundance of components of the endocannabinoid system within microglia. Here we show that lipopolysaccharide and interferon gamma influence messenger RNA abundances of the microglial endocannabinoid system in a concentration-dependent manner. Furthermore, we demonstrate that the efficacy of different synthetic cannabinoid treatments with respect to inhibition of microglia nitric oxide release is dependent on the concentration and type of pro-inflammatory stimuli presented to the microglia. This indicates that different pro-inflammatory stimuli influence the capacity of microglia to synthesize, degrade, and respond to cannabinoids which has implications for the development of cannabinoid-based treatments for neuroinflammation.

3.2 Introduction

The endocannabinoid system (ECS) plays roles in mood, memory, appetite, pain, immune function, and thermoregulation (Wenger and Moldrich 2002; Marsicano and Lafenêtre 2009; Pandey et al. 2009; Woodhams et al. 2015). The ECS comprises endogenously produced cannabinoids, the receptors for these molecules, and the enzymes required to biosynthesize and degrade them. The primary endocannabinoids are anandamide (AEA) and 2-arachidonylglycerol (2-AG) which bind to the cannabinoid type 1 (CB_1) and type 2 (CB_2) receptors to regulate synaptic activity or neuroinflammation and partially mimic the effects of the psychoactive constituents of cannabis (Lu and Mackie 2016; Young and Denovan-Wright 2022a). AEA is synthesized by N-acyl phosphatidylethanolamine-specific phospholipase D (NAPE-PLD) and metabolized by fatty acid amide hydrolase (FAAH) whereas 2-AG is synthesized by diacylglycerol lipase (DAGL) and metabolized by monoacylglycerol lipase (MAGL)(Lu and Mackie 2021). Components of the ECS are primarily located in brain cells including GABAergic interneurons and microglia, but are also distributed throughout the periphery in the immune system and the gut (Stella 2010; Lu and Mackie 2021). The ECS is dynamic, and the abundance of its components fluctuate under pathological conditions including inflammation and neurodegeneration (Young and Denovan-Wright 2022a). Perturbation of the ECS at a global scale may subsequently inhibit immune function and synaptic plasticity, or increase the risk to develop psychiatric disorders (Heifets and Castillo 2009; Leweke 2012; Lu and Mackie 2016, 2021; Young and Denovan-Wright 2022a). Thus, it is important to understand how endocannabinoids and the associated receptors and metabolic machinery are regulated under pathological conditions.

Microglia, the resident immune cells of the brain, possess a self-contained ECS including receptors for cannabinoid-like molecules and the capacity to biosynthesize and metabolize AEA and 2-AG (Stella 2009, 2010). In the brain, endocannabinoids released by post-synaptic neurons interact with pre-synaptic neuronal cannabinoid receptors to inhibit the release of transmitters, primarily glutamate or GABA, through modulation of calcium mobilization, cyclic AMP signaling, and inwardly rectifying potassium currents (Howlett 2002). Endocannabinoids also interact with microglial cannabinoid receptors to

suppress neuroinflammation (Correa et al. 2010, 2011; Malek et al. 2015; Mecha et al. 2015). Infusion with AEA or 2-AG has been neuroprotective in animal models of multiple sclerosis (Lourbopoulos et al. 2011; Hernangómez et al. 2012). However, 2-AG is also an intermediate metabolite in prostaglandin synthesis and excess quantities of 2-AG could promote neuroinflammation and subsequent neurodegeneration via prostaglandin-mediated microglial activity (Nomura et al. 2011; Klawonn et al. 2021). Thus, control of the microglial ECS is critical to the regulation of neuroinflammation.

Microglia exhibit extraordinary phenotypic plasticity and pro-inflammatory stimuli such as IFNγ and LPS have been demonstrated to induce the release of pro-inflammatory cytokines, stimulate migration, and regulate phagocytosis (Kettenmann et al. 2011). Upon exposure to pro-inflammatory stimuli, there are conflicting reports with respect to perturbation to the ECS (Young and Denovan-Wright 2022a). Studies using various single concentrations of IFNγ and LPS alone or in combination have reported both upregulation and downregulation of cannabinoid receptors and the associated regulatory enzymes (Carlisle et al. 2002; Maresz et al. 2005; Mecha et al. 2015). These conflicting reports have made it difficult to discern the true effects of inflammatory conditions on the regulation of the ECS in microglia.

Given the importance of microglia and the ECS in the maintenance of proper brain function and the control of neuroinflammation, we aimed to delineate the effects of pro-inflammatory stimuli on the regulation of the microglial ECS. We used two distinct pro-inflammatory stimuli, IFNγ and LPS, in a broad range of concentrations to entirely assess the dose-dependent fluctuation in the components of the microglial ECS. We also aimed to determine whether these molecules would behave in an additive or synergistic manner when combined. Lastly, we used a panel of selective and nonselective synthetic cannabinoids to measure the responsiveness of microglia to cannabinoid ligands across a range of pro-inflammatory conditions.

3.3 Results

3.3.1. IFNγ and LPS induce NO release from microglia in a concentration dependent manner

To compare the effects of IFNγ and LPS on NO release in SIM-A9 microglia, a concentration-response curve was prepared for each pro-inflammatory stimulus. Both molecules induced the release of NO from microglia in a concentration-dependent manner. IFNγ induced the release of NO up to a maximum of 13.41 ± 0.17 nmol per 100 µg protein with an EC_{50} of 1.80 ± 0.12 ng/mL (Fig. 3. 1A). LPS stimulated NO release to a maximum of 17.77 ± 0.49 nmol per 100 µg protein with an EC_{50} of 56.89 ± 9.86 ng/mL (Fig. 3. 1B). In subsequent experiments, concentrations of 1, 5, and 20 ng/mL were used for IFNγ and concentrations of 10, 100, and 1000 ng/mL were used for LPS. These values represent the concentrations required to elicit a low, moderate, and maximal pro-inflammatory response as denoted by the release of NO.

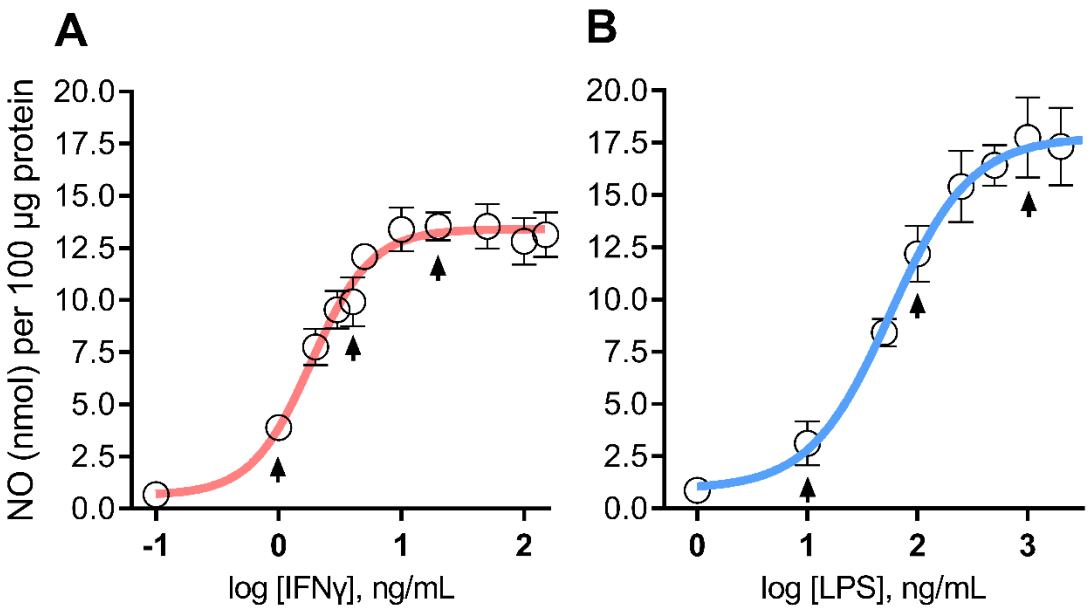

Figure 3. 1. IFNγ and LPS stimulate NO release from cultured microglia in a concentration-dependent manner. A-B SIM-A9 microglia were stimulated with **A** IFNγ (0.1 – 150.0 ng/mL) or **B** LPS (1 – 4000 ng/mL) for 16 h and NO release was measured from the cell supernatant. Arrowheads indicate the concentrations that were selected for subsequent experiments (1, 5, 20 ng/mL for IFNγ; 10, 100, 1000 ng/mL for LPS). Data are presented as the mean ± standard deviation of the mean for four independent experiments performed in technical duplicates.

3.3.2. Pro-inflammatory stimuli modulate microglial cannabinoid receptor abundance

To determine if IFNγ or LPS influence the abundance of mRNA or protein for the cannabinoid receptors, SIM-A9 microglia were treated with increasing concentrations of each stimulus. Treatment with either stimulus at any concentration resulted in a decrease in *Cnr1* mRNA (Fig. 3. 2A). The abundance of *Cnr2* mRNA was increased by 3.1-fold by the lowest concentration of IFNγ but was unaffected by the maximal concentration (Fig. 3. 2B). The lowest concentration of LPS increased *Cnr2* mRNA by 2.1-fold but the maximal concentration of LPS also had no effect. In contrast, treatment with the maximal concentration of IFNγ increased the abundance of CB_1 receptors to 213 ± 68% of baseline whereas LPS resulted in a CB_1 protein abundance of 135 ± 44% and was deemed to have no affect (Fig. 3. 2C). A similar pattern was observed for CB_2 receptor protein abundance where treatment with IFNγ elevated CB_2 protein to 150 ± 19% relative to baseline whereas LPS treatment resulted in 108 ± 5% (Fig. 3. 2D). These data indicate that treatment with IFNγ stimulated the upregulation of CB_1 and CB_2 receptors, but LPS did not.

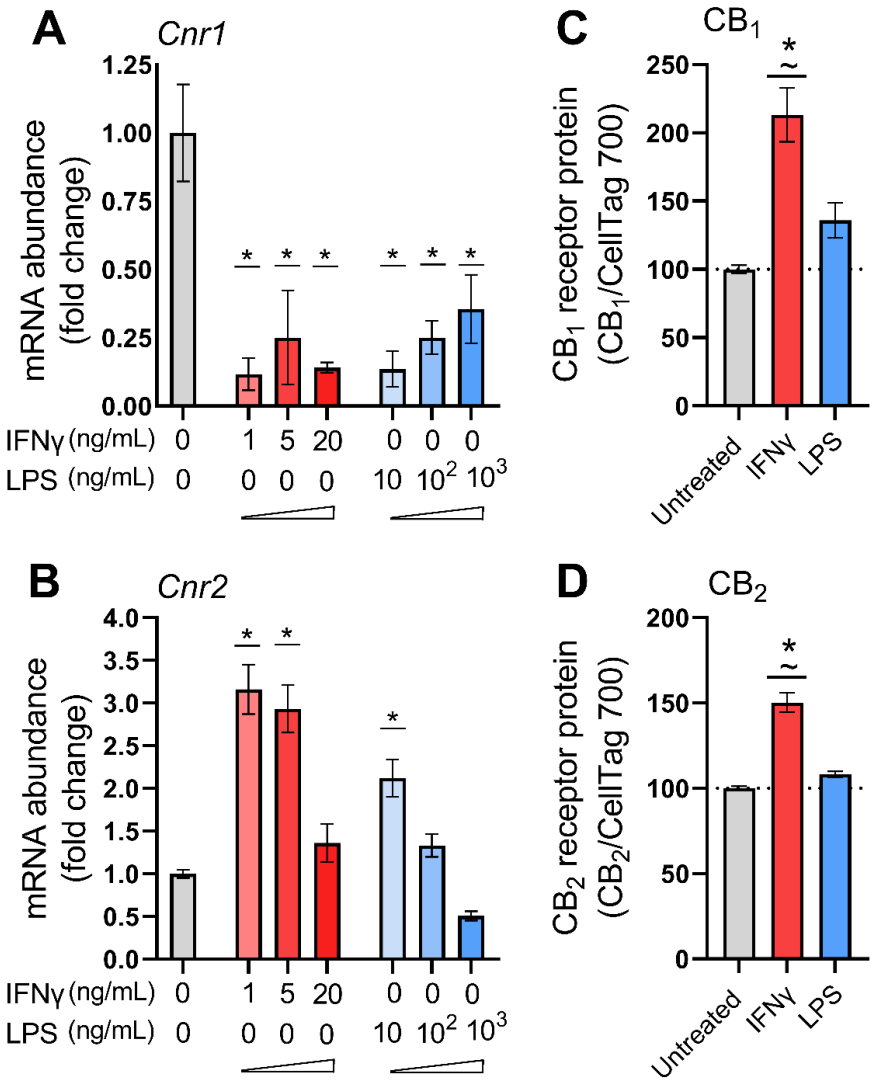

Figure 3. 2. IFNγ and LPS differentially influence mRNA and protein abundance of CB₁ and CB₂ receptors. A-B SIM-A9 microglia were treated with IFNγ or LPS for 16 h and mRNA abundance of **A** *Cnr1* or **B** *Cnr2* (n = 3) was quantified via RT-qPCR relative to cells that were treated with vehicle only. * $p < 0.01$ compared to untreated; significance was determined via one-way ANOVA with Holm-Sidak post-hoc test. **C-D** SIM-A9 microglia were treated with IFNγ (20 ng/mL) or LPS (1000 ng/mL). Protein abundance of **C** CB_1 receptors or **D** CB_2 (n = 12) receptors was quantified via in-cell western relative to cells that were treated with vehicle only, data are presented relative to untreated cells which are constrained to 100%. * $p < 0.01$ relative to untreated; ~ $p < 0.01$ relative to LPS. Significance was determined via Kruskal-Wallis test with Dunn's correction for multiple comparisons.

3.3.3. Pro-inflammatory stimuli modulate quantities of enzymes of the endocannabinoid system

We next aimed to assess whether pro-inflammatory stimuli may alter the capacity of microglia to synthesize or metabolize endocannabinoids. SIM-A9 cells were treated with increasing concentrations of IFNγ or LPS and the quantities of mRNA for *NAPEPLD*, *FAAH*, *DAGLA*, and *MGLL* were assessed. *NAPEPLD* mRNA was unaffected by IFNγ but was decreased upon treatment with the maximal concentration of LPS (Fig. 3. 3A). *FAAH* mRNA was increased only by the maximal concentration of IFNγ and the low concentration of LPS (Fig. 3. 3B). These data indicate that microglia in a pro-inflammatory phenotype could synthesize less AEA and degrade more AEA depending on the degree of stimulus. *DAGLA* mRNA was increased by the low concentration of LPS but was unaffected otherwise (Fig. 3. 3C). *MGLL* mRNA was suppressed by both IFNγ and LPS at all concentrations (Fig. 3. 3D). These data indicate that 2-AG synthesis may be unaffected under pro-inflammatory conditions, but 2-AG degradation may be enhanced.

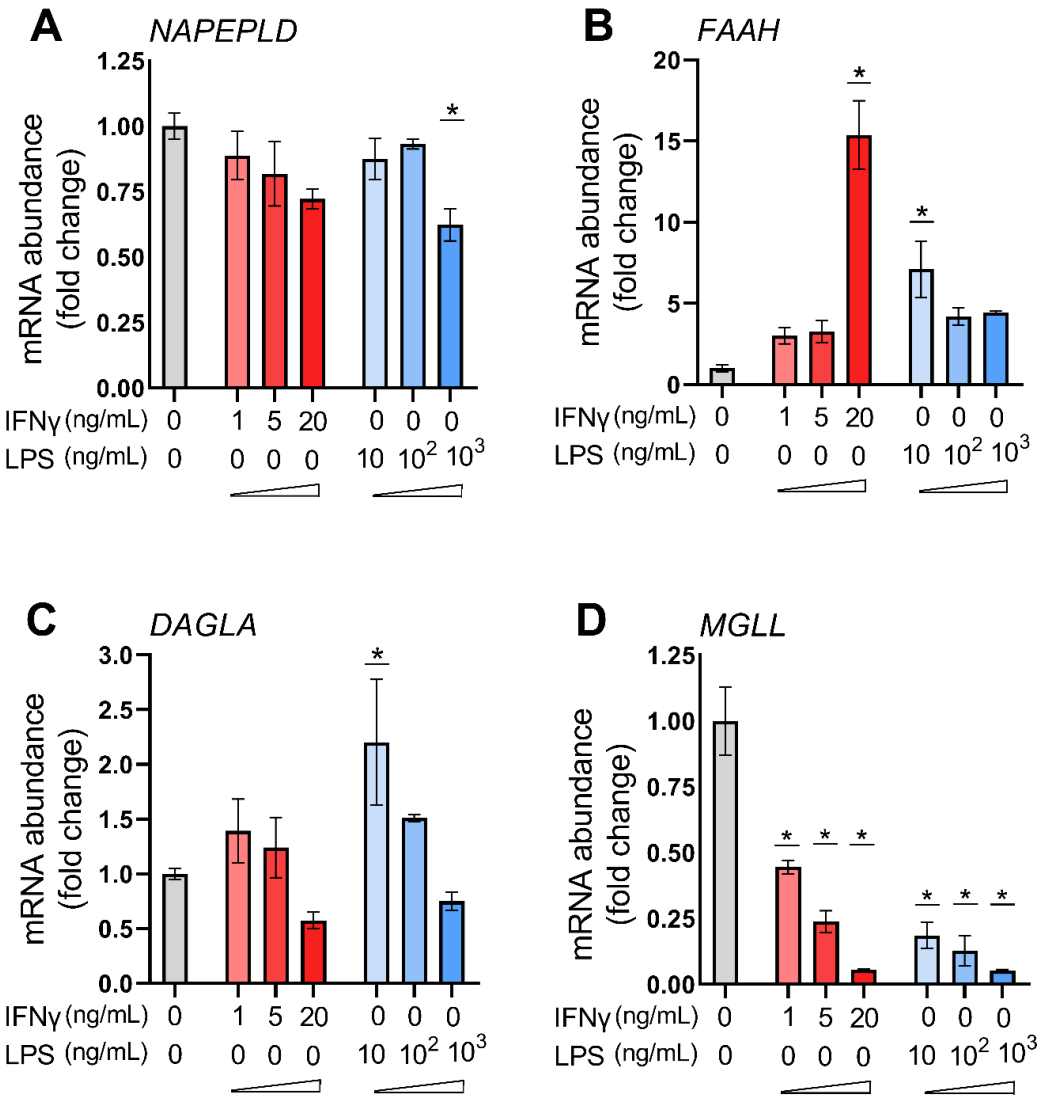

Figure 3. 3. IFNγ and LPS differentially influence mRNA abundance of enzymes of the endocannabinoid system. A-D SIM-A9 microglia were treated with increasing doses of IFNγ or LPS for 16 h and mRNA abundance of **A** *NAPEPLD*, **B** *FAAH*, **C** *DAGLA*, ***D*** *MGLL* (n = 3) was quantified via RT-qPCR relative to cells that were treated with vehicle only. * $p < 0.01$ compared to untreated; significance was determined via one-way ANOVA with Holm-Sidak post-hoc test.

3.3.4. Combinations of IFNγ and LPS differentially influence components of the endocannabinoid system

To determine whether IFNγ and LPS could exhibit synergistic effects on the mRNA abundance of components of the endocannabinoid system, SIM-A9 microglia were treated with combinations of dosages of each stimulus. Combinations were prepared using either a maximal concentration of IFNγ and a low concentration of LPS or vice-versa. The results are summarized in Table 2. 1. The combination treatments did not significantly affect *Cnr1* mRNA compared to the treatments with IFNγ or LPS alone. In contrast, the combination treatments appeared to block the upregulation of *Cnr2* mRNA observed upon treatment with low concentrations of either stimulus. This indicated that *Cnr2* mRNA was only elevated in the presence of low concentrations of either IFNγ or LPS. *NAPEPLD* mRNA was generally unchanged although treatment with the maximal concentration of IFNγ and a low concentration of LPS resulted in elevated *NAPEPLD* mRNA compared to treatment with IFNγ alone. Interestingly, co-treatment with the maximal concentration of IFNγ and the low concentration of LPS induced a 37-fold increase in *FAAH* mRNA compared to the 15-fold increase induced by the same concentration of IFNγ alone or the 7-fold increase induced by LPS alone. *DAGLA* mRNA was not significantly influenced by the combination treatments of IFNγ and LPS and *MGLL* mRNA was suppressed whether cells were treated with IFNγ or LPS alone or in combination.

Table 2. 1. Combinations of IFNγ and LPS differentially influence mRNA abundance of some components of the endocannabinoid system. Treatments were prepared using either a maximal concentration (E_{max}) of IFNγ and a low concentration (E_{min}) of LPS or vice-versa. SIM-A9 microglia were treated with IFNγ or LPS alone or in combination and mRNA abundance of mRNA for, *Cnr1*, *Cnr2*, *NAPEPLD*, *FAAH*, *DAGLA*, *MGLL* (n = 3) was quantified via RT-qPCR relative to cells that were treated with vehicle only. Values represent the fold-change in mRNA abundance relative to vehicle-treated cells. * $p < 0.01$ compared to vehicle; # $p < 0.05$ compared to IFNγ (20 ng/mL) and LPS (10 ng/mL); ~ $p < 0.05$ compared to IFNγ (1 ng/mL) and LPS (1000 ng/mL); significance was determined via one-way ANOVA with Holm-Sidak post-hoc test.

Gene	**Vehicle**	**IFNγ (E_{max})**	**LPS (E_{min})**	**IFNγ (E_{max}) + LPS (E_{min})**	**IFNγ (E_{min})**	**LPS (E_{max})**	**IFNγ (E_{min}) + LPS (E_{max})**
Cnr1	1 (0.31)	0.14 (0.03)*	0.14 (0.11)*	0.50 (0.13)	0.12 (0.1)*	0.36 (0.22)*	0.49 (0.35)*
Cnr2	1 (0.08)	1.40 (0.38)	2.10 (0.38)*	0.94 (0.1)	3.20 (0.5)*~	0.51 (0.09)*	0.61 (0.23)*
NAPEPLD	1 (0.08)	0.72 (0.07)#	0.88 (0.14)	1.20 (0.36)	0.89 (0.16)	0.62 (0.11)	0.66 (0.06)
FAAH	1 (0.37)	15.38 (3.66)* #	7.12 (3.01) #	37.37 (6.72)*	3.01 (0.87)	4.43 (0.17)	4.81 (0.91)
DAGLA	1 (0.09)	0.58 (0.13)	2.20 (0.99)	1.30 (0.51)	1.40 (0.5)	0.75 (0.14)	0.95 (0.15)
MAGL	1 (0.23)*	0.06 (0.01)*	0.19 (0.09)*	n.d.[a]	0.45 (0.04)*~	0.05 (0.01)*	0.06 (0.01)*

[a] Not detected.

3.3.5. Treatment with synthetic cannabinoids influenced microglial NO release upon exposure to IFNγ and LPS

Finally, we aimed to assess whether a panel of synthetic cannabinoid molecules would inhibit NO release from SIM-A9 microglia upon treatment with increasing concentrations of IFNγ and LPS. Concentration-response curves for IFNγ and LPS were prepared in the presence of ACEA, HU-308, or CP 55,940 at a concentration of 1 μM or a combination of ACEA and HU-308 each at a concentration of 0.5 μM. Shifts in the EC_{50} and E_{max} were modeled and analyzed to assess the impact of the cannabinoid treatments (Table 2. 2). When microglia were treated with increasing concentrations of LPS, each of the treatment groups exhibited a reduction in both the EC_{50} and the E_{max} (Fig. 3. 4A). However, when IFNγ was present, the cannabinoid treatments reduced the E_{max} of NO release but no longer influenced the EC_{50} (Fig. 3. 4B). This indicated that cannabinoid signaling may have potentiated NO release stimulated by a low concentration of LPS but suppressed NO release in the presence of a high concentration of LPS. When microglia were treated with increasing concentrations of IFNγ, co-treatment with ACEA or HU-308 reduced the E_{max} whereas treatment with CP 55,940 or ACEA and HU-308 increased the E_{max} (Fig. 3. 4C). This indicated that individual stimulation of CB_1 or CB_2 receptors inhibited NO release whereas co-activation of both receptors potentiated NO release in the presence of high concentrations of IFNγ. However, the E_{max} of NO release was reduced by all cannabinoid treatments upon co-treatment with LPS and increasing concentrations of IFNγ (Fig. 3. 4D). Taken together, the results indicated that the cannabinoid treatments suppressed microglial NO release in the presence of high concentrations of pro-inflammatory stimuli but were less efficacious in the presence of moderate concentrations of LPS.

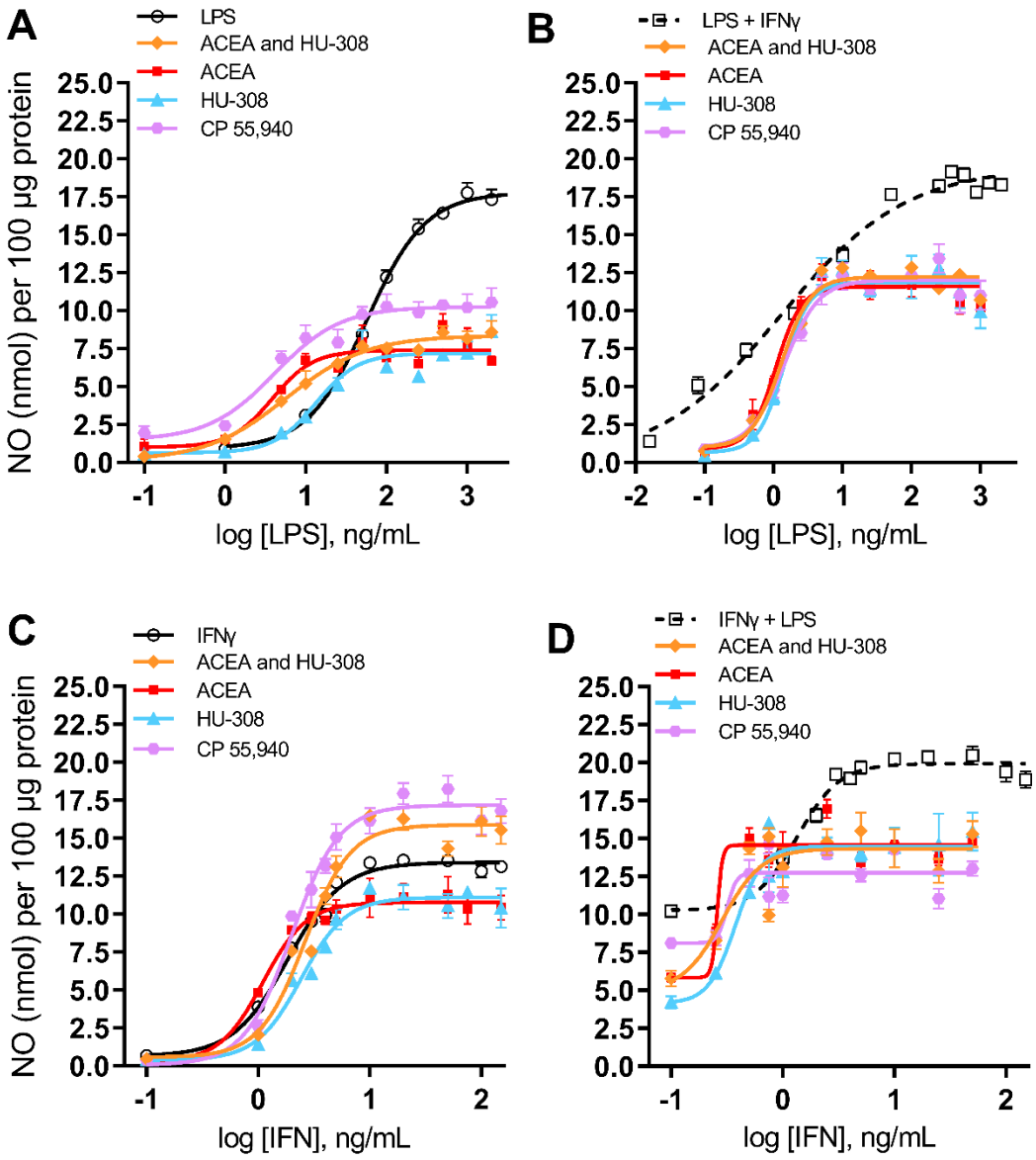

Figure 3. 4. Cannabinoid treatments differentially influenced NO release from microglia. SIM-A9 microglia were treated concurrently with LPS and/or IFNγ in the presence of different cannabinoid treatments for 16 h (n = 4). The cannabinoid treatments included ACEA and HU-308 (0.5 µM each), ACEA (1 µM), HU-308 (1 µM), or CP 55,940 (1 µM). NO release was monitored following treatment of microglia with **A** increasing concentrations of LPS, **B** increasing concentrations of LPS in the presence of IFNγ (1 ng/mL), **C** increasing concentrations of IFNγ, **D** increasing concentrations of IFNγ in the presence of LPS (10 ng/mL).

Table 2. 2. Cannabinoid treatments differentially influenced the E_{max} and EC_{50} of LPS and IFNγ with respect to NO release from microglia. SIM-A9 microglia were treated with LPS and/or IFNγ in the presence of different cannabinoid treatments. The cannabinoid treatments included ACEA and HU-308 (0.5 μM each), ACEA (1 μM), HU-308 (1 μM), or CP 55,940 (1 μM).

Stimulus[a]	Concurrent treatment[b]	E_{max} (95% CI)[c]	EC_{50} (95% CI)[c]
LPS	Vehicle	17.77 (17.11 to 18.44)	56.89 (47.03 to 68.82)
	ACEA + HU-308	8.35 (7.81 to 8.90)*	5.74 (3.51 to 9.39)*
	ACEA	7.39 (6.80 to 7.98)*	3.85 (1.95 to 7.61)*
	HU-308	7.19 (6.55 to 7.82)*	13.36 (8.52 to 20.96)*
	CP 55,940	10.26 (9.57 to 10.95)*	4.12 (2.18 to 7.80)*
LPS	IFNγ + Vehicle	19.46 (18.48 to 20.45)	1.29 (0.68 to 2.47)
	IFNγ + ACEA + HU-308	12.21 (11.41 to 13.01)*	1.31 (0.90 to 1.90)
	IFNγ + ACEA	11.58 (11.00 to 12.17)*	1.08 (0.83 to 1.39)
	IFNγ + HU-308	11.86 (11.15 to 12.58)*	1.39 (1.02 to 1.89)
	IFNγ + CP 55,940	12.02 (11.35 to 12.68)*	1.43 (1.02 to 2.02)
IFNγ	Vehicle	13.41 (13.07 to 13.75)	1.84 (1.65 to 2.06)
	ACEA + HU-308	15.88 (15.14 to 16.63)*	2.64 (2.25 to 3.09)*
	ACEA	10.78 (10.15 to 11.41)*	1.10 (0.85 to 1.43)*
	HU-308	11.11 (10.47 to 11.74)*	2.42 (1.98 to 2.96)
	CP 55,940	17.18 (16.41 to 17.95)*	1.99 (1.68 to 2.37)
IFNγ	LPS + Vehicle	19.93 (19.52 to 20.35)	1.34 (1.13 to 1.60)
	LPS + ACEA + HU-308	14.33 (13.32 to 15.33)*	0.29 (0.16 to 0.52)*
	LPS + ACEA	14.56 (14.07 to 15.06)*	~0.2584 (N.D.)
	LPS + HU-308	14.49 (13.61 to 15.36)*	0.38 (0.28 to 0.51)*
	LPS + CP 55,940	12.74 (12.13 to 13.34)*	0.32 (0.07 to 1.54)

[a] Applied as a concentration-response curve.
[b] Applied as a fixed concentration.
[c] Determined by nonlinear regression with four-parameter analysis.
* Significantly different from vehicle as indicated by non-overlapping 95% CI.

3.4 Discussion

Endocannabinoids and their receptors on microglia have previously been implicated in neuroinflammation, but conflicting reports have made it unclear whether inflammation may stimulate or suppress the ECS. We used two unique pro-inflammatory stimuli, IFNγ and LPS, at low, medium, and high concentrations to examine the effects on the microglial ECS. We observed that IFNγ and LPS exhibited differential effects relative to one another at different concentrations (Fig. 3. 5). Furthermore, in some cases, the combination of both pro-inflammatory stimuli produced results that were not observed upon treatment with either IFNγ or LPS alone.

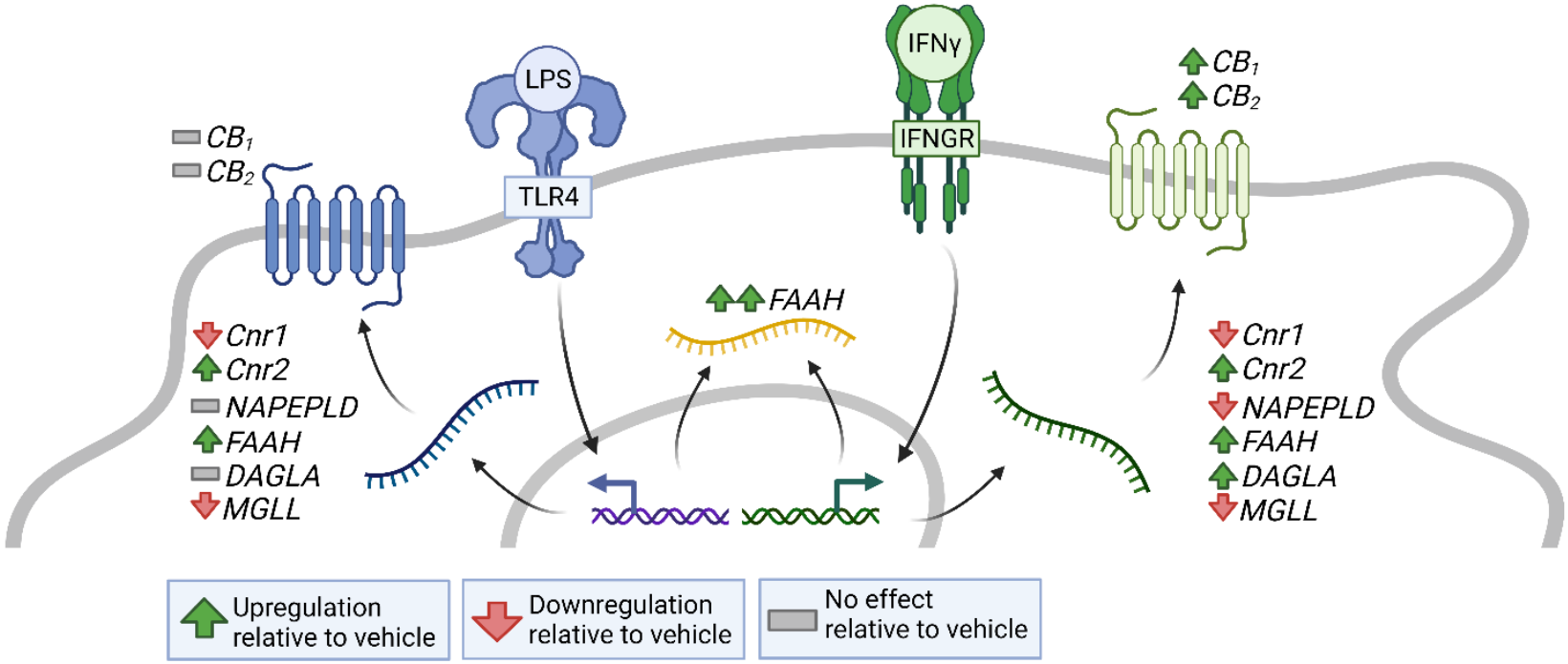

Figure 3. 5. Schematic summary of the effects of LPS and IFNγ on the abundance of mRNA and protein for components of the endocannabinoid system. The effects of LPS or IFNγ are indicated for the mRNA abundance of *Cnr1*, *Cnr2*, *NAPEPLD*, *FAAH*, *DAGLA*, and *MAGL*, as well as the protein abundance of CB_1 and CB_2 receptors. Figure created with BioRender.

The pro-inflammatory stimuli influenced the mRNA and protein abundance of the cannabinoid receptors. The *Cnr1* mRNA was suppressed by either IFNγ or LPS regardless of concentration. In contrast, *Cnr2* mRNA was elevated following treatment with a low concentration of either stimulus but subsequently reduced in a dose-dependent manner. Furthermore, IFNγ enhanced the abundance of protein for both CB_1 and CB_2 whereas LPS had no impact on the protein abundance for either receptor. Carlisle et al. (2002) previously reported that IFNγ (~10 ng/mL) had no effect on *Cnr2* mRNA whereas LPS (1000 ng/ml) suppressed *Cnr2* mRNA in RAW264.7 macrophage-like cells. Maresz et al. (2005) also reported that IFNγ (~15 ng/mL) did not influence *Cnr2* mRNA whereas LPS (100 ng/ml) had a suppressive effect in primary cultured microglia. Using cultured N9 microglia, it has been reported that LPS (1 μM) induced *Cnr2* mRNA by roughly 15-fold (Navarro et al. 2018a). Using primary rat microglia, it has also been demonstrated that LPS (50 ng/mL) suppressed *Cnr1* and *Cnr2* mRNA after 6 hours, but the abundance of these transcripts returned to normal within 24 h (Mecha et al. 2015). These conflicting reports have created confusion with respect to the regulation of *Cnr2* mRNA in myeloid cells under pro-inflammatory conditions (Young and Denovan-Wright 2022a). Our results support that high concentrations of IFNγ in fact do not influence *Cnr2* mRNA in SIM-A9 microglia but low or moderate concentrations stimulate its upregulation. Similarly, our findings support that a low concentration (10 ng/mL) of LPS could upregulate *Cnr2* mRNA whereas high concentrations may suppress it. Taken together, these data provide evidence that these pro-inflammatory stimuli influence the regulation of CB_2 receptors in a biphasic concentration-dependent manner

We observed that IFNγ and LPS also exhibited concentration-dependent effects on mRNA for *NAPEPLD*, *FAAH*, *DAGLA*, and *MGLL*, the enzymes that synthesize and degrade AEA and 2-AG, respectively. The highest concentration of LPS resulted in a reduction of mRNA for *NAPEPLD* and *MGLL* which would correspond to reduced synthesis of AEA and breakdown of 2-AG, respectively. However, the lowest concentration of LPS resulted in elevated mRNA for *FAAH* and *DAGLA* which would correspond to increased breakdown of AEA and synthesis of 2-AG. IFNγ-mediated signaling generally had a smaller influence on ECS enzymes compared to LPS, but the

highest concentration of IFNγ greatly enhanced the mRNA for *FAAH* and suppressed *MGLL*. Mecha et al. (2015) previously reported that treatment with LPS (50 ng/mL) suppressed mRNA for *NAPEPLD*, *FAAH*, and *MGLL* within 6 hours. However, after 24 hours, only *FAAH* and *MGLL* remained downregulated. These data indicate that microglia in a pro-inflammatory phenotype generally exhibit altered quantities of ECS enzymes that may result in reduced biosynthesis of AEA but elevated production of 2-AG. However, these effects are influenced by several variables including type of pro-inflammatory stimuli as well as concentration and length of exposure to stimuli.

When combined, IFNγ and LPS exhibited some effects on the ECS that were not observed when the microglia were exposed to either pro-inflammatory stimulus alone. To assess the effects of dual treatment with IFNγ and LPS, we combined the stimuli using the highest concentration of IFNγ (20 ng/mL) and the lowest concentration of LPS (10 ng/mL) and vice-versa. Generally, the net effect of the dual treatments produced an effect that was like the stimuli of the greater concentration. However, there were some examples of synergy. Most notably, the combination of IFNγ and LPS upregulated *FAAH* mRNA by 37-fold compared to a 15-fold increase induced by IFNγ alone or the 7-fold increase caused by LPS alone. Interestingly, the same upregulation of *FAAH* mRNA was not observed when the lowest concentration of IFNγ was combined with the highest concentration of LPS. This indicates that there is crosstalk between toll-like receptor 4 (TLR4) and the interferon-gamma receptor (IFNGR) which is sensitive to the concentrations of ligand for either receptor. Non-additive interactions between the effects of LPS and IFNγ have been previously observed in myeloid cells (Häusler et al. 2002; Zhao et al. 2006; Papageorgiou et al. 2016). Our data supports that these interactions can also affect components of the ECS in microglia.

Pharmacological activation of CB_1 and CB_2 receptors influenced the release of NO from microglia upon exposure to IFNγ and/or LPS. Several previous studies have demonstrated that different cannabinoid molecules could inhibit microglial NO release *in vitro* using single concentrations of pro-inflammatory stimuli (Waksman et al. 1999; Ma et al. 2015; Malek et al. 2015; Young and Denovan-Wright 2022b). However, the concentration-response curves used in this work revealed that different synthetic

cannabinoid treatments could produce a variety of effects that were dependent on the type of cannabinoid as well as the concentration of IFNγ and/or LPS. When the microglia were exposed to LPS alone, co-treatment with any of the cannabinoid treatments substantially reduced the E_{max} of LPS as well as the EC_{50}. This pattern was also reported by Ross *et al.* (2000) following treatment of RAW264.7 macrophages with LPS and (-)-WIN 55,212-2 or palmitoylethanolamide. These observed effects of cannabinoids on LPS-mediated NO release resemble the expected effects of a modulator which would increase the affinity of LPS but decrease its efficacy (Kenakin 2007). However, to our knowledge, there is currently no evidence that cannabinoids bind directly to TLR4 in an orthosteric or allosteric manner. Thus, this was likely a summative effect that emerged based on the overlap of common signaling pathways among TLR4, and CB_1 and CB_2 receptors. When microglia were stimulated with IFNγ alone, only co-treatment with ACEA or HU-308 suppressed NO release whereas co-treatment with ACEA and HU-308 or CP 55,940 enhanced NO release. This indicates that co-activation of CB_1 and CB_2 receptors may produce a different effect than selective activation of either receptor under specific circumstances.

We found that when microglia were stimulated by LPS and IFNγ, all cannabinoid treatments also reduced the maximal NO release but without an effect on the EC_{50}. This is potentially because co-treatment with IFNγ masked the cannabinoid-mediated effects on the EC_{50} of LPS. When microglia were treated with combinations of IFNγ and LPS, all cannabinoids reduced the maximal NO release with variable effects on the EC_{50} of the pro-inflammatory stimuli. Furthermore, there was an observed downward shift in NO release at the lower concentrations of LPS and IFNγ which resembles the operational model for an allosteric modulator with direct agonist efficacy (Kenakin 2007). However, it is likely that the synthetic cannabinoids did not act in an allosteric manner but have direct agonist efficacy via cannabinoid receptors and suppression of NO release was simply masked by a floor effect upon treatment with low concentrations of LPS or IFNγ alone.

CB_1 and CB_2 have previously been reported to physically associate to form heteromers which can alter the response to endogenous or exogenous cannabinoids

(Callén et al. 2012; Navarro et al. 2018b; Young et al. 2022). Although CB_1-CB_2 heteromers have demonstrated the potential to mediate synergy among cannabinoids (Navarro et al. 2018a), the heteromers generally have a propensity to exhibit negative cross-talk which reduces the efficacy of cannabinoid drugs when presented in combination (Callén et al. 2012; Young et al. 2022; Young and Denovan-Wright 2022b). As this specific pattern was only observed in the presence of a high concentration of IFNγ and a lower concentration of LPS, it appeared that the pro-inflammatory environment also influenced the efficacy of the cannabinoid treatments.

It has been frequently reported that components of the ECS, especially CB_2 receptors, are upregulated under conditions of neurodegeneration such as in Alzheimer's disease (AD) and Huntington's disease (HD) (Benito et al. 2003; Sagredo et al. 2009; Palazuelos et al. 2009; Mulder et al. 2011). We found that microglial *Cnr2* mRNA was upregulated upon exposure to relatively low to moderate concentrations of IFNγ and LPS but not in response to relatively high concentrations of either stimulus. It is unclear whether microglial CB_2 receptors are upregulated in AD and HD due to the microglial activation associated with chronic neuroinflammation or other disease-specific mechanisms. Furthermore, it remains to be determined whether more severe neuroinflammation in these diseases would also result in suppression of *Cnr2* and other components of the ECS as observed in the present study. Regardless of the mechanism, the elevated quantities of microglial CB_2 receptors in AD and HD are indicative of an increased sensitivity to CB_2 receptor-selective agonists that have anti-inflammatory properties without the psychoactive effects of CB_1 receptor-selective or nonselective cannabinoid agonists (Ashton and Glass 2007; Navarro et al. 2016; Cassano et al. 2017; Young and Denovan-Wright 2022a). In future work, it will be important to determine whether CB_2 receptors and synthetic enzymes for endocannabinoids are most elevated in specific AD or HD stages of disease. This could be indicative of a window of opportunity where cannabinoid-based interventions could have the greatest therapeutic efficacy.

There are limitations to the present study which highlight the value of future experiments *in vivo*. In this work, concentrations of IFNγ and LPS were defined as low, moderate, and maximal based on the degree of NO release stimulated by each molecule.

Although we observed concentration-dependent effects of IFNγ and LPS on the microglial ECS, it is unclear whether these differences may translate to microglia *in situ*. Furthermore, we only assessed microglia at a single time point following exposure to the pro-inflammatory stimuli. We selected the time point of 16 hours as it corresponded to the point in which the cells exhibit a maximal pro-inflammatory response. Components of the ECS have been shown to fluctuate from 6 to 24 hours following a single exposure to LPS (50 ng/mL) (Mecha et al. 2015). Thus, the element of time which is missing from this study is also worthy of independent exploration. Finally, it would be useful to measure the release of endocannabinoids from microglia in response to IFNγ and LPS. Although the abundance of ECS enzymes can provide an indication of the propensity of microglia to release AEA and 2-AG, lipidomic analyses could provide further insight into these results.

In conclusion, the current study demonstrated that stimulation of cultured microglia with distinct pro-inflammatory stimuli, IFNγ and LPS, differentially influenced the abundance of mRNA and protein for different components of the ECS. We observed that low concentrations of these molecules stimulated the ECS whereas high concentrations of these stimuli were neutral or suppressed the ECS. Furthermore, treatment with exogenous synthetic cannabinoids inhibited the microglial pro-inflammatory response. Generally, activation of CB_1 or CB_2 receptors alone was more effective than co-activation of both receptors which highlighted the value of selective cannabinoid compounds as anti-inflammatory molecules.

Chapter 4: Enantiomeric agonists of cannabinoid type 2 receptors differentially regulate the pro-inflammatory activity of microglia

Copyright statement

This article is currently unpublished and thus does not require copyright permission to be included in this thesis. The publication status of first-author articles included or excluded from this thesis are in Table A1 (Appendix A).

Contribution statement

All experiments were performed, and data were collected by myself. Analysis and interpretation of the data were performed in consultation Dr. Eileen Denovan-Wright. Current *in vivo* experiments are ongoing in the lab of Dr. Melanie Kelly and the additional data will be integrated into this manuscript prior to publication. This work was completed as part of an industry collaboration with Panag Pharma Inc. and Tetra-Bio Pharma.

Preface

This chapter further explores the anti-inflammatory effects of CB_2 receptor activation in microglia. The purpose of the chapter was to determine potential functional differences between two enantiomers, HU-308 and HU-433. Tetra-Bio Pharma is developing HU-308 as a therapeutic for inflammation, pain, and ophthalmology indications. As synthesis of HU-308 tends to generate HU-433 as well, there was industry interest to determine the functional differences between these molecules and identify whether HU-433 may be independently useful.

4.1 Abstract

Microglia are the resident immune cells of the brain and are the primary regulators of inflammation in the central nervous system. Hyperactivation of microglia is characterized by chronic upregulation of cytokine release and is a common element of several neurodegenerative diseases. Microglial CB_2 receptors are an emerging therapeutic target to suppress the excessive inflammation associated with hyperactive microglia. HU-308 and HU-433 are enantiomers and are both selective agonists of CB_2 receptors with the demonstrated ability to reduce inflammation *in vivo*. We compared the effects of HU-308 and HU-433 with respect to β-arrestin2 and $G\alpha_i$ recruitment at the human CB_2 receptor and the anti-inflammatory effects in cultured SIM-A9 microglia. We observed that HU-308 more strongly recruited both β-arrestin2 and $G\alpha_i$. However, HU-433 more strongly suppressed LPS- and IFNγ-mediated signaling in microglia which culminated in a greater influence over the release of NO and TNF. This demonstrated that the effects on downstream signaling were not directly linked to the magnitude of effector recruitment, and that the signaling effects were more predictive of anti-inflammatory capacity. This work provides insight into the mechanism by which CB_2 receptor activation leads to suppression of microglial inflammatory activity which is relevant to the treatment of neuroinflammation.

4.2 Introduction

The endocannabinoid system (ECS) contributes broadly to the physiology of animals and is involved in thermoregulation as well as memory, appetite, and immune function (Wenger and Moldrich 2002; Marsicano et al. 2002; Cabral et al. 2008). Type 2 cannabinoid (CB_2) receptors are expressed in myeloid, monocytic, and lymphoid cells and mediate the immune-related functions of the ECS (Munro et al. 1993; Galiègue et al. 1995). This contrasts with type 1 cannabinoid (CB_1) receptors which mediate the effects of endocannabinoids in the central nervous system (CNS) as well as the psychoactive effects of exogenous cannabinoids (Mechoulam and Parker 2013). Although CB_2 receptors were once reported to be absent from the brain, they have since been identified primarily within microglia with some expression by neurons (Benito et al. 2003; Palazuelos et al. 2009; Lanciego et al. 2011; Zhang et al. 2014, 2021b; Stempel et al. 2016; Chen et al. 2017; Navarro et al. 2018a). CB_2 receptors within the CNS have now successfully been targeted to treat neurodegenerative diseases such as Alzheimer's and Parkinson's disease in animal models (Price et al. 2009; Martín-Moreno et al. 2012; Aso et al. 2013; Javed et al. 2016; Li et al. 2019a). Although CB_2 receptors have demonstrated therapeutic potential, there are few ligands that maintain high selectivity to target these anti-inflammatory functions of the ECS without psychoactivity or other off-target effects.

Selective CB_2 receptor agonists have shown promise for the modulation of inflammation, pain, neurodegeneration, and osteoporosis (Tabrizi et al. 2016). HU-308 is a synthetic cannabinoid and structural analog of cannabidiol (CBD) that behaves as a CB_2 receptor agonist with greater than 440-fold selectivity over CB_1 receptors (Hanus et al. 1999). HU-308 is synthesized from molecules with multiple chiral centers, thus, its production yields multiple enantiomers. One such enantiomer includes HU-433 which has demonstrated a lower binding affinity for human CB_2 receptors than HU-308, but increased efficacy *in vivo* to reduce xylene-induced ear swelling and ovariectomy-induced bone loss in mice (Smoum et al. 2015). Thus, HU-308 and HU-433 are enantiomers that differ with respect to receptor binding and efficacy. However, it is unclear whether these agonists differ in terms of arrestin recruitment, downstream signaling, or anti-inflammatory capacity in microglia. As these intracellular effects

greatly influence the clinical relevance of a potential anti-inflammatory compound, it is important that these pharmacological properties are defined.

Microglia are the resident immune cells of the brain and possess the necessary components to biosynthesize and degrade endocannabinoids or respond to cannabinoids that target either CB_1 or CB_2 receptors (Stella 2010; Young and Denovan-Wright 2022a). Microglia express CB_2 receptors and are the primary target cells for anti-inflammatory cannabinoids in the CNS (Stella 2010). Although microglia are known to propagate neuroinflammation in response to immunogenic stimuli such as lipopolysaccharides (LPS) and interferon gamma (IFNγ), selective activation of microglial CB_2 receptors has been demonstrated to suppress the pro-inflammatory response to these stimuli (Ehrhart et al. 2005; Ashton and Glass 2007; Young and Denovan-Wright 2022b). However, it is unclear which signaling pathways are modulated by CB_2 receptor agonists to elicit these immunosuppressive effects.

Agonists of CB_2 receptors have shown promise for the treatment of neuroinflammation but there are gaps in our understanding of how CB_2 receptors influence the inflammatory activity of microglia to mediate these effects. In this work, we utilize the HU-308 molecular scaffold to examine the differential cellular effects of HU-308 and HU-433 via CB_2 receptors. Specifically, we investigate how CB_2 receptor activation can influence cellular signaling of microglia in response to LPS and IFNγ. Our findings suggest that HU-308 and HU-433 exhibit differences in the recruitment of $G\alpha_i$ and β-arrestin2 which translate to subtle differences in the canonical signaling responses to pro-inflammatory stimuli. Ultimately, these differences in signaling culminate in increased efficacy of HU-433 to suppress microglial inflammation *in vitro*.

4.3 Results

4.3.1. HU-308 exhibits enhanced recruitment of β-arrestin2 and mini-$G\alpha_i$ compared to HU-433

HU-308 and HU-433 are enantiomers and HU-308 was reported to exhibit higher binding affinity for the human CB_2 receptor relative to HU-433, but the compounds were not compared with respect to effector recruitment (Fig. 4. 1)(Smoum et

al. 2015). To assess the relative efficacies of HU-308 and HU-433 on the human CB_2 receptor, NanoBiT assays were performed to measure the concentration-dependent recruitment of β-arrestin2 or a mini-$G\alpha_i$ protein (Fig. 4. 2A). The mini-$G\alpha_i$ protein constitutes only the activate GTPase domain of $G\alpha_i$ which interacts with the receptor upon ligand binding (Nehmé et al. 2017). Preliminary experiments were performed with the fusion proteins in different permutations, and it was determined that the assays were most sensitive when the small nanoluciferase fragment was fused to the C-terminus of the CB_2 receptor and the large nanoluciferase fragment was fused to the N-terminus of the β-arrestin2 or mini-$G\alpha_i$ (Fig. 4. S1). It was also confirmed that any effect of HU-308 or HU-433 was reversed by the CB_2 receptor inverse agonist, SR144528 (Fig. 4. S2A-B). SR144528 alone also reduced the luminescent signal below baseline in a concentration-dependent manner which suggested that the assay could detect constitutive activity of the transfected CB_2 receptors (Fig. 4. S2C).

We measured β-arrestin2 recruitment over the course of 42 min for HU-308 (Fig. 4. 2B) and HU-433 (Fig. 4. 2C) and the areas under the curve were used to prepare concentration-response curves. HU-308 (EC_{50} = 530.4 nM) exhibited increased β-arrestin2 recruitment at concentrations above 100 nM compared to HU-433 (EC_{50} = 2.42 μM; $p < 0.0001$) (Fig. 4. 2D). Relative to HU-308, CP 55,940 exhibited increased potency with an EC_{50} of 52.4 nM but reduced efficacy with respect to β-arrestin2 recruitment. When mini-$G\alpha_i$ recruitment was measured, HU-308 (EC_{50} = 14.9 μM) and HU-433 (EC_{50} not determined) had low potency and efficacy relative to CP 55,940 (EC_{50} = 239.6 nM) (Fig. 4. 2E). However, HU-308 did exhibit increased recruitment of mini-$G\alpha_i$ compared to HU-433 at concentrations above 100 nM ($p < 0.001$).

As HU-308 and HU-433 are both expected to bind the orthosteric site of CB_2 receptors, we investigated whether these molecules would compete with each other to influence β-arrestin2 recruitment. To test this, HEK 293T cells expressing human CB_2 receptors were treated with the EC_{80} of HU-308 (1.8 μM) or HU-433 (5.9 μM) in conjunction with increasing concentrations of the other molecule. We observed that at concentrations above 10 μM, HU-433 did appear to outcompete HU-308 at the orthosteric site which reduced the overall recruitment of β-arrestin2 (Fig. 4. 2F). A

similar pattern was observed in the inverse experiments as HU-308 appeared to outcompete HU-433 to increase β-arrestin2 recruitment at concentrations above 10 μM. These data indicate that although HU-308 and HU-433 compete for the CB_2 receptor orthosteric site, relatively high levels of cross-contamination would likely be required to have an observable influence at the cellular level.

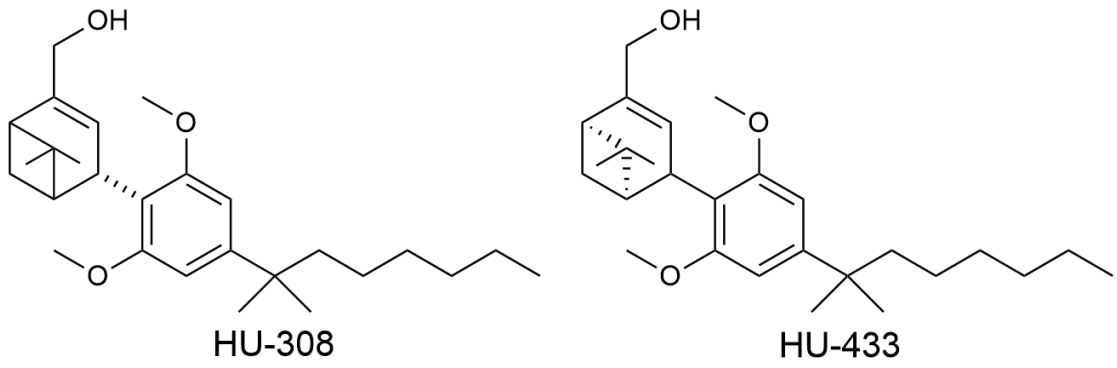

Figure 4. 1. Structures of the enantiomers, HU-308 and HU-433, used as CB_2 receptor agonists.

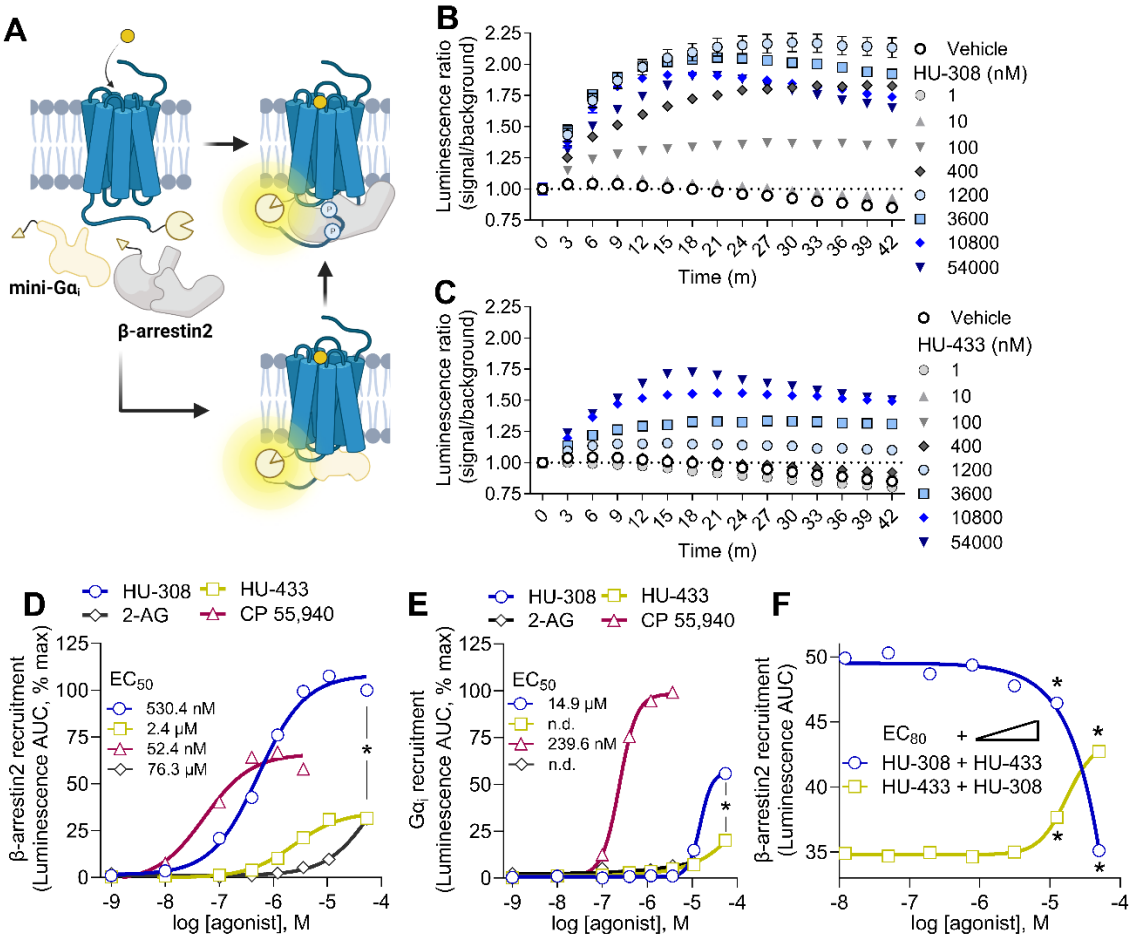

Figure 4. 2. HU-308 exhibits enhanced recruitment of β-arrestin2 and mini-Gαi compared to HU-433. A NanoBiT assays were developed to facilitate the detection of β-arrestin2 or mini-$G\alpha_i$ recruitment to human CB_2 receptors in HEK 293T cells. NanoBiT assays were utilized to measure the recruitment of β-arrestin2 over the course of 42 minutes upon stimulation with increasing concentrations of **B** HU-308 or **C** HU-433 (n = 4). **D** Concentration-dependent recruitment of β-arrestin2 in response to HU-308 (1 nM – 54 μM), HU-433 (1 nM – 54 μM), CP 55,940 (1 nM – 5 μM), or 2-AG (1 nM – 54 μM) (n = 4). * $p < 0.05$; HU-308 vs. HU-433. **E** Concentration-dependent recruitment of mini-$G\alpha_i$ in response to HU-308 (1 nM – 54 μM), HU-433 (1 nM – 54 μM), CP 55,940 (1 nM – 5 μM), or 2-AG (1 nM – 54 μM) (n = 4). **F** β-arrestin2 recruitment to CB_2 receptors following treatment with the EC_{80} of HU-308 (1.8 μM) combined with increasing concentrations of HU-433, or the EC_{80} of HU-433 (5.9 μM) combined with increasing concentrations of HU-308 (n = 4). * $p < 0.05$ vs. vehicle.

4.3.2. HU-308 and HU-433 blunted LPS- and IFNγ-mediated signaling in SIM-A9 microglia

The effects of HU-308 and HU-433 on microglial pro-inflammatory signaling were next determined in response to two pro-inflammatory stimuli, LPS and IFNγ. We observed that the pro-inflammatory signaling of SIM-A9 microglia displayed an early wave (10 min) and a late wave (8 h) for ERK1/2, JNK, p38, and Akt signaling (Fig. 4. S3A-D). NF-κB was stimulated early by LPS and only at a later timepoint by IFNγ (Fig. 4. S3E) whereas STAT1 was only stimulated late by IFNγ and unaffected by LPS. In the absence of a pro-inflammatory stimulus, HU-308 and HU-433 stimulated ERK1/2 phosphorylation (Fig. 4. S4A) but inhibited JNK and p38 phosphorylation (Fig. 4. S4B,C) with no effect on Akt phosphorylation (Fig. 4. S4D).

When SIM-A9 microglia were stimulated with LPS, HU-308 and HU-433 delayed the initial signaling peak of ERK1/2 and JNK phosphorylation and greatly suppressed the second wave of signaling (Fig. 4. 3A,B). Both HU-308 and HU-433 inhibited the early phosphorylation of p38 although HU-433 exhibited a greater capacity to block the late wave of p38 signaling (Fig. 4. 3C). Similarly, HU-433 more strongly inhibited the late wave of Akt signaling compared to HU-308 (Fig. 4. 3D). Both HU-308 and HU-433 inhibited NF-κB signaling at the 8 h timepoint but had no effect on STAT1 signaling (Fig. 4. 3E,F). When SIM-A9 microglia were stimulated with IFNγ, HU-308 and HU-433 suppressed the initial wave of ERK1/2 signaling at the 10 min and 60 min timepoints, however, HU-433 was more efficacious with respect to suppression of ERK1/2 signaling at the later 6 and 8 h timepoints (Fig. 4. 4A). HU-308 and HU-433 also suppressed the initial wave of JNK phosphorylation at the 10 min and 30 min timepoints whereas only HU-433 reduced JNK phosphorylation at the 16 h timepoint (Fig. 4. 4B). With respect to IFNγ-mediated signaling, neither HU-308 or HU-433 affected the phosphorylation of p38, Akt, NF-κB, or STAT1 relative to the vehicle (Fig. 4. 4C-F). The data indicate that CB_2 receptor activation influenced the downstream kinetics of LPS and IFNγ differentially, and that HU-433 was generally more efficacious with respect to suppression of pro-inflammatory signaling.

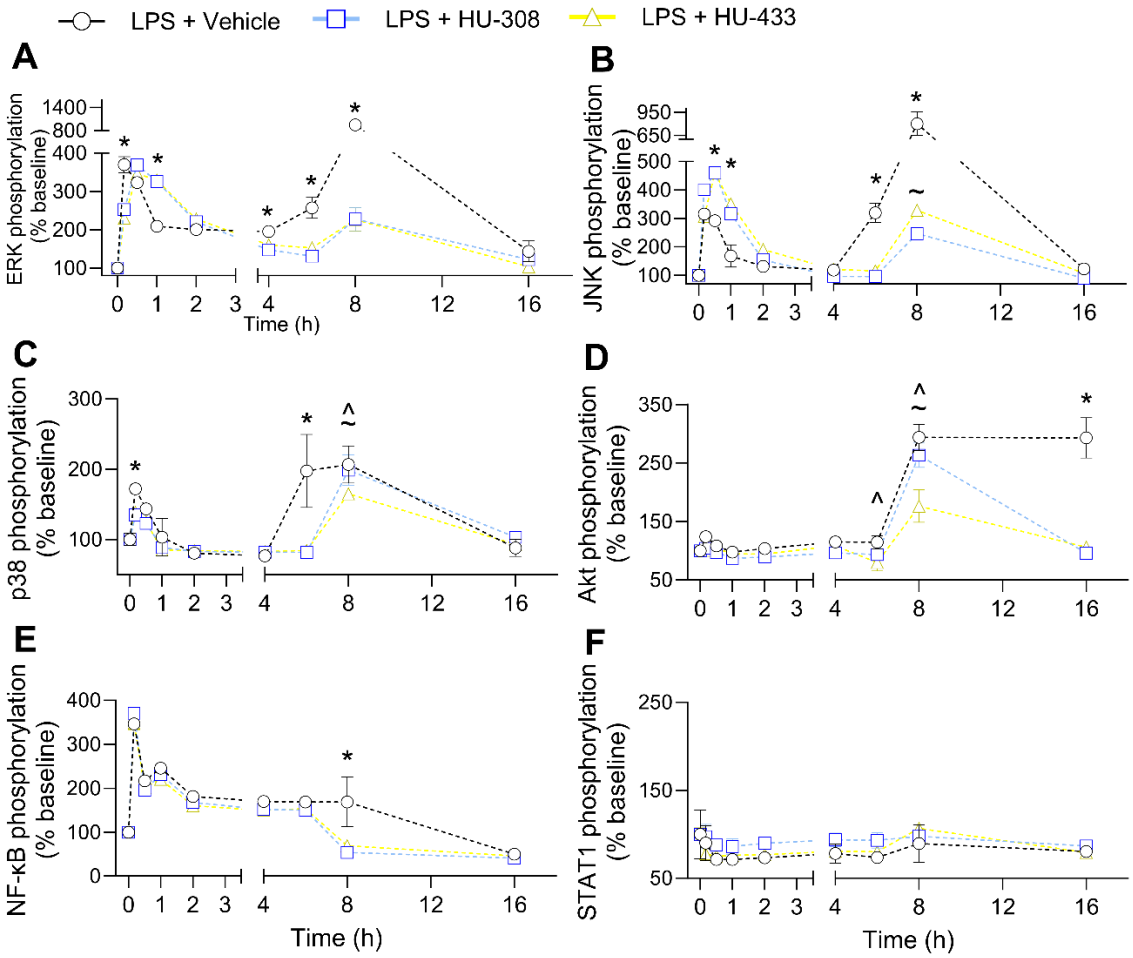

Figure 4. 3. HU-308 and HU-433 modulate the kinetics and magnitude of microglial pro-inflammatory signaling in response to LPS. Cultured SIM-A9 microglia were stimulated with LPS (1000 ng/mL) for 16 h, and in-cell western assays were used to monitor the phosphorylation of **A** ERK1/2 (Thr202/Tyr204), **B** JNK (Thr183/Tyr185), **C** p38 (Thr180/Tyr182), **D** Akt (Ser473), **E** NF-κB (Ser536), **F** STAT1 (Tyr701) (n = 4). Each time-point represents an independent preparation of cultured SIM-A9 microglia. Statistical significance was determined using two-way ANOVA with Tukey post-hoc test. * $p < 0.05$, vehicle vs. HU-308 and HU-433; ~ $p < 0.05$, HU-308 vs. HU-433; ^ $p < 0.05$, vehicle vs. HU-433 only.

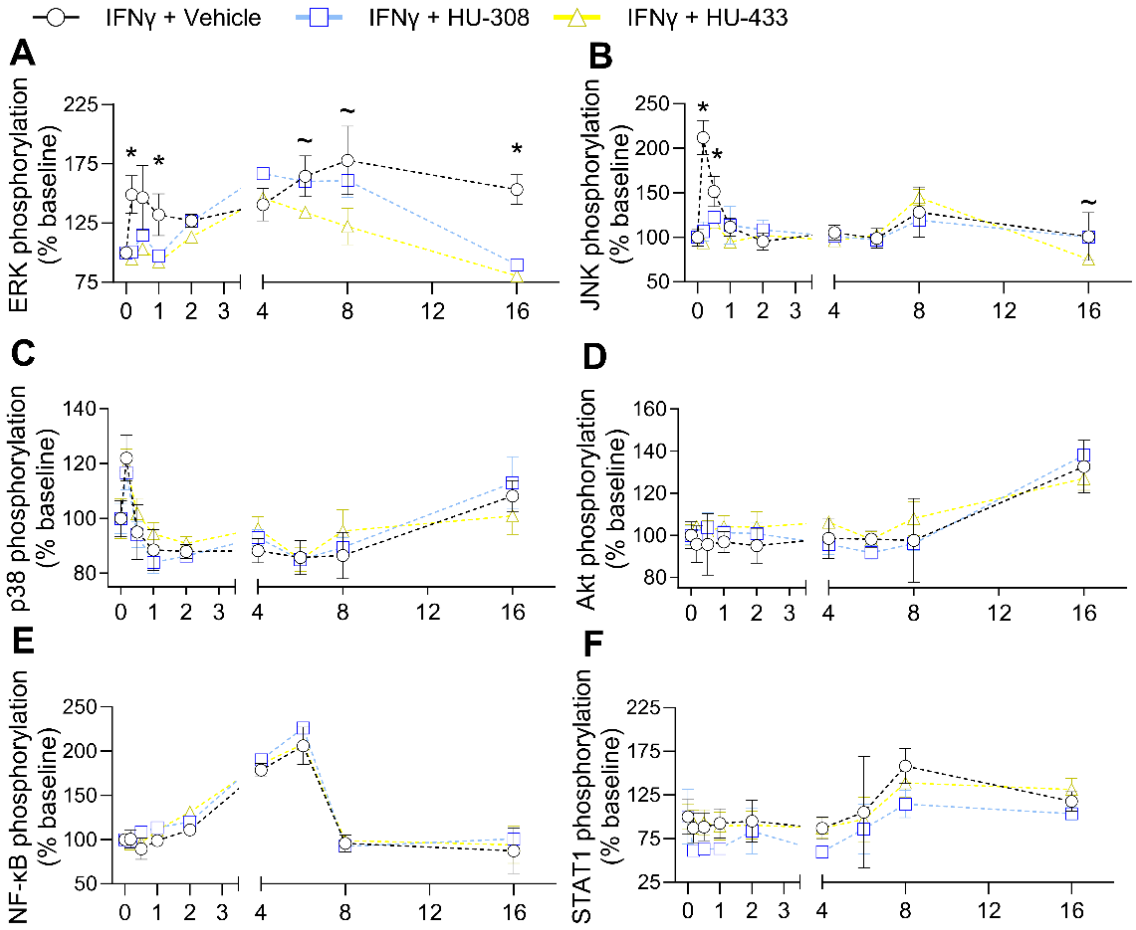

Figure 4. 4. HU-308 and HU-433 modestly affect the kinetics and magnitude of microglial pro-inflammatory signaling in response to LPS. Cultured SIM-A9 microglia were stimulated with IFNγ (20 ng/mL) for 16 h, and in-cell western assays were used to monitor the phosphorylation of **A** ERK1/2 (Thr202/Tyr204), **B** JNK (Thr183/Tyr185), **C** p38 (Thr180/Tyr182), **D** Akt (Ser473), **E** NF-κB (Ser536), **F** STAT1 (Tyr701) (n = 4). Each time-point represents an independent preparation of cultured SIM-A9 microglia. Statistical significance was determined using two-way ANOVA with Tukey post-hoc test. * $p < 0.05$, vehicle vs. HU-308 and HU-433; ~ $p < 0.05$, HU-308 vs. HU-433.

4.3.3. Microglial CB_2 receptor activation inhibited the pro-inflammatory activity of microglia

To assess functional differences between HU-308 and HU-433, the microglial response to each was compared with respect to the release of NO and TNF, and the capacity to induce secondary neurotoxicity. The microglial release of NO was suppressed by HU-308 (IC_{50}: 4.39 μM) as well as HU-433 (IC_{50}: 3.25 μM), and HU-433 was more efficacious at concentrations above 1 μM (Fig. 4. 5A). Microglial cells that were stimulated with LPS (500 ng/mL) and IFNγ (5 ng/mL) released TNF to a concentration of 7318 ± 222 pg/mL within 16 h (Fig. 4. 5B). Treatment with HU-308 (5 μM) reduced the concentration of released TNF to 3541 ± 837 pg/mL and HU-433 treatment (5 μM) reduced TNF to 1794 ± 665 pg/mL. This effect on TNF release was reversed by co-incubation with the inverse agonist, SR144528 (20 μM) which supports the CB_2 receptor-specific effects of HU-308 and HU-433. These data suggest that both HU-308 and HU-433 had anti-inflammatory effects on SIM-A9 microglial cells via activation of CB_2 receptors, however, HU-433 was more efficacious.

The influence of HU-308 and HU-433 on secondary neurotoxicity was determined using conditioned media and ST*Hdh*$^{Q7/Q7}$ neuronal cells as previously described (Young and Denovan-Wright 2022b). SIM-A9 microglia were stimulated with LPS (500 ng/mL) and IFNγ (5 ng/mL) in conjunction with HU-308 or HU-433 at concentrations of 500 nM or 5 μM. Co-treatment of microglia with HU-433 at either concentration improved subsequent neuronal viability whereas HU-308 was only efficacious at the 5 μM concentration (Fig. 4. 5C). Co-treatment with SR144528 (20 μM) reduced the effects of HU-308 and HU-433 (5 μM), however, there was still an improvement in ST*Hdh*$^{Q7/Q7}$ cell viability which is consistent with a partial blockade of the receptor-mediated effects. This was likely a consequence of the high agonist concentration relative to the antagonist (Rinaldi-Carmona et al. 1998). These data suggest that HU-308 and HU-433 reduced the pro-inflammatory activity of SIM-A9 microglia which subsequently reduced the secondary damage to cultured ST*Hdh*$^{Q7/Q7}$ cells.

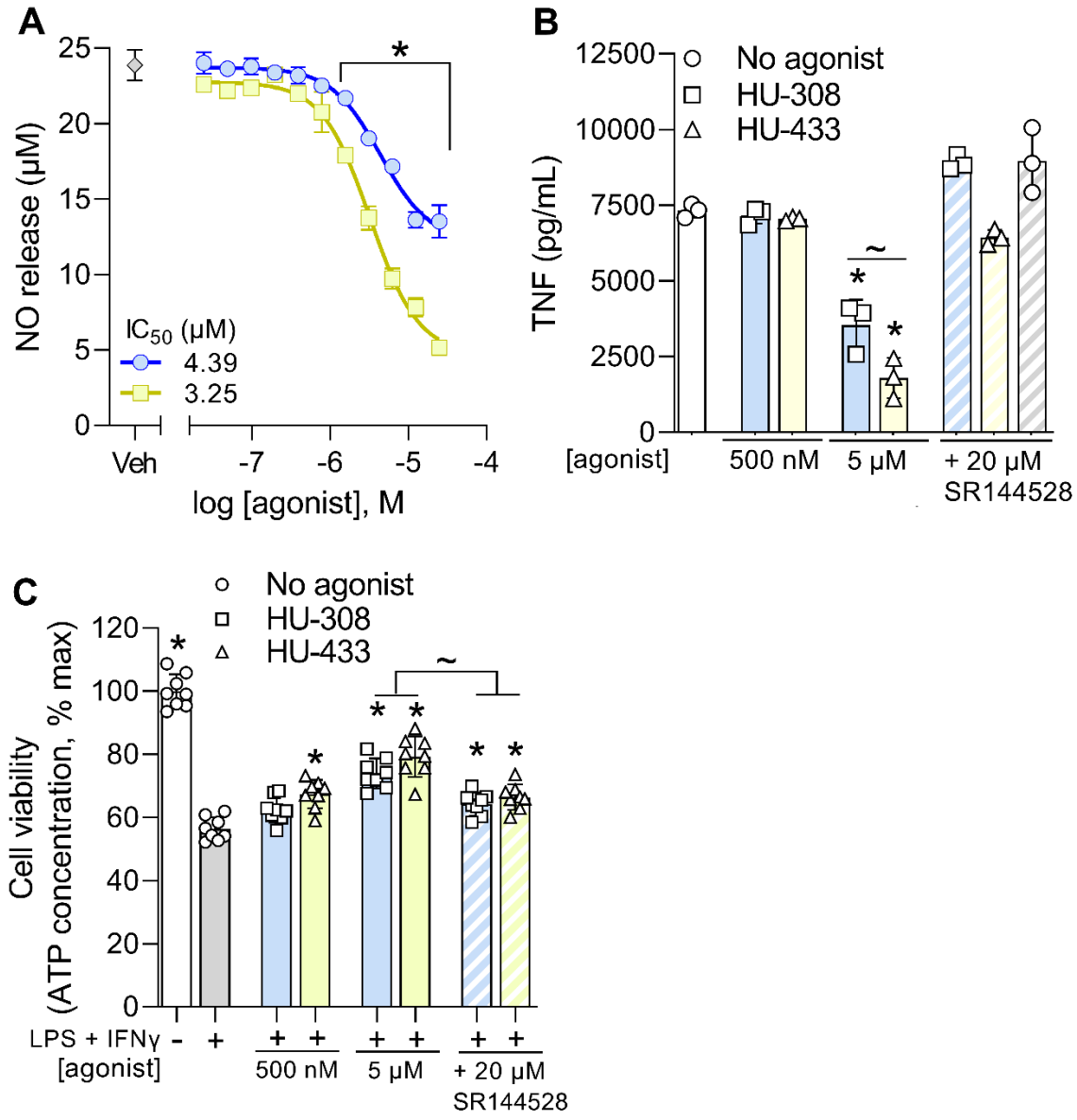

Figure 4. 5. HU-308 and HU-433 differentially suppress the release of NO and TNF from SIM-A9 microglia which impacts secondary neurotoxicity. Cultured SIM-A9 microglia were stimulated with LPS (500 ng/mL) and IFNγ (5 ng/mL) for 16 h. **A** NO release was measured using the Griess assay (n = 4). * $p < 0.05$; two-way ANOVA with Sidak post-hoc test. **B** TNF release was determined by enzyme-linked immunosorbent assay (n = 3). Significance was determined using one-way ANOVA with Tukey post-hoc test. * $p < 0.05$ vs. no agonist; ~ $p < 0.05$, HU-308 vs. HU-433. **C** SIM-A9 microglia were stimulated with LPS (500 ng/mL) and IFNγ (5 ng/mL) in conjunction with HU-308, HU-433, and SR144528 as indicated for 16 h. The conditioned media was applied to cultured ST*Hdh*$^{Q7/Q7}$ cells and ATP concentrations were measured as a proxy for cell viability after 24 h. * $p < 0.05$ vs. LPS + IFNγ with no agonist. ~ $p < 0.05$, agonist (5 μM) vs. agonist (5 μM) + SR144528 (20 μM).

4.4 Discussion

In this work, we investigated a CB_2 receptor agonist, HU-308, and its enantiomer, HU-433. The goal was to unravel a previously observed phenomenon whereby HU-308 exhibited greater affinity for CB_2 receptors in *in vitro* binding assays whereas HU-433 demonstrated greater efficacy in mouse models of inflammation and osteoporosis (Smoum et al. 2015). We measured the effects of HU-308 and HU-433 on the recruitment of effector proteins to CB_2 receptors as well as on the signaling dynamics of microglia in response to LPS or IFNγ. HU-308 recruited β-arrestin2 and mini-$G\alpha_i$ more strongly than HU-433 which was consistent with the previously observed differences in binding affinity (Smoum et al. 2015). In response to LPS, HU-308 and HU-433 modulated the canonical pro-inflammatory signaling response including the suppression of MAPK and Akt signaling. More specifically, CB_2 receptor activation was associated with inhibition of the second wave of signaling which has been linked to inflammatory activity (Rodems and Spector 1998; Chen et al. 2004; Hadi et al. 2013). Ultimately, despite reduced recruitment of effector proteins, HU-433 exhibited greater influence over the pro-inflammatory signaling of cultured SIM-A9 microglia which culminated in stronger anti-inflammatory effects.

We observed that HU-308 more strongly recruited both mini-$G\alpha_i$ and β-arrestin2 to human CB_2 receptors compared to HU-433. It was previously reported that HU-308 induces greater binding of [^{35}S]-GTPγS and also displays an increased binding affinity to CB_2 receptors as measured by displacement of [^{3}H]-CP 55,940 (Smoum et al. 2015). We also found that CP 55,940 recruited β-arrestin2 to human CB_2 receptors with 10-fold greater potency relative to HU-308 which was previously observed (Soethoudt et al. 2017). However, we observed greater maximal β-arrestin2 recruitment in response to HU-308. Taken together, these data suggest that HU-308 binds strongly to CB_2 receptors and elicits a greater response than HU-433 with respect to the recruitment of proteins required for canonical GPCR-mediated signaling. With respect to binding of CB_2 receptors, docking studies suggest that HU-308 and HU-433 both bind to the orthosteric binding pocket in a very similar orientation (Smoum et al. 2015). However, the model demonstrated that HU-308 exhibits stronger hydrogen bonding overall and the bicyclic

ring is buried deeper into the binding pocket. This information is consistent with our finding that HU-308 and HU-433 compete to influence β-arrestin2 recruitment. Together, these data strongly suggest that HU-308 and HU-433 both bind to the same orthosteric binding site rather than different potential allosteric sites.

We identified that HU-308 and HU-433 both subtly modulated the early signaling responses of microglial cells to LPS and IFNγ. The effects of the CB_2 agonists in response to LPS were most notable on the phosphorylation of mitogen-activated protein kinases (MAPKs), ERK1/2, JNK, and p38. It has been previously demonstrated that the phosphorylation of ERK1/2 is a characteristic of microglia following treatment with LPS, and that this response is blunted by stimulation of either CB_1 or CB_2 receptors (Ribeiro et al. 2013). LPS was also shown to stimulate ERK1/2 and p38 in primary mouse microglia and JNK in BV-2 immortalized microglia (Ribeiro et al. 2013; Liu et al. 2021). Consistent with past findings, we found that treatment with HU-308 and HU-433 blunted the early phosphorylation of p38 in SIM-A9 microglia stimulated with LPS. However, while ERK1/2 phosphorylation was suppressed by CB_2 receptor activation at the earliest timepoint, there was a greater response at the one-hour timepoint which is indicative of delayed ERK1/2 signaling rather than suppression. Furthermore, HU-308 and HU-433 enhanced the early phosphorylation of JNK. This was unexpected as JNK has been associated with the pro-inflammatory activity of primary microglia from both mice and rats (Waetzig et al. 2005; Ribeiro et al. 2013). This suggests that the LPS-mediated signaling response is multifaceted and CB_2 receptor activation has multiple effects that are dependent on specific signaling pathways. Microglia stimulated with IFNγ exhibited rapid phosphorylation of ERK1/2, JNK, and p38. This IFNγ-mediated effect on ERK1/2 and JNK was blunted by treatment with either HU-308 or HU-433. Thus, the early pro-inflammatory response of microglia to LPS or IFNγ was broadly suppressed by CB_2 receptor activation.

The activation of microglial MAPK and Akt pathways was biphasic in response to LPS, but not IFNγ, and was characterized by an early wave and a late wave. Late activation of ERK1/2 in immortalized microglia was previously identified and the stimulation of CB_1 receptors by anandamide suppressed ERK1/2 phosphorylation at the

late 24 h timepoint (Eljaschewitsch et al. 2006). We observed that although HU-308 and HU-433 influenced the early wave of pro-inflammatory signaling, the effects of CB_2 receptor activation on MAPK signaling were most prominent in the late wave. Together, these data indicate that targeting the endocannabinoid system through either CB_1 or CB_2 receptors is a viable method to suppress the late wave of MAPK signaling associated with pro-inflammatory activation following LPS treatment. Biphasic ERK1/2 signaling in response to growth factors has been observed in smooth muscle and epithelial cells (Finlay et al. 2003; Chen et al. 2004; Hadi et al. 2013; Huang et al. 2017). The second wave of ERK1/2 phosphorylation is associated with proliferative activity as well as the inflammatory response to infection in human fibroblasts and mammary epithelial cells (Rodems and Spector 1998; Chen et al. 2004; Hadi et al. 2013). A matrix metalloprotease inhibitor specifically blunted the second wave of ERK signaling in human mammary epithelial cells (Chen et al. 2004). A second wave of LPS-mediated IL-8 secretion has been demonstrated in human neutrophils and was dependent on TNF release (Cassatella et al. 1993). This indicates that the second wave of signaling is an autocrine mechanism involving secreted proteins. Although it is unclear whether the pro-inflammatory activity of microglia is primarily linked to the second wave of MAPK signaling, future work is warranted to determine whether this could be a primary mechanism for the anti-inflammatory effects of CB_2 receptor agonists.

Despite the structural similarities between HU-308 and HU-433, we observed differences in the efficacy of the ligands to suppress the inflammatory activity of microglia. HU-308 previously suppressed the release of NO and TNF from SIM-A9 microglia and reduced the secondary neurotoxicity in a CB_2 receptor-dependent manner (Young and Denovan-Wright 2022b). CB_2 receptor activation has also been shown to inhibit LPS- and IFNγ-mediated effects in other models of microglia, including immortalized N9 cells and primary mouse and rat microglia (Ehrhart et al. 2005; Correa et al. 2010; Ma et al. 2015; Mecha et al. 2015). In contrast, HU-433 was also shown to have greater efficacy *in vivo* to inhibit xylene-mediated ear swelling (Smoum et al. 2015). In this work, we also demonstrated that HU-433 suppressed the release of NO and TNF

to a greater extent than HU-308 despite the reduced degree of effector recruitment to CB_2 receptors.

Although the activity of CB_2 receptors has generally been anti-inflammatory and neuroprotective in various *in vivo* models, there is evidence that CB_2 receptors promote inflammation under specific conditions. In a mouse model of graft-versus-host disease, CB_2 receptor-knockout mice displayed reduced infiltration of donor $CD4^+$ and $CD8^+$ T cells into the brain which was accompanied by reduced caspase-3 cleavage in neurons (Moe et al. 2023). These results were replicated with the use of a brain-penetrant inverse agonist of CB_2 receptors, SMM-189. An additional study identified that primary microglia from CB_2 receptor-knockout mice were less sensitive to LPS and IFNγ (Schmöle et al. 2015). Blockade of CB_2 receptors with SR144528 reduced swelling, neutrophil recruitment, and leukotriene production in a mouse model of acute ear inflammation (Oka et al. 2005). CB_2 receptor blockade also reduced the recruitment of eosinophils and the release of pro-inflammatory cytokines such as TNF in mice with oxazolone-induced contact dermatitis (Oka et al. 2006). These past findings suggest that the constitutive activity of CB_2 receptors may be required to initiate the pro-inflammatory activity of peripheral immune cells as well as microglia.

Substantial attention has been directed toward understanding the pharmacology of CB_2 receptors to develop therapeutics for several indications including inflammation, itch, osteoporosis, and neuropathic pain (Guindon and Hohmann 2008; Kusakabe et al. 2013; Han et al. 2013; Rossi et al. 2019). However, HU-308 and most other CB_2 receptor agonists are highly lipophilic molecules with poor solubility and other undesirable physicochemical properties (Soethoudt et al. 2017; Whiting et al. 2022). Thus, although HU-308 has been demonstrated to be suitable for topical treatment in multiple mouse models of ocular inflammation, it may have unfavorable pharmacokinetic properties when administered orally (Toguri et al. 2014; Thapa et al. 2018). As CB_2 receptor agonists, including HU-308, have repeatedly shown promise in pre-clinical models, further optimization of CB_2-selective scaffolds with suitable pharmacokinetic properties may be critical to the development of CB_2 receptors as targets for neuroinflammation.

Receptor selectivity has been another challenge in the development of CB_2 receptor agonists with therapeutic potential in the absence of psychoactivity. HU-308 has demonstrated very high selectivity for CB_2 over CB_1 receptors and does not elicit catalepsy, antinociception, or hypothermia in mice at doses of up to 100 mg/kg (Soethoudt et al. 2017). Furthermore, HU-308 is among the CB_2 receptor agonists with the fewest off-target effects based on a panel of over 64 human proteins (Soethoudt et al. 2017). This suggests that HU-308 has the potential to specifically target CB_2 receptors *in vivo*. However, it is unclear whether the effects of HU-433 are mediated exclusively by CB_2 receptors. We found that a much greater concentration of the inverse agonist, SR144528, was required to suppress the recruitment of β-arrestin2 and mini-$G\alpha_i$ in response to HU-433 compared to HU-308. SR144528 also reversed the anti-inflammatory effects of HU-433 on microglia to a lesser degree relative to HU-308. The effects of HU-433 on mouse osteoblast proliferation were shown to be absent in CB_2 receptor-knockout mice (Smoum et al. 2015). However, anti-inflammatory effects through either CB_1 receptors or other receptors such as GPR55 have not been ruled out.

Despite enhanced effector protein recruitment upon treatment with HU-308, the enantiomer HU-433 had greater anti-inflammatory properties to counter the effects of LPS and IFNγ on cultured SIM-A9 microglia. These data support that microglial CB_2 receptors are a useful target to suppress the pro-inflammatory activity of microglia. Furthermore, these data highlight that properties such as β-arrestin recruitment are insufficient to judge the efficacy of a GPCR agonist, and that other properties including the signaling response may be more predictive of the functional activity.

4.5 Supplementary data

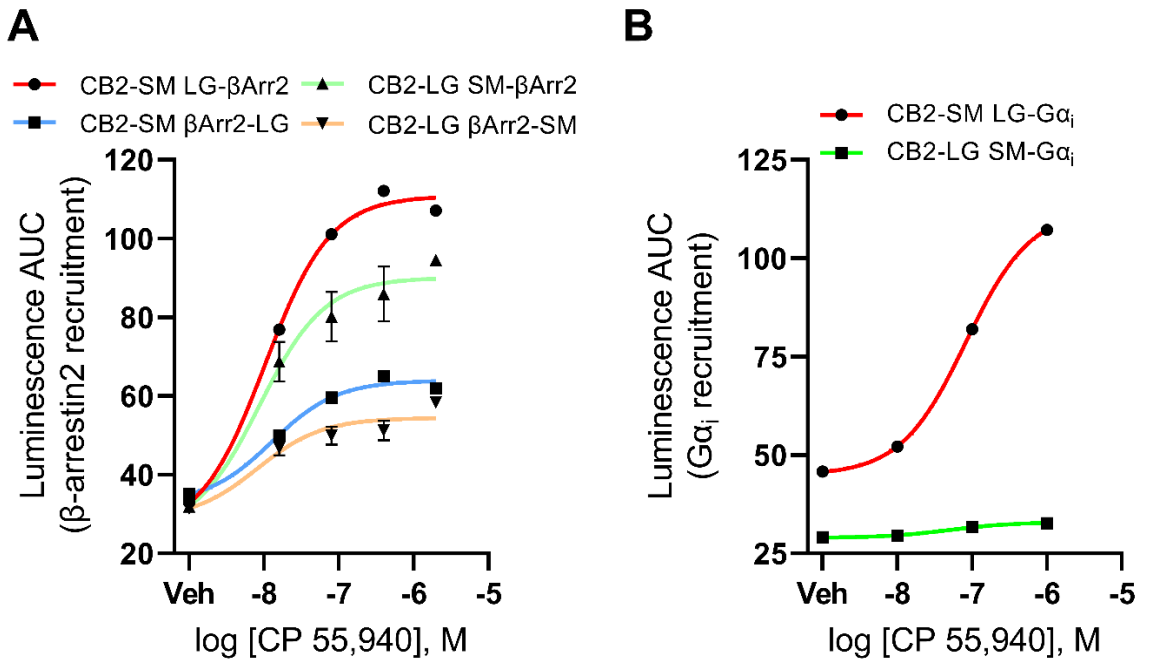

Figure 4. S1. Determination of proper orientations for small and large nanoluciferase fragments. A NanoBiT assays were performed using the human CB_2 receptor sequence fused to either the small (CB2-SM) or large (CB2-LG) fragment of nanoluciferase in conjunction with β-arrestin2 fused to either the small or large fragment fused to the N-terminal end (SM- and LG-βArr2, respectively) or the C-terminal end (βArr2-SM and -LG, respectively). **B** NanoBiT assays were performed using the CB_2 receptor sequence fused to the small or large fragment of nanoluciferase fused to the C-terminal end (CB2-SM and -LG, respectively) in conjunction with the mini-$G\alpha_i$ sequence with the small or large fragment of nanoluciferase fused to the N-terminal end (SM- and LG-$G\alpha_i$, respectively). Luminescence was recorded as a kinetic measurement over 42 min for β-arrestin2 and 30 min for $G\alpha_i$ and concentration-response curves were prepared from the area under the curve for each concentration of CP 55,940 which was used as the test agonist.

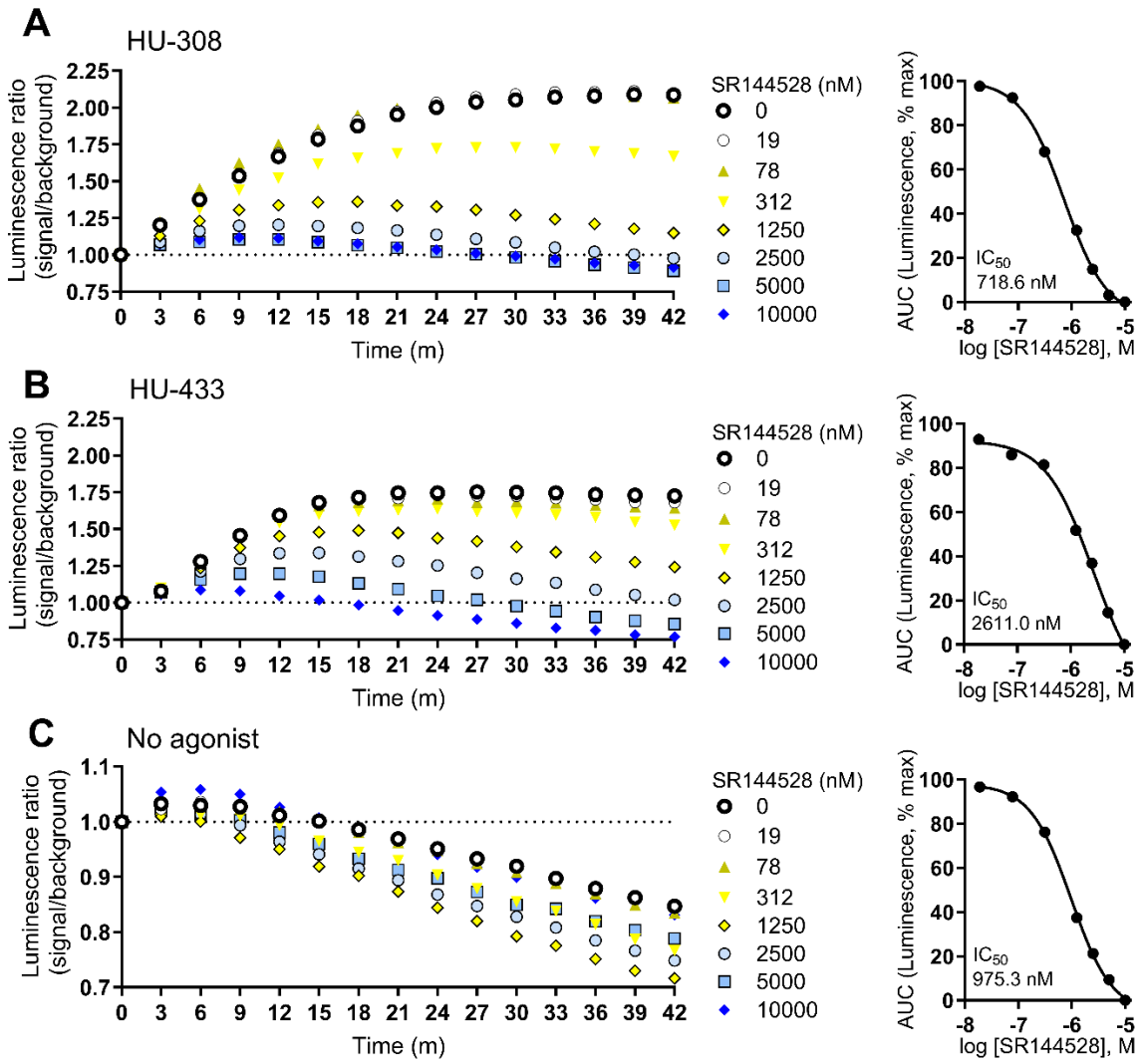

Figure 4. S2. Assessment of β-arrestin2 recruitment in response to SR144528. NanoBiT assays were performed in HEK 293T cells transfected with human CB_2 receptor fused to the small nanoluciferase fragment in conjunction with β-arrestin2 fused to the large nanoluciferase fragment at the N-terminal end. The effect of increasing concentrations of SR144528 (19 nM – 10 μM) on **A** HU-308 (1.8 μM), **B** HU-433 (5.9 μM), or **C** vehicle only on the recruitment of β-arrestin2 was determined over the course of 42 min. Areas under the curves (AUCs) were used to prepare concentration-response curves.

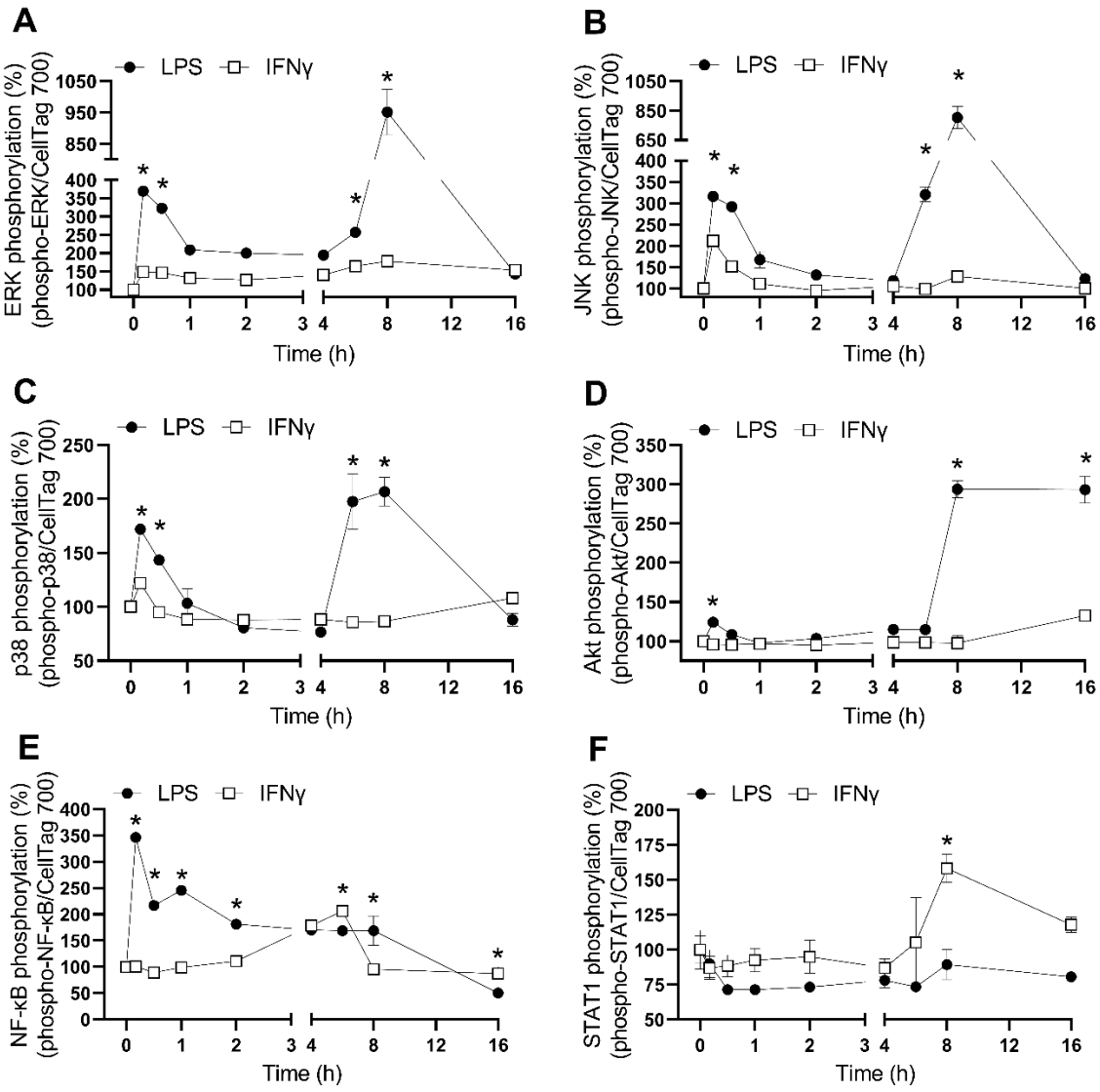

Figure 4. S3. Signaling kinetics of SIM-A9 microglia in response to LPS and IFNγ. Cultured SIM-A9 microglia were stimulated with LPS (1000 ng/mL) or IFNγ (20 ng/mL) over the course of 16 h, and in-cell western assays were used to monitor the phosphorylation of **A** ERK1/2, **B** JNK, **C** p38, **D** Akt, **E** NF-κB, **F** STAT1 (n = 4). Statistical significance was determined using two-way ANOVA with Tukey post-hoc test. * $p < 0.05$ vs. baseline (0 min).

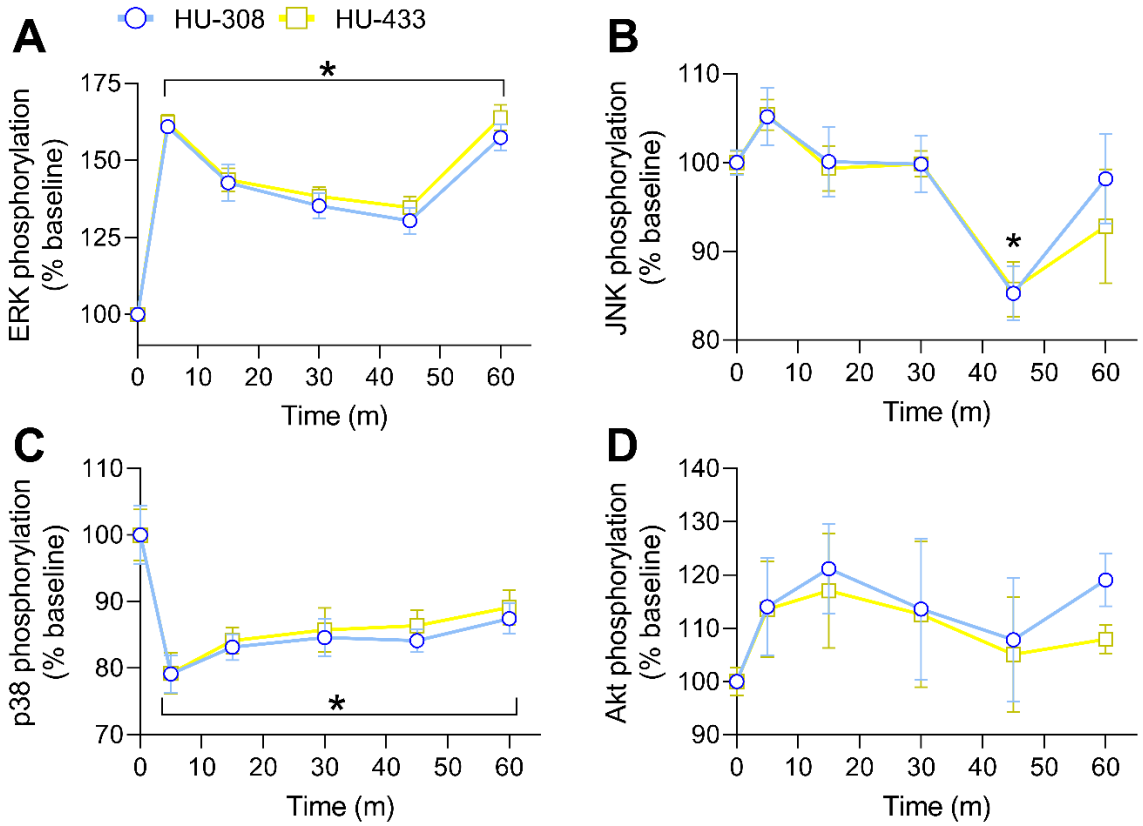

Figure 4. S4. Signaling kinetics of SIM-A9 microglia in response to HU-308 and HU-433. Cultured SIM-A9 microglia were stimulated with HU-308 or HU-433 (1 μM) over the course of 60 min, and in-cell western assays were used to monitor the phosphorylation of **A** ERK1/2, **B** JNK, **C** p38, **D** Akt (n = 4). Statistical significance was determined using two-way ANOVA with Tukey post-hoc test. * $p < 0.05$ vs. baseline (0 min).

Chapter 5: JAK1/2 regulates synergy between interferon gamma and lipopolysaccharides in microglia

Copyright statement

This article is in revision with the *Journal of Neuroimmune Pharmacology* and does not currently require copyright permission to be included in this thesis. The publication status of first-author articles included or excluded from this thesis are in Table A1 (Appendix A).

Contribution statement

All experiments were performed, and data were collected by myself. Analysis and interpretation of the data were performed in consultation Dr. Eileen Denovan-Wright. Preparation of the manuscript was done by me with support from Dr. Eileen Denovan-Wright.

Preface

This chapter investigates the pharmacological activity of LPS and IFNγ in microglia. The purposes of this chapter were to identify whether LPS and IFNγ acted on microglia in an additive or synergistic manner, and to determine which signaling pathways were likely the most critical to the microglial inflammatory response. Past reports of associations between altered gut microbiota and neurodegeneration also prompted the use of LPS from different bacteria that were considered more harmful or beneficial gut microbes.

5.1 Abstract

Microglia, the resident immune cells of the brain, regulate neuroinflammation which can lead to secondary neuronal damage and cognitive impairment under pathological conditions. Two of the many molecules that can elicit an inflammatory response from microglia are lipopolysaccharide (LPS), a component of gram-negative bacteria, and interferon gamma (IFNγ), an endogenous pro-inflammatory cytokine. We thoroughly examined the concentration-dependent relationship between LPS from multiple bacterial species and IFNγ in cultured microglia and macrophages. We measured the effects that these immunostimulatory molecules have on pro-inflammatory activity of microglia and used a battery of signaling inhibitors to identify the pathways that contribute to the microglial response. We found that LPS and IFNγ interacted synergistically to induce a pro-inflammatory phenotype in microglia, and that inhibition of JAK1/2 completely blunted the response. We determined that this synergistic action of LPS and IFNγ was likely dependent on JNK and Akt signaling rather than typical pro-inflammatory mediators such as NF-κB. Finally, we demonstrated that LPS derived from *Escherichia coli, Klebsiella pneumoniae,* and *Akkermansia muciniphila* can elicit different inflammatory responses from microglia and macrophages, but these responses could be consistently prevented using ruxolitinib, a JAK1/2 inhibitor. Collectively, this work reveals a mechanism by which microglia may become hyperactivated when levels of LPS and IFNγ rise above normal. Given that elevations in circulating LPS and IFNγ occur in a wide variety of pathological conditions, it is critical to understand the pharmacological interactions between these molecules to develop safe and effective treatments for neuroinflammation.

5.2 Introduction

Microglia are specialized brain-resident macrophages that are uniquely equipped to support neuronal function as well as regulate inflammatory processes (Nimmerjahn et al. 2005; Perry et al. 2010). Although microglia can suppress inflammation and promote tissue repair in the central nervous system, these cells are phenotypically plastic and are also the primary initiators and propagators of inflammation in the brain (Cherry et al. 2014). The pro-inflammatory activity of microglia is typically protective against pathogens or the aggregation of debris within the brain (Davalos et al. 2005; Lehnardt 2010). However, microglial hyperactivity accelerates neuronal death associated with chronic neurodegenerative diseases, like Alzheimer's disease (AD), as well as acute conditions such as sepsis-associated encephalopathy (Perry et al. 2010; Widmann and Heneka 2014; Guzman-Martinez et al. 2019). Although microglia regulate innate immunity in the brain, microglia are also sensitive to immunostimulatory molecules in peripheral circulation (Hoogland et al. 2015). By this mechanism, systemic inflammation induces the priming of microglia, resulting in a heightened pro-inflammatory response upon detection of a second stimulus. In this context, individuals with chronic systemic inflammation may be more susceptible to subsequent neurodegeneration, and likewise, individuals with established brain pathology may exhibit an exaggerated microglial response to peripheral infection (Perry and Holmes 2014; Brown 2019).

Interferon gamma (IFNγ), a pro-inflammatory cytokine, can be released by microglia as well as peripheral immune cells and is commonly elevated in patients with chronic inflammatory diseases such as type 2 diabetes, obesity, or rheumatoid arthritis (Kasahara et al. 1983; Ye et al. 1995; Tsiavou et al. 2005; Monteiro et al. 2017; Zhang et al. 2019a; Bradley et al. 2022). IFNγ serves as a primary activator of myeloid cells upon binding the interferon gamma receptor (IFNGR), and can prime microglia or macrophages for an enhanced response to other pro-inflammatory stimuli such as lipopolysaccharide (LPS)(Hayes et al. 1995; Held et al. 1999; Schroder et al. 2006; Monteiro et al. 2017). LPS is a component of gram-negative bacterial cell membranes that interacts with toll-like receptor 4 (TLR4), present on immune cells (Wright et al. 1990; Lu et al. 2008). When LPS enters the blood stream, it generates a systemic

inflammatory response and elicits sickness behavior in humans at relatively low concentrations (Rietschel et al. 1994; Sandiego et al. 2015). LPS may enter general circulation during acute bacterial infection or from the gut microbiome via damaged intestinal epithelia (Evans and Pollack 1993; van Langevelde et al. 1998). Although LPS and IFNγ have typically been investigated in the context of the peripheral immune system, both molecules interact with microglia, especially under conditions of systemic inflammation when the blood-brain barrier may be more permeable (Murray et al. 2011; Chai et al. 2014; Too et al. 2014; Banks et al. 2015; Vargas-Caraveo et al. 2017).

Some links have been drawn between circulating LPS and the development of neurodegenerative disease. High concentrations of LPS have been observed in the blood of patients with AD, and intestinal permeability is increased in Parkinson's disease (Zhang et al. 2009b; Forsyth et al. 2011). This highlights a potential mechanism whereby LPS enters peripheral circulation to induce neuroinflammation in concert with IFNγ. Combined stimulation with IFNγ and LPS has been demonstrated to elicit pro-inflammatory activity from microglia that induces neurotoxicity (Navarro et al. 2018a; Young and Denovan-Wright 2022b). However, the interactions between LPS and IFNγ at the level of microglial signaling are unclear which impedes the rational development of drugs to suppress neuroinflammation.

In this study, we addressed the hypothesis that LPS and IFNγ stimulate microglia to elicit a greater inflammatory response than treatment with either molecule alone. We also probed downstream signaling pathways to identify those most closely linked with the microglial response. LPS from multiple bacterial species, *Escherichia coli*, *Klebsiella pneumoniae*, and *Akkermansia muciniphila*, were also assessed to determine whether microglia and macrophage cells respond differently based on the source of LPS. We provide evidence that co-activation of TLR4 and IFNGR stimulates microglial-derived inflammation in a synergistic manner which can be prevented by blockade of Janus kinase 1 and 2 (JAK1/2) in microglia and macrophages, despite evidence that TLR4 does not primarily signal via the JAK-STAT pathway. These data highlight a single pharmacological target that may be used to nullify the pro-inflammatory activity of myeloid cells under a variety of pathological conditions.

5.3 Results

5.3.1. IFNγ and LPS from E. coli induce microglial inflammation in a synergistic manner

Although it has been well established that IFNγ and LPS elicit a pro-inflammatory response from microglia (Chhor et al. 2013; Navarro et al. 2018a; Young and Denovan-Wright 2022b), we aimed to determine whether the combination of both molecules would produce an additive, synergistic, or antagonistic response. Microglial cells were treated with increasing concentrations of IFNγ and LPS in combination with increasing concentrations of the other molecule. NO release was measured as a proxy for pro-inflammatory activity (Bal-Price and Brown 2001; Chhor et al. 2013).

IFNγ stimulated NO release from microglia in a concentration-dependent manner (Fig. 5. 1A). When LPS was added in combination, there was a concentration-dependent leftward shift in the curve as well as an increase in baseline and maximal NO release. Similarly, LPS induced NO release from microglia, and the potency as well as basal and maximal NO release was elevated in the presence of IFNγ at concentrations as low as 0.1 ng/mL (Fig. 5. 1B). NO release that was stimulated by IFNγ or LPS was completely blocked by the inducible nitric oxide synthase (iNOS) inhibitor, 1400W, which indicated that the reactive NO release was controlled by the inducible form of NOS (Fig. 5. S1)(Garvey et al. 1997).

To determine whether the microglial response to the combination of IFNγ and LPS was additive or synergistic, isobolograms were prepared from the EC_{50} values and a combination index analysis was performed. The combination index provides an indication of whether two molecules may act in a synergistic (< 1), additive (= 1), or antagonistic (> 1) manner (Chou and Talalay 1984; Chou 2006, 2018). The EC_{50} values were determined for IFNγ or LPS alone and in the presence of the other molecule (Fig. 5. 1C). The combination indices for IFNγ combined with increasing concentrations of LPS were 0.745 (0.05 ng/mL), 0.534 (0.5 ng/mL), and 0.343 (5 ng/mL). This indicated that the potency of IFNγ increased synergistically with increasing concentrations of LPS. The inverse experiments revealed a similar pattern as the combination indices for LPS combined with increasing concentrations of IFNγ were 0.813 (0.01 ng/mL), 0.459 (0.1

ng/mL), and 0.633 (1 ng/mL) (Fig. 5. 1D). This indicated that the addition of IFNγ also enhanced the potency of LPS in a synergistic manner. Taken together, these data suggest that IFNγ and LPS induced NO release from microglia in a synergistic manner, with pronounced effects even at relatively low concentrations.

Induction of mRNA for four pro-inflammatory markers was measured to further assess the microglial response to IFNγ and LPS. The mRNA markers used were *Nos2* (iNOS), *Tnf* (TNF), *Il6* (IL-6), and *Il1b* (IL-1β), as these markers are strongly associated with microglial pro-inflammatory activity (Chhor et al. 2013). Low, medium, and high concentrations of IFNγ or LPS relative to the maximal effect were chosen based on the concentration-response curves for NO release. These concentrations corresponded to 1, 5, and 20 ng/mL for IFNγ (Fig. 5. 1E) and 10, 100, and 1000 ng/mL for LPS (Fig. 5. 1F). *Nos2* was the only marker elevated by IFNγ and was only elevated by the highest concentration of IFNγ (Fig. 5. 1G). In contrast, LPS upregulated the mRNA abundance of *Nos2*, *Tnf*, *Il6*, and *Il1b* at all concentrations (Fig. 5. 1H-J). These data indicated that LPS was a more robust stimulus than IFNγ alone to elevate the mRNA abundance of specific pro-inflammatory markers in cultured microglia.

The measurements of mRNA abundance were repeated to assess whether combinations of IFNγ and LPS would produce different effects compared to either stimulus alone. SIM-A9 microglia were treated with a low concentration of IFNγ and a high concentration of LPS or vice versa. For comparison, cells were also treated with a high concentration of both stimuli. Treatment with high IFNγ (20 ng/mL) and low LPS (10 ng/mL) increased the mRNA for *Nos2*, *Tnf*, and *Il6* compared to the same concentration of IFNγ or LPS alone (Table 5. S1). This pattern was also observed upon treatment with low IFNγ (1 ng/mL) and high LPS (1000 ng/mL). When maximal concentrations of each were combined, *Nos2* and *Tnf* were elevated compared to any other combination of concentrations, but the same pattern was not observed for *Il6.* This suggests that TLR4 and IFNGR co-activation produces great increases in mRNA for some pro-inflammatory markers, especially *Nos2* and *Tnf*.

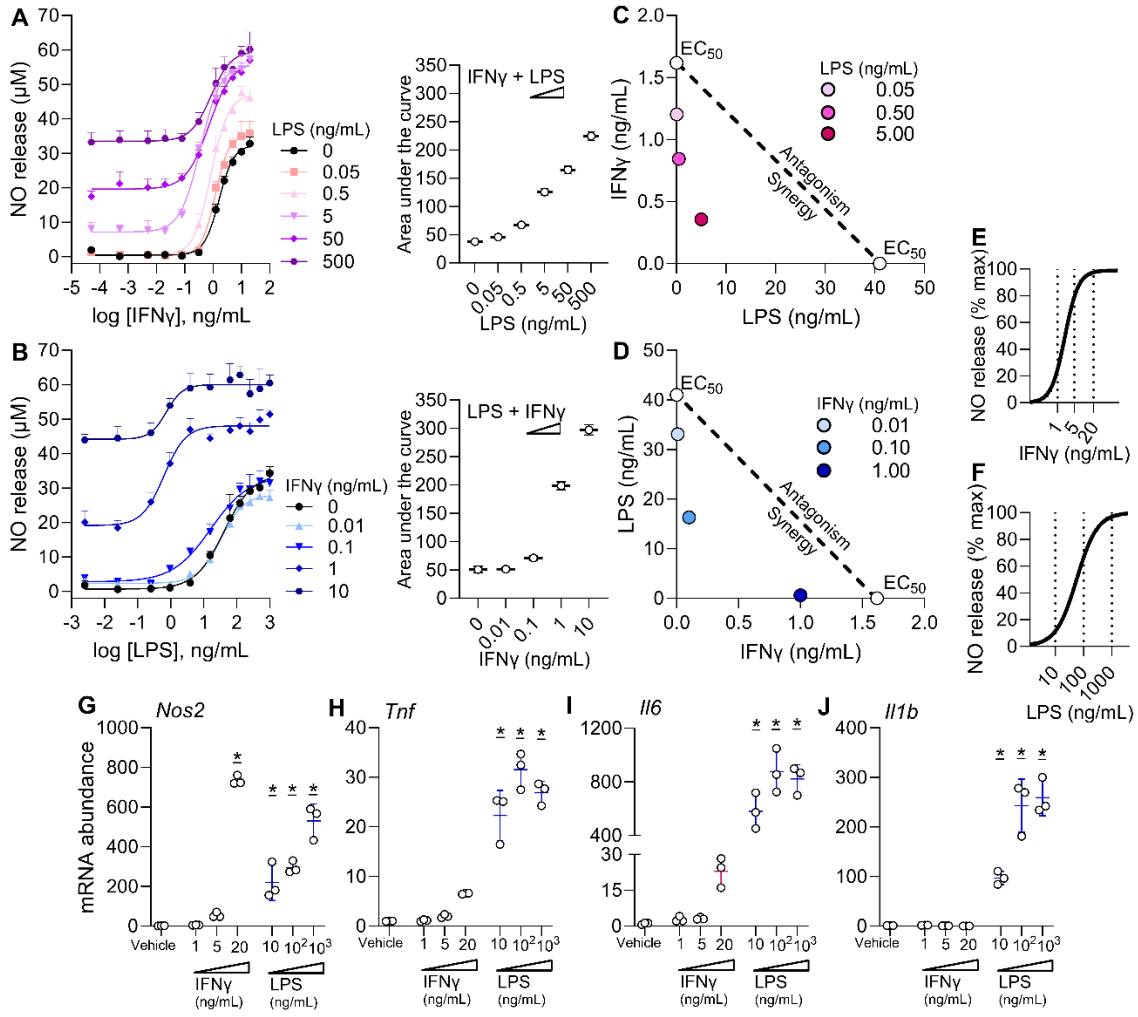

Figure 5. 1. IFNγ and LPS from *E. coli* stimulated a pro-inflammatory response from microglia in a concentration-dependent and synergistic manner. A SIM-A9 microglial cells were treated with increasing concentrations of IFNγ (50 fg/mL – 20 ng/mL) with vehicle (PBS) or increasing concentrations of LPS. **B** Microglial cells were treated with increasing concentrations of LPS (2.5 pg/mL – 1000 ng/mL) with vehicle (PBS) or increasing concentrations of IFNγ. NO release was monitored via the Griess assay (n = 4) after 16 h. Data points represent the means ± SEM. Area under the curve was calculated and plotted for each concentration-response curve. **C** An isobologram was prepared using EC_{50} values for IFNγ and LPS alone or IFNγ combined with LPS (0.05, 0.50, 5.00 ng/mL). **D** An isobologram was prepared using EC_{50} values for IFNγ and LPS alone or LPS combined with IFNγ (0.01, 0.10, 1.00 ng/mL). Combination indices were calculated for the co-treatments based on the method of Chou and Talalay (1984). The dashed line represents a predicted additive response whereby a position to the lower left of the dashed line indicates synergy and a position to the upper right of the dashed line indicates antagonism between the two molecules. Concentration-response curves for NO release were used to identify relatively low, medium, and high concentrations of **E** IFNγ (1, 5, or

20 ng/mL) or **F** LPS (10, 100, or 1000 ng/mL) to use in RT-qPCR experiments. The relative abundance of mRNA was quantified for **G** *Nos2*, **H** *Tnf*, **I** *Il1b*, and **J** *Il6* (n = 3) following treatment with IFNγ (1, 5, or 20 ng/mL) or LPS (10, 100, or 1000 ng/mL). The mRNA abundance is presented as the fold-change relative to vehicle. Statistical significance was determined using a one-way ANOVA with Dunnett's correction for multiple comparisons; * $p < 0.05$ vs. vehicle.

5.3.2. Synergy is consistent between IFNγ and LPS from K. pneumoniae and A. muciniphila

LPS from additional bacterial species, *K. pneumoniae* and *A. muciniphila*, were used to determine whether the bacterial species of origin would influence the observed synergy between TLR4 and IFNGR. We observed that IFNγ induced NO release in a concentration-dependent manner, and that the combination of LPS from *K. pneumoniae* increased both the maximal and the basal NO release (Fig. 5. 2A). The increase in basal NO release occurred at a concentration of 5 ng/mL and there was a decrease in the EC_{50} of IFNγ in the presence of only 0.05 ng/mL LPS from *K. pneumoniae* (Table 5. 1). A similar pattern was observed when the inverse experiments were performed as there was an increase in basal and maximal NO release as well as an increase in the potency of LPS from *K. pneumoniae* when combined with increasing concentrations of IFNγ (Fig. 5. 2B). When the concentration-response curves of LPS from *K. pneumoniae* were combined with increasing concentrations of IFNγ, there was a shift in the combination index from 0.885 (0.001 ng/mL) to 0.317 (1 ng/mL) which indicated that the potency of LPS from *K. pneumoniae* was increasingly enhanced by increasing concentrations of IFNγ (Fig. 5. 2C).

The same experiments were performed using LPS from *A. muciniphila* as this species of bacteria has been demonstrated to be a beneficial gut microbe rather than a potential pathogen (Zhou 2017). As with LPS from *E. coli* and *K. pneumoniae*, LPS from *A. muciniphila* enhanced the IFNγ-mediated NO release from SIM-A9 microglia. However, basal NO release was only influenced at a concentration of 500 ng/mL LPS, and the potency of IFNγ was only increased by the LPS from *A. muciniphila* at a concentration of 5 ng/mL (Fig. 5. 2D). This indicated that LPS from *A. muciniphila* had less of a potentiation effect on IFNγ compared to LPS from *E. coli* or *K. pneumoniae*. Similarly, a higher concentration of IFNγ was required to enhance the effects of LPS from *A. muciniphila* compared to LPS from *K. pneumoniae* (Fig. 5. 2E)(Table 5. 1). When the concentration-response curves of LPS from *A. muciniphila* were combined with increasing concentrations of IFNγ, there was a shift in the combination index from

0.743 (0.001 ng/mL) to 0.290 (1 ng/mL) which indicated that the potency of LPS was enhanced by increasing concentrations of IFNγ (Fig. 5. 2F)(Table 5. 1).

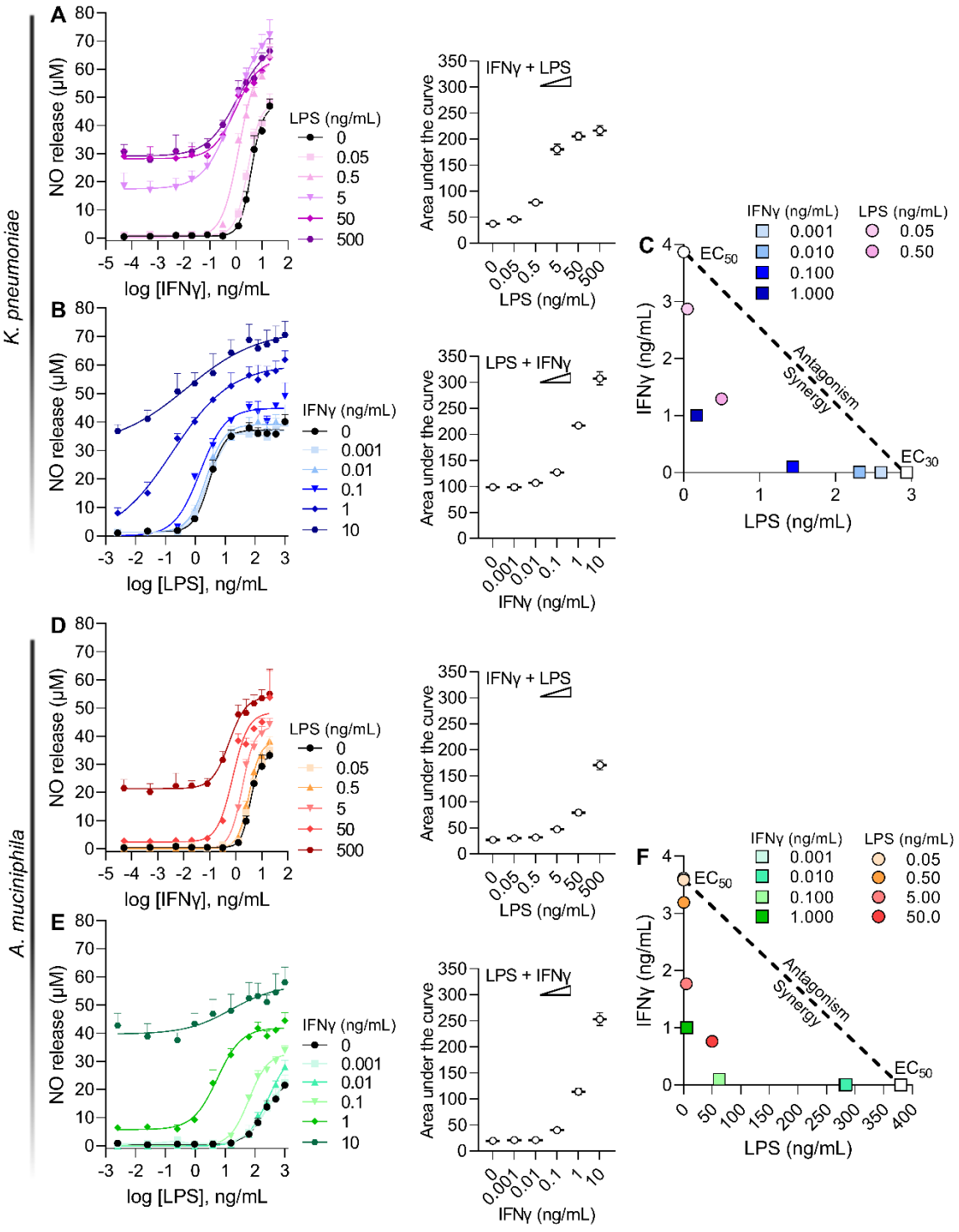
K. pneumoniae
A
NO release (μM)
log [IFNγ], ng/mL
LPS (ng/mL)
0
0.05
0.5
5
50
500
B
log [LPS], ng/mL
IFNγ (ng/mL)
0
0.001
0.01
0.1
1
10
IFNγ + LPS
Area under the curve
LPS (ng/mL)
LPS + IFNγ
IFNγ (ng/mL)
C
EC50
EC30
Antagonism
Synergy
IFNγ (ng/mL)
LPS (ng/mL)
0.001
0.010
0.100
1.000
0.05
0.50
A. muciniphila
D
E
F
5.00
50.0

Figure 5. 2. LPS from *K. pneumoniae* and *A. muciniphila* acted synergistically with IFNγ to induce NO release from SIM-A9 microglial cells. A SIM-A9 microglial cells were treated with increasing concentrations of IFNγ (50 fg/mL – 20 ng/mL) with vehicle (PBS) or increasing concentrations of LPS from *K. pneumoniae*. **B** Microglial cells were treated with increasing concentrations of LPS from *K. pneumoniae* (2.5 pg/mL – 1000 ng/mL) with vehicle (PBS) or increasing concentrations of IFNγ. **C** An isobologram was prepared using EC_{50} values for IFNγ combined with LPS (0, 0.05, 0.5 ng/mL) or LPS combined with IFNγ (0, 0.001, 0.01, 0.1, 1 ng/mL). **D** SIM-A9 microglial cells were treated with increasing concentrations of IFNγ (50 fg/mL – 20 ng/mL) with vehicle (PBS) or increasing concentrations of LPS from *A. muciniphila*. **E** Microglial cells were treated with increasing concentrations of LPS from *A. muciniphila* (2.5 pg/mL – 1000 ng/mL) with vehicle (PBS) or increasing concentrations of IFNγ. **F** An isobologram was prepared using EC_{50} values for IFNγ combined with LPS (0, 0.05, 0.5, 5, 50 ng/mL) or LPS combined with IFNγ (0, 0.001, 0.01, 0.1, 1 ng/mL). In all cases, NO release was measured using the Griess assay 16 h following the treatment (n = 4). Data points represent the means ± SEM. Area under the curves were calculated and plotted for each concentration-response curve.

Table 5. 1. SIM-A9 microglia were treated with increasing concentrations of IFNγ or LPS in the presence of multiple concentrations of the other molecule (n = 4). Minimum NO release (E_{min}), maximal NO release (E_{max}), and the EC_{50} were calculated using nonlinear regression with four-parameter analysis. The combination indices were determined for the EC_{50} of IFNγ and LPS the presence of multiple concentrations of the other molecule. Combination indices could not be calculated when the concentration of the concurrent treatment exceeded its EC_{50}. The E_{min}, E_{max} and EC_{50} are presented as the 95% confidence intervals (CI).

Treatment[a]	**Concurrent treatment**	**E_{min} (NO, µM)**	**E_{max} (NO, µM)**	**EC_{50} (ng/mL)**	**Combination index**
	LPS from *E. coli* (ng/mL)				
IFNγ	0	-0.11 to 0.97	31.25 to 33.74	1.474 to 1.783	1
	0.05	-0.51 to 1.24	33.98 to 37.30*	1.055 to 1.373*	0.745
	0.5	-0.65 to 1.28	45.43 to 48.90*	0.740 to 0.960*	0.534
	5	5.58 to 8.63*	53.62 to 58.20*	0.291 to 0.443*	0.343
	50	18.29 to 20.82*	54.22 to 59.81*	0.562 to 0.943*	-
	500	31.99 to 34.92*	57.18 to 64.04*	0.578 to 1.336*	-
	IFNγ (ng/mL)				
LPS from *E. coli*	0	-0.62 to 1.86	31.53 to 37.77	30.26 to 58.25	1
	0.01	1.54 to 3.13	26.84 to 29.50	27.11 to 40.26	0.813
	0.1	1.14 to 4.22	31.20 to 36.83^	10.84 to 25.80^	0.459
	1	16.76 to 21.28^	46.84 to 49.34^	0.45 to 0.85^	0.633
	10	41.49 to 46.63^	58.58 to 61.51^	0.40 to 1.34^	-
	LPS from *K. pneumoniae* (ng/mL)				
IFNγ	0	-0.3136 to 1.648	43.76 to 51.06	0.5335 to 0.6554	1
	0.05	0.2366 to 1.775	45.73 to 50.60	0.4164 to 0.5053*	0.758
	0.5	-1.082 to 1.640	60.03 to 67.14*	0.04661 to 0.1831*	0.504

Treatment[a]	Concurrent treatment	E_{min} (NO, µM)	E_{max} (NO, µM)	EC_{50} (ng/mL)	Combination index
	5	15.16 to 19.53*	71.38 to 86.20*	-0.1966 to 0.1947*	-
	50	26.47 to 29.82*	59.76 to 71.06*	-0.1859 to 0.2642*	-
	500	26.82 to 31.17*	63.91 to 84.62*	-0.2048 to 0.5614	-
	IFNγ (ng/mL)				
LPS from *K. pneumoniae*	0	-0.3136 to 1.648	43.76 to 51.06	0.5335 to 0.6554	1
	0.001	0.2366 to 1.775	45.73 to 50.60	0.4164 to 0.5053^	0.885
	0.01	-1.082 to 1.640	60.03 to 67.14^	0.04661 to 0.1831^	0.791
	0.1	15.16 to 19.53^	71.38 to 86.20^	-0.1966 to 0.1947^	0.515
	1	26.47 to 29.82^	59.76 to 71.06^	-0.1859 to 0.2642^	0.317
	10	26.82 to 31.17^	63.91 to 84.62^	-0.2048 to 0.5614	-
	LPS from *A. muciniphila* (ng/mL)				
IFNγ	0	-0.1857 to 1.017	31.35 to 34.64	0.5210 to 0.5984	1
	0.05	-0.2169 to 1.433	32.81 to 38.26	0.4965 to 0.6237	0.991
	0.5	-0.3372 to 0.4994	36.89 to 39.43*	0.4770 to 0.5329	0.884
	5	-0.6463 to 0.7297	41.80 to 45.03*	0.2127 to 0.2843*	0.502
	50	0.2994 to 4.408	44.73 to 53.83*	-0.2404 to 0.0278*	0.342
	500	19.28 to 23.28*	51.16 to 58.30*	-0.4241 to -0.0807*	-
	IFNγ (ng/mL)				
LPS from *A. muciniphila*	0	0.0028 to 0.96	21.64 to 29.51	179.50 to 358.31	1
	0.001	-0.11 to 1.43	22.15 to 42.74	182.83 to 851.43	0.743
	0.01	-0.59 to 0.33	30.61 to 39.88*	226.07 to 401.48	0.751

Treatment[a]	Concurrent treatment	E_{min} (NO, µM)	E_{max} (NO, µM)	EC_{50} (ng/mL)	Combination index
	0.1	-0.75 to 0.53	31.53 to 34.66*	55.19 to 71.60*	0.192
	1	4.15 to 7.24*	40.49 to 43.61*	4.24 to 7.06*	0.290
	10	22.66 to 42.76*	52.19 to n.d.*	1.969 to n.d.	-

[a] Applied as a concentration-response curve

* Significantly different from IFNγ alone as indicated by non-overlapping 95% CI.

^ Significantly different from LPS alone as indicated by non-overlapping 95% CI.

5.3.3. JAK1/2 exerts control over the microglial response to IFNγ and LPS

IFNGR signaling is transduced via JAK1 and JAK2 whereas TLR4 signals primarily via myeloid differentiation primary response 88 (MyD88)(Vogel et al. 2003; Schroder et al. 2004, 2006). Despite little overlap in upstream effector proteins, the receptors share several downstream signaling pathways activated by IFNγ and LPS, including NF-κB and MAP kinases (MAPKs)(Fig. 5. 3A). We hypothesized that if there was no crosstalk between IFNGR and TLR4 signaling, then inhibition of JAK1/2 would block only IFNγ-mediated effects and inhibition of MyD88 would block only LPS-mediated effects. To test this, microglia were stimulated using fixed concentrations of IFNγ and LPS alone or in combination. These treatments were delivered concurrently with TAK-242 or ruxolitinib. TAK-242 is a selective inhibitor of TLR4 that disrupts the interaction with MyD88 to suppress LPS-mediated signaling (Takashima et al. 2009; Matsunaga et al. 2011). Ruxolitinib is a dual inhibitor of JAK1 and JAK2 that suppresses signaling mediated by IFNγ and other JAK-dependent cytokines, such as IL-6 (Quintás-Cardama et al. 2010; Albeituni et al. 2019).

We observed that inhibition of TLR4 prevented the response to LPS, however, it did not block the microglial response to IFNγ. TAK-242 suppressed LPS-mediated NO release with an IC_{50} of 36.48 nM (Fig. 5. 3B). In the presence of a moderate concentration of IFNγ (5 ng/mL), the IC_{50} of TAK-242 was 1.62 μM, a shift of nearly 45-fold, this also increased the total AUC (Fig. 5. S2A). When microglia were treated with IFNγ alone, TAK-242 inhibited IFNγ-mediated NO release with an IC_{50} of 32.81 μM which is three orders of magnitude higher than the inhibition of LPS and may be indicative of nonspecific effects at extremely high concentrations (Fig. 5. 3C). These results were expected as TAK-242 is known to inhibit TLR4 but has not been shown to influence IFNGR or IFNγ-mediated signaling.

The inverse experiments revealed that inhibition of JAK1/2 using ruxolitinib blocked the microglial response to IFNγ and LPS when presented alone or in combination. Ruxolitinib inhibited IFNγ-mediated NO release with an IC_{50} of 320.63 nM (Fig. 5. 3D). In the presence of additional LPS (50 ng/mL), the IC_{50} of ruxolitinib was shifted only to 397.19 nM which was not different from IFNγ alone, and there was no

change in the total AUC (Fig. 5. S2B). This indicated that inhibition of JAK1/2 completely prevented NO release in response to IFNγ, even in the presence of LPS, without a loss in potency or efficacy. When microglia were stimulated with LPS alone, ruxolitinib inhibited NO release with an IC_{50} of 26.48 nM (Fig. 5. 3E). These data indicated that inhibition of IFNGR signaling via blockade of JAK1/2 could blunt the pro-inflammatory effects of IFNγ and LPS when presented to microglia alone or in combination.

We assessed the effects of TLR4 or JAK1/2 inhibition with respect to the secondary effects on cultured ST*Hdh*$^{Q7/Q7}$ neuronal cells. We approached this using a conditioned media system as previously described (Young and Denovan-Wright 2022b). ST*Hdh*$^{Q7/Q7}$ cells were treated with media from SIM-A9 microglia that had been previously treated with LPS or IFNγ in combination with vehicle, TAK-242, or ruxolitinib. ATP concentrations were measured as a proxy for cell viability. When ST*Hdh*$^{Q7/Q7}$ cultures were exposed to media from microglia previously treated with LPS, the ATP concentration fell from 0.99 ± 0.06 μM to 0.17 ± 0.03 μM, and the ATP concentration was 0.29 ± 0.05 μM upon exposure to media from microglia that were treated with IFNγ (Fig. 5. 3F). However, direct exposure of ST*Hdh*$^{Q7/Q7}$ cells to LPS or IFNγ had no effect on cell viability which suggested that cell death was a result of microglial-secreted factors (data not shown). Co-treatment with either TAK-242 or ruxolitinib attenuated the effects of LPS-conditioned media on ST*Hdh*$^{Q7/Q7}$ cell viability. However, only ruxolitinib blunted the effects of IFNγ-conditioned media whereas TAK-242 had no effect. A similar pattern was observed for the glutamate-mediated calcium uptake in ST*Hdh*$^{Q7/Q7}$ cells. Conditioned media from microglia that were treated with LPS induced a loss of glutamate-mediated calcium uptake which was likely a result of the reduced number of viable cells (Fig. 5. 3G). As observed with NO release and secondary neuronal death, TAK-242 and ruxolitinib each blocked the LPS-mediated effects on calcium uptake in ST*Hdh*$^{Q7/Q7}$ cells. Conditioned media from microglia that were treated with IFNγ also reduced calcium uptake in ST*Hdh*$^{Q7/Q7}$ cells. These effects were partially blocked by TAK-242 but completely reversed by ruxolitinib (Fig. 5. 3H). Together, these

data were consistent with the notion that blockade of JAK1/2 is sufficient to inhibit LPS-mediated effects in microglia.

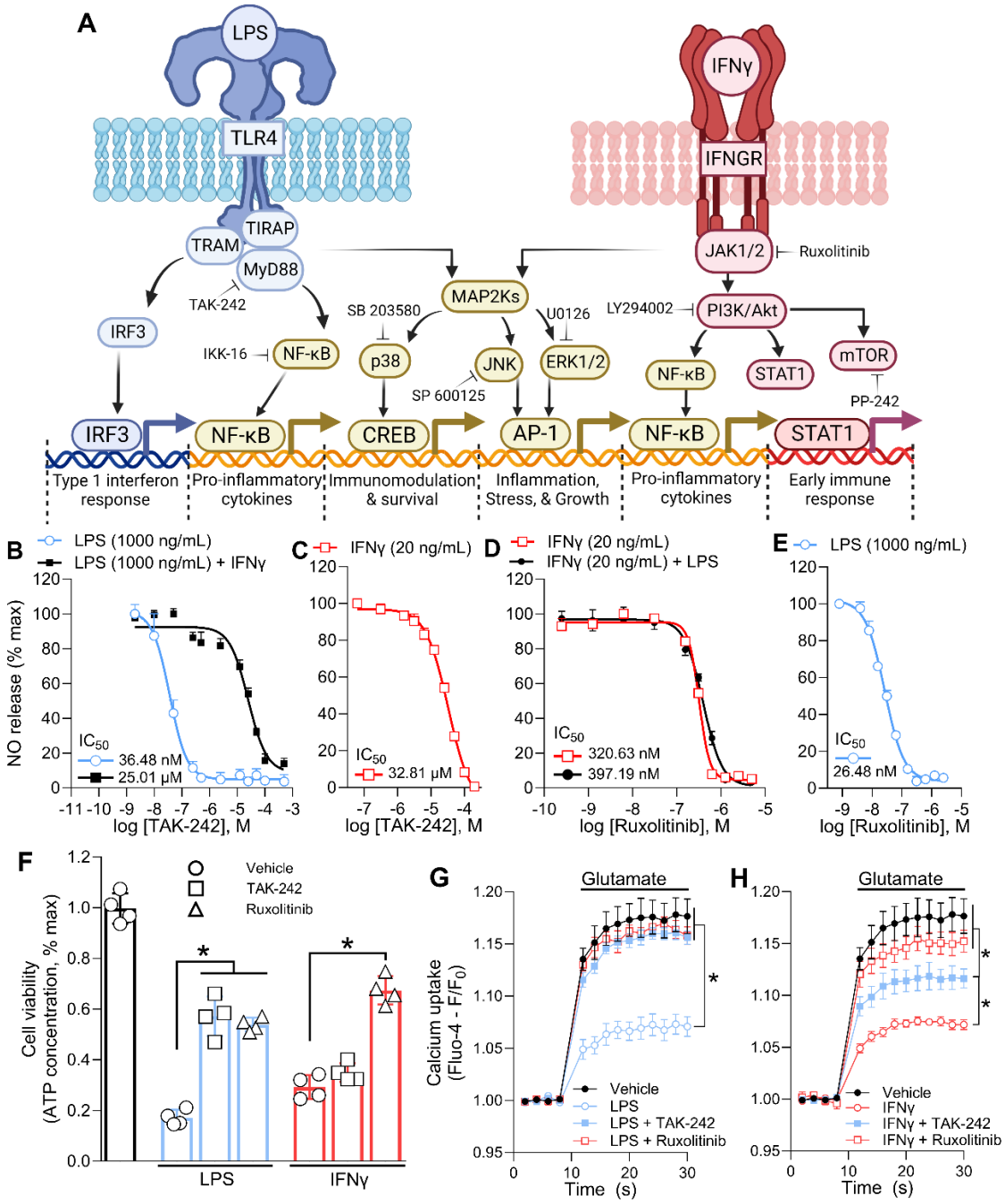

Figure 5. 3. JAK1/2 inhibition negatively regulates TLR4-mediated signaling in microglia but not vice-versa. A Microglia exhibit substantial overlap in canonical signaling pathways. Blue and red colors indicate signaling pathways specific to TLR4 and IFNGR, respectively, whereas gold colour indicates signaling pathways known to overlap. All signaling inhibitors used within the study are indicated. Created with BioRender. **B** Microglia were stimulated with LPS (1000 ng/mL) alone or in combination with IFNγ (5

ng/mL) in the presence of increasing concentrations of a TLR4 signaling inhibitor, TAK-242 (2 nM – 500 μM). **C** Microglia were stimulated with IFNγ (20 ng/mL) in the presence of TAK-242 (60 nM – 200 μM). **D** Microglia were stimulated with IFNγ alone (20 ng/mL) or in combination with LPS (50 ng/mL) in the presence of increasing concentrations of a selective JAK1/2 inhibitor, ruxolitinib (200 pM – 5 μM). **E** Microglia were stimulated with LPS (1000 ng/mL) in the presence of ruxolitinib (1 nM – 10 μM). **F** Microglia were stimulated with vehicle, or LPS (1000 ng/mL) or IFNγ (20 ng/mL) in conjunction with TAK-242 (1 μM) or ruxolitinib (1 μM) to generate conditioned media. The conditioned media was applied to ST*Hdh*$^{Q7/Q7}$ neuronal cells and cell viability was measured after 24 h (n = 4). * $p \leq 0.05$ as determined by one-way ANOVA with Tukey *post-hoc* test. ST*Hdh*$^{Q7/Q7}$ neuronal cells were incubated for 24 h with conditioned media from microglia that had been treated with **G** LPS (1000 ng/mL) or **H** IFNγ (20 ng/mL) in conjunction with TAK-242 (1 μM) or ruxolitinib (1 μM). Calcium uptake in response to glutamate (500 μM) was then measured using fluo-4 calcium-sensitive dye (n = 4). Significance was determined using 95% confidence intervals of the area under the curve.

5.3.4. Bacterial species of origin influences the pro-inflammatory effect of LPS on microglia

The structure of LPS can differ among gram-negative bacterial species which creates opportunities for differential effects upon interaction with TLR4 (Mohr et al. 2022). *K. pneumoniae* is part of a normal microbiome in many humans but may also cause community-associated infections, including pneumonia (Calfee 2017). In contrast, *A. muciniphila* is inversely correlated with the onset of obesity and diabetes and is known as a beneficial gut microbe (Zhou 2017). Thus, we compared the pro-inflammatory effects of LPS from *K. pneumoniae* and *A. muciniphila* in addition to *E. coli*. We observed that LPS from *K. pneumoniae* stimulated microglia with the greatest potency (EC_{50}; 2.13 ng/mL) and efficacy whereas LPS from *A. muciniphila* was the least potent (EC_{50}; 33.67 ng/mL) but elicited a similar response to LPS from *E. coli* at the highest concentration (Fig. 5. 4A).

To better understand the spectrum of species-specific effects, microglia were treated with LPS (100 ng/mL) from *K. pneumoniae*, *E. coli*, or *A. muciniphila* and microglia were profiled for an array of functional markers. LPS from all three species upregulated the mRNA for *Nos2, Tnf, Il6, Il1b,* and *Ccl2* (Fig. 5. 4B). However, LPS from *A. muciniphila* elicited a smaller response with respect to upregulation of *Tnf*, *Il1b*, and *Il6* compared to LPS from other species (Table 5. S2). Furthermore, LPS from *E. coli* and *A. muciniphila* upregulated *Nos2* mRNA to a similar degree which was less than LPS from *K. pneumoniae*. This coincides with the observation that LPS from *K. pneumoniae* elicited greater NO release compared to LPS from *E. coli* and *A. muciniphila*. LPS from all species upregulated *Csf3* but LPS from *A. muciniphila* had the smallest effect (Fig. 5. 4C). Furthermore, LPS from *A. muciniphila* was the only type to upregulate *Sirpa* and *Cd11b* which are phagocytic markers. LPS from all species induced a reduction in mRNA abundance for the microglial homeostatic markers, *Cx3cr1* and *P2ry12*. There was no effect on anti-inflammatory markers (*Arg1, Cd206, Fizz1, Il10*) from LPS of any species or IFNγ (data not shown).

At a stimulatory concentration of 100 ng/mL, conditioned media from microglia stimulated with *K. pneumoniae* LPS induced the greatest proportion of cell death in

cultured ST*Hdh*$^{Q7/Q7}$ neuronal cells (Fig. 5. 4D). In contrast, conditioned media from microglia stimulated with *A. muciniphila* LPS was the least damaging to cultured neurons. Together, these data suggest that LPS from *K. pneumoniae* elicited the greatest pro-inflammatory response from microglia and LPS from *A. muciniphila* had the smallest effect, whereas LPS from *E. coli* had a comparatively moderate effect. Regardless of species of origin, ruxolitinib blocked the LPS-mediated NO release in a concentration-dependent manner (Fig. 5. 4E). Ruxolitinib most potently blocked the effects of LPS from *A. muciniphila* (IC_{50}; 12.33 nM) and was the least potent against LPS from *K. pneumoniae* (IC_{50}; 45.31 nM). Thus, the effects mediated by LPS from all species were ultimately sensitive to the inhibition of JAK1/2.

We next aimed to assess whether LPS from multiple bacterial species could elicit a stronger pro-inflammatory response compared to a single form. The cells were first exposed to the EC_{50} of LPS from one species with increasing concentrations of LPS from another species. We observed that combining LPS from multiple bacterial species elicited a response from microglia that was comparable to the expected maximal effect from a single form of LPS (Fig. 5. 4F). The experiments were repeated using the EC_{max} of one type of LPS with increasing concentrations of another. We observed that once the E_{max} was reached using LPS from *K. pneumoniae* or *E. coli*, addition of a different LPS had no effect on NO release (Fig. 5. 4G). However, when cells were treated with the EC_{max} of *A. muciniphila*, addition of LPS from *E. coli* or *K. pneumoniae* induced a further increase in NO release. Thus, once the pro-inflammatory effect was saturated by LPS from *E. coli* or *K. pneumoniae*, further addition of another type of LPS had no effect. However, when a saturating concentration of *A. muciniphila* was used, subsequent addition of LPS from *E. coli* or *K. pneumoniae* induced a greater effect. This may be suggestive of differences in the affinity of different types of LPS for TLR4, or differences in the proportion of total TLR4 that each LPS must bind to reach the maximal effect.

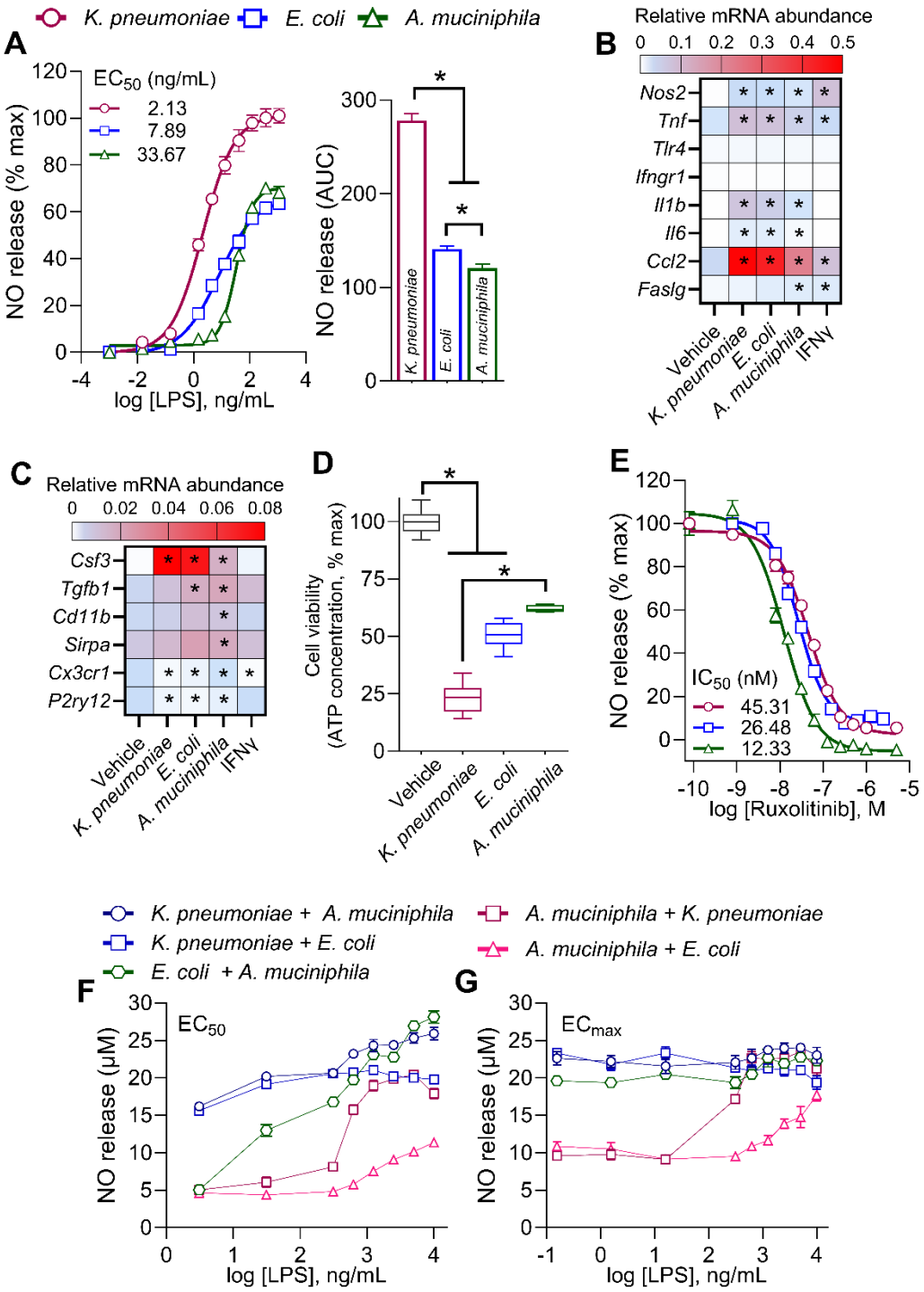

Figure 5. 4. Lipopolysaccharides from *E. coli*, *K. pneumoniae*, and *A. muciniphila* stimulate microglia in a JAK1/2-sensitive manner. A SIM-A9 microglial cells were stimulated with LPS from *E. coli*, *K. pneumoniae*, and *A. muciniphila* (1 pg/mL – 1111 ng/mL) and NO release was measured after 16 h (n = 4). Data points represent the mean ± SEM. Significant differences between areas under the curve (AUC) are indicated by an

asterisk and were determined using non-overlapping 95% confidence intervals. SIM-A9 cells were treated with 100 ng/mL LPS from *E. coli*, *K. pneumoniae*, or *A. muciniphila* or 5 ng/mL IFNγ for 16 h and the mRNA for **B** pro-inflammatory or **C** other functional microglial markers was assessed (n = 4). * $p \leq 0.05$ vs. vehicle as determined by non-overlapping confidence intervals. **D** Conditioned media from microglia that received the same treatment was applied to ST*Hdh*$^{Q7/Q7}$ neuronal cells, cell viability was measured after 24 h (n = 8). * $p \leq 0.05$ as determined by one-way ANOVA with Tukey *post-hoc* test. **E** SIM-A9 cells were treated with the EC_{80} of LPS from each species with increasing concentrations of ruxolitinib, a selective JAK1/2 inhibitor, and NO release was measured after 16 h (n = 4). Data points represent the mean ± SEM. SIM-A9 cells were treated with the **F** EC_{50} or **G** EC_{max} of LPS from one bacterial species in combination with an increasing concentration of LPS from another species, as indicated, and NO release was measured after 16 h (n = 4). Data points represent the mean ± SEM.

5.3.5. Crosstalk between IFNGR and TLR4 is distinct among downstream signaling pathways

We dissected the crosstalk between IFNGR and TLR4 in microglia using a battery of inhibitors for known signaling pathways downstream of MyD88 and JAK1/2. This included specific inhibitors of JNK, Akt, ERK, mTOR, NF-κB, and p38. NO release was used as a proxy for pro-inflammatory activity as induction of iNOS and subsequent NO release is tightly linked to microglial inflammatory activity (Bal-Price and Brown 2001; Chhor et al. 2013; Young and Denovan-Wright 2022a, 2022c). We hypothesized that if a specific pathway contributed to the synergy between IFNγ and LPS, combination of both stimuli would produce a rightward shift in the concentration-response curve. In contrast, if a pathway does not contribute to the synergy between IFNγ and LPS, we would expect inhibition of that pathway to have a similar effect on NO release regardless of whether IFNγ and LPS are presented alone or in combination.

Signaling inhibition experiments were performed using LPS alone or in the presence of IFNγ and vice-versa. Inhibition of JNK and Akt effectively blocked NO release mediated by LPS or IFNγ alone with reduced efficacy and a rightward shift in the IC_{50}s when stimuli were presented together (Fig. 5. 5A-D). The bidirectional reduction in potency and efficacy was clear upon quantification of the AUC for all concentration-response curves. Inhibition of ERK signaling blocked both LPS and IFNγ-mediated NO release but the curve was only shifted when the IFNγ treatment was spiked with LPS and not vice-versa (Fig. 5. 5E-F). Conversely, mTOR inhibition shifted the curve to the right only when LPS was spiked with IFNγ (Fig. 5. 5G-H). Inhibition of NF-κB-mediated signaling blocked NO release regardless of the stimulus, but the IC_{50} values and AUC were not affected when both stimuli were presented together (Fig. 5. 5I-J). Finally, inhibition of p38 did not produce a measurable reduction in NO release from microglia (Fig. 5. 5K-L). These data suggest that JNK and Akt facilitate synergy between TLR4 and IFNGR whereas crosstalk may be unidirectional and more selective at the level of ERK and mTOR signaling, with no crosstalk observed at the level of NF-κB or p38 (Table 5. S3).

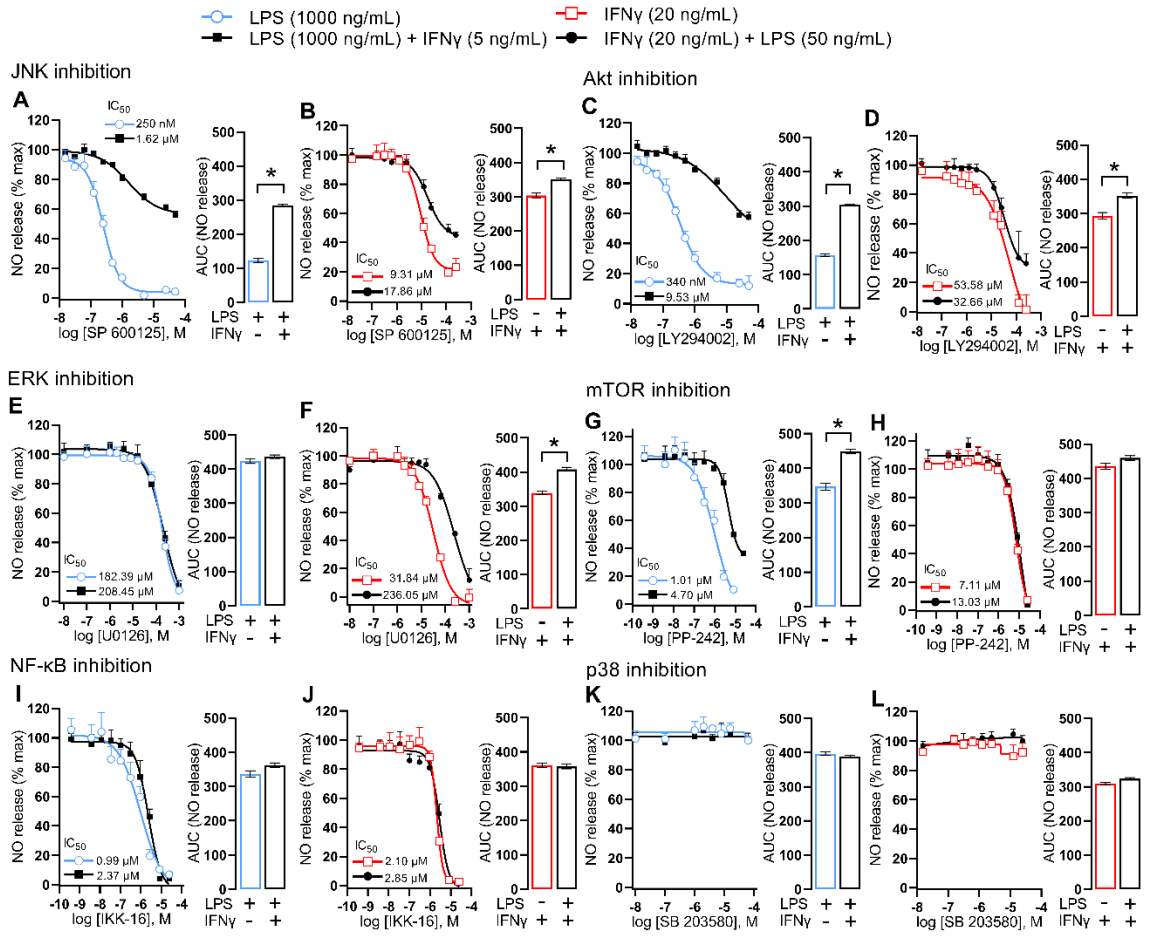

Figure 5. 5. Inhibition of pathways downstream of TLR4 and IFNGR signaling differentially influences NO release from microglia stimulated with LPS and/or IFNγ. SIM-A9 microglia were stimulated with LPS (1000 ng/mL) alone or with IFNγ (5 ng/mL). Alternatively, microglia were stimulated with IFNγ (20 ng/mL) alone or with LPS (50 ng/mL) (n = 4). Microglia were concurrently treated with increasing concentrations of inhibitors for **A-B** JNK (SP 600125; 15 nM – 250 µM), **C-D** PI3K-Akt (LY294002; 15 nM – 250 µM), **E-F** ERK (U0126; 10 nM – 1 mM), **G-H** mTOR (PP-242; 380 pM – 25 µM), **I-J** NF-κB (IKK-16; 380 pM – 25 µM), or **K-L** p38 (SB 203580; 15 nM – 25 µM). Data points represent the mean ± SD. Significant differences between areas under the curve (AUC) are indicated by an asterisk and were determined using non-overlapping 95% confidence intervals.

5.3.6. JAK1/2 blockade inhibits LPS-mediated NO release in cultured macrophages

Microglia and macrophages have a shared developmental origin and exhibit many similar properties with respect to innate immune function (Ginhoux et al. 2010). We used cultured RAW 264.7 macrophages to determine whether LPS from different bacterial species and inhibition of JAK1/2 would produce similar results compared to microglia. As with the microglia, we found that LPS from *K. pneumoniae* stimulated the macrophage cells with the greatest potency (EC_{50}; 4.14 ng/mL) and LPS from *A. muciniphila* was the least potent (EC_{50}; 17.41 ng/mL) (Fig. 5. 6A). LPS from *E.coli* elicited a maximal response from macrophages that was the same as *K. pneumoniae*, whereas in microglia, the response to LPS from *E. coli* was lower and more comparable to that of *A. muciniphila*. IFNγ stimulated macrophages with an EC_{50} of 4.18 ng/mL which was less potent than in microglia (Fig. 5. 6B). As in microglia, TAK-242 inhibited the effects of all types of LPS and affected IFNγ-mediated NO release to a lesser extent (Fig. 5. 6C). Inhibition of JAK1/2 by ruxolitinib did block LPS-mediated NO release in macrophages, but the inhibition was not complete in macrophages as observed in microglia (Fig. 5. 6D). Taken together, these results suggest that LPS from various bacterial species have differential effects on cultured macrophages and that JAK1/2 also controlled TLR4-mediated signaling in these cells.

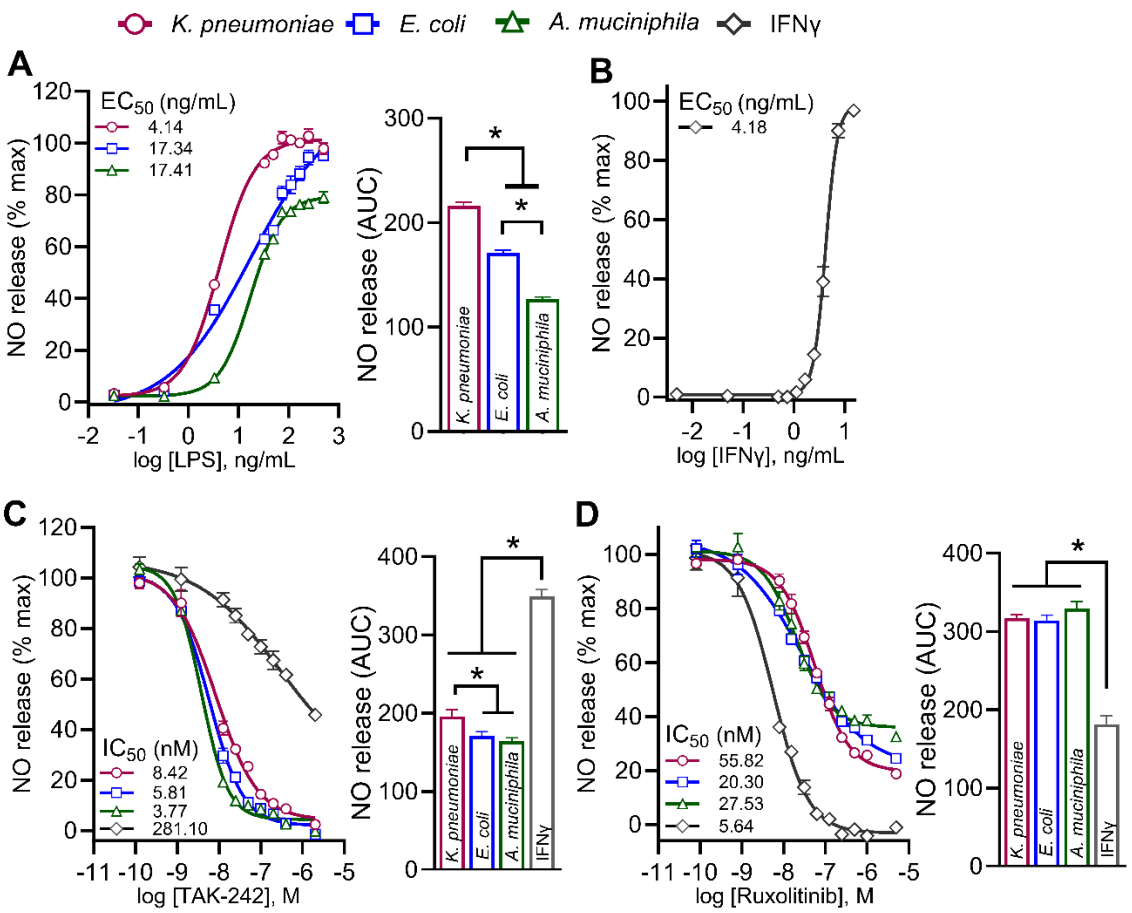

Figure 5. 6. Unidirectional control of JAK1/2 over TLR4-mediated NO release is recapitulated in RAW 264.7 macrophage cells. RAW 264.7 macrophages were stimulated with **A** LPS from *E. coli*, *K. pneumoniae*, and *A. muciniphila* (1 pg/mL – 1111 ng/mL)(n = 4). Data points represent the mean ± SEM. B Macrophage cells were stimulated with IFNγ, and NO release was measured after 16 h (n = 4). Data points represent the mean ± SEM. Cells were stimulated with a maximal concentration of LPS or IFNγ in conjunction with increasing concentrations of **C** ruxolitinib or **D** TAK-242 (n = 4). Significant differences between areas under the curve (AUC) are indicated by an asterisk and were determined using non-overlapping 95% confidence intervals.

5.4 Discussion

Here, we have investigated the molecular basis of pro-inflammatory microglial activity following stimulation with LPS and IFNγ. Both molecules stimulated NO release and the induction of mRNA for *Nos2*, *Tnf*, and *Il6* in a concentration-dependent manner. A drug combination analysis indicated that the interaction between LPS and IFNγ was synergistic. The signaling pathways downstream of TLR4 and IFNGR made unequal contributions to the microglial response as blockade of JAK1/2, immediately downstream of IFNGR, inhibited the effects of IFNγ and LPS whereas inhibition of TLR4 blocked only the effects of LPS and not IFNγ. An in-depth probing of downstream signaling pathways revealed the effect was dependent on JNK and PI3K-Akt signaling rather than more canonical pro-inflammatory signaling pathways such as NF-κB. We found that LPS from *K. pneumoniae* was more efficacious and potent in the stimulation of microglia compared to LPS from *E. coli* or *A. muciniphila* which indicated that LPS from different bacterial species may have different capacities to initiate inflammation in the brain. These findings were consistent in cultured macrophages. Ultimately, this work highlights the interactions that can occur between bacterial components and endogenous cytokines at the cellular signaling level and the influence over the immune response when these molecules are upregulated under pathological conditions.

It has been long established that microglial priming by IFNγ is a contributor to neuroinflammation and neurodegeneration (Perry and Holmes 2014). Microglial priming has been operationally defined by an initial stimulus, typically IFNγ, which induces a small initial response but facilitates an enhanced subsequent response upon exposure to a secondary stimulus, typically LPS (Schroder et al. 2006). We found that LPS elicited a greater response from SIM-A9 cells compared to IFNγ alone, however, concurrent stimulation with both molecules mediated a pharmacologically synergistic response. Elevated systemic IFNγ is associated with several conditions, including viral infection, alcohol abuse, obesity, and ageing (Bandrés et al. 2000; Katze et al. 2002; Pacifico et al. 2006; Lowe et al. 2020). These conditions are each associated with increased risk of neurodegeneration, including the development of AD (Mazon et al. 2017; Hou et al. 2019; Kamal et al. 2020; Sun et al. 2022). Furthermore, elevated serum LPS

concentrations are observed in AD, amyotrophic lateral sclerosis (ALS), liver cirrhosis, chronic HIV infection, as well as in transient bacterial infection (Brenchley et al. 2006; Zhang et al. 2009b; Kell and Pretorius 2015; Raparelli et al. 2017; Brown 2019). Thus, chronic inflammatory diseases characterized by elevated IFNγ may induce neurological changes via microglial activation in a manner that is enhanced in the presence of LPS due to infection or leaky gut (Fig. 5. 7).

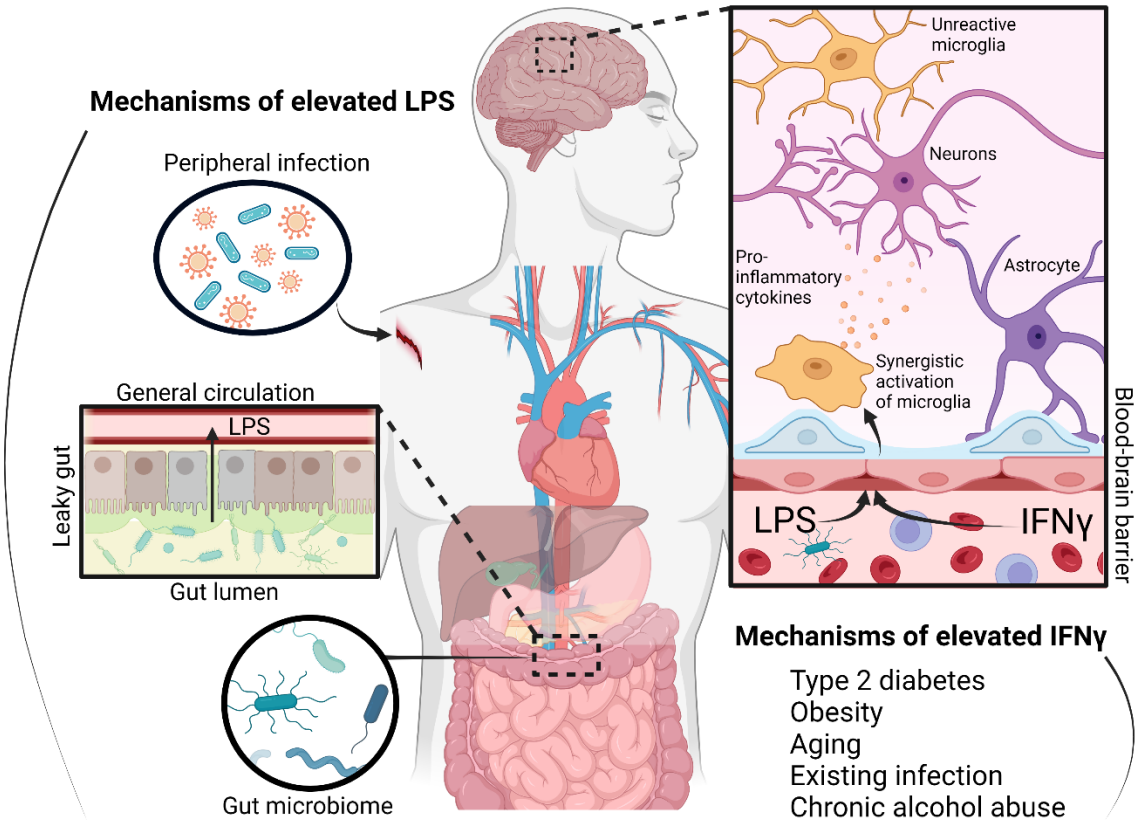

Figure 5. 7. Summary of potential mechanisms by which circulating levels of LPS and IFNγ may become elevated to synergistically activate microglia in the brain. Humans have an abundance of microbial species that reside within the gut. The composition of these species may vary depending on the health status of the individual. Gram-negative bacteria shed LPS which may enter general circulation, especially under conditions of increased intestinal permeability, generally known as leaky gut. Alternatively, LPS may enter peripheral circulation upon infection of a wound by a bacterial species such as *E. coli*. The concentration of circulating IFNγ may be elevated in type 2 diabetes, obesity, and several other conditions. When LPS and IFNγ are elevated in general circulation, the two molecules act together to activate microglia in a synergistic manner. This triggers the release of cytokines and other pro-inflammatory factors that may negatively impact surrounding cells. Figure created with BioRender.

The JAK-STAT pathway is the canonical signaling pathway immediately downstream of IFNGR whereas LPS typically engages MyD88- or TRIF-dependent pathways to mediate gene transcription via NF-κB or IRF3 (Schroder et al. 2004, 2006; Lu et al. 2008). We found that blockade of JAK1/2 by ruxolitinib was sufficient to completely inhibit NO release from microglial cells that had been stimulated with LPS or IFNγ, or both. However, interference with TLR4-mediated signaling by TAK-242 only inhibited NO release from cells treated with LPS alone. These data suggest that LPS-mediated activation of microglia is regulated by JAK1/2. LPS has been reported to directly engage JAK2 in RAW 264.7 macrophage cells (Okugawa et al. 2003; Kimura et al. 2005) and in primary glial cultures (Minogue et al. 2012). In these works, LPS was not found to activate JAK1. Thus, it is possible that ruxolitinib completely inhibited the JAK1/2-mediated effects of IFNγ as well as the JAK2-mediated effects of LPS in microglia and macrophage cells. Although TLR4 and IFNGR have not been demonstrated to form heteromers, this is commonly observed with G protein-coupled receptors, and TLR4 has been demonstrated to physically interact with other receptors such as TLR5 which alters its signaling profile (Bagher et al. 2020; Hussain et al. 2020; Zrein et al. 2020; Young et al. 2022). It is also possible that inhibition of JAK1/2 by ruxolitinib influenced the shift in cellular metabolism from oxidative phosphorylation to aerobic glycolysis that occurs in innate immune cells upon stimulation with LPS or IFNγ (Gaber et al. 2017; Yang et al. 2021). This metabolic shift is known to occur downstream of JAK1/2 and Akt (Orihuela et al. 2016). A JAK1/3 inhibitor, tofacitinib, has been previously shown to reverse the metabolic shift back to oxidative phosphorylation and simultaneously reduce pro-inflammatory cytokine release in an *ex vivo* model of rheumatoid arthritis (McGarry et al. 2018). It has also been demonstrated that a panel of different JAK inhibitors can shift metabolism away from glycolysis toward oxidative phosphorylation in primary synovial fibroblasts from human patients with psoriatic arthritis (O'Brien et al. 2021). Thus, it may be possible that JAK inhibitors blunt the pro-inflammatory effects of LPS via inhibition of the metabolic shift that is associated with pro-inflammatory microglial phenotypes. Ultimately, these regulatory mechanisms by

which JAK inhibits TLR4, which does not primarily signal via the JAK-STAT pathway, are worthy of further exploration.

Different bacterial species exhibit structural differences in the LPS presented on the outer membrane which creates differences in the immune response generated by these different LPS molecules (Vatanen et al. 2016; Mohr et al. 2022). We utilized LPS derived from *E. coli*, *K. pneumoniae*, and *A. muciniphila* to stimulate SIM-A9 microglial cells as well as RAW 264.7 macrophages and observed that LPS from *K. pneumoniae* was the most potent stimulator of NO release whereas LPS from *A. muciniphila* elicited the smallest response. Each of these species of bacteria can be found in the mammalian gut and an increased abundance of *K. pneumoniae* has been associated with inflammatory bowel diseases in mice as well as humans (Rashid et al. 2013; Federici et al. 2022; Zhang et al. 2022b). In contrast, *A. muciniphila* is negatively associated with such inflammatory bowel diseases as well as obesity and diabetes (Everard et al. 2013; Chevalier et al. 2015; Li et al. 2016; Zhou 2017). Furthermore, colonization with *A. muciniphila* is associated with reduced disease severity in a mouse model of ALS (Blacher et al. 2019). Although the abundances of *K. pneumoniae* and *A. muciniphila* in the gut are linked to the severity of inflammation in several pathologies, it is unclear whether the underlying mechanisms are related to LPS release and TLR4 activation.

JAK-mediated signaling is implicated in a number of inflammatory conditions that primarily include autoimmune diseases, however, there is increasing attention on the value of JAK as a pharmacological target for neurodegenerative diseases (Villarino et al. 2017; Lashgari et al. 2021; Rusek et al. 2023). The JAK1/3 inhibitor, tofacitinib, is approved for the treatment of rheumatoid arthritis but has also demonstrated success in the treatment of autoimmune encephalitis in individuals that did not benefit from typical anti-inflammatory therapies including corticosteroids (Schwartz et al. 2016; Jang et al. 2021). Machine learning algorithms were also used to identify ruxolitinib and several other JAK inhibitors as potential treatments for AD which is consistent with current evidence that excessive IFN-mediated signaling contributes to disease progression (Taylor et al. 2018; Rodriguez et al. 2021). A recent report indicated that rheumatoid arthritis patients taking tofacitinib did not have a reduced risk of AD or related dementia

compared to the control patients who took abatacept, a T cell inhibitor (Desai et al. 2022). However, it remains to be determined whether blockade of JAK in high-risk healthy patients could delay the onset of AD. In a mouse model of Parkinson's disease, an experimental JAK2 inhibitor, AZD1480, effectively prevented the pro-inflammatory response of microglia to alpha-synuclein and preserved the viability of dopaminergic neurons (Qin et al. 2016). Given that alpha-synuclein and amyloid-beta interact with microglial TLR4 receptors which we observed to be regulated by JAK1/2, it is possible that JAK inhibitors would be effective inhibitors of microglial activation by these proteins, especially in the presence of elevated endogenous IFNγ (Reed-Geaghan et al. 2009; Fellner et al. 2013; De et al. 2019; Hughes et al. 2020). In addition to the effects on microglia, tofacitinib also prevented IFNγ-mediated intestinal leakage in human colonic organoids via suppression of claudin-2 (Sayoc-Becerra et al. 2020). Thus, epithelial JAK-STAT signaling is involved in the regulation of intestinal permeability (Lei et al. 2021). As elevations in gut permeability and circulating LPS have been observed in AD and Parkinson's disease, it is possible that blockade of JAK signaling could also be useful to reduce the initial leakage of LPS from the gut into general circulation (Zhang et al. 2009b; Forsyth et al. 2011).

Microglia exhibit different responses to priming and changes in phenotypic plasticity that are dependent on the developmental stage of the cells. Primary microglia from newborn mice generally exhibit reduced basal release of pro-inflammatory cytokines, an enhanced response to LPS, as well as increased sensitivity to priming compared to microglia from aged mice (Lajqi et al. 2020). Furthermore, the concentration of LPS used for priming is important as an ultra-low concentration (1 fg/mL) provokes trained immunity whereas priming with a higher initial concentration (100 ng/mL) induces tolerance and subsequent resistance to a second stimulus (Lajqi et al. 2019). These effects on cytokine release and priming were dependent on upregulation of PI3Kγ which is congruent with our observation that blockade of PI3K-Akt signaling potently inhibited the LPS-mediated inflammatory response. Although the SIM-A9 cells used in this work were spontaneously immortalized microglia derived from one-day old mouse pups, it is difficult to assess whether these cells behave more like neonatal or aged

microglia. However, there are data to support that the mechanisms reported in this work are likely similar in cells derived from young or old animals. Baricitinib, a JAK1/2 inhibitor, has been shown to reduce microglial activation *in vivo* in response to infection with HIV in 5-week old male mice (Gavegnano et al. 2019). Similarly, an experimental JAK2 inhibitor, TG101209, inhibited the IFNγ-induced pro-inflammatory response in primary microglia prepared from 12- to 14-month old APPswe/PS1dE9 (APP/PS1) mice (Jones et al. 2015). Thus, blockade of microglial JAK-STAT signaling likely has therapeutic potential in young as well as aged animals.

There are limitations to the current study which highlight the value of future work using *in vivo* models. We found that LPS and IFNγ acted in a synergistic manner to promote a pro-inflammatory phenotype in cultured microglia. Within the brain, microglia interact with several different cytokines, hormones, and cell types that were not present in our cell culture system. The associated cell types primarily include perivascular macrophages and astrocytes which modulate the central immune response to pro-inflammatory stimuli (Quan et al. 1998; Schiltz and Sawchenko 2002; Liddelow et al. 2017). Future studies *in vivo* would be helpful to determine how basal circulating levels of IFNγ influence the microglial response to LPS, and vice versa, and whether the synergistic response remains consistent. We also identified that LPS derived from different bacterial species variably induced a pro-inflammatory response from microglia as well as macrophages. There is currently a dearth of information to suggest whether LPS derived from different bacterial species may influence the pro-inflammatory response of microglia *in vivo*. However, it has been reported that LPS from species such as *Bacteroides dorei* may antagonize TLR4 and inhibit the response to LPS from *E. coli* (Vatanen et al. 2016). Additionally, it has been established that the abundance of specific bacteria can be positively or negatively correlated with the development of neurodegenerative diseases (Blacher et al. 2019; Chandra et al. 2023). Thus, there is a clear need to improve our understanding of how LPS derived from the microbiome is linked to chronic systemic inflammation and subsequent neurodegeneration.

In summary, the current study demonstrates that LPS and IFNγ induce a pro-inflammatory microglial phenotype in a pharmacologically synergistic manner via

activation of their cognate receptors, TLR4 and IFNGR, respectively. The inflammatory response of microglial and macrophage cells differed depending on whether the LPS was derived from *E. coli*, *K. pneumoniae*, or *A. muciniphila* which indicates that the source of LPS is critical to the response from myeloid cells. Inhibition of JAK1/2 was sufficient to completely block the microglial response to the co-activation of TLR4 and IFNGR, even though TLR4 activation is not canonically linked to JAK-STAT signaling. This work highlights a mechanism whereby microglia may become hyperactivated when levels of LPS and IFNγ rise above normal and demonstrates a single pharmacological target to block this response. Future work to unravel the mechanisms of microglial hyperactivation and neurotoxicity will be critical to the eventual treatment of diseases with a neuroinflammatory component.

5.5 Supplementary data

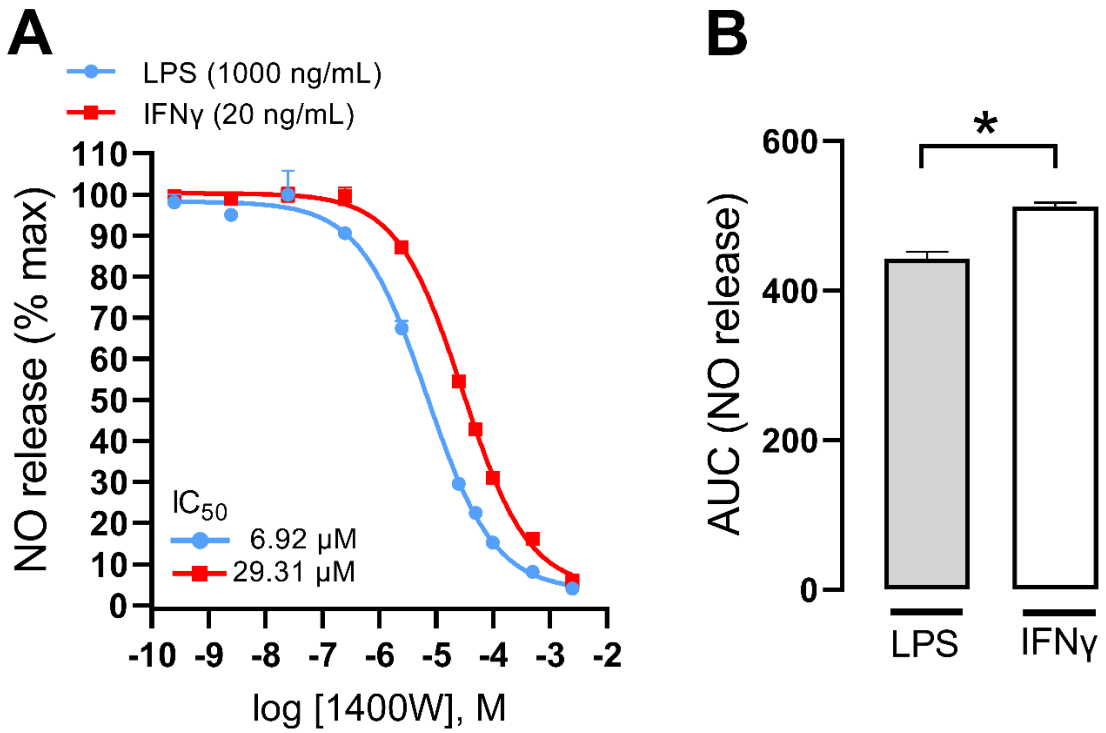

Figure 5. S1. Inhibition of microglial NO release by the iNOS inhibitor 1400W. A Microglia were stimulated with LPS (1000 ng/mL) or IFNγ (20 ng/mL) in the presence of increasing concentrations of an iNOS enzyme inhibitor (1400W; 250 pM – 2.5 mM) (n = 4). **B** Concentration-response curves were converted to area under the curve (AUC) to allow for direct comparison of the overall effect of iNOS inhibition. Data is presented as the mean ± SEM AUC. Significant differences are indicated by an asterisk and were determined using non-overlapping 95% confidence intervals.

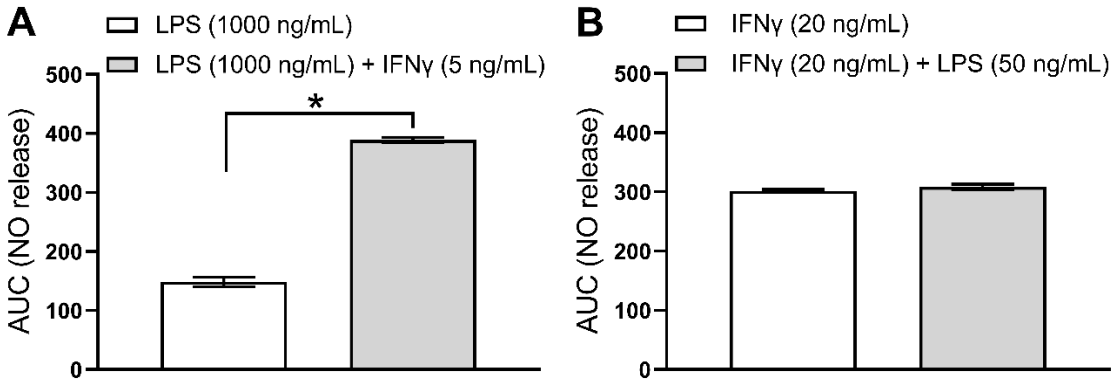

Figure 5. S2. Areas under the curve for NO release from SIM-A9 microglia stimulated with LPS and IFNγ in conjunction with TAK-242 or ruxolitinib. Microglia were stimulated with LPS and/or IFNγ in the presence of **A** increasing concentrations of a TLR4 signaling inhibitor (TAK-242; 2 nM – 500 μM) or **B** increasing concentrations of a selective JAK1/2 inhibitor (ruxolitinib; 200 pM – 5 μM) and cumulative nitric oxide release was measured after 16 hours (n = 4). Concentration-response curves were prepared and area under the curve (AUC) was used to compare overall nitric oxide release between treatments. Data is presented as the mean ± SEM. Significant differences are indicated by an asterisk and were determined using non-overlapping 95% confidence intervals.

Table 5. S1. SIM-A9 microglia were treated with IFNγ at the E_{min} (1 ng/mL) or E_{max} (20 ng/mL), LPS at the E_{min} (10 ng/mL) or E_{max} (1000 ng/mL), or a combination of both as indicated (n = 3). The E_{min} and E_{max} concentrations were determined by NO release analysis. The relative abundance of mRNA was quantified for *Nos2*, *Tnf*, *Il1b*, and *Il6*. Values presented are the mean (standard deviation). Statistical significance was determined using a one-way ANOVA with Dunnett's correction for multiple comparisons; $p < 0.05$.

Gene	**IFNγ (E_{min})**	**IFNγ (E_{max})**	**LPS (E_{min})**	**LPS (E_{max})**	**IFNγ (E_{max}) + LPS (E_{min})**	**IFNγ (E_{min}) + LPS (E_{max})**	**IFNγ (E_{max}) + LPS (E_{max})**
Nos2	4.52 (1.35)	734.57 (23.02)	219.69 (90.67)	530.16 (85.33)	5497.53 (1344.42)*	1201.30 (16.85)#	3655.57 (331.49)†
Tnf	1.11 (0.19)	6.55 (0.12)	22.29 (5.05)	26.87 (2.31)	75.01 (18.75)*	50.59 (4.11)#	187.34 (4.34)†
Il1b	1.71 (0.23)	0.35 (0.04)	97.01 (13.42)	258.94 (36.16)	24.48 (13.7)	160.71 (20.14)	94.84 (9.47)
Il6	2.77 (1.18)	22.94 (6.25)	581.21 (133.84)	821.64 (106.76)	1465.11 (254.45)*	1346.8 (75.23)#	590.30 (167.84)

* Higher than IFNγ (E_{max}) and LPS (E_{min}) alone.
\# Higher than IFNγ (E_{min}) and LPS (E_{max}) alone.
† Higher than IFNγ (E_{max}) and LPS (E_{max}) alone.

Table 5. S2. SIM-A9 cells were treated with 100 ng/mL LPS from *K. pneumoniae, E. coli*, or *A. muciniphila* or 5 ng/mL IFNγ for 16 h and the mRNA for pro-inflammatory or other functional microglial markers was assessed by RT-qPCR (n = 4). Data are presented as the fold-change relative to the vehicle mean (with 95% confidence intervals).

	K. pneumoniae	***E. coli***	***A. muciniphila***	**IFNγ**
Nos2	39.51 (34.71 - 44.31)	30.13 (17.72 - 42.54)	23.36 (17.63 - 29.1)	162.1 (108.05 - 216.16)
Tnf	6.64 (4.54 - 8.73)	6.16 (4.38 - 7.94)	3.51 (2.9 - 4.12)	1.69 (1.24 - 2.15)
Tlr4	1.34 (0.60 - 2.08)	1.46 (0.43 - 2.50)	1.17 (0.55 - 1.8)	0.99 (0.60 - 1.37)
Ifngr1	0.67 (0.25 - 1.09)	0.83 (0.21 - 1.46)	0.79 (0.41 - 1.18)	0.58 (0.18 - 0.97)
Il1b	641.99 (534.89 - 749.08)	455.91 (307.06 - 604.76)	110.73 (79.86 - 141.6)	0.92 (0.35 - 1.5)
Il6	30.66 (14.88 - 46.44)	32.1 (21.53 - 42.66)	10.78 (8.67 - 12.9)	0.81 (0.48 - 1.15)
Ccl2	18.99 (13.39 - 24.58)	16.71 (1.65 - 31.77)	8.6 (4.74 - 12.47)	3.02 (1.39 - 4.65)
Flt1	1.77 (0.87 - 2.66)	3.03 (0.68 - 5.39)	3.24 (2.09 - 4.39)	3.41 (1.18 - 5.64)
Csf3	12334.58 (9544.69 - 15124.46)	10539.24 (6414.89 - 14663.59)	2428.39 (2231.65 - 2625.14)	4.42 (-0.01 - 8.84)
Tgfb1	3.53 (0.33 - 6.73)	6 (3.05 - 8.95)	6.85 (5.87 - 7.84)	4.18 (0.84 - 7.52)
Cd11b	2.6 (0.77 - 4.44)	5.59 (1.28 - 9.91)	4.3 (3.66 - 4.93)	1.39 (0.46 - 2.32)
Sirpa	1.65 (1.05 - 2.26)	2.76 (0.87 - 4.66)	2.32 (1.75 - 2.88)	1.34 (0.23 - 2.46)
Cx3cr1	0.05 (-0.02 - 0.12)	0.09 (0.04 - 0.14)	0.24 (0.12 - 0.35)	0.02 (-0.01 - 0.05)
P2ry12	0.17 (-0.23 - 0.58)	0.12 (0.03 - 0.20)	0.26 (0.04 - 0.48)	1.12 (0.66 - 1.58)

Table 5. S3. SIM-A9 microglia were stimulated with LPS (1000 ng/mL) alone or with IFNγ (5 ng/mL). Alternatively, microglia were stimulated with IFNγ (20 ng/mL) alone or with LPS (50 ng/mL). Microglia were co-treated with an inhibitor of JNK (SP 600125; 15 nM – 250 μM), PI3K-Akt (LY294002; 15 nM – 250 μM), ERK (U0126; 10 nM – 1 mM), mTOR (PP-242; 380 pM – 25 μM), or NF-κB (IKK-16; 380 pM – 25 μM). Concentration-response curves were prepared using four-parameter analysis and used to calculate the IC_{50} as well as the bottom of the curve (IC_{max}) for NO release relative to vehicle. Data are presented as the mean (95% confidence interval).

Inhibited pathway	**Treatments**	**Bottom (% vehicle)**	**IC_{50} (μM)**
JNK	LPS	2.93 (2.57 - 3.28)	0.25 (0.19 - 0.31)
	LPS + IFNγ (5 ng/mL)	26.36 (24.33 - 28.39)*	1.62 (1.03 - 3.44)*
	IFNγ	8.24 (6.66 - 9.82)	9.31 (7.49 - 11.29)
	IFNγ + LPS (50 ng/mL)	21.91 (21.06 - 22.76)^	17.86 (14.48 - 24.94)^
Akt	LPS	4.42 (3.08 - 5.76)	0.34 (0.27 - 0.40)
	LPS + IFNγ (5 ng/mL)	28.53 (27.07 - 30.00)*	9.53 (4.23 - 805.37)*
	IFNγ	2.41 (0.25 - 5.08)	53.58 (29.24 - 1745.82)
	IFNγ + LPS (50 ng/mL)	15.63 (12.87 - 18.39)^	32.66 (23.55 - 76.20)
ERK	LPS	5.35 (3.12 - 7.57)	182.39 (154.52 - 222.33)
	LPS + IFNγ (5 ng/mL)	7.35 (6.01 - 8.68)	208.45 (159.95 - 316.22)
	IFNγ	2.86 (1.08 - 4.64)	31.84 (27.03 - 37.67)
	IFNγ + LPS (50 ng/mL)	8.57 (4.85 - 12.29)^	236.05 (156.31 - 503.50)^
mTOR	LPS	10.43 (9.29 - 11.57)	1.01 (0.60 – 3.01)
	LPS + IFNγ (5 ng/mL)	36.43 (35.35 - 37.52)*	4.70 (3.77 – 6.35)*
	IFNγ	7.07 (5.42 - 8.72)	7.11 (5.49 - 11.99)
	IFNγ + LPS (50 ng/mL)	3.58 (2.94 - 4.23)^	13.03 (8.18 - 54.57)
NF-κB	LPS	6.91 (5.92 - 7.90)	0.99 (0.61 - 2.17)
	LPS + IFNγ (5 ng/mL)	3.98 (2.38 - 5.57)*	2.37 (1.90 - 2.99)
	IFNγ	2.58 (2.22 - 2.95)	2.10 (1.87 - 2.34)
	IFNγ + LPS (50 ng/mL)	2.64 (0.64 - 4.64)	2.85 (2.39 - 3.41)^

* Significantly different from LPS alone as indicated by non-overlapping 95% CI.
^ Significantly different from IFNγ alone as indicated by non-overlapping 95% CI.

Chapter 6: Microglia-mediated neuron death requires TNF and is exacerbated by mutant huntingtin

Copyright statement

This article is currently unpublished and does not currently require copyright permission to be included in this thesis. The publication status of first-author articles included or excluded from this thesis are in Table A1 (Appendix A).

Contribution statement

All experiments were performed, and data were collected by myself. Analysis and interpretation of the data were performed in consultation Dr. Eileen Denovan-Wright. Preparation of the manuscript was done by me with support from Dr. Eileen Denovan-Wright.

Preface

The primary aim of this chapter was to identify which specific microglial-secreted factors were required to cause neuronal death in the conditioned media model. It had been well established that there are excessive quantities of pro-inflammatory factors in the brains of patients with Huntington's disease and that this is correlated with neuronal loss in the striatum. However, no mechanistic link had been drawn. Thus, as a secondary objective, I aimed to determine whether neuronal cells that express mutant huntingtin were inherently more sensitive to the pro-inflammatory environment produced by microglia.

6.1 Abstract

Microglia, the resident immune cells of the brain, regulate the balance of inflammation in the central nervous system under healthy and pathogenic conditions. Chronic hyperactivation of microglia is associated with neuronal death. However, the specific secreted factors required to kill neurons are unknown. We used a conditioned media system to assess the profile of microglia-secreted proteins in response to LPS and IFNγ and the effects of these proteins on cultured neuronal cells. ST*Hdh*$^{Q7/Q7}$ and ST*Hdh*$^{Q111/Q111}$ neuronal cells were used a model for wild-type and Huntington's disease neurons, respectively. We found that pro-inflammatory microglial media induced the hyperactivation of ERK1/2, Akt, and CREB pathways in ST*Hdh*$^{Q111/Q111}$ cells compared to ST*Hdh*$^{Q7/Q7}$ cells. This culminated in apoptosis and necroptosis which was dependent on TNF and elevated in ST*Hdh*$^{Q111/Q111}$ cells. We also determined that survival of ST*Hdh*$^{Q7/Q7}$ cells could be improved by activation of CB_1 or D_2 receptors whereas survival of ST*Hdh*$^{Q111/Q111}$ cells was improved only by stimulation of D_2 receptors. These data indicate that pro-inflammatory microglia kill neurons in a TNF-dependent manner, that these effects can be blocked upon neutralization of TNF, and that neuronal resilience can possibly be enhanced by modulation of the endocannabinoid and dopamine systems.

6.2 Introduction

Microglia are recognized as the resident immune cells of the brain which survey brain parenchyma and regulate several processes including synaptic activity and maintenance, permeability of the blood-brain barrier, and clearance of cellular waste and debris (Stevens et al. 2007; Neumann et al. 2009; Bilimoria and Stevens 2015; Haruwaka et al. 2019; Badimon et al. 2020). Under healthy conditions, microglia secrete trophic factors and support proper neuronal function (Ueno et al. 2013; Badimon et al. 2020). However, pathogen or damage-associated molecular patterns in the brain evoke pro-inflammatory responses from microglia (Kreutzberg 1996). Under conditions of chronic neuroinflammation, pro-inflammatory microglia fail to clear waste, engulf synapses in excessive quantities, and facilitate entry of peripheral immune cells into the brain (Prinz and Priller 2017; Norris et al. 2018; Jafari et al. 2021). In addition to the dysregulation of homeostatic processes, pro-inflammatory microglia secrete large quantities of pro-inflammatory cytokines which can induce neuronal dysfunction and death (Hu et al. 1997; Chhor et al. 2013; Frakes et al. 2014; Young and Denovan-Wright 2022b).

TNF is a pleiotropic cytokine that is released in abundance by pro-inflammatory microglia *in vitro* as well as *in vivo* (Gregersen et al. 2000; Lambertsen et al. 2005; Ajami et al. 2018; Young and Denovan-Wright 2022b). Elevated TNF protein in the cerebrospinal fluid and serum has been associated with the progression of MS, AD, and PD (Tarkowski et al. 2003; Magaki et al. 2007; Swardfager et al. 2010; Chen et al. 2018; Magliozzi et al. 2021; Fu et al. 2023). This would suggest that TNF release by microglia and other immune cells is associated with neurodegeneration. TNF can directly induce apoptosis upon activation of TNFR1 but may also trigger cell death by necroptosis when caspase-8 is inhibited (Webster and Vucic 2020). TNF is the primary inducer of extrinsic apoptosis in the CNS and is thus relevant to several neurodegenerative diseases (Siegel 2006). However, elevated neuronal necroptosis has also been implicated in several diseases of the human CNS (Yuan et al. 2019). Microglia may efficiently clear apoptotic cells from the CNS whereas necroptosis of neurons involves the leakage of intracellular contents which promotes the further recruitment and pro-inflammatory stimulation of

microglia (Ofengeim and Yuan 2013). Thus, the specific mechanisms by which microglia induce neuronal death can impact the progression of the neuroinflammation.

Huntington's disease (HD) is a progressive neurodegenerative disease characterized by dysfunction and death of medium-spiny neurons (MSNs) which manifests in global cognitive impairment and chorea (Sieradzan and Mann 2001; MacDonald et al. 2003; Pérez-Navarro et al. 2006). MSN death has been partially attributed to an excitotoxic mechanism linked to dysfunctional handling of dopamine and glutamate mediated by mutant huntingtin (mHTT) (Jakel and Maragos 2000; Pérez-Navarro et al. 2006; Paoletti et al. 2008). However, it is now recognized that there are several other factors that contribute to MSN death, including inflammation, which emerges from the brain as well as the periphery (Crotti and Glass 2015; Rocha et al. 2016; Valadão et al. 2020). In the brain, pro-inflammatory microglia begin to gather in the striatum of pre-symptomatic HD patients, and continue to accumulate throughout the progression of the disease (Sapp et al. 2001; Pavese et al. 2006; Tai et al. 2007). Cerebrospinal fluid from HD patients also has higher concentrations of pro-inflammatory cytokines such as IL-6 and TNF (Björkqvist et al. 2008). In the periphery, innate immune cells in the blood have upregulated expression of immediate early genes and increased circulating IL-6 can be reliably detected 15 years prior to the onset of symptoms (Runne et al. 2007; Björkqvist et al. 2008). Thus, systemic inflammation and propagation of neuroinflammation by microglia likely contribute to neuronal death in the pathogenesis of HD.

Microglia that express mHTT exhibit constitutively elevated markers of activation and have an increased capacity to induce neuronal death *in vivo* and *ex vivo* (Crotti et al. 2014; O'Regan et al. 2021). Monocytes and macrophages isolated from HD patients also release more pro-inflammatory cytokines such as IL-1β, IL-6, IL-8, and TNF upon stimulated with lipopolysaccharides (LPS) compared to cells isolated from healthy controls (Björkqvist et al. 2008; Träger et al. 2014). This indicates that microglia and other immune cells are dysfunctional in HD and generate excessive inflammation, even in the absence of extrinsic pro-inflammatory stimuli. When expressed in neurons, wild-type (wt)HTT has pro-survival functionality whereas mHTT can promote caspase-

dependent cell death (Sánchez et al. 1999; Rigamonti et al. 2000). This could be indicative of a mechanism whereby neurons in the HD brain have reduced pro-survival capacity and are less resilient to potentially neurotoxic factors released by microglia. Although HD pathophysiology appears to create a pro-inflammatory environment within the brain, it is unclear whether neurons that express mutant HTT are inherently sensitive to this environment.

In this work, we investigated mechanisms of microglia-mediated neurotoxicity using cultured neurons that originated from wild-type and HD mice (Trettel et al. 2000). The primary goal was to identify the minimum necessary factors released by microglia to elicit a pro-death response from neurons. We also aimed to determine whether the expression of mHTT would hypersensitize neurons to pro-inflammatory factors released by microglia and enhance cell death.

6.3 Results

6.3.1. mHTT conferred enhanced sensitivity to microglial-derived factors

To assess the early neuronal response to conditioned microglial media, we applied media from microglia that had been stimulated with LPS and IFNγ to cultured neuronal cells. ST*Hdh*$^{Q7/Q7}$ and ST*Hdh*$^{Q111/Q111}$ neuronal cells were used and are homozygous for a humanized *huntingtin* allele with 7 or 111 CAG repeats, respectively. The activation of eight signaling pathways was monitored for three hours upon exposure of the neurons to microglial pro-inflammatory media (Fig 6. 1A). We observed an exaggerated response from ST*Hdh*$^{Q111/Q111}$ cells with respect to phosphorylation of ERK1/2 (Fig. 6. 1B; $F(5, 36) = 4.751$), Akt (Fig. 6. 1C; $F(5, 36) = 3.689$), and CREB (Fig. 6. 1D; $F(5, 36) = 3.420$). In each case, the elevated signaling relative to ST*Hdh*$^{Q7/Q7}$ cells was clear within 10 minutes, and signaling via these pathways remained elevated after 3 h. Phosphorylation of p38 was elevated in ST*Hdh*$^{Q111/Q111}$ cell after 30 mintes, and in ST*Hdh*$^{Q7/Q7}$ cells only at the 120-minute time point. However, there was no difference between groups (Fig. 6. 1E). NF-κB p65 phosphorylation was elevated in both cell types from the 10-minute time point until 60 minutes following stimulation, and remained significantly higher in ST*Hdh*$^{Q7/Q7}$ cells at the 120-minute time point (Fig. 6. 1F). There

was no observed elevation in the phosphorylation of JNK (Fig. 6. 1G), PLCβ3 (Fig. 6. 1H), or STAT1 (Fig. 6. 1I) relative to baseline with no difference between cell types.

To assess whether ST*Hdh*$^{Q7/Q7}$ and ST*Hdh*$^{Q111/Q111}$ cells exhibit differences in cell viability in response to pro-inflammatory microglial media, both cell types were exposed to the conditioned media and monitored for 24 h. We observed that the viability of ST*Hdh*$^{Q7/Q7}$ fell below baseline after 16 h, whereas the viability of ST*Hdh*$^{Q111/Q111}$ cells fell below baseline and was different from ST*Hdh*$^{Q7/Q7}$ after 8 h (Fig. 6. 1J). These differences were maintained after 24 h. Taken together, these data suggest that pro-inflammatory microglial media reduced the viability of neuronal cells which was exacerbated by mHTT, and this response was linked to the early hyperactivation of ERK1/2, Akt, and CREB pathways.

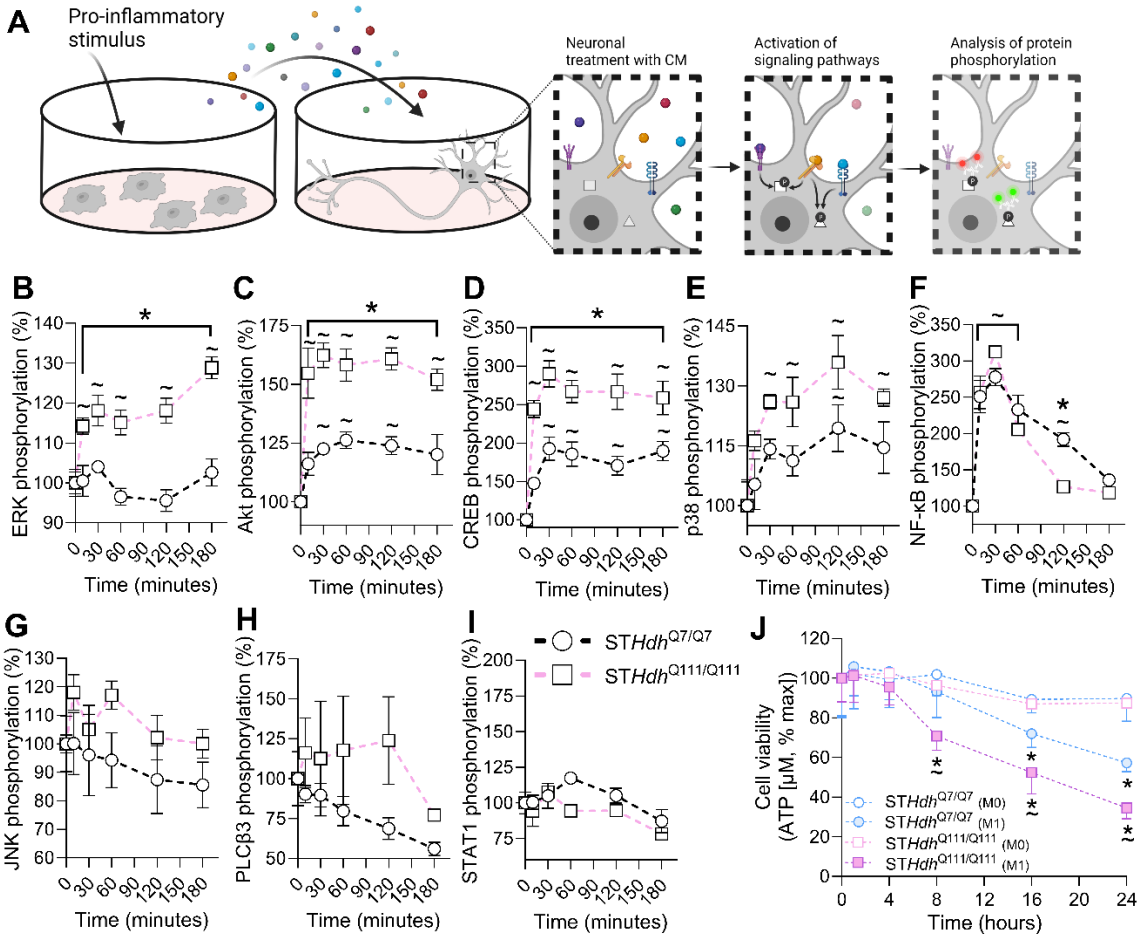

Figure 6. 1. ST*Hdh*$^{Q111/Q111}$ cells exhibit an exaggerated early signaling response in ERK, Akt, and CREB pathways compared to ST*Hdh*$^{Q7/Q7}$ cells upon treatment with microglial conditioned media. A SIM-A9 microglia were stimulated with LPS and IFNγ, conditioned media was applied to cultured ST*Hdh*$^{Q7/Q7}$ and ST*Hdh*$^{Q111/Q111}$ neuronal cells. Phosphorylation of **B** ERK1/2 (Thr202/Tyr204), **C** Akt (Ser473), **D** CREB (Ser133), **E** JNK (Thr183/Tyr185), **F** p38 (Thr180/Tyr182), **G** PLCβ3 (Ser537), **H** NF-κB (Ser536), and **I** STAT1 (Tyr701) was determined using the in-cell western technique (n = 4). Each time-point represents an independent preparation of cells. **J** Conditioned media from unstimulated microglia (M0) or microglia treated with LPS and IFNγ (M1) was applied to cultured ST*Hdh*$^{Q7/Q7}$ and ST*Hdh*$^{Q111/Q111}$ neuronal cells and the ATP concentration was monitored over 24 h (n = 8). Each time-point represents an independent preparation of cells. Significance was determined using two-way ANOVA with Sidak post-hoc test; * $p < 0.05$; ST*Hdh*$^{Q7/Q7}$ vs. ST*Hdh*$^{Q111/Q111}$ cells. ~ $p < 0.05$ vs. baseline (0 minutes).

6.3.2. Microglia engaged in robust pro-inflammatory activity in response to LPS and IFNγ

We first assessed the profile of proteins released by SIM-A9 microglial cells in an unreactive state and upon treatment with LPS or IFNγ. In the basal phenotype, microglia released several chemokines, such as chemokine ligand (CCL)2 and CCL3, and relatively low quantities of pro- and anti-inflammatory cytokines (Fig. 6. 2A). Upon treatment with LPS, there was an upregulation of chemokines such as CCL5, CCL12, and CXCL9, as well as the pro-inflammatory cytokines, IL-6 and TNF (Fig. 6. S1). Upon treatment with IFNγ, there was a substantial increase in the release of chemokines CCL12, CXCL10, and CXCL11, as well as IL-6 and TNF. When microglia were treated with LPS and IFNγ in combination, there was an upregulation of IL-6 (Fig. 6. 2B), TNFα (Fig. 6. 2C), with no change in the anti-inflammatory cytokines, IL-4 (Fig. 6. 2D) and IL-10 (Fig. 6. 2E). Intercellular adhesion molecule 1 (ICAM-1), which promotes entry of peripheral immune cells through the blood-brain barrier, was stimulated by IFNγ but not LPS (Fig. 6. 2F). However, the growth factor, granulocyte colony stimulating factor (G-CSF), was upregulated more in response to LPS (Fig. 6. 2G). These data support that LPS and IFNγ robustly induce pro-inflammatory microglial phenotypes but do not completely overlap in their effects.

The abundance of iNOS (Fig. 6. 2H) and COX2 (Fig. 6. 2I) proteins were qualitatively monitored over the course of 16 h upon stimulation with LPS or IFNγ. At the endpoint, the population of cells exhibited strong iNOS- and COX2-like immunoreactivity. As iNOS and COX2 are robust indicators of pro-inflammatory microglia, these experiments provided visual confirmation that microglia engage in pro-inflammatory activity upon stimulation with LPS and IFNγ (Chhor et al. 2013). These data demonstrate that in the unreactive state, the microglia constitutively released several chemokines with relatively low amounts of pro- and anti-inflammatory cytokines. However, activation of TLR4 and/or IFNGR induced the microglia into a pro-inflammatory phenotype, characterized by upregulation of intracellular iNOS and COX2 as well as the release of IL-6 and TNF.

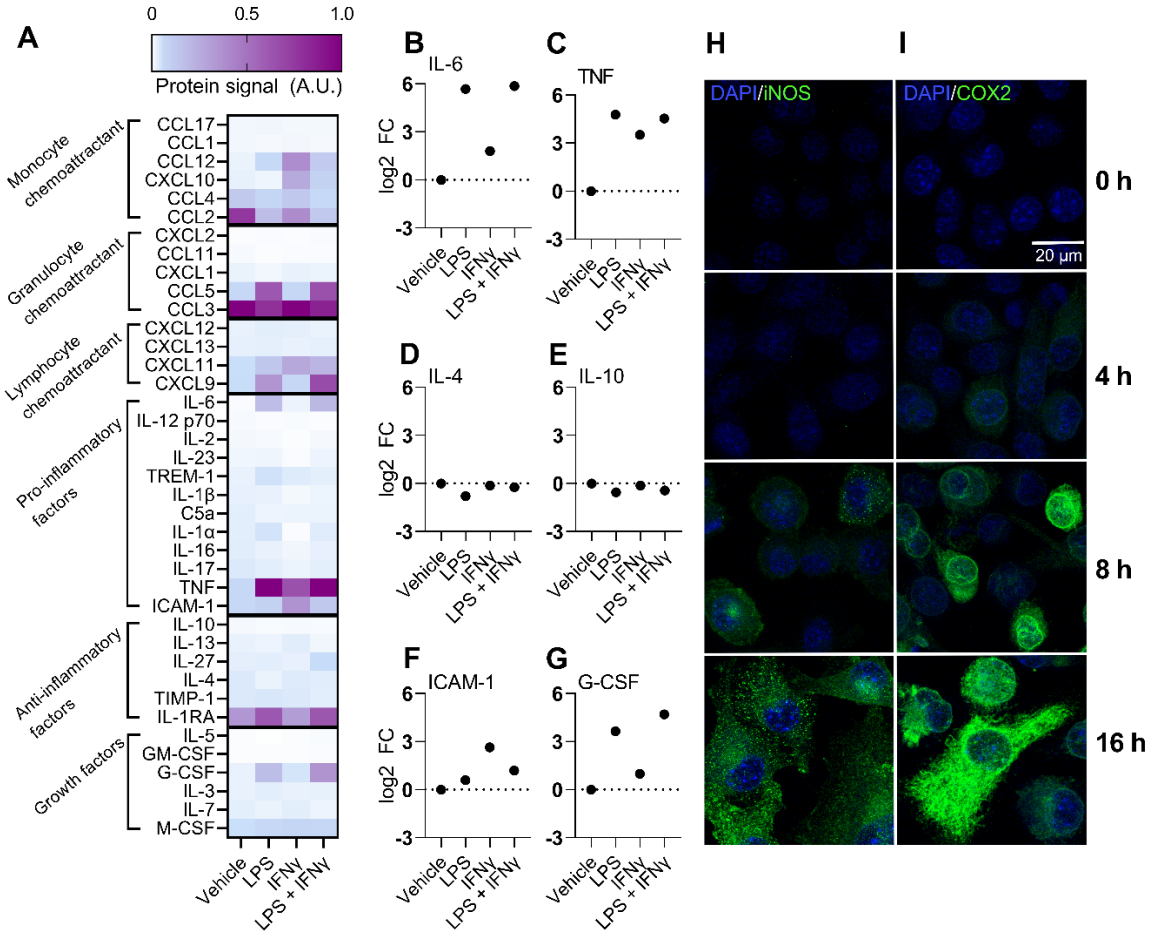

Figure 6. 2. Microglia exhibit pro-inflammatory properties upon stimulation with LPS and IFNγ. A. SIM-A9 microglia were stimulated with vehicle (PBS), LPS (1000 ng/mL), IFNγ (20 ng/mL), or LPS and IFNγ, and the media was assessed for the protein abundance of 39 cytokines and chemokines. Proteins were measured using a Proteome Profiler™ antibody array; cell culture supernatant from 24 technical replicates was pooled and incubated with each membrane with antibodies spotted in duplicate. **B-G.** The log2 fold-change relative to vehicle was determined for all proteins and plotted for **B.** IL-6, **C.** TNFα, **D.** IL-4, **E.** IL-10, **F.** G-CSF, **G.** CCL2. **H-I.** Microglial cells were stimulated with LPS and IFNγ and **H.** iNOS- and **I.** COX2-like immunoreactivity was assessed after 16 h. Scale bar; 20 μm.

6.3.3. Microglial pro-inflammatory activity and secondary neurotoxicity were modulated favourably by blockade of JAK1/2

We used a battery of signaling inhibitors to prevent the activation of pathways that are known to contribute to the effects of LPS or IFNγ, or both. SIM-A9 microglial cells were stimulated with half-maximal concentrations of LPS and IFNγ in conjunction with increasing concentrations of each signaling inhibitor. The inhibited pathways in these experiments were TLR4, JAK1/2, NF-κB, p38, mTOR, ERK, JNK, and Akt. NO release was used as a proxy for pro-inflammatory activity as it correlates with release of many pro-inflammatory cytokines and the upregulation of mRNA for markers of inflammation (Young and Denovan-Wright 2022b).

We observed that blockade of TLR4 (Fig. 6. 3A) and JAK1/2 (Fig. 6. 3B) resulted in the most potent inhibition of NO release from the cultured microglia. This was expected, as TLR4 and JAK1/2 are the most upstream targets to inhibit the effects of LPS and IFNγ, respectively. However, blockade of TLR4 via TAK-242 resulted in the inhibition of NO release to 75.2 ± 2.7% of the vehicle whereas blockade of JAK1/2 via ruxolitinib inhibited NO release to 1.7 ± 0.9%. These data suggest that dual inhibition of JAK1/2 was sufficient to block the effects of LPS and IFNγ. Inhibition of NF-κB (Fig. 6. 3C), p38 (Fig. 6. 3D), mTORC1/2 (Fig. 6. 3E), ERK1/2 (Fig. 6. 3F), JNK (Fig. 6. 3G), and Akt (Fig. 6. 3H) using a variety of inhibitors reduced the release of NO from microglia with various degrees of potency and efficacy. Blockade of NF-κB, mTOR, ERK, and Akt reduced NO release by more than 80% whereas inhibition of p38 had no effect on microglial NO release. This demonstrated that the JAK1/2 inhibitor, ruxolitinib, was the most useful to inhibit microglial NO release compared to other experimental inhibitors with respect to potency and efficacy.

To assess the effect of signaling inhibition on subsequent neuronal viability, microglia were stimulated with LPS and IFNγ in conjunction with vehicle or a signaling inhibitor and neuronal viability was assessed following treatment with the conditioned media. Blockade of NF-κB, p38, ERK1/2, JNK, or Akt further reduced cell viability compared to conditioned media in the absence of a signaling inhibitor (Fig. 6. 3I). Inhibition of mTOR improved the relative cellular viability of only ST*Hdh*$^{Q111/Q111}$ cells

and inhibition of JAK1/2 improved cell viability in both celltypes. Thus, JAK1/2 were the only proteins downstream of TLR4 and IFNGR that regulated the pro-inflammatory activity of microglia and improved subsequent neuronal viability when inhibited by ruxolitinib.

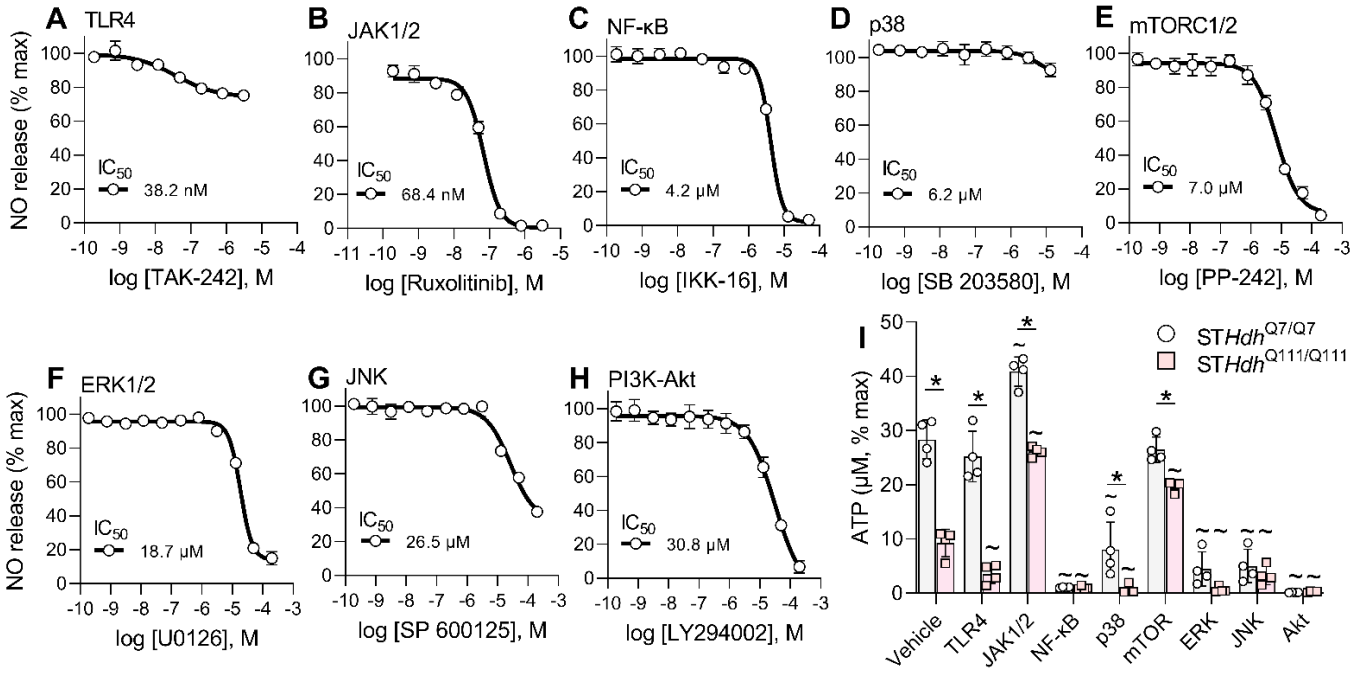

Figure 6. 3. Microglial NO release downstream of TLR4 and IFNGR and subsequent neuronal survival is modulated favourably by inhibition of JAK1/2. SIM-A9 microglia were stimulated with LPS and IFNγ (EC_{50} concentrations), and treated with inhibitors of **A** TLR4 (TAK-242; 190 pM – 3.1 μM), **B** JAK1/2 (Ruxolitinib; 190 pM – 3.1 μM), **C** NF-κB (IKK-16; 190 pM – 50 μM), **D** p38 (SB 203580; 190 pM – 13 μM), **E** mTORC1/2 (PP-242; 190 pM – 200 μM), **F** ERK1/2 (U0126; 190 pM – 200 μM), **G** JNK (SP 600125; 190 pM – 200 μM), and **H** PI3K-Akt (LY294002; 190 pM – 200 μM). **I** SIM-A9 microglia were stimulated with LPS and IFNγ in conjunction with vehicle or an inhibitor of TLR4, JAK1/2, NF-κB, p38, mTORC1/2, ERK1/2, JNK, or PI3K-Akt (10 μM for each). The ATP concentration was measured after 24 h as a proxy for cell viability. Significance was determined using two-way ANOVA with Sidak post-hoc test; * $p < 0.05$; ST*Hdh*$^{Q7/Q7}$ vs. ST*Hdh*$^{Q111/Q111}$ cells. ~ $p < 0.05$ vs. vehicle.

6.3.4. Microglial-secreted TNF was necessary but insufficient to mediate neuronal death

TNF is a known mediator of cell death and was the most abundant pro-inflammatory factor released by SIM-A9 microglia in response to LPS and IFNγ. For this reason, we investigated whether TNF released by microglia was a primary mediator of cell death in the ST*Hdh*$^{Q7/Q7}$ and ST*Hdh*$^{Q111/Q111}$ cells. We observed that recombinant TNF had no negative effect on cell viability except for ST*Hdh*$^{Q111/Q111}$ cells at a concentration of 150 ng/mL (Fig. 6. 4A). However, when recombinant TNF was added to pro-inflammatory media, the proportion of cell death was increased in a concentration-dependent manner (Fig. 6. 4B). TNF was neutralized from the pro-inflammatory media using polyclonal antibodies to determine whether removal of TNF could prevent the neuronal death associated with the microglial media. The pro-inflammatory media contained TNF at a concentration of 14,669 ± 891 pg/mL which was decreased to 1,721 ± 83 pg/mL at a 1:100 antibody dilution and 190 ± 10 pg/mL at a 1:20 dilution (Fig. 6. 4C). When pro-inflammatory media that had been treated with the anti-TNF antibodies was applied to ST*Hdh*$^{Q7/Q7}$ and ST*Hdh*$^{Q111/Q111}$ cells, there was a significant improvement in viability at the 1:100 dilution (Fig. 6. 4D). When the media had been treated with the 1:20 antibody dilution to remove 98.7% of the TNF, there was no effect of the media on overall cell viability as measured by ATP concentration.

When cell viability was measured by penetration of zombie red dye, we observed that pro-inflammatory media induced cell death in 40 ± 6% of ST*Hdh*$^{Q7/Q7}$ cells and 72 ± 7% ST*Hdh*$^{Q111/Q111}$ cells which was blocked by anti-TNF antibodies in both cases (Fig. 6. 4E). The effects of pro-inflammatory media on the reductive capacities of the ST*Hdh*$^{Q7/Q7}$ and ST*Hdh*$^{Q111/Q111}$ cells were examined using calcein and reazurin substrates. The addition of recombinant TNF (15 ng/mL) reduced the ability of ST*Hdh*$^{Q7/Q7}$ cells to metabolize calcein but did not affect ST*Hdh*$^{Q111/Q111}$ cells (Fig. 6. 4F). The pro-inflammatory media negatively impacted the ability of both cell types to metabolize calcein, this effect was partially ameliorated but not completely reversed by neutralization of TNF. This pattern was also observed when reazurin was used as a substrate (Fig. 6. 4G). Taken together, these data suggest that among the microglial secretome, TNF is a component that was necessary but not sufficient to mediate cell

death. Thus, neutralization of TNF ameliorated the damaging effects of pro-inflammatory media on ST*Hdh*$^{Q7/Q7}$ and ST*Hdh*$^{Q111/Q111}$ cells.

To further assess the specific mechanisms of neuronal cell death, ST*Hdh*$^{Q7/Q7}$ and ST*Hdh*$^{Q111/Q111}$ cells were stained for caspase-3 cleavage and receptor interacting protein kinase 3 (RIP3) phosphorylation. Cleavage of caspase-3 is indicative of apoptotic cell death whereas phosphorylated RIP3 (pRIP3) suggests that a cell is fated for necroptotic cell death, and both mechanisms of cell death have been linked to TNF (Zhao et al. 2001; Wang et al. 2008; Zhang et al. 2009a; Sun et al. 2012). In response to pro-inflammatory microglial media, 15.9 ± 2.8% of ST*Hdh*$^{Q7/Q7}$ cells were positive for cleavage of caspase-3 compared to 20.3 ± 2.0% of ST*Hdh*$^{Q111/Q111}$ cells (Fig. 6. 4H). This was in contrast with >90% cells that stained positive for caspase-3 cleavage in response staurosporine which served as a positive control. This suggests that although pro-inflammatory media induced apoptosis in a relatively small subset of cells, there was no difference between ST*Hdh*$^{Q7/Q7}$ and ST*Hdh*$^{Q111/Q111}$ cells. In response to the same stimulus, 28.0 ± 5.6% of ST*Hdh*$^{Q7/Q7}$ cells were positive for pRIP3 compared to 41.8 ± 5.5% of ST*Hdh*$^{Q111/Q111}$ cells (Fig. 6. 4I). This phosphorylation of RIP3 was blocked by necrostatin-1 which inhibits the phosphorylation of RIP1 downstream of TNF receptor 1 (TNFR1) activation (Degterev et al. 2005; Christofferson et al. 2014). Taken together, these data demonstrated that conditioned media from pro-inflammatory microglia induced a combination of apoptosis and necroptosis in both cell types. However, a necroptotic mechanism of cell death accounted for the increased proportion of death observed in ST*Hdh*$^{Q111/Q111}$ cells.

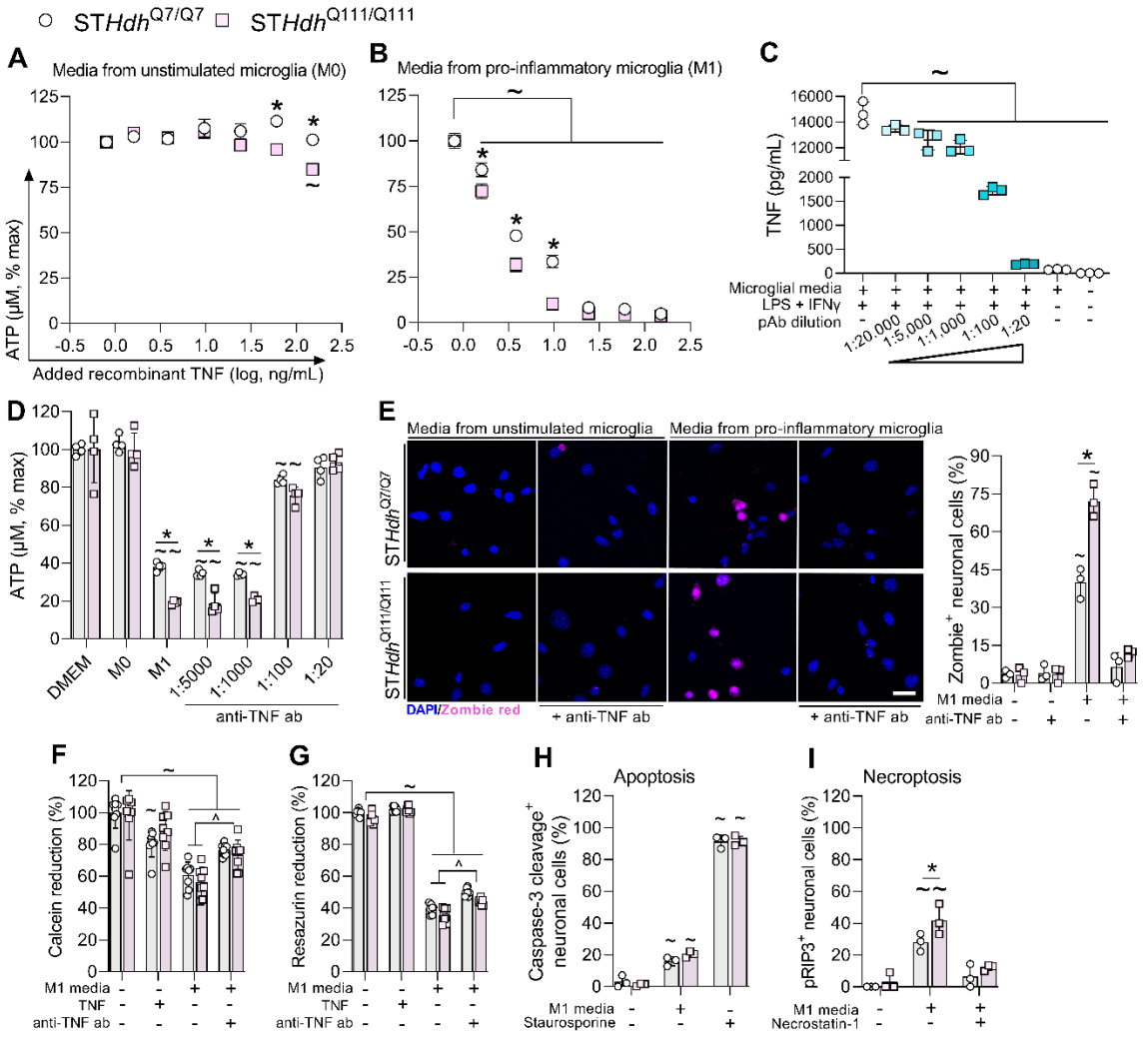

Figure 6. 4. TNF is necessary but not sufficient to mediate neuronal cell death by pro-inflammatory microglial media. ST*Hdh*$^{Q7/Q7}$ and ST*Hdh*$^{Q111/Q111}$ cells were treated with increasing concentrations of mouse recombinant TNF (0.8 – 150 ng/mL) that had been added to media derived from **A** unstimulated microglia or **B** microglia that were stimulated with LPS (1000 ng/mL) and IFNγ (20 ng/mL), and ATP was measured after 24 h as a proxy for cell viability (n = 4). Significance was determined using two-way ANOVA with Sidak post-hoc test. * $p < 0.05$, ST*Hdh*$^{Q7/Q7}$ vs. ST*Hdh*$^{Q111/Q111}$. ~ $p < 0.05$ vs. baseline. **C** Media from microglia treated with LPS and IFNγ or vehicle was incubated with increasing concentrations of polyclonal anti-TNF antibodies (1:20,000 – 1:20) and concentrations of TNF were measured by enzyme-linked immunosorbent assay. Significance was determined by one-way ANOVA with Tukey post-hoc test. ~ $p < 0.05$ vs. baseline. **D** Conditioned media from stimulated or unstimulated microglia was incubated with vehicle or anti-TNF antibodies and applied to ST*Hdh*$^{Q7/Q7}$ and ST*Hdh*$^{Q111/Q111}$ cells, ATP concentrations were measured after 24 h. Significance was determined using two-way ANOVA with Sidak post-hoc test. * $p < 0.05$, ST*Hdh*$^{Q7/Q7}$ vs. ST*Hdh*$^{Q111/Q111}$. ~ $p < 0.05$ vs. baseline. **E** Conditioned media from stimulated or unstimulated microglia was

incubated with vehicle or anti-TNF antibodies and applied to ST*Hdh*$^{Q7/Q7}$ and ST*Hdh*$^{Q111/Q111}$ cells, proportions of cells penetrated by zombie red dye were manually counted. Conditioned media from stimulated or unstimulated microglia was incubated with vehicle, recombinant TNF, or anti-TNF antibodies and applied to ST*Hdh*$^{Q7/Q7}$ and ST*Hdh*$^{Q111/Q111}$ cells. Reduction of **F** calcein or **G** resazurin was measured after 24 h. Following the same conditioned media treatments, ST*Hdh*$^{Q7/Q7}$ and ST*Hdh*$^{Q111/Q111}$ were stained for **H** caspase-3 cleavage as a marker of apoptosis, or **I** RIP3 phosphorylation as a marker of necroptosis. Significance was determined using two-way ANOVA with Sidak post-hoc test. * $p < 0.05$, ST*Hdh*$^{Q7/Q7}$ vs. ST*Hdh*$^{Q111/Q111}$; ~ $p < 0.05$ vs. baseline; ^ $p < 0.05$, M1 media vs. M1 media + anti-TNF antibodies.

6.3.5. Inhibitory stimuli promoted resilience of neuronal cells

Differentiated ST*Hdh*$^{Q7/Q7}$ and ST*Hdh*$^{Q111/Q111}$ cells are models of striatal medium spiny neurons of the indirect pathway (Trettel et al. 2000). These cells express cannabinoid type 1 (CB_1) and dopamine type 2 (D_2) receptors which are linked to $G\alpha_i$, as well as adenosine 2a (A_{2A}) receptors which are linked to $G\alpha_s$ and N-methyl-D-aspartate (NMDA) receptors which mediate calcium uptake (Gerfen et al. 1990; Ferré et al. 2010, 2016; Galvan et al. 2012; Gardoni and Bellone 2015). Thus, agonists of CB_1 or D_2 receptors provide an inhibitory stimulus whereas agonists of A_{2A} or NMDA receptors provide distinct excitatory stimuli. We stimulated the neuronal cells with an agonist for each receptor subtype concurrently with the pro-inflammatory stimulus to determine whether stimulation or inhibition of the cells could improve survival.

The selective CB_1 receptor agonist, ACEA, as well as dopamine had no effect at the low concentration (500 nM) but substantially improved survival of ST*Hdh*$^{Q7/Q7}$ cells at a concentration of 5 μM ($F [9, 70] = 37.87$; $p < 0.0001$). In contrast, treatment with the A_{2A} receptor-selective agonist, CGS 21680, or NMDA had no effect on cell viability at either concentration (Fig. 6. 5A). A similar pattern was observed in ST*Hdh*$^{Q111/Q111}$ cells, however, the effect of CB_1 receptor activation was lost (Fig. 6. 5B)($F [9, 70] = 118.2$). It is possible that this was due to a loss of CB_1 receptor expression as we observed a reduction in *Cnr1* mRNA in ST*Hdh*$^{Q111/Q111}$ cells ($p = 0.0286$) with no change in *Drd2* (Fig. 6. 5C). ST*Hdh*$^{Q111/Q111}$ cells also exhibited increased mRNA for *Tnfrsf1a* ($p = 0.0412$) but reduced mRNA for *Tnfrsf1b* ($p = 0.0286$) which is consistent with the increased TNF-mediated cell death (Fig. 6. S2). Furthermore, the ST*Hdh*$^{Q111/Q111}$ cells had increased mRNA for *Ifngr1* and *Tlr4* which would indicate increased sensitivity to IFNγ and LPS, however, no direct effects of these molecules were observed with respect to cell viability (data not shown). Together, these data show that stimulation of D_2 receptors was protective against the pro-inflammatory microglial media in both cell types whereas CB_1 receptor stimulation was protective only in the wild-type ST*Hdh*$^{Q7/Q7}$ cells.

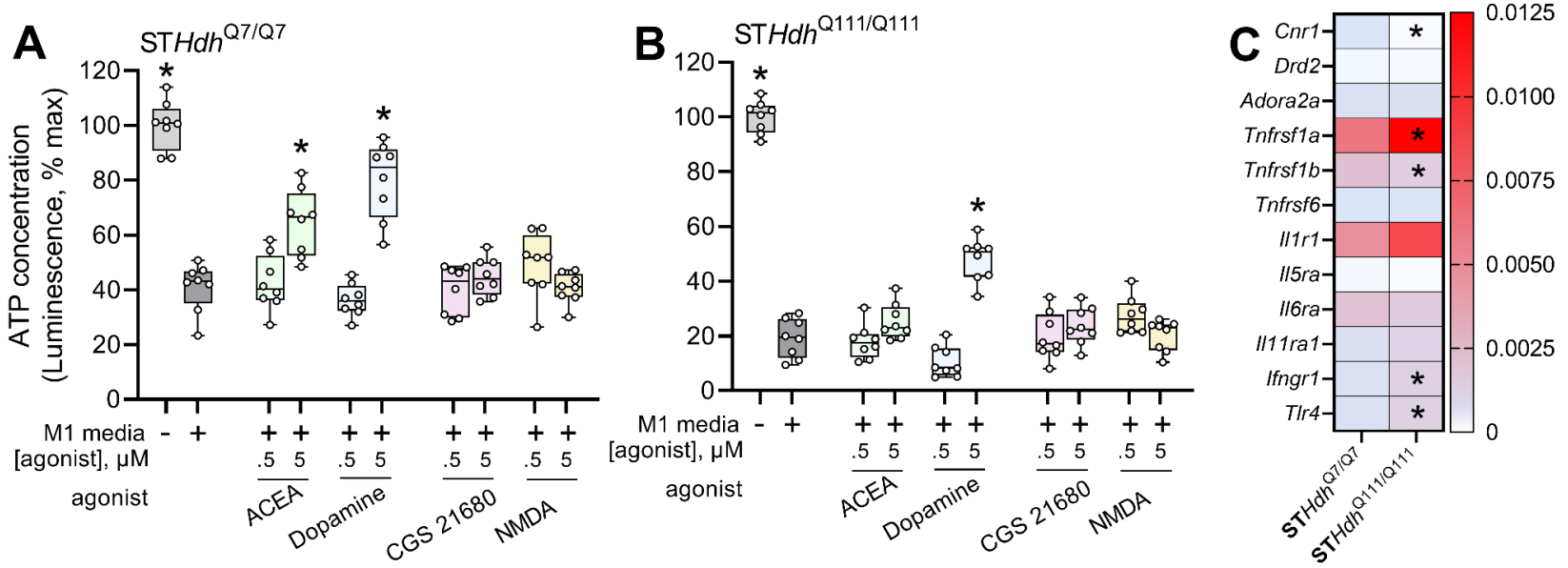

Figure 6. 5. Neuronal cell survival was improved by stimulation of CB_1 and D_2 receptors. Conditioned media from microglia treated with LPS (1000 ng/mL) and IFNγ (20 ng/mL) was combined with ACEA, dopamine, CGS 21680, or NMDA (500 nM or 5 µM) and added to **A** ST*Hdh*$^{Q7/Q7}$ or **B** ST*Hdh*$^{Q111/Q111}$ cells. ATP concentrations were measured after 24 h as a proxy for cell viability. Significance was determined using one-way ANOVA with Tukey post-hoc test. * $p < 0.05$ vs. pro-inflammatory media. **C** mRNA for several G protein-coupled receptors and cytokine receptors was measured to assess baseline differences between ST*Hdh*$^{Q7/Q7}$ and ST*Hdh*$^{Q111/Q111}$ cells. Significance was determined using two-tailed Mann-Whitney tests. * $p < 0.05$ vs. ST*Hdh*$^{Q7/Q7}$.

6.4 Discussion

We have investigated the differential effects of microglial-secreted factors on the cellular survival of wild-type ST*Hdh*$^{Q7/Q7}$ cells as well as ST*Hdh*$^{Q111/Q111}$ cells which express humanized mHTT. We have also investigated the mechanisms by which pro-inflammatory microglial media induces neuronal cell death. The results demonstrated that ST*Hdh*$^{Q111/Q111}$ cells exhibited hyperactivation of ERK, Akt, and CREB signaling pathways in the initial 3 h upon exposure to the pro-inflammatory media. This culminated in an overall increase in cell death which was attributed specifically to an increase in necroptosis. This mechanism of cell death in both cell types was dependent on TNF as neuronal survival could be maintained through the selective neutralization of TNF from the conditioned media. Thus, the results of this work suggest that TNF is required for microglia to promote neuronal death without phagocytosis, and highlights a mechanism by which mHTT may sensitize neurons to microglia-mediated death.

We observed enhanced death in cultured neuronal cells that expressed humanized mHTT compared to cells that expressed wtHTT. This death was preceded by the hyperactivation of ERK, Akt, and CREB. ERK was shown to play a critical role in glutamate-mediated necroptosis in cultured HT-22 mouse hippocampal neurons, necrostatin-1 inhibited early ERK phosphorylation but had no effect on JNK or p38 (Zhang et al. 2013). This necroptosis was also prevented by the ERK inhibitor, U0186, which suggests that ERK signaling can initiate necroptotic cell death (Zhang et al. 2013). Biphasic phosphorylation of ERK has been specifically associated with necroptosis as opposed to apoptosis in mouse L929 adipocytes (Sipieter et al. 2021). We also observed biphasic ERK phosphorylation in ST*Hdh*$^{Q111/Q111}$ cells, with an initial peak at 30 min and a second peak approaching by 3 h. This would be consistent with the increased proportion of necroptosis in ST*Hdh*$^{Q111/Q111}$ cells compared to ST*Hdh*$^{Q7/Q7}$ cells. TNF-mediated necroptosis was preceded by the activation of Akt and mTOR and subsequent generation of mitochondrial reactive oxygen species in HT-22 cells (Liu et al. 2014). In this case, cell death was prevented by necrostatin-1 as well as selective inhibitors of Akt and mTOR. This suggests that Akt as well as mTOR may also be an important distinguishing factor as we observed increased Akt phosphorylation in ST*Hdh*$^{Q111/Q111}$

cells compared to ST*Hdh*$^{Q7/Q7}$ cells in response to pro-inflammatory microglial media. We also observed increased phosphorylation of CREB in ST*Hdh*$^{Q111/Q111}$ cells. CREB is phosphorylated upon stimulation by pro-inflammatory cytokines, however, CREB is typically associated with an anti-apoptotic response rather than a pro-death response (Saha et al. 2009; Wen et al. 2010). CREB signaling was specifically associated with a neuroprotective response to TNF in HT-22 cells (Jensen et al. 2017). It is possible that CREB phosphorylation was elevated in ST*Hdh*$^{Q111/Q111}$ cells as a compensatory mechanism for the ERK- and Akt-dependent pro-death signaling but further probing of these pathways would be required to confirm this.

The contributions of microglia to neuronal death have been documented in a variety of experimental models of neurodegeneration disease, both *in vitro* and *in vivo* (Hickman et al. 2018). We found that pro-inflammatory media from microglia induced a mixture of apoptosis and necroptosis in cultured neuronal cells expressing wtHTT and mHTT. Specifically, ST*Hdh*$^{Q7/Q7}$ and ST*Hdh*$^{Q111/Q111}$ cells demonstrated equal levels of apoptosis whereas ST*Hdh*$^{Q111/Q111}$ cells exhibited more necroptosis. This distinction is relevant as necroptosis propagates inflammation via leakage of damage-associated molecular patterns whereas apoptosis does not (Pasparakis and Vandenabeele 2015). TNF is a potent inducer of apoptosis through the death-domain of TNFR1 which recruits several pro-apoptotic signal transducers (Dhuriya and Sharma 2018). TNF can also mediate necroptosis under certain circumstances (Sun et al. 1999). Necroptosis is driven by the formation of a RIP1-RIP3 complex which is favoured when RIP1 is unable to activate caspase-8 to initiate apoptosis (Holler et al. 2000; Sun et al. 2002; Cho et al. 2009; Berghe et al. 2014). In neurons, necroptosis is favoured when mitochondrial dysfunction leads to the depletion of ATP or nicotinamide adenine dinucleotide (NAD^+)(Kristian et al. 2011). Excitotoxic insults mediated by glutamate promote an excessive calcium influx which can promote necroptosis via mitochondrial calcium overload (Sattler and Tymianski 2001; Nakagawa et al. 2005). Neurons expressing mHtt have dysregulated mechanisms of intracellular calcium handling which sensitizes the cells to excitotoxic cell death (Tang et al. 2003, 2005; Wu et al. 2011). Necroptotic neurons have been observed multiple sclerosis (MS), amyotrophic lateral sclerosis (ALS),

and Parkinson's disease (PD) (Re et al. 2014; Ofengeim et al. 2015; Wu et al. 2015). TNF-mediated neuronal necroptosis also appeared to be elevated based on post-mortem analyses in tissues from Alzheimer's disease (AD) patients which were corroborated using human inducible pluripotent stem cells (iPSCs)(Jayaraman et al. 2021). The process of necroptosis is an emerging therapeutic target for the treatment of AD (Xu et al. 2021; Richard and Mousa 2022). Future work will determine whether necroptosis is a useful therapeutic target or if it is more beneficial to reduce molecules that initiate necroptosis, such as TNF.

It has been repeatedly demonstrated that TNF alone has limited capacity to induce neuronal injury but can be potentiated by several different stimuli when presented concurrently. A single dose of TNF (50 ng/mL) was found insufficient to induce either apoptosis or necrosis in cultured neurons in the absence of microglia (Neniskyte et al. 2014). This is consistent with our finding that recombinant TNF did not negatively affect the viability of ST*Hdh*$^{Q7/Q7}$ or ST*Hdh*$^{Q111/Q111}$ cells at concentrations of up to 150 ng/mL. TNF alone was also not neurotoxic to primary human co-cultures that consisted of neurons, astrocytes, and microglia (Chao et al. 1995). However, in the presence of IL-1β, TNF induced marked neuronal injury which could be prevented using an anti-TNF antibody (Chao et al. 1995). Similarly, conditioned media from microglia stimulated with amyloid-β induced death of mouse primary cortical neurons but was inhibited by co-treatment with recombinant soluble TNFR1 (Floden et al. 2005). It was also shown that TNF was only neurotoxic in the presence of microglia and that secondary neurotoxicity was dependent on the release of Fas ligand (Taylor et al. 2005). IFNγ was previously shown to potentiate cytotoxic effects of TNF on a cervical cancer cell line (Suk et al. 2001). In this case, it appeared that IFNγ inhibited the pro-survival response and shifted the effects of TNF toward a pro-death response. IFNγ also potentiated the pro-inflammatory response of microglia to TNF in Parkinsonian monkeys but it was not determined whether this enhanced neuronal death (Barcia et al. 2011). IFNγ induced neuronal death in co-cultures of primary neurons and glia, but IFNγ had no effect on neuronal survival in the absence of microglia (Mount et al. 2007). These reports suggest that IFNγ may also be required along with TNF to induce neurotoxicity. TNF has also

been demonstrated to induce neuronal death indirectly via microglia in several cell culture systems. In a co-culture model of microglia and neurons, microglia were observed to phagocytose otherwise viable neurons upon stimulation with TNF (Neniskyte et al. 2014). Microglia also elicited neuronal death via excitotoxicity through the release of glutamate upon TNF treatment (Takeuchi et al. 2006). Together, these reports suggest that TNF, IL-1β, IFNγ, and glutamate each play important roles in microglia-mediated cell death.

We observed that stimulation of D_2 receptors improved survival in ST*Hdh*$^{Q7/Q7}$ and ST*Hdh*$^{Q111/Q111}$ cells whereas stimulation of CB_1 receptors was only beneficial in ST*Hdh*$^{Q7/Q7}$ cells. A loss of CB_1 receptors is a well established characteristic of striatal neurons in HD, as well as in these cell lines (Glass et al. 1993; Laprairie et al. 2013). As we also observed a loss in *Cnr1* mRNA, it is possible that the reduced efficacy of ACEA in ST*Hdh*$^{Q111/Q111}$ cells was due to reduced receptor density. Although a loss of D_2 and A_{2A} receptors has also been observed in the progression of HD, we did not find a difference in *Drd2* or *Adora2a* mRNA between cell types (Richfield et al. 1991; Glass et al. 2000). There are conflicting reports regarding whether it is more beneficial to enhance or suppress striatal dopamine in HD (Chen et al. 2013; Cepeda et al. 2014). The D_2 receptor agonist, quinpirole, has been shown to reduce striatal excitotoxicity in rats (Cepeda et al. 1998). Antidopaminergic drugs reduced the motor symptoms of HD in humans, but worsened cognition (Harris et al. 2020). Thus, dopaminergic signaling appears to be pleiotropic and promotes neuronal survival and dysfunction. In addition to D_2 receptors, stimulation of CB_1 receptors has been proposed as a useful treatment for HD. The use of a positive allosteric modulator of CB_1 receptors delayed the onset of symptoms in the R6/2 mouse model of HD (Laprairie et al. 2019). Direct stimulation of CB_1 receptors using delta(9)-tetrahydrocannabinol (THC) improved outcomes in the mouse experimental autoimmune encephalomyelitis (EAE) model of MS (Maresz et al. 2007). However, such treatments would likely be associated with an intolerable degree of psychoactivity (Kleine-Brueggeney et al. 2015). Direct activation of CB_1 receptors has been demonstrated to reduce neurogenic inflammation in the periphery, as well as microglial cytokine release (McKenna and McDougall 2020; Young and Denovan-

Wright 2022b). Together, these reports suggest that CB_1 receptors would be viable therapeutic targets to improve neuronal survival and reduce inflammation. However, dose is important and the adverse effects of chronic global CB_1 receptor activation may limit the usefulness of this strategy.

There are several FDA-approved TNF inhibitors which are typically prescribed to treat chronic inflammatory conditions, including autoimmune disorders (Kodama et al. 2005; Meier et al. 2013; Meroni et al. 2015). However, there is growing attention toward the use of TNF inhibitors for the treatment of neurodegenerative diseases (Chang et al. 2017; Torres-Acosta et al. 2020). Patients that took TNF blocking agents for rheumatoid arthritis, psoriasis, and ankylosing spondylitis have shown a reduced risk of developing AD (Zhou et al. 2020; Watad et al. 2022). However, TNF inhibitors did not reduce the risk of dementia among rheumatoid arthritis patients when compared to abatacept or methotrexate (Kern et al. 2021; Desai et al. 2022). Among patients with inflammatory bowel disease, early exposure to anti-TNF therapy reduced the incidence of PD by 78% (Peter et al. 2018). Thus, the use of TNF inhibitors has shown promise among patients that use them to treat chronic inflammatory conditions. TNF inhibitors have also shown therapeutic potential with respect to cognitive performance, neuroinflammation, and motor performance in mouse models of tauopathy, AD, PD, and HD (McCoy et al. 2006; Shi et al. 2011; Hsiao et al. 2014; Kim et al. 2016; Ou et al. 2021). In the future, it will be important to determine whether the early blockade of TNF in the brain is a viable treatment for slow the progression of neurodegeneration in healthy individuals at high-risk for neurodegeneration such as those that carry mutant *huntingtin* or familial AD risk genes.

6.5 Supplementary data

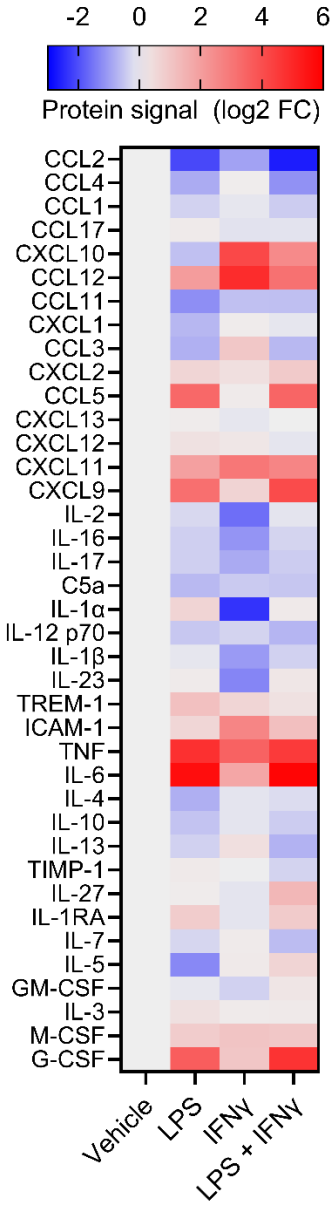

Figure 6. S1. Proteome Profiler antibody array results. SIM-A9 microglia were stimulated with vehicle (PBS), LPS (1000 ng/mL), IFNγ (20 ng/mL), or LPS and IFNγ, and the media was assessed for the protein abundance of 39 cytokines and chemokines. Proteins were measured using a Proteome Profiler™ antibody array; cell culture supernatant from 24 technical replicates was pooled and incubated with each membrane with antibodies spotted in duplicate. Data are presented as the $\log_2$ fold-change relative to vehicle treatment.

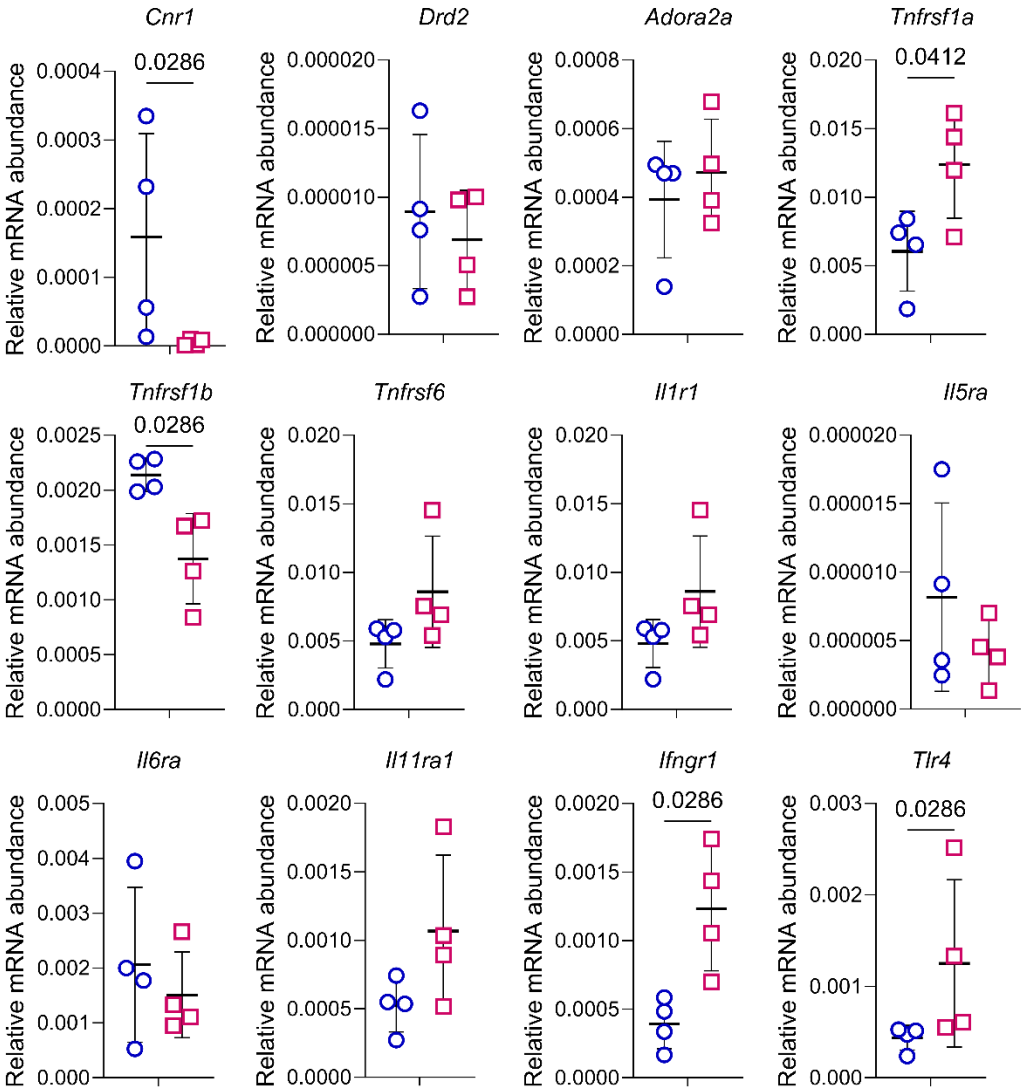

Figure 6. S2. mRNA for several G protein-coupled receptors and cytokine receptors in ST*Hdh*$^{Q7/Q7}$ and ST*Hdh*$^{Q111/Q111}$ cells. Significance was determined using two-tailed Mann-Whitney tests. * $p < 0.05$ vs. ST*Hdh*$^{Q7/Q7}$.

Chapter 7: Methods

7.1 Pharmacological compounds and preparation of treatments

All compounds used in this research are detailed in Table 7. 1. Small molecules were dissolved in dimethyl sulfoxide (DMSO) and recombinant proteins were diluted in phosphate buffered saline (PBS) with 0.1% bovine serum albumin (BSA). All compounds were stored at -20°C at concentrations of at least 1 mM or 100 µg/mL. Compounds were prepared in serum-free media and negative control groups received the vehicle of DMSO and/or PBS with 0.1% BSA as appropriate. Treatments and corresponding vehicle solutions were also prepared in serum-free media so that media for all treatment groups contained 0.1% DMSO.

7.2 Cell culture

Spontaneously immortalized microglia (SIM)-A9 cells (ATCC CRL-3265; Nagamoto-Combs et al., 2014) were purchased from Cedarlane (Burlington, ON, Canada). SIM-A9 microglia were maintained at 37°C with 5% CO_2 in complete media containing Dulbecco's modified eagle's medium (DMEM):F12 (ATCC 30-2006), supplemented with 10% heat-inactivated fetal bovine serum (Gibco, #A31607), 5% heat-inactivated donor horse serum (Sigma-Aldrich, #H1270), and 100 U/mL penicillin-streptomycin (Gibco, #15140122). Cells were dissociated from plates using PBS with 0.5 mM EDTA (Sigma-Aldrich, #D8537). SIM-A9 microglia are of female origin (Krasnow et al. 2017).

Conditionally immortalized ST*Hdh*$^{Q7/Q7}$ cell lines were derived from striatal progenitor cells of female embryonic day 14 C57BL/6J mice. The ST*Hdh*$^{Q7/Q7}$ cells possess mutant huntingtin loci with a humanized exon 1 containing 7 polyglutamine repeats. Cells were maintained at 33°C, 5% CO_2 in DMEM that was supplemented with 10% fetal bovine serum, 2 mM L-glutamine, 100 U/mL penicillin-streptomycin, and 400 µg/mL Geneticin. To promote differentiation into an adult neuron-like phenotype, the complete media was replaced with serum-free DMEM that contained the following differentiation cocktail: acidic fibroblast growth factor (10 ng/mL), 3-isobutyl-1-

methylxanthine (250 μM), phorbol 12-myristate 13-acetate (200 nM), forskolin (50 μM), and dopamine (10 μM). The cells were allowed to differentiate for 16 hours prior to experimentation (Hauber 1998; Trettel et al. 2000).

RAW 264.7 macrophage-like cells (ATCC® TIB-71) were routinely maintained at 37˚C with 5% CO_2 up to the 15th passage. Cells were grown in complete media containing DMEM (Gibco, #10313021), supplemented with 10% fetal bovine serum and 100 U/mL penicillin-streptomycin. Cells were dissociated from plates using 0.5 mM EDTA in Dulbecco's Phosphate Buffered Saline. Immortalized RAW 264.7 cells were established from a male mouse.

Human embryonic kidney (HEK) 293T cells (ATCC® CRL-3216) were routinely maintained at 37˚C with 5% CO_2. Cells were grown in complete media containing DMEM (Gibco, #10313021), supplemented with 10% fetal bovine serum and 100 U/mL penicillin-streptomycin. Cells were dissociated from plates using 0.5 mM EDTA in Dulbecco's Phosphate Buffered Saline. HEK 293T cells were established from the kidney epithelium of a human female fetus.

7.3 Microglial NO release

NO release from microglial and macrophage cells was determined using a Griess reagent system. Briefly, 30,000 cells were seeded into 96-well plates and allowed to adhere to the plate for at least 3 h. Treatments were added at the desired concentration in 100 μL serum-free media. After 16 h, 50 μL of media was moved to a new clear 96-well plate and combined with 50 μL of Griess solution (Sigma, #G4410). Following an incubation of 10 minutes in the dark, absorbance of the samples was measured at 540 nm with a FLUOstar Omega plate reader (BMG Labtech; Ortenberg, DE). Standard preparations of nitrite were used to prepare standard curves to quantify NO release (μM).

7.4 Enzyme-linked immunosorbent assays

SIM-A9 microglia were seeded into 96-well plates at a density of 30,000 cells per well in serum-free media and allowed to adhere for at least 3 h. Cells were treated as indicated and the media was measured to determine the concentration of TNF, IL-1β, and

IL-6. The protocols for the ELISAs were followed as per the manufacturer's instructions for the mouse TNF (R&D Systems, #MTA00B; Minneapolis, MN, USA), IL-1β (R&D Systems, #DY401-05) and IL-6 (R&D Systems, #DY406-05) kits. Dilution factors of 1:50, 1:1, and 1:10 were used for TNF, IL-1β and IL-6, respectively.

7.5 Reverse transcription quantitative PCR

To isolate total RNA, cells were seeded into 6-well plates at 500,000 cells per well in serum-free media and allowed at least 3 h to adhere to the plate. Following treatment, cells were dissociated from the plates and pelleted in 1.5 mL microcentrifuge tubes. RNA was isolated via the TRIzol method using 1 mL of TRIzol reagent per sample (Invitrogen, #LS15596026; Burlington, ON, Canada). Genomic DNA was removed using DNase I (NEB, #M0303) as per manufacturer's recommendations and RNA was purified by ethanol precipitation. Total RNA (1 µg) was reverse transcribed in a 20 µL reaction using the LunaScript RT SuperMix Kit (NEB, #E3010) at 25°C for two minutes, 55°C for ten minutes, and 95°C for one minute. The complementary DNA (cDNA) was diluted 1:3 with DEPC-treated water and stored at -20°C. To amplify each gene of interest, 2 µL of diluted cDNA was combined with 10 µL of Luna Universal qPCR Master Mix (NEB, #M3003), 500 nM of forward and reverse primers, and topped to 20 µL with DEPC-treated water. The details of all primers used are included in Table 7. 2. The reactions took place in a Bio-Rad CFX96 Touch system (Bio-Rad Laboratories; Hercules, CA, USA) with an initial denaturation of 95°C for one minute, followed by 45 cycles of 95°C for 15 seconds and 56°C for 30 seconds. Fluorescence was measured after each cycle.

Data were converted to delta Cq (dCq) values by subtraction of the Cq of the gene of interest from the mean Cq value of the reference genes. The dCq values were transformed using the formula $2^{\wedge dCq}$ to determine the mean number of mRNA molecules present for the gene of interest relative to the reference genes. The data were either presented as the $2^{\wedge dCq}$ values or as the fold-change of the vehicle control mean. Elongation factor 1-alpha (*Eef1a*) and beta-2 microglobulin (*B2m*) were used as reference genes and were determined to be stable among treatment groups as per the methods of Young et al. (2019) and Mishra et al. (2023).

7.6 Immunofluorescence

SIM-A9 microglia or ST*Hdh*$^{Q7/Q7}$ neurons were seeded onto round 18 mm coverslips (ThermoFisher Scientific, #NC0301187) in 12-well plates at a density of 150,000 cells per coverslip in serum-free media and allowed at least 3 h to adhere to the coverslip. Cells were treated as indicated, rinsed thrice with TBS, and fixed in 4% paraformaldehyde (ThermoFisher Scientific, #AA433689M) in TBS for 12 minutes. Coverslips were washed in TBS with 0.3% Triton X-100 for 20 minutes to permeabilize the cells. The cells were blocked for at least 45 minutes in 20% Intercept blocking buffer (LI-COR Biosciences, #927-60001; Lincoln, NE, USA) in TBS. Coverslips were incubated overnight at 4°C in primary antibody at a dilution of 1:500. The details of antibodies used are available in Table 7. 3. Coverslips were washed thrice in TBS with 0.1% Tween-20 for at least five minutes each and incubated in secondary antibody at a dilution of 1:500 at room temperature for two hours. Coverslips were again washed thrice in TBS with 0.1% Tween-20 for at least five minutes each and mounted in ProLong Diamond Antifade Mountant (ThermoFisher Scientific, #P36965). Slides were viewed on a Leica SP8 inverted confocal microscope (Leica Microsystems; Wetzlar, Germany) at 64-100X objective using oil immersion. Images were captured using Leica LAS X software. Adjustments to brightness and contrast were made to entire images, and equal adjustments were made to all images within each experiment.

7.7 Preparation of conditioned media

SIM-A9 microglia were grown to confluence in 10 cm dishes and treated with LPS and IFNγ in 5 mL of serum-free DMEM:F12 for 16 h. The media was aspirated from the 10 cm dishes and centrifuged at 300 x g for five minutes to pellet any cells. The supernatant was aspirated and stored at -20°C until needed. Control (M0) media was prepared in parallel from microglia that did not receive LPS or IFNγ.

7.8 Cell viability assays

The LIVE/DEAD Viability/Cytotoxicity Kit for mammalian cells (Invitrogen, #L3224) was used to measure the proportion of dead cells following treatment with conditioned media. The viability assay relies on ethidium homodimer-1 which penetrates dead cells and fluoresces upon intercalation of DNA. ST*Hdh*$^{Q7/Q7}$ neurons or HEK 293T cells were seeded into white clear-bottom 96-well plates in complete media. ST*Hdh*$^{Q7/Q7}$ cells were treated with the differentiation cocktail and allowed 16 hours to differentiate to a neuronal phenotype. The cells were incubated with conditioned media for 24 h, rinsed twice with warm PBS, and then equilibrated in 200 µL PBS that contained 2 µM EthD-1. Fluorescence (544/620 nm) was measured using a FLUOstar Omega plate reader (BMG Labtech). Data were reported as cell death (%) where 0% was defined by untreated cells and 100% was defined by cells treated with 70% methanol for 20 minutes to permeabilize the membrane and allow maximal EthD-1 penetration.

ATP concentrations were measured as a proxy for cell viability using the CellTiter Glo viability kit (Promega) as per the manufacturer's instructions. ST*Hdh*$^{Q7/Q7}$ neurons were plated and treated as described, and 100 µL of CellTiter Glo reagent was added to lyse the cells and provide a luminescent signal proportional to the concentration of ATP. Total luminescence was measured using a FLUOstar Omega plate reader (BMG Labtech). A standard curve of ATP was used to determine the absolute concentration within each sample.

The penetration of Zombie red dye was used as a proxy for cell death of neuronal cells in response to microglial media. The Zombie Red™ Fixable Viability Kit (BioLegend, #423109) was used as per the manufacturer's recommendation. Briefly, ST*Hdh*$^{Q7/Q7}$ neurons were plated and treated as described, fixed in 4% PFA for 15 minutes, incubated with Zombie red dye at a 1:1,000 dilution for 30 minutes in the dark, rinsed in complete media to quench extracellular staining, and mounted for viewing on the confocal microscope.

Resazurin reduction was also assessed as a measure of cell viability using the CellTiter Blue viability kit (Promega) as per the manufacturer's instructions. Briefly, ST*Hdh*$^{Q7/Q7}$ neurons were plated in clear-bottom black 96-well plates and treated as

described, 20 µL of CellTiter blue reagent was added and the plates were incubated at 37°C for 2 h. Fluorescence was measured using the resorufin filter of a CLARIOstar plate reader to determine the reduction of resazurin to resorufin.

7.9 In-cell western assays

SIM-A9 microglia were seeded into black clear-bottom 96-well plates (ThermoFisher Scientific, #12-566-70) at a density of 30,000 cells per well in serum-free media and allowed a minimum of 3 h to adhere to the plate. Cells were stimulated as indicated and fixed in 4% PFA in Tris buffered saline (TBS; 137 mM sodium chloride, 20 mM Tris, pH 7.6) for 15 minutes at room temperature. Cells were rinsed in TBS, permeabilized in TBS with 0.3% Triton X-100 for 15 minutes, rinsed in TBS again, and blocked in 20% Intercept blocking buffer (LI-COR Biosciences, #927-60001) diluted in TBS with 0.1% Tween-20 for at least 45 minutes. Phosphorylated proteins were detected using the primary antibodies diluted in blocking buffer to a final dilution of 1:200. Primary antibody incubations took place overnight at 4°C without agitation. Cells were rinsed thrice in TBS + 0.1% Tween-20 and incubated at room temperature for two hours with the secondary antibodies conjugated to IRDye 800CW at a dilution of 1:500. Cells were co-incubated with CellTag 700 (LI-COR Biosciences, #926-41090; 1:500 dilution) to allow for normalization to cell number. Cells were rinsed thrice in TBS and allowed to dry for at least 20 minutes prior to imaging. Plates were imaged on an Odyssey CLx platform (LI-COR Biosciences) using Image Studio version 5.0 software at medium quality, 4.0 mm focus offset, and automated channel intensities. The fluorescence of the 800 nm channel was normalized to the fluorescence of the 700 nm channel to provide normalized signal intensities for each sample. Normalized signals were used for statistical purposes and data were presented as the fold-change compared to the mean of the negative control or vehicle treatment.

7.10 NanoLuc binary technology assay and construct preparation

To prepare the CB_2-SmBiT construct, the sequence for the human CB_2 receptor was subcloned into the pBiT3.1-C [CMV/SmBiT] Vector (Promega). The CB_2 receptor sequence was obtained from Dr. Bryan Roth (University of North Carolina at Chapel Hill) via Addgene (plasmid # 66255). The CB_2 receptor sequence was amplified using primers harboring XhoI and HindIII sites and the PCR product was gel purified using the Monarch® DNA gel extraction kit (NEB, # T1020). The CB_2 receptor fragment and the pBiT3.1-SmBiT backbone were digested using the XhoI and HindIII restriction enzymes and purified using the Monarch® PCR & DNA clean-up kit (NEB, # T1030). The digested fragments were ligated using instant sticky-end ligase master mix (NEB, #M0370), transformed into NEB® 5-alpha competent *E. coli* (high efficiency; NEB, #C2987), and plasmid DNA was isolated using the Monarch® plasmid miniprep kit (NEB, #T1010). The CB_2-SmBiT construct was verified by next-generation sequencing prior to use (Plasmidsaurus; Eugene, OR). The sequences and annotated maps of the CB_2-smBiT and lgBiT-mini-$G\alpha_i$ plasmids are included in Figures 7.1 and 7.2, respectively. The sequence of the sm-BiT-β-arrestin2 plasmid can be obtained directly from the manufacturer, Promega.

To perform the NanoBiT assay, HEK 293T cells were distributed into white 96-well plates and allowed 3 h to adhere. To transiently transfect HEK 293T cells, 50 ng of the CB_2-BiT construct and 50 ng of the effector (β-arrestin2 or mini-$G\alpha_i$) construct was diluted in OptiMEM media with 0.3 µL FuGENE HD (Promega) in a final volume of 8 µL per well and the transfection mixture was added directly to the cells. Cells were incubated with the transfection mixture for 24 h prior to experimentation. Immediately prior to experimental treatment, media was aspirated from the cells and replaced with 100 µL of Nano-Glo reagent from the Nano-Glo® Live Cell Assay System (Promega, #N2012). Luminescence was monitored to ensure that the nanoluciferase signal was stable (30 minutes), the mean luminescence over the final 9 minutes was used to establish the basal luminescence value for each well. To stimulate the cells, 10 µL of the experimental treatment (11X concentrated) was added directly to the cells. Luminescence was recorded from each well at 3-min intervals for 42 minutes using a FLUOstar Omega

plate reader (BMG Labtech). To calculate the corrected luminescence values, the raw luminescence values at each time-point were divided by the basal luminescence value which was established immediately prior to treatment. For experiments that used SR144528 (inverse agonist), the cells were incubated with the compound for 10 min after the basal luminescence was established and before the addition of the agonist.

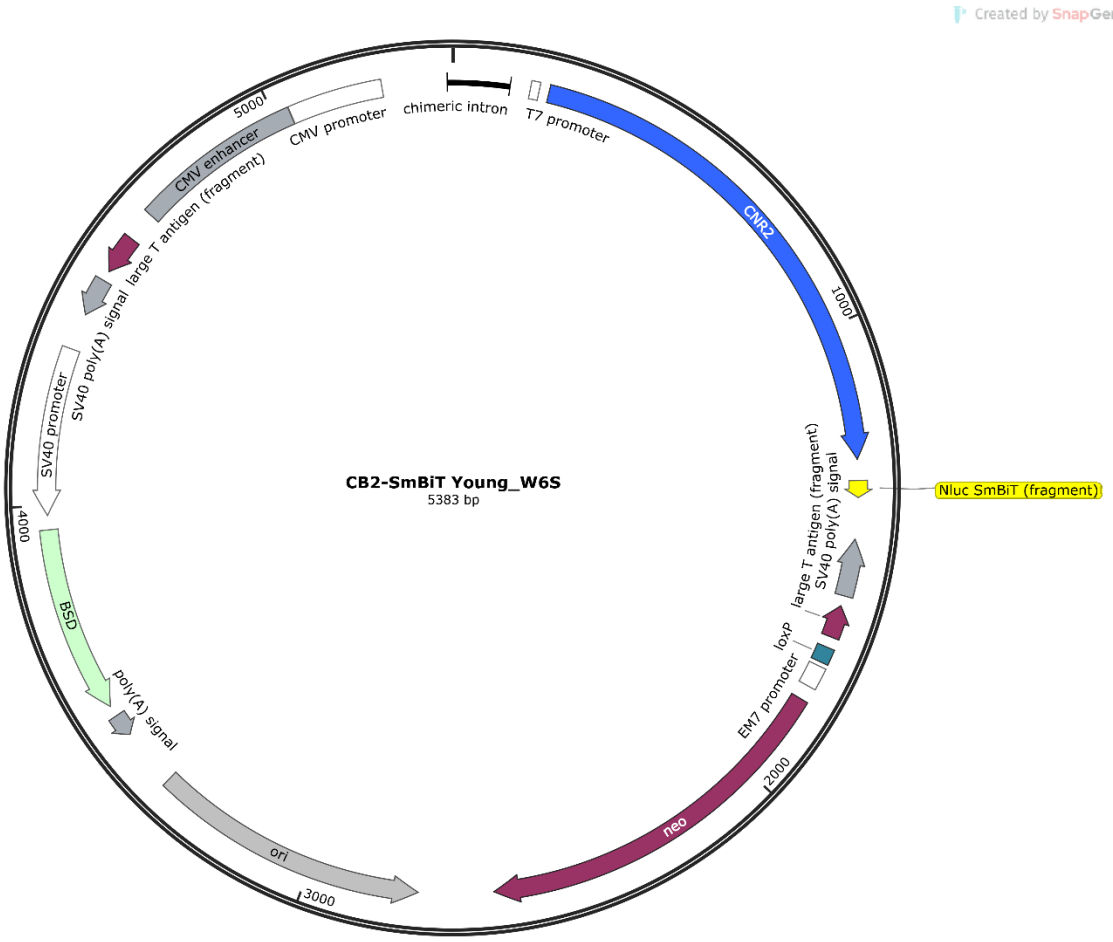

Figure 7. 1. Plasmid map of the CB_2-smBiT plasmid used for the nanoluciferase assays. The complete sequence of the plasmid is:

>GGTTACAAGACAGGTTTAAGGAGACCAATAGAAACTGGGCTTGTCGAGACA
GAGAAGACTCTTGCGTTTCTGATAGGCACCTATTGGTCTTACTGACATCCACT
TTGCCTTTCTCTCCACAGGTGTCCACTCCCAGTTCAATTACAGCTCTTAAGGCT
AGAGTATTAATACGACTCACTATAGGGGCGATCGCAACAAGCTTACCATGGA
GGAATGCTGGGTGACAGAGATAGCCAATGGCTCCAAGGATGGCTTGGATTCC
AACCCTATGAAGGATTACATGATCCTGAGTGGTCCCCAGAAGACAGCTGTTG
CTGTGTTGTGCACTCTTCTGGGCCTGCTAAGTGCCCTGGAGAACGTGGCTGTG
CTCTATCTGATCCTGTCCTCCCACCAACTCCGCCGGAAGCCCTCATACCTGTT
CATTGGCAGCTTGGCTGGGGCTGACTTCCTGGCCAGTGTGGTCTTTGCATGCA
GCTTTGTGAATTTCCATGTTTTCCATGGTGTGGATTCCAAGGCTGTCTTCCTGC
TGAAGATTGGCAGCGTGACTATGACCTTCACAGCCTCTGTGGGTAGCCTCCTG
CTGACCGCCATTGACCGATACCTCTGCCTGCGCTATCCACCTTCCTACAAAGC
TCTGCTCACCCGTGGAAGGGCACTGGTGACCCCGGGCATCATGTGGGTCCTC
TCAGCACTAGTCTCCTACCTGCCCCTCATGGGATGGACTTGCTGTCCCAGGCC

CTGCTCTGAGCTTTTCCCACTGATCCCCAATGACTACCTGCTGAGCTGGCTCC
TGTTCATTGCCTTCCTCTTTTCCGGAATCATCTACACCTATGGGCATGTTCTCT
GGAAGGCCCATCAGCATGTGGCCAGCTTGTCTGGCCACCGGGACAGGCAGGT
GCCGGGAATGGCCCGAATGAGGCTGGATGTGAGGTTGGCCAAGACCCTAGG
GCTAGTGTTGGCTGTGCTCCTCATCTGTTGGTTCCCAGTGCTGGCCCTCATGG
CCCACAGCCCGGCCACTACGCTCAGTGACCAGGTCAAGAAGGCCTTTGCTTT
CTGCTCCATGCTGTGCCTCATCAACTCCATGGTCAATCCTGTCATCTATGCTCT
ACGGAGTGGAGAGATCCGCTCCTCTGCCCATCACTGCCTGGCTCACTGGAAG
AAGTGTGTGAGGGGCCTTGGGTCAGAGGCAAAAGAAGAAGCCCCGAGATCC
TCAGTCACCGAGACAGAGGCTGATGGGAAAATCACTCCGTGGCCAGATTCCA
GAGATCTAGACCTCTCTGATTGCGGCTCGAGCGGTGGTGGCGGGAGCGGAGG
TGGAGGGTCGTCAGGTGTGACCGGCTACCGGCTGTTCGAGGAGATTCTGTAA
GTTTAAACGGCCGCGACTCTAGACTGCAGGCATGCAAGCTGATTTGGCTGCT
GCCACCGCTGAGCAAGGCCGCTTCGAGCAGACATGATAAGATACATTGATGA
GTTTGGACAAACCACAACTAGAATGCAGTGAAAAAAATGCTTTATTTGTGAA
ATTTGTGATGCTATTGCTTTATTTGTAACCATTATAAGCTGCAATAAACAAGT
TAACAACAACAATTGCATTCATTTTATGTTTCAGGTTCAGGGGGAGATGTGGG
AGGTTTTTTTAAGCAAGTAAAACCTCTACAAATGTGGTAAAATCTTAATTAAG
ACTTCTAATATAACTTCGTATAGCATACATTATACGAAGTTATGGTTCCACTG
TTGACAATTAATCATCGGCATAGTATATCGGCATAGTATAATACGACAAGGT
GAGGAACTAAACCCAGGAGGCAGATCATGATTGAACAAGATGGATTGCACG
CAGGTTCTCCGGCCGCTTGGGTGGAGAGGCTATTCGGCTATGACTGGGCACA
ACAGACAATCGGCTGCTCTGATGCCGCCGTGTTCCGGCTGTCAGCGCAGGGG
CGCCCGGTTCTTTTTGTCAAGACCGACCTGTCCGGTGCCCTGAATGAACTGCA
GGACGAGGCAGCGCGGCTATCGTGGCTGGCCACGACGGGCGTTCCTTGCGCA
GCTGTGCTCGACGTTGTCACTGAAGCGGGAAGGGACTGGCTGCTATTGGGCG
AAGTGCCGGGGCAGGATCTCCTGTCATCTCACCTTGCTCCTGCCGAGAAAGT
ATCCATCATGGCTGATGCAATGCGGCGGCTGCATACGCTTGATCCGGCTACCT
GCCCATTCGACCACCAAGCGAAACATCGCATCGAGCGAGCACGTACTCGGAT
GGAAGCCGGTCTTGTCGATCAGGATGATCTGGACGAAGAGCATCAGGGGCTC
GCGCCAGCCGAACTGTTCGCCAGGCTCAAGGCGCGCATGCCCGACGGCGAGG
ATCTCGTCGTGACCCATGGCGATGCCTGCTTGCCGAATATCATGGTGGAAAAT
GGCCGCTTTTCTGGATTCATCGACTGTGGCCGGCTGGGTGTGGCGGACCGCTA
TCAGGACATAGCGTTGGCTACCCGTGATATTGCTGAAGAGCTTGGCGGCGAA
TGGGCTGACCGCTTCCTCGTGCTTTACGGTATCGCCGCTCCCGATTCGCAGCG
CATCGCCTTCTATCGCCTTCTTGACGAGTTCTTCTGATTCGAAATGACCGACC
AAGCGACGCCCAACCGGTATCAGCTCACTCAAAGGCGGTAATACGGTTATCC
ACAGAATCAGGGGATAACGCAGGAAAGAACATGTGAGCAAAAGGCCAGCAA
AAGGCCAGGAACCGTAAAAAGGCCGCGTTGCTGGCGTTTTTCCATAGGCTCC
GCCCCCCTGACGAGCATCACAAAAATCGACGCTCAAGTCAGAGGTGGCGAA
ACCCGACAGGACTATAAAGATACCAGGCGTTTCCCCCTGGAAGCTCCCTCGT
GCGCTCTCCTGTTCCGACCCTGCCGCTTACCGGATACCTGTCCGCCTTTCTCCC
TTCGGGAAGCGTGGCGCTTTCTCATAGCTCACGCTGTAGGTATCTCAGTTCGG
TGTAGGTCGTTCGCTCCAAGCTGGGCTGTGTGCACGAACCCCCCGTTCAGCCC
GACCGCTGCGCCTTATCCGGTAACTATCGTCTTGAGTCCAACCCGGTAAGAC

ACGACTTATCGCCACTGGCAGCAGCCACTGGTAACAGGATTAGCAGAGCGAG
GTATGTAGGCGGTGCTACAGAGTTCTTGAAGTGGTGGCCTAACTACGGCTAC
ACTAGAAGGACAGTATTTGGTATCTGCGCTCTGCTGAAGCCAGTTACCTTCGG
AAAAAGAGTTGGTAGCTCTTGATCCGGCAAACAAACCACCGCTGGTAGCGGT
GGTTTTTTTGTTTGCAAGCAGCAGATTACGCGCAGAAAAAAAGGATTTCAAG
AAGATCCTTTGATCTTTTCTACGGGGTCTGACGCTCAGTGGAACGAAAACTCA
CGTTAAGGGATTTTGGTCATGAGATTATCAAAAAGGATCTTCACCTAGATCCT
TTTATAGTCCGGAATCGTCACACAAAAAACCAACACACAGATGTAATGAAAA
TAAAGATATTTTATTGCGGCCATCGTGATGGCTAGAGTTTAGCCCTCCCACAC
ATAACCAGAGGGCAGCAATTCACGAATCCCAACTGCCGTCGGCTGTCCATCA
CTGTCCTTCACTATGGCTTTGATCCCAGGATGCAGATCGAGAAGCACCTGTCG
GCACCGTCCGCAGGGGCTCAAGATGCCCCTGTTCTCATTTCCGATCGCGACG
ATACAAGTCAGGTTGCCAGCTGCCGCAGCAGCAGCAGTGCCCAGCACCACGA
GTTCTGCACAAGGTCCCCCAGTAAAATGATATACATTGACACCAGTGAAGAT
GCGGCCGTCGCTAGAGAGAGCTGCGCTGGCGACGCTGTAGTCTTCAGAGATG
GGGATGCTGTTGATTGTAGCCGTTGCTCTTTCAATGAGGGTGGATTCTTCTTG
AGACAAAGGCTTGGCCATGGTGGCGCTAGTGTCAGAAGAATCGAGCTTTTTG
CAAAAGCCTAGGCCTCCAAAAAAGCCTCCTCACTACTTCTGGAATAGCTCAG
AGGCCGAGGCGGCCTCGGCCTCTGCATAAATAAAAAAAATTAGTCAGCCATG
GGGCGGAGAATGGGCGGAACTGGGCGGAGTTAGGGGCGGGATGGGCGGAGT
TAGGGGCGGGACTATGGTTGCTGACTAATTGAGATGCATGCTTTGCATACTTC
TGCCTGCTGGGGAGCCTGGGGACTTTCCACACCTGGTTGCTGACTAATTGAGA
TGCATGCTTTGCATACTTCTGCCTGCTGGGGAGCCTGGGGACTTTCCACACCC
TAACTGACACACATTCCACAGCTGGTTCTTTCCGCCTCAGAAGGTACCTAACC
AAGTTCCTCTTTCAGAGGTTATTTCAGGCCATGGTGCTGCGCAAGACGCGTTA
ATTAAGACGTCGGCAGTGAAAAAAATGCTTTATTTGTGAAATTTGTGATGCTA
TTGCTTTATTTGTAACCATTATAAGCTGCAATAAACAAGTTAACAACAACAAT
TGCATTCATTTTATGTTTCAGGTTCAGGGGGAGGTGTGGGAGGTTTTTTAAAG
CAAGTAAAACCTCTACAAATGTGGTATGGCTGATTATGATCCGCGGCCGCAA
TACGTCGACGTTATCAGCTGACTTCGTACGAGAGCCTAGGATTATGGCGCGC
CACTAGTTATTAATAGTAATCAATTACGGGGTCATTAGTTCATAGCCCATATA
TGGAGTTCCGCGTTACATAACTTACGGTAAATGGCCCGCCTGGCTGACCGCC
CAACGACCCCCGCCCATTGACGTCAATAATGACGTATGTTCCCATAGTAACG
CCAATAGGGACTTTCCATTGACGTCAATGGGTGGAGTATTTACGGTAAACTG
CCCACTTGGCAGTACATCAAGTGTATCATATGCCAAGTCCGCCCCCTATTGAC
GTCAATGACGGTAAATGGCCCGCCTGGCATTATGCCCAGTACATGACCTTAC
GGGACTTTCCTACTTGGCAGTACATCTACGTATTAGTCATCGCTATTACCATG
GTGATGCGGTTTTGGCAGTACACCAATGGGCGTGGATAGCGGTTTGACTCAC
GGGGATTTCCAAGTCTCCACCCCATTGACGTCAATGGGAGTTTGTTTTGGCAC
CAAAATCAACGGGACTTTCCAAAATGTCGTAATAACCCCGCCCCGTTGACGC
AAATGGGCGGTAGGCGTGTACGGTGGGAGGTCTATATAAGCAGAGCTGGTTT
AGTGAACCGTCAGATCACTAGAATCTTTATTGCGGTAGTTTATCACAGTTAAA
TTGCTAACGCAGTCAGTGCTTCTGACACAACAGTCTCGAACTTAAGCTGCAG
AAGTTGGTCGTGAGGCACTGGGCAGGTAAGTATCAA.

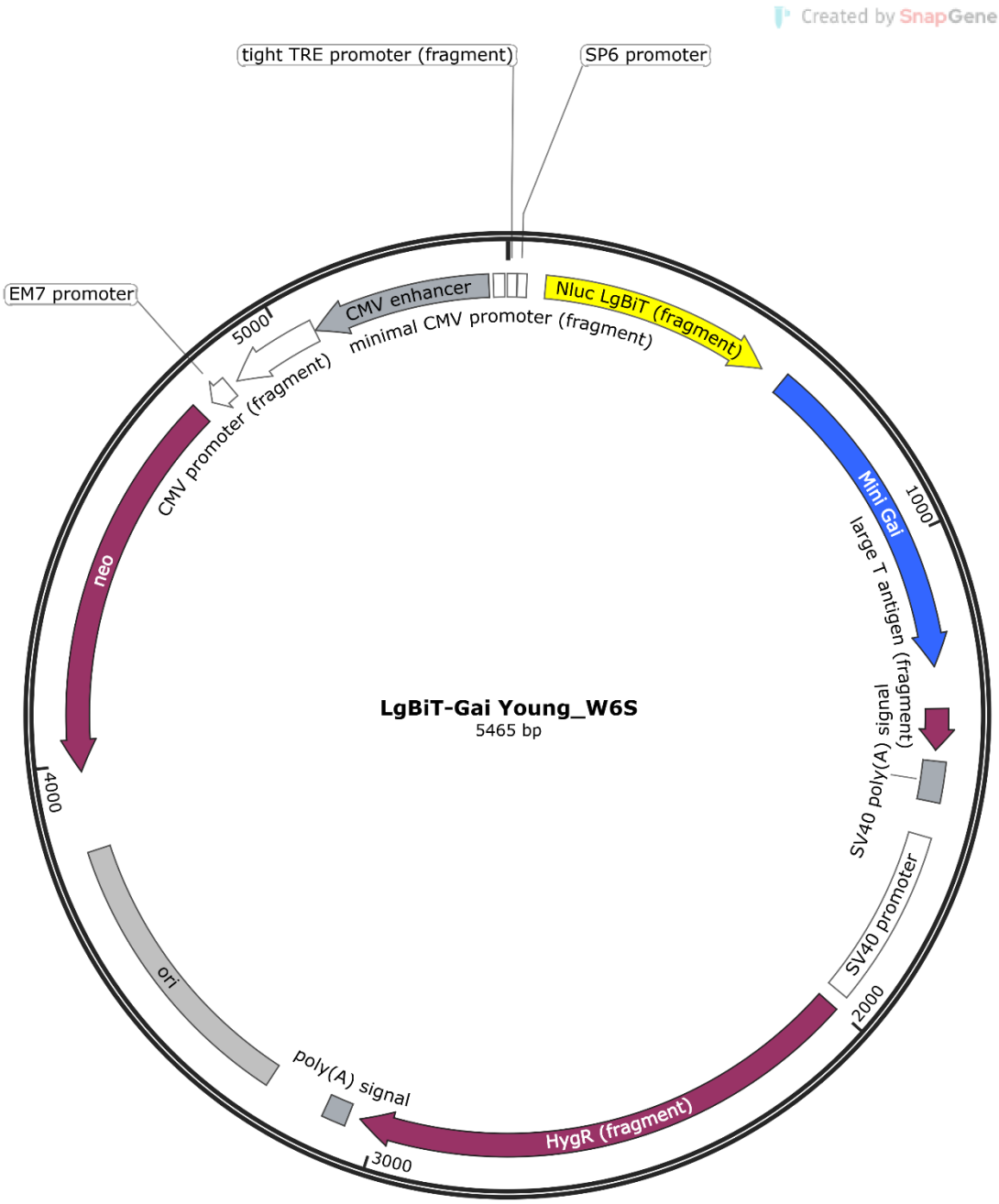

Figure 7. 2. Plasmid map of the LgBiT-mini-Gα$_i$ plasmid used for the nanoluciferase assays. The complete sequence of the plasmid is:

>AGTGAACCGTCAGATCGCCCATTTAGGTGACACTATAGAATACAAGCTACT
TGTTCTTTTTGCAGCTAGCGCTCACCATGGTCTTCACACTCGAAGATTTCGTTG
GGGACTGGGAACAGACAGCCGCCTACAACCTGGACCAAGTCCTTGAACAGG
GAGGTGTGTCCAGTTTGCTGCAGAATCTCGCCGTGTCCGTAACTCCGATCCAA
AGGATTGTCCGGAGCGGTGAAAATGCCCTGAAGATCGACATCCATGTCATCA
TCCCGTATGAAGGTCTGAGCGCCGACCAAATGGCCCAGATCGAAGAGGTGTT

TAAGGTGGTGTACCCTGTGGATGATCATCACTTTAAGGTGATCCTGCCCTATG
GCACACTGGTAATCGACGGGGTTACGCCGAACATGCTGAACTATTTCGGACG
GCCGTATGAAGGCATCGCCGTGTTCGACGGCAAAAAGATCACTGTAACAGGG
ACCCTGTGGAACGGCAACAAAATTATCGACGAGCGCCTGATCACCCCCGACG
GCTCCATGCTGTTCCGAGTAACCATCAACAGTGGGAGCTCCGGTGGTGGCGG
GAGCGGAGGTGGAGGCTCGAGCGGTATTGAAAAGCAACTGCAGAAAGACAA
ACAAGTCTACCGGGCCACGCATCGACTGTTGCTCCTCGGTGCAGACAACTCC
GGGAAGTCCACCATAGTCAAACAGATGCGCATCCTTCACGGGGGGTCCGGTG
GTAGTGGAGGTACAAGCGGCATCTTTGAGACCAAATTCCAGGTGGATAAAGT
AAATTTCCATATGTTCGATGTGGGGGGCCAAAGAGATGAGCGGAGAAAGTGG
ATTCAATGCTTCAATGACGTGACCGCCATTATATTTGTTGTAGATTCCTCAGA
TTACAATAGATTGCAAGAAGCACTTAATGACTTTAAGTCTATTTGGAACAATA
GGTGGTTGCGAACCATATCAGTAATACTCTTTTTGAATAAGCAGGACTTGCTG
GCCGAGAAAGTACTCGCAGGTAAAAGTAAGATCGAGGACTACTTCCCTGAAT
TTGCCCGATATACCACTCCAGAAGATGCGACACCGGAACCTGGGGAAGATCC
TAGAGTAACAAGGGCGAAATACTTTATCCGAGATGAGTTCTTGAGGATTTCA
ACCGCGAGCGGCGATGGCAGACATTATTGTTATCCGCACTTCACATGTGCCGT
GGATACAGAGAACGCGCGGAGAATCTTTAACGATGTTACGGACATTATAATT
AAGATGAACCTGCGCGACTGTGGCCTCTTTTAGGGATCCTCTAGAAACACCT
AGGCTCTCGTACGAAGTCAGCTGATAACGTCGACGTATTGCGGCCGCGGATC
ATAATCAGCCATACCACATTTGTAGAGGTTTTACTTGCTTTAAAAAACCTCCC
ACACCTCCCCCTGAACCTGAAACATAAAATGAATGCAATTGTTGTTGTTAACT
TGTTTATTGCAGCTTATAATGGTTACAAATAAAGCAATAGCATCACAAATTTC
ACAAATAAAGCATTTTTTTCACTGCCGACGTCACGCGTCTTGCGCAGCACCAT
GGCCTGAAATAACCTCTGAAAGAGGAACTTGGTTAGGTACCTTCTGAGGCGG
AAAGAACCAGCTGTGGAATGTGTGTCAGTTAGGGTGTGGAAAGTCCCCAGGC
TCCCCAGCAGGCAGAAGTATGCAAAGCATGCATCTCAATTAGTCAGCAACCA
GGTGTGGAAAGTCCCCAGGCTCCCCAGCAGGCAGAAGTATGCAAAGCATGC
ATCTCAATTAGTCAGCAACCATAGTCCCGCCCCTAACTCCGCCCATCCCGCCC
CTAACTCCGCCCAGTTCCGCCCATTCTCCGCCCCATGGCTGACTAATTTTTTTT
ATTTATGCAGAGGCCGAGGCCGCCTCGGCCTCTGAGCTATTCCAGAAGTAGT
GAGGAGGCTTTTTTGGAGGCCTAGGCTTTTGCAAAAAGCTCGATTCTTCTGAC
ACTAGCGCCACCATGAAGAAGCCCGAACTCACCGCTACCAGCGTTGAAAAAT
TTCTCATCGAGAAGTTCGACAGTGTGAGCGACCTGATGCAGTTGTCGGAGGG
CGAAGAGAGCCGAGCCTTCAGCTTCGATGTCGGCGGACGCGGCTATGTACTG
CGGGTGAATAGCTGCGCTGATGGCTTCTACAAAGACCGCTACGTGTACCGCC
ACTTCGCCAGCGCTGCACTACCCATCCCCGAAGTGTTGGACATCGGCGAGTT
CAGCGAGAGCCTGACATACTGCATCAGTAGACGCGCCCAAGGCGTTACTCTC
CAAGACCTCCCCGAAACAGAGCTGCCTGCTGTGTTACAGCCTGTCGCCGAAG
CTATGGATGCTATTGCCGCCGCCGACCTCAGTCAAACCAGCGGCTTCGGCCC
ATTCGGGCCCCAAGGCATCGGCCAGTACACAACCTGGCGGGATTTCATTTGC
GCCATTGCTGATCCCCATGTCTACCACTGGCAGACCGTGATGGACGACACCG
TGTCCGCCAGCGTAGCTCAAGCCCTGGACGAACTGATGCTGTGGGCCGAAGA
CTGTCCCGAGGTGCGCCACCTCGTCCATGCCGACTTCGGCAGCAACAACGTC
CTGACCGACAACGGCCGCATCACCGCCGTAATCGACTGGTCCGAAGCTATGT

TCGGGGACAGTCAGTACGAGGTGGCCAACATCTTCTTCTGGCGGCCCTGGCT
GGCTTGCATGGAGCAGCAGACTCGCTACTTCGAGCGCCGGCATCCCGAGCTG
GCCGGCAGCCCTCGTCTGCGAGCCTACATGCTGCGCATCGGCCTGGATCAGC
TCTACCAGAGCCTCGTGGACGGCAACTTCGACGATGCTGCCTGGGCTCAAAG
CCGCTGCGATGCCATCGTCCGCAGCGGGGCCGGCACCGTCGGTCGCACACAA
ATCGCTCGCCGGAGCGCAGCCGTATGGACCGACGGCTGCGTCGAGGTGCTGG
CCGACAGCGGCAACCGCCGGCCCAGTACACGACCGCGCGCTAAGGAGGTAG
GTCGAGTTTAGACTCTAGCCATCACGATGGCCGCAATAAAATATCTTTATTTT
CATTACATCTGTGTGTTGGTTTTTTGTGTGACGATTCCGGACTATAAAAGGAT
CTAGGTGAAGATCCTTTTTGATAATCTCATGACCAAAATCCCTTAACGTGAGT
TTTCGTTCCACTGAGCGTCAGACCCCGTAGAAAAGATCAAAGGATCTTCTTGA
AATCCTTTTTTTCTGCGCGTAATCTGCTGCTTGCAAACAAAAAAACCACCGCT
ACCAGCGGTGGTTTGTTTGCCGGATCAAGAGCTACCAACTCTTTTTCCGAAGG
TAACTGGCTTCAGCAGAGCGCAGATACCAAATACTGTCCTTCTAGTGTAGCC
GTAGTTAGGCCACCACTTCAAGAACTCTGTAGCACCGCCTACATACCTCGCTC
TGCTAATCCTGTTACCAGTGGCTGCTGCCAGTGGCGATAAGTCGTGTCTTACC
GGGTTGGACTCAAGACGATAGTTACCGGATAAGGCGCAGCGGTCGGGCTGAA
CGGGGGGTTCGTGCACACAGCCCAGCTTGGAGCGAACGACCTACACCGAACT
GAGATACCTACAGCGTGAGCTATGAGAAAGCGCCACGCTTCCCGAAGGGAG
AAAGGCGGACAGGTATCCGGTAAGCGGCAGGGTCGGAACAGGAGAGCGCAC
GAGGGAGCTTCCAGGGGGAAACGCCTGGTATCTTTATAGTCCTGTCGGGTTTC
GCCACCTCTGACTTGAGCGTCGATTTTTGTGATGCTCGTCAGGGGGGCGGAGC
CTATGGAAAAACGCCAGCAACGCGGCCTTTTTACGGTTCCTGGCCTTTTGCTG
GCCTTTTGCTCACATGTTCTTTCCTGCGTTATCCCCTGATTCTGTGGATAACCG
TATTACCGCCTTTGAGTGAGCTGATACCGGTTGGGCGTCGCTTGGTCGGTCAT
TTCGAATCAGAAGAACTCGTCAAGAAGGCGATAGAAGGCGATGCGCTGCGA
ATCGGGAGCGGCGATACCGTAAAGCACGAGGAAGCGGTCAGCCCATTCGCC
GCCAAGCTCTTCAGCAATATCACGGGTAGCCAACGCTATGTCCTGATAGCGG
TCCGCCACACCCAGCCGGCCACAGTCGATGAATCCAGAAAAGCGGCCATTTT
CCACCATGATATTCGGCAAGCAGGCATCGCCATGGGTCACGACGAGATCCTC
GCCGTCGGGCATGCGCGCCTTGAGCCTGGCGAACAGTTCGGCTGGCGCGAGC
CCCTGATGCTCTTCGTCCAGATCATCCTGATCGACAAGACCGGCTTCCATCCG
AGTACGTGCTCGCTCGATGCGATGTTTCGCTTGGTGGTCGAATGGGCAGGTA
GCCGGATCAAGCGTATGCAGCCGCCGCATTGCATCAGCCATGATGGATACTT
TCTCGGCAGGAGCAAGGTGAGATGACAGGAGATCCTGCCCCGGCACTTCGCC
CAATAGCAGCCAGTCCCTTCCCGCTTCAGTGACAACGTCGAGCACAGCTGCG
CAAGGAACGCCCGTCGTGGCCAGCCACGATAGCCGCGCTGCCTCGTCCTGCA
GTTCATTCAGGGCACCGGACAGGTCGGTCTTGACAAAAAGAACCGGGCGCCC
CTGCGCTGACAGCCGGAACACGGCGGCATCAGAGCAGCCGATTGTCTGTTGT
GCCCAGTCATAGCCGAATAGCCTCTCCACCCAAGCGGCCGGAGAACCTGCGT
GCAATCCATCTTGTTCAATCATGATCTGCCTCCTGGGTTTAGTTCCTCACCTTG
TCGTATTATACTATGCCGATATACTATGCCGATGATTAATTGTCAACAGTATT
AGAATTCGATTTGACCTCCCACCGTACACGCCTACCGCCCATTTGCGTCAACG
GGGCGGGGTTATTACGACATTTTGGAAAGTCCCGTTGATTTTGGTGCCAAAAC
AAACTCCCATTGACGTCAATGGGGTGGAGACTTGGAAATCCCCGTGAGTCAA

ACCGCTATCCACGCCCATTGGTGTACTGCCAAAACCGCATCACCATGGTAAT
AGCGATGACTAATACGTAGATGTACTGCCAAGTAGGAAAGTCCCGTAAGGTC
ATGTACTGGGCATAATGCCAGGCGGGCCATTTACCGTCATTGACGTCAATAG
GGGGCGGACTTGGCATATGATACACTTGATGTACTGCCAAGTGGGCAGTTTA
CCGTAAATACTCCACCCATTGACGTCAATGGAAAGTCCCTATTGGCGTTACTA
TGGGAACATACGTCATTATTGACGTCAATGGGCGGGGGTCGTTGGGCGGTCA
GCCAGGCGGGCCATTTACCGTAAGTTATGTAACGCGGAACTCCATATATGGG
CTATGAACTAATGACCCCGTAATTGATTACTATTAATAACTAGTGGCGCGCCA
GGGAGGCCTATATAAGCAGAGCTGGTTT.

7.11 Calcium uptake assays

ST*Hdh*$^{Q7/Q7}$ neuronal cells were seeded at 20,000 cells per well in black clear-bottom 96-well plates in the differentiation cocktail. Neurons were incubated at 37°C for 4 h to allow adherence to the plate and promote differentiation to a mature neuron-like phenotype. Conditioned media from microglia was applied to the ST*Hdh*$^{Q7/Q7}$ cells for a total exposure of 24 h. To measure calcium uptake, the fluo-4 no wash calcium assay kit (Invitrogen, #F36206) was used as per the manufacturer's protocol. Briefly, ST*Hdh*$^{Q7/Q7}$ cells were rinsed with PBS which was then replaced with 100 µL dye loading solution with 2.5 mM probenecid. ST*Hdh*$^{Q7/Q7}$ cells were incubated at 37 °C for 1 h and a further 30 min at room temperature. Glutamate was delivered in a 10 µL volume to a final concentration of 500 µM using a CLARIOstar Plus microplate reader (BMG Labtech). The bottom of each well was scanned in a spiral pattern every 2 s for 30 s using the fluo-4 filter set (excitation: 488 nm, emission: 530 nm), glutamate was delivered after 10 s. To assess calcium uptake, the mean fluorescence for each replicate was normalized to the basal fluorescence (prior to glutamate injection) within the replicate. Data were presented as the fold-change in fluorescence compared to the baseline prior to glutamate delivery.

7.12 Antibody arrays

To assess proteins released by SIM-A9 microglia, the Proteome Profiler Mouse Cytokine Array Kit, Panel A was used (R&D Systems, #ARY006) was used as per the manufacturer's recommendation. Briefly, microglia were seeded into clear 96-well plates at a density of 30,000 cells per well. Microglia were treated with vehicle (PBS), LPS (1000 ng/mL), IFNγ (20 ng/mL), or LPS and IFNγ in 24 technical replicates. Media from all replicates was pooled, centrifuged to remove particulate matter, and 500 µL of the conditioned media samples from each treatment group were incubated with the antibody-spotted membranes overnight at 4°C. The membranes were analyzed using Empiria studio (v2.3; LI-COR) such that the positive control was used as the reference signal and the negative control was used as the background. The signal for each protein was calculated based on the pixel density relative to the reference after global subtraction of the background signal.

7.13 Statistical analysis

Statistical significance among groups was assessed using several different statistical tests or by overlap between 95% confidence intervals, as indicated in specific figure captions. Briefly, the non-parametric Mann-Whitney test was used for single comparisons and the Kruskal-Wallis test with Dunn's post-hoc test were used for multiple comparisons with unequal variance among groups. Brown-Forsythe and Welch ANOVA tests with Dunnett correction, or two-way ANOVA with Sidak correction for multiple comparisons as deemed appropriate based on the number of comparisons and normality of the data. Only *p*-values of less than 0.05 based on post-hoc tests or non-overlapping confidence intervals were considered statistically significant. Sample sizes (n) for cell culture experiments were selected based on the expected variability from previous work using similar methods or using pilot experiments for cases where similar experiments had not been published. Sample sizes are indicated within individual figure legends and represent the number of independent cell culture preparations included in the statistical calculations. Concentration-response curves were fit using non-linear regression with 4-parameters to account for variable Hill coefficients using GraphPad Prism (v. 9.3.1). These curves were used to calculate the half maximal effective concentrations (EC_{50}) and maximal effective concentrations (EC_{max}) for agonists, or the half maximal inhibitory concentration (IC_{50}) for the different signaling inhibitors, as well as the minimal effect (E_{min}), maximum effect (E_{max}), and area under the curve (AUC).

7.14 Materials

Table 7. 1. Details of small molecules and recombinant proteins within the thesis. Items are presented in the order in which they appear.

Ligand/protein	Mechanism of action	Supplier	Catalog #	Chapter(s)
LPS (*E. coli)*	TLR4 agonist	Sigma-Aldrich	LPS25	2-6
Mouse IFNγ	IFNGR agonist	Cell Signaling Technology	39127	2-6
ACEA	CB_1 agonist	Tocris Bioscience	1319	2,3,6
HU-308	CB_2 agonist	Tocris Bioscience	3088	2,3
CP 55,940	CB_1/CB_2 agonist	Cayman Chemical Company	90084	2,3
AM251	CB_1 inverse agonist	Tocris Bioscience	1117	2
AM630	CB_2 inverse agonist	Tocris Bioscience	1120	2
SR144528	CB_2 inverse agonist	Tocris Bioscience	5039	2,4,6
HU-308	CB_2 agonist	Dalton Pharma Services	N/A	4
HU-433	CB_2 agonist	Dalton Pharma Services	N/A	4
LPS (*K. pneumoniae*)	TLR4 agonist	Sigma-Aldrich	L4268	5
LPS (*A. muciniphila*)	TLR4 agonist	Sigma-Aldrich	SBR00027	5
TAK-242	TLR4 inhibitor	Sigma-Aldrich	614316	5,6
Ruxolitinib	JAK1/2 inhibitor	Cell Signaling Technology	83405S	5,6
Glutamic acid	Pan-glutamate receptor agonist	Tocris Bioscience	0218	5
SP 600125	JNK1/2/3 inhibitor	Tocris Bioscience	1496	5,6
LY294002	PI3Kα/β/δ inhibitor	Tocris Bioscience	1130	5,6
U0126	MEK1/2 inhibitor	Cell Signaling Technology	9903S	5,6
PP-242	mTORC1/2 inhibitor	Tocris Bioscience	4257	5,6

Ligand/protein	Mechanism of action	Supplier	Catalog #	Chapter(s)
IKK-16	IKKα/β inhibitor	Tocris Bioscience	2539	5,6
SB 203580	p38 inhibitor	Tocris Bioscience	1202	5,6
1400W	iNOS inhibitor	Sigma-Aldrich	100050	5
Mouse TNF	TNFR1/2 agonist	Cell Signaling Technology	24095	6
Staurosporine	Nonselective kinase inhibitor	Tocris Bioscience	1285	6
Necrostatin-1	Inhibitor of RIP1 kinase	Cayman Chemical Company	11658	6
Dopamine	Pan-dopamine receptor agonist	Tocris Bioscience	3548	6
CGS 21680	A_{2A} agonist	Tocris Bioscience	1063	6
NMDA	NMDAR agonist	Cayman Chemical Company	14581	6

Table 7. 2. Details of the primers used for reverse transcription quantitative PCR (RT-qPCR) within the thesis. Primers are presented in the order in which they first appear as many primers are used in multiple chapters.

Gene of interest (protein)	Sequence	Amplicon size (bp)
Cnr1 (CB_1)	For: 5'-AAGTCGATCTTAGACGGCCTT-3' Rev: 5'-TCCTAATTTGGATGCCATGTCTC-3'	123
Cnr2 (CB_2)	For: 5'-ACGGTGGCTTGGAGTTCAAC-3' Rev: 5'-GCCGGGAGGACAGGATAAT-3'	147
Napepld (NAPE-PLD)	For: 5'-AGCGCCAAGCTATCAGTATCC-3' Rev: 5'-ACGTCCTCCTCTAGTCTGTAATC-3'	132
Faah (FAAH)	For: 5'-GTATCGCCAGTCCGTCATTG-3' Rev: 5'-GCCTATACCCTTTTTCATGCCC-3'	274
Dagla (DAGLα)	For: 5'-GTCCTGCCAGCTATCTTCCTC-3' Rev: 5'-CGTGTGGGTTATAGACCAAGC-3'	91
Daglb (DAGLβ)	For: 5'- AGCGACGACTTGGTGTTCC-3' Rev: 5'- GCTGAGCAAGACTCCACCG-3'	126
Mgll (MAGL)	For: 5'-CGGACTTCCAAGTTTTTGTCAGA-3' Rev: 5'-GCAGCCACTAGGATGGAGATG-3'	127
Nos2 (iNOS)	For: 5'-CCGAAGCAAACATCACATTCA-3' Rev: 5'-GGTCTAAAGGCTCCGGGCT-3'	101
Tnf (TNF)	For: 5'-GGTGCCTATGTCTCAGCCTCTT-3' Rev: 5'-GCCATAGAACTGATGAGAGGGAG-3'	139
Il1b (IL-1β)	For: 5'-TGGACCTTCCAGGATGAGGACA-3' Rev: 5'-GTTCATCTCGGAGCCTGTAGTG-3'	145
Il6 (IL-6)	For: 5'-GGCCTTCCCTACTTCACAAG-3' Rev: 5'-ATTTCCACGATTTCCCAGAG-3'	126
Eef1a1 (EF1α)	For: 5'-TAGACGAGGCAATGTTGCTG-3' Rev: 5'-AGCGTAGCCAGCACTGATTT-3'	115
B2m (B2M)	For: 5'-TGGTGCTTGTCTCACTGACC-3' Rev: 5'-TATGTTCGGCTTCCCATTCT-3'	98
Tlr4 (TLR4)	For: 5'-ATGGCATGGCTTACACCACC-3' Rev: 5'-GAGGCCAATTTTGTCTCCACA-3'	129
Ifngr1 (IFNGR1)	For: 5'-GTGGAGCTTTGACGAGCACT-3' Rev: 5'-ATTCCCAGCATACGACAGGGT-3'	105
Ccl2 (CCL2)	For: 5'-TTAAAAACCTGGATCGGAACCAA-3' Rev: 5'-GCATTAGCTTCAGATTTACGGGT-3'	121
Faslg (FASLG)	For: 5'-CACTGACATACCCAAACTTGTGC-3' Rev: 5'-GTCCCATGTTATTCTTTGCCCAT-3'	145

Gene of interest (protein)	**Sequence**	**Amplicon size (bp)**
Csf3 (G-CSF)	For: 5'-ATGGCTCAACTTTCTGCCCAG-3' Rev: 5'-CTGACAGTGACCAGGGGAAC-3'	249
Tgfb1 (TGFB1)	For: 5'-GTGCCCGAACCCCCATTGCT-3' Rev: 5'-CGTTTGGGGCTGATCCCGTTGAT-3'	299
Cd11b (CD11b)	For: 5'-ATGGACGCTGATGGCAATACC-3' Rev: 5'-TCCCCATTCACGTCTCCCA-3'	203
Sirpa (SIRPα)	For: 5'-CTCTCCGCGTCCTGTTTCTG-3' Rev: 5'-TCTGTACCACCTAATGGGTCC-3'	153
Cx3cr1 (CX3CR1)	For: 5'-GAGTATGACGATTCTGCTGAGG-3' Rev: 5'-CAGACCGAACGTGAAGACGAG-3'	102
P2ry12 (P2RY12)	For: 5'-CCCTGTGCGTCAGAGACTAC-3' Rev: 5'-CAAGCTGTTCGTGATGAGCC-3'	92
Drd2 (D_2)	For: 5'-ACCTGTCCTGGTACGATGATG-3' Rev: 5'-GCATGGCATAGTAGTTGTAGTGG-3'	105
Adora2a (A_{2A})	For: 5'-GCCATCCCATTCGCCATCA-3' Rev: 5'-GCAATAGCCAAGAGGCTGAAGA-3'	122
Tnfrsf1a (TNFR1)	For: 5'-CCGGGAGAAGAGGGATAGCTT-3' Rev: 5'-TCGGACAGTCACTCACCAAGT-3'	113
Tnfrsf1b (TNFR2)	For: 5'-ACACCCTACAAACCGGAACC-3' Rev: 5'-AGCCTTCCTGTCATAGTATTCCT-3'	66
Tnfrsf6 (FAS)	For: 5'-GCGGGTTCGTGAAACTGATAA-3' Rev: 5'-GCAAAATGGGCCTCCTTGATA-3'	61
Il1r1 (IL1R1)	For: 5'-GTGCTACTGGGGCTCATTTGT-3' Rev: 5'-GGAGTAAGAGGACACTTGCGAAT-3'	134
Il5ra (IL5RA)	For: 5'-AGGAAGTCCTTGGTAGAATGGC-3' Rev: 5'-CCTGGTCCATAGATGACACACTC-3'	105
Il6ra (IL6R)	For: 5'-CCTGAGACTCAAGCAGAAATGG-3' Rev: 5'-AGAAGGAAGGTCGGCTTCAGT-3'	108
Il11ra1 (IL11RA)	For: 5'-GATCAATGTGACCGAGGTGAACC-3' Rev: 5'-GTATGTCCAGCTGGCATGCAG-3'	151

Table 7. 3. Details of the primary antibodies used within the thesis. Antibodies are presented in the order in which they first appear.

Antigen	Host	Supplier	Clonality	Application	RRID
CB_1 receptor	Mouse	Santa Cruz Biotechnology	Monoclonal	IF	AB_2889069
CB_1 receptor	Rabbit	Cell Signaling Technology	Monoclonal	ICW	AB_2756361
CB_2 receptor	Rabbit	Cayman Chemical Company	Polyclonal	IF/ICW	AB_10079370
p-ERK1/2	Rabbit	Cell Signaling Technology	Monoclonal	ICW	AB_331775
p-JNK	Rabbit	Cell Signaling Technology	Polyclonal	ICW	AB_331659
p-p38	Mouse	Cell Signaling Technology	Monoclonal	ICW	AB_331296
p-Akt	Mouse	Cell Signaling Technology	Monoclonal	ICW	AB_331158
p-p65	Rabbit	Cell Signaling Technology	Monoclonal	ICW	AB_331284
p-STAT1	Rabbit	Cell Signaling Technology	Monoclonal	ICW	AB_561284
iNOS	Rabbit	Cell Signaling Technology	Monoclonal	IF	AB_2687529
COX2	Rabbit	Cell Signaling Technology	Monoclonal	IF	AB_2571729
Cleaved Caspase-3	Rabbit	Cell Signaling Technology	Monoclonal	IF	AB_2070042
p-RIP3	Rabbit	Cell Signaling Technology	Monoclonal	IF	AB_2937060

Chapter 8: Discussion

I have investigated the mechanisms by which microglia take on a pro-inflammatory phenotype in response to LPS and IFNγ, and the mechanisms by which microglia may induce neuronal dysfunction or death. This thesis represents a contribution to a rapidly growing field at the interface of neuroscience and immunology. Traditional approaches to the treatment of neurodegeneration have involved drugs that directly target neuronal processes such as mitochondrial function and autophagy. Although this approach may still yield a benefit in the future, there is accumulating evidence to suggest that drugs traditionally used to treat immunological disorders may also be useful for neurological disorders. Currently emerging targets in the field of neuroimmune pharmacology, not explored within this thesis, include the complement cascade as well as mechanisms of neuron-glia communication. Herein, the major questions and future directions that stem directly from this work will be addressed as well as some anticipated future directions in the field of neuroimmunology as whole.

8.1 Future directions of this research

This thesis provides some new findings with respect to the pro-inflammatory activity of microglia and the secondary effects on neurons. Cultured immortalized microglia were differentially activated by LPS and IFNγ and these molecules acted synergistically via a JAK1/2-dependent mechanism. Among all cytokines released by the activated microglia, TNF was determined to be specifically responsible for the neurotoxic effects of microglial media on cultured neuronal cells. Early phosphorylation of neuronal ERK1/2, Akt, and CREB ultimately culminated in neuronal death by a combination of apoptosis and necroptosis. These pro-death effects were enhanced in ST*Hdh*$^{Q111/Q111}$ cells which indicated that mHTT sensitized the cells to inflammatory factors.

Based on the results within this thesis, there are several open questions that are worthy of further exploration to improve our understanding of microglia and the potential contributions of these cells to neurodegeneration. Three of the most compelling among these questions include: 1) How does JAK1/2 regulate the pro-inflammatory activity of microglia? 2) What are the soluble factors required to potentiate the neurotoxic effects of

microglial-secreted TNF? 3) What are the major determinants of whether these findings will be relevant *in vivo*?

8.1.1. Regulation of microglia by JAK1/2

We observed the blockade of JAK1/2 by the nonselective JAK inhibitor, ruxolitinib, suppressed the pro-inflammatory activity of microglia in response to LPS and IFNγ (Chapter 5). This was an unexpected finding as LPS acts on TLR4 and the canonical pro-inflammatory effects of TLR4 are not dependent on JAK-mediated signaling. Subsequently, we determined that of all canonical signaling pathways downstream of TLR4 and IFNGR, JAK1/2 were the only proteins that could be safely inhibited in microglia as well as neurons and not enhance neuronal death (Chapter 6). This indicated that blockade of JAK1/2 suppressed the pro-inflammatory activity of microglia, and that neuronal JAK1/2 was not required to promote cell survival. These findings highlight JAK1/2 as a potential target for neuroinflammation.

It has been previously demonstrated that LPS could stimulate the release of cytokines from macrophages which then act in an autocrine or paracrine manner to subsequently activate JAK-STAT signaling (Carl et al. 2004; Pattison et al. 2012). These secondary JAK-dependent effects of LPS could then be blocked by ruxolitinib (Pattison et al. 2012). Ruxolitinib also inhibited the response of *ex vivo* human lung macrophages to LPS and prevented the release of TNF, IL-6 and several other cytokines and chemokines (Mantov et al. 2022). In the experiments within this thesis, microglia were co-incubated over the course of 16 h so the effects of ruxolitinib on the direct early LPS-mediated effects cannot be ascertained. Thus, it cannot be ruled out that inhibition of JAK1/2 in microglia prevented the secondary response to secreted factors rather than the LPS treatment itself. We observed that LPS induced the biphasic activation of several signaling pathways including ERK, JNK, p38, and Akt (Chapter 4). Time-course experiments to assess the effects of JAK1/2 inhibition on the time-course of LPS-dependent signaling would shed light on the mechanism by which JAK1/2 regulates pro-inflammatory activity of microglia downstream of TLR4 activation.

The ideal strategy to target JAK-mediated signaling will depend on the cytokines that are responsible for microglial activation or neuronal death. IFNγ and IL-6 both rely on JAK1 and JAK2 to facilitate pro-inflammatory signaling (Schwartz et al. 2017). Next-generation selective JAK inhibitors are in development to regulate inflammation with reduced adverse effects. Selective JAK2 inhibition prevented the IFNγ-mediated release of NO and TNF from primary microglia derived from wild-type as well as AD mice (Jones et al. 2015). A brain-penetrant JAK2 inhibitor also suppressed microglial activation in a mouse model of metastatic brain cancer (Jin et al. 2022). These data suggest that selective inhibition of JAK2 could treat neuroinflammation without the need to inhibit JAK1. This may reduce adverse effects of nonselective JAK inhibition.

8.1.2. Potentiation of neurotoxicity by TNF

We observed that recombinant TNF, when presented alone, had no effect on neuronal viability. However, TNF was the primary determinant of neuronal death when presented with other factors secreted by microglia in response to LPS and IFNγ (Chapter 6). This suggests that other proteins are required to unmask the harmful effects of TNF on neurons. Based on current knowledge of cytokine-induced cell death, some potential candidates include IFNγ, IL-1β, and IL-6. TNF and IFNγ induced cell death in bone marrow-derived macrophages by a mixture of pyroptosis, apoptosis, and necroptosis (known as PANoptosis) whereas no other combinations had the same effect among TNF, IL-1α, IL-1β, IL-2, IL-6, IL-15, IL-18, and IFNγ (Karki et al. 2021). In this work, TNF produced by macrophages and IFNγ produced by natural killers induced cytokine shock with subsequent damage to the lungs and gut in mice. These effects were dependent on STAT1 which is downstream of JAK1/2 (Karki et al. 2021). In neuronal cultures, IFNγ was shown to have no direct effect on neuronal viability but induced neuronal death when neurons were co-cultured with glia (Mount et al. 2007). Although the involvement of TNF was not tested, IFNγ induces TNF release from microglia which could have been subsequently potentiated by IFNγ (Chhor et al. 2013). An earlier study using whole-brain primary co-cultures demonstrated that TNF and IL-1β induced neuronal damage whereas neither cytokine alone had an effect (Chao et al. 1995). However, this appeared to be

dependent on NO release from activated astrocytes rather than a direct effect on neurons. We found that IL-6 was the most upregulated cytokine by microglia in terms of fold-change upon LPS and IFNγ treatment (Chapter 6). IL-6 has enhanced the TNF-induced apoptosis of multiple cancer cell lines (Sano et al. 2021). These reports suggest that there is complex interplay among TNF, IFNγ, IL-1β, and IL-6 and that two or more of these proteins may be required to mediate neuronal death.

8.1.3. Considerations for the translation of these findings

There are a plethora of factors that must be considered with respect to the translatability of *in vitro* results to an *in vivo* model. In particular for this work, the role of astrocytes in microglia-mediated neuron death are unclear based on the conditioned media model. Secondly, appropriate pharmacological strategies must also be employed to target cytokines for neuroinflammation. It is generally not detrimental to completely remove a cytokine for *in vitro* experiments, however, cytokines are pleiotropic molecules and must be targeted carefully *in vivo*.

We observed that secreted factors from microglia induced secondary neuronal damage *in vitro*, however, astrocytes have also demonstrated neuroprotective and neurotoxic properties. It is unclear whether the presence of astrocytes would be likely to enhance or reduce secondary neuronal death in response to LPS and IFNγ. The pro-inflammatory astrocyte (A1) phenotype requires the presence of TNF, IL-1α, and C1q released by microglia (Liddelow et al. 2017). These A1 astrocytes can induce neuronal damage via secretion of specific saturated lipids (Nagai et al. 2007; Guttenplan et al. 2020a, 2021). Global knockdown of TNF, IL-1α, and complement component 1q (C1q) prevented the formation of A1 astrocytes and slowed disease progression in a mouse model of ALS (Guttenplan et al. 2020b). This suggests that microglial activation of astrocytes enhances neuronal damage. Astrocytes have been shown to exhibit neuroprotective activity *in vivo* and *in vitro* through mechanisms that primarily relate to attenuation of excitotoxicity (Ye and Sontheimer 1998; Lamigeon et al. 2001; Zhang et al. 2016). As neuronal death in this work was mediated by cytokines rather than

excitotoxicity, it would be likely that the introduction of astrocytes would enhance secondary neuronal damage by microglia rather than reduce damage.

Cytokines are pleiotropic molecules that can contribute to tissue damage but are also useful for homeostatic physiological processes. TNF deficiency has been associated with increased tumour growth as well as a compensatory increase in other pro-inflammatory cytokines (Li et al. 2009; Tuazon Kels et al. 2020). The blockade of TNF signaling via TNFR1 has demonstrated benefits in a humanized mouse model of MS (Williams et al. 2018). However, a clinical trial of etanercept in human MS patients revealed a worsening of symptoms by the treatment (Group 1999; Sicotte and Voskuhl 2001). It has since become clear that TNF signaling via TNFR2 is neuroprotective in animal models of MS which has highlighted a mechanism whereby too little TNF exacerbates the disease (Fischer et al. 2019; Ortí-Casañ et al. 2022; Pegoretti et al. 2023). Ultimately, it will be important to understand the pleiotropic properties of cytokines and target them appropriately to treat neurodegeneration. For cytokines with multiple receptors such as TNF, this may involve the use of selective receptor antagonists rather than removal of the cytokine.

8.2 Targeting neuronal cells for neurodegeneration

There are ongoing efforts to develop drugs that directly target neuronal processes to prevent neurodegeneration. Two of these processes include mitochondrial metabolism and autophagy. These processes are dysregulated during neurodegeneration and pharmacological strategies to correct them have shown promise.

Neurons require large amounts of energy to regulate synaptic plasticity, synthesize neurotransmitters, and maintain electrical conductivity. The primary energy source of neurons is ATP which is produced through oxidative phosphorylation in the mitochondria. Mitochondrial function is impaired during neurodegeneration and has been linked to the dysfunction of several GTPases in AD (Koshiba et al. 2004; Wang et al. 2009). Neuronal mitochondria in these contexts exhibit proton leakage, lowered oxidative capacity, and increased production of reactive oxygen species (Kim et al. 2018). This may also sensitize neurons to the reactive oxygen and nitrogen species released by

microglia as inhibition of mitochondrial respiration by such molecules can induce neuronal death (Brown and Vilalta 2015). Suppression of mitochondrial calcium uptake via blockade of the mitochondrial calcium uniporter has shown to be neuroprotective against oxygen-glucose deprivation *in vitro* as well as *in vivo* (Baughman et al. 2011; Novorolsky et al. 2020; Woods et al. 2023). Resveratrol and number of other antioxidants such as coenzyme Q10 have been used to suppress the production of reactive oxygen species and have shown therapeutic benefit in mouse models of AD and PD and a human iPSC-derived model of ALS (Ghosh et al. 2010; Dumont et al. 2011; McManus et al. 2011; Zhelev et al. 2013; Stefanova et al. 2016; Kolosova et al. 2017; Pavshintsev et al. 2017; Yu et al. 2020; Yadav et al. 2022).

Neuronal autophagy is a catabolic mechanism to clear protein aggregates and functionally compromised organelles, and defective autophagy has been linked to the degeneration of axons and dendrites (Yang et al. 2013). Autophagy is stimulated by AMP-activated protein kinase (AMPK) and inhibited by mTOR which has established these pathways as therapeutic targets to manipulate this process (Liang et al. 2007; Chang et al. 2009; Kim et al. 2011). Rapamycin is an mTOR inhibitor and a potent inducer of autophagy in cultured neurons as well as in animal models of neurodegeneration (Sarkar et al. 2009; Rubinsztein and Nixon 2010). Rapamycin treatment improved lifespan in both wild-type and AD mice and improved cognitive performance and reduced the Aβ-plaque load in AD mice (Harrison et al. 2009; Spilman et al. 2010; Caccamo et al. 2010). Rapamycin has also reduced the loss of dopaminergic neurons in a mouse model of PD and improved motor coordination in animal models of PD and HD (Ravikumar et al. 2004; Malagelada et al. 2010; Bai et al. 2015). We determined that inhibition of mTOR using an experimental inhibitor, PP-242, was effective to suppress the microglial production of reactive nitrogen species (Chapters 5 and 6) and improve cell viability in the ST*Hdh*$^{Q111/Q111}$ cellular model of HD (Chapter 6). Although it is unclear whether these effects were related to autophagy, these findings were consistent with the notion that inhibition of mTOR may be neuroprotective.

8.3 Emerging targets in neuroimmune pharmacology

There have been significant advances in recent years toward understanding the contributions of the immune system to neuroinflammation and neurodegeneration. However, the field of neuroimmunology is still relatively nascent. There are several emerging targets including the complement system and mechanisms of neuron-glia communication. There are also major open questions such as how early neuroinflammation must be targeted to influence the course of neurodegeneration.

8.3.1. The complement cascade

The classical complement cascade has long been recognized to facilitate host defense by the peripheral immune system, however, the complement system is also a primary mechanism by which microglia eliminate synapses in the CNS (Dunkelberger and Song 2010; Stevens and Johnson 2021). It was originally reported that C1q was produced by postnatal neurons and would become localized to synapses during refinement of the retinogeniculate pathway (Stevens et al. 2007). It was later demonstrated that microglia facilitated the removal of complement-tagged and that less active synapses were preferentially removed whereas active synapses were preserved and strengthened (Schafer et al. 2012). Excessive synaptic engulfment by microglia has been implicated in AD, HD, and schizophrenia (Sekar et al. 2016; Hong et al. 2016; Sellgren et al. 2019; Wilton et al. 2021). Anti-complement drugs have been developed to reduce excessive synapse elimination as well as microglial pro-inflammatory activity (Zelek and Morgan 2022). The direct blockade of synaptic C1q using monoclonal antibodies (mAbs) preserved corticostriatal synapses in HD mice and reduced complement-dependent cytotoxicity in a mouse model of neuromyelitis optica (Phuan et al. 2013; Wilton et al. 2021), ANX005, a C1q-neutralizing mAb produced by Annexon, Inc., recently completed a phase 2a trial in patients with or at risk for HD (ClinicalTrials.gov identifier: NCT04514367) and is currently recruiting for a phase 2a trial in ALS patients (ClinicalTrials.gov identifier: NCT04569435). ANX005 was well-tolerated in HD patients and patients exhibited stable clinical scores over the nine-month trial as opposed to the expected decline observed in untreated patients (Kumar et al. 2023).

8.3.2. Mechanisms of neuron-glia communication

Neurons communicate with microglia as a part of the normal surveillance functions of microglia (Szepesi et al. 2018). Neurons present glycoproteins such as cluster of differentiation 200 ligand (CD200L) and C-X3-C motif ligand 1 (CX3CL1) at the cell surface which interact with receptors on microglia and macrophages to oppose pro-inflammatory activation (Hoek et al. 2000; Biber et al. 2007; Eyo and Wu 2013). Enhanced expression of CD200L and its receptor, CD200R, is associated with reduced susceptibility to experimental autoimmune encephalomyelitis in mice and reduced TNF production in response to LPS (Chitnis et al. 2007; Boudakov et al. 2007). Downregulation of CD200L and CX3CL1 and the respective receptors has been associated with neuroinflammation in several animal models of neurodegenerative disease as well as in human post-mortem AD and HD brains (Zujovic et al. 2001; Walker et al. 2009; Wynne et al. 2010; Pabon et al. 2011; Castro-Sánchez et al. 2018; Zhang et al. 2018; Kim et al. 2020; Pawelec et al. 2020). We observed a loss of mRNA for *Cd200* and *Cx3cl1* in ST*Hdh*$^{Q111/Q111}$ neuronal cells (Chapter 6) as well as a reduction in mRNA for *Cx3cr1* in microglia that had been stimulated with LPS or IFNγ (Chapter 5). These findings suggested that mHTT may reduce the surface expression of these ligands by neurons, and that pro-inflammatory conditions also reduce the sensitivity of microglia to these signals. We have post-mortem striatal and motor cortex tissue from HD patients and efforts to determine the protein abundance and localization of CD200L-CD200R and CX3CL1-CX3CR1 are ongoing. Drugs to target these mechanisms of neuron-glia communication have not yet entered clinical trials, however, direct stimulation of CD200R and CX3CR1 has shown promise to reduce microglial activation and neuroinflammation in animal models of MS, PD, and natural ageing (Cardona et al. 2006; Cox et al. 2012; Rabaneda-Lombarte et al. 2021; Almeida et al. 2023).

8.3.3. Timing of anti-inflammatory treatments

Arguably, one of the greatest challenges in the development of treatments for neurodegenerative diseases is related to the time course of potential treatments relative to

the onset of symptoms. As an example, with respect to AD, efforts have been largely concentrated on the removal of Aβ plaques using mAbs. However, the removal of plaques has not consistently improved cognitive function or other outcomes of the disease (Doody et al. 2014; Honig et al. 2018; Panza et al. 2019; Knopman et al. 2021; Decourt et al. 2021; Haeberlein et al. 2022). This has raised the question of whether plaques must be removed from the brain prior to the onset of disease to achieve clinical benefits. Similarly, with neuroinflammation, it is unclear how early treatments must begin relative to the onset of symptoms. The risk of AD is reduced by the use of NSAIDs, particularly ibuprofen, with the greatest benefits observed in long-term users (in t' Veld et al. 2001; Vlad et al. 2008). However, trials of NSAIDs in symptomatic AD patients failed to produce a clinical benefit (Scharf et al. 1999; Aisen et al. 2002, 2003; Reines et al. 2004). This suggests that suppression of inflammation does not alter the course of AD at the symptomatic stage. However, it may be possible to gain a benefit from the modulation of inflammation at the pre-clinical stage.

Although much of the clinical trials with respect to anti-inflammatory drugs and neurodegeneration have focused on AD, premanifest and symptomatic HD patients may be a more effective population to explore the potential of neuroinflammation as a therapeutic target. HD is a monogenic disease with complete penetrance in m*HTT* gene carriers with greater than 40 CAG repeats (Caron et al. 1993). The rate of disease progression and age of death with HD are also predicted by the number of *HTT* CAG repeats (Brinkman et al. 1997; Keum et al. 2016). These features of HD allow premanifest carriers to be easily identified, and benefits of treatment to be measured against the predicted trajectory within each subject. Furthermore, there is a shift toward a pro-inflammatory state that occurs long before the onset of the motor symptoms characteristic of HD. Activated microglia have been observed using positron emission tomography in the brains of living premanifest m*HTT* gene carriers (Pavese et al. 2006; Tai et al. 2007; Politis et al. 2011, 2015). Elevated IL-6 concentrations were also found in the blood of m*HTT* gene carriers up to 16 years prior to disease onset (Björkqvist et al. 2008). Although it poses an incredible challenge to test anti-inflammatory treatments in premanifest HD patients to assess the effects on long-term disease progression, such a

trial could finally shed light on whether the success of treatments for neuroinflammation depends on the timing.

8.4 General limitations

8.4.1. Immortalized microglial and neuronal cell lines cultured separately

The results of each chapter within this thesis relied on the use of immortalized microglial (SIM-A9) and neuronal (ST*Hdh*) cells. It has been well established that immortalized cell lines do not necessarily behave the same way in response to various stimuli compared to primary cells or cells *in vivo*. In this work, spontaneously immortalized microglia were used. Spontaneously immortalized cells do not require genetic modification with oncogenes as with genetically immortalized microglial cell lines such as N9 or BV-2 cells (Righi et al. 1989; Blasi et al. 1990). However, as the mechanism of immortalization is unknown with SIM-A9 cells, it is difficult to directly compare these cells to primary microglia. It has been previously shown that BV-2 cells behave in a similar manner to primary mouse microglia but the primary cells released greater quantities of TNF, IL-6, IL-1β, and reactive nitrogen species in response to the same concentrations of LPS (Horvath et al. 2008). This suggests that although primary microglia may exhibit enhanced sensitivity to stimuli, general mechanisms of microglial cellular physiology are conserved upon immortalization.

Immortalized neuronal cells are commonly used for high-throughput pharmacological testing, and immortalized lines have been prepared to model neurons of the retina, spinal cord, striatum, hypothalamus, and several other brain regions (Hammang et al. 1990; Raymon et al. 1999; Trettel et al. 2000; Dalvi et al. 2011; Cocks et al. 2013). However, when compared to microglia, much greater differences have been observed between immortalized neuronal cells and primary neurons. For example, PC12 immortalized rat neuronal cells have been widely used to model catecholaminergic neurons for the study of NMDA receptor physiology, however, PC12 cells were shown to express an atypical complement of NMDA receptor subunits which influenced the behaviour of the cells in response to excitatory stimuli (Edwards et al. 2007). Neuro-2a neuroblastoma lines are also commonly used for neurotoxic compound screens, but

neuro-2a cells have been demonstrated to behave differently from primary neurons and have exhibited resistance to several neurotoxic compounds, likely due to differences in receptor and ion channel surface expression (Calderón et al. 1999; LePage et al. 2005). ST*Hdh* neuronal cells were used in this work to identify mechanisms of microglia-mediated cell death. However, ST*Hdh* cells have not been compared directly to primary neurons with respect to the response to a pro-inflammatory environment. Thus, it would be highly informative to replicate aspects of this work using primary microglia and neurons.

Perhaps the greatest limitation of individually cultured microglia and neurons is the lack of input from other cell types and the brain microenvironment more broadly. Microglia *in vivo* are continuously exposed to direct interactions with neural cells as well as infiltrating immune cells and blood borne soluble factors. These inputs could cause microglia to behave very differently even compared to primary cells *ex vivo*. In recent years, a surge of single-cell RNA sequencing (scRNA-seq) experiments have targeted microglia in a range of brain regions and stages of development and disease, and the data have indicated that microglia are highly heterogeneous within the mouse brain (Keren-Shaul et al. 2017; Hammond et al. 2019; Masuda et al. 2019). Thus, microglia may perform a wide variety of tasks that differ during development or ageing, or in response to brain region-specific stimuli. In the future, further research into the specific culture conditions of microglia to better mimic the CNS environment may be fruitful to increase the fidelity of cultured microglia compared to microglia *in situ*.

8.4.2. Cells derived only from female animals

Microglia tend to differ substantially between the sexes which adds a layer of complexity to these cells as therapeutic targets. Microglia express both androgen receptors as well as estrogen receptors which have been shown to regulate motility, cytokine release, and phagocytosis during neuroinflammation (García-Ovejero et al. 2002; Loiola et al. 2019). Glial expression of aromatase, the enzyme that converts testosterone to estrogen, was upregulated following injury in rats, songbirds, and human children (Duncan and Saldanha 2011; Zhong et al. 2017; Wright et al. 2019). The actions

of exogenous estrogen have also been shown to be neuroprotective in animal models of neurotoxicity and stroke (Gillies and McArthur 2010; Céspedes Rubio et al. 2018). This suggests that an environment that favors estrogen over androgens promotes microglia to shift toward a pro-resolution state rather than a pro-inflammatory state. The microglial cells and neuronal cells used in this work were derived from female mice but were cultured in the absence of hormones. Substantial transcriptional differences have been identified between male and female microglia *in vitro*, and male microglia have been shown to be more sensitive to pro-inflammatory stimuli even in the absence of sex steroids in the culture media (Villa et al. 2018; Guneykaya et al. 2018; Han et al. 2021). However, conflicting evidence has shown that microglia in female rats and mice were more sensitive to acute LPS challenge *in vivo* (Doyle et al. 2017; Murtaj et al. 2019). Ultimately, sex differences are important to consider as the differences affect the response to stimuli *in situ* and the responses of cultured microglia, possibly even when cultured in the absence of sex hormones.

8.4.3. LPS and IFNγ as immune stimulants

To stimulate microglia toward a pro-inflammatory phenotype, LPS and IFNγ were used to activate TLR4 and IFNG receptors, respectively. LPS is commonly used in both *in vitro* and *in vivo* models to simulate infection or induce a general inflammatory response (Lewis et al. 2016; Skrzypczak-Wiercioch and Sałat 2022). As with most immune cells, microglia express TLR4 receptors at the cell surface and are sensitive to the presence of LPS. LPS-based models of neurodegeneration have been criticized as bacterial penetration of the brain parenchyma is not a component of AD, PD, HD, or other neurodegenerative disease. However, it has been shown that LPS can be shed from bacteria in the gut, and this free LPS may enter general circulation and eventually affect the brain. Elevated concentrations of circulating LPS has been observed in AD and PD as well as ALS and has been correlated with increased gut permeability (Zhang et al. 2009b; Forsyth et al. 2011; Brown 2019). Although a healthy BBB is generally resistant to the entry of LPS, the BBB exhibits increased permeability under conditions of systemic inflammation which promotes the entry of peripheral pro-inflammatory factors into the

parenchyma (Banks et al. 2015; Galea 2021). In mice, a peripheral injection of LPS is sufficient to induce robust activation of microglia in the CNS (Chen et al. 2012). Thus, there is evidence to suggest that the actions of circulating LPS on microglia makes relevant contributions to the initiation and maintenance of neuroinflammation.

IFNγ is primarily secreted by T cells and natural killer cells to stimulate the antibacterial and antiviral response of macrophages (Tau and Rothman 1999). IFNγ is systemically upregulated in patients with a variety of chronic inflammatory diseases including type 2 diabetes, obesity, or rheumatoid arthritis (Kasahara et al. 1983; Ye et al. 1995; Tsiavou et al. 2005; Monteiro et al. 2017; Zhang et al. 2019a; Bradley et al. 2022). Although the mechanisms are unclear, the incidence of chronic inflammatory conditions such as diabetes and rheumatoid arthritis has been correlated with an increased risk of dementia (Sangha et al. 2020; Barbiellini Amidei et al. 2021). This suggests that there may be a link between mediators of peripheral immune responses and microglia-mediated neuroinflammation. IFNγ has also been shown to induce a primed state of microglia which can enhance the subsequent response to an additional stimulus such as LPS (Hayes et al. 1995; Held et al. 1999; Schroder et al. 2006; Perry and Holmes 2014; Monteiro et al. 2017). For these reasons, we examined the effects of IFNγ on microglia when presented as an individual treatment or in combination with LPS.

8.5 Concluding remarks

The data presented within this thesis provide some new insights into the mechanisms by which microglia respond to common pro-inflammatory stimuli and how this may induce secondary neuronal damage. The work supports the hypothesis that microglia may directly inflict neuronal damage via secreted factors, and that this is dependent on activation of microglial JAK1/2 and subsequent release of TNF. The findings also suggest that direct suppression of microglia is sufficient to reduce secondary neurotoxicity. Promising pharmacological strategies to accomplish this included anti-TNF biologics, JAK inhibitors, and CB_2 receptor agonists. Future work *in vivo* will be critical to understand the roles of other neural cells such as astrocytes and determine the translatability of these findings.

Appendix A: Associated publications

Table A1. 1. The status of all first-author publications associated with this doctoral research, regardless of inclusion within the thesis.

Article type	Title	Publication status	Journal/book	Date of publication	Included in thesis
Research	Synthetic cannabinoids reduce the inflammatory activity of microglia and subsequently improve neuronal survival *in vitro*	Published	Brain, Behavior, and Immunity	Jun 2022	Chapter 2
Research	The microglial endocannabinoid system is similarly regulated by lipopolysaccharide and interferon gamma	Published	Journal of Neuroimmunology	Sep 2022	Chapter 3
Research	Enantiomeric agonists of cannabinoid type 2 receptors differentially regulate the pro-inflammatory activity of microglia	In preparation			Chapter 4
Research	JAK1/2 regulates synergy between interferon gamma and lipopolysaccharides in microglia	In revision	Journal of Neuroimmune Pharmacology		Chapter 5
Research	Microglia-mediated neuron death requires TNF and is exacerbated by mutant Huntingtin	In preparation			Chapter 6
Review	The dynamic role of microglia and the endocannabinoid system in neuroinflammation	Published	Frontiers in Pharmacology	Feb 2022	No
Book chapter	Protein-protein allosteric effects on cannabinoid receptor heteromer signaling	Published	Allosteric Modulation of G Protein-Coupled Receptors	Jan 2022	No
Research	Endothelin B receptor dysfunction mediates elevated myogenic tone in cerebral arteries from aged male Fischer 344 rats	Published	GeroScience	Jan 2021	No

References

Aisen, P.S., Schafer, K.A., Grundman, M., Pfeiffer, E., Sano, M., Davis, K.L., Farlow, M.R., Jin, S., Thomas, R.G., Thal, L.J., and Alzheimer's Disease Cooperative Study. 2003. Effects of rofecoxib or naproxen vs placebo on Alzheimer disease progression: a randomized controlled trial. JAMA **289**(21): 2819–2826. doi:10.1001/jama.289.21.2819.

Aisen, P.S., Schmeidler, J., and Pasinetti, G.M. 2002. Randomized pilot study of nimesulide treatment in Alzheimer's disease. Neurology **58**(7): 1050–1054. doi:10.1212/wnl.58.7.1050.

Ajami, B., Samusik, N., Wieghofer, P., Ho, P.P., Crotti, A., Bjornson, Z., Prinz, M., Fantl, W.J., Nolan, G.P., and Steinman, L. 2018. Single cell mass cytometry reveals distinct populations of brain myeloid cells in mouse models of neuroinflammatory and neurodegenerative diseases. Nat. Neurosci. **21**(4): 541–551. doi:10.1038/s41593-018-0100-x.

Albeituni, S., Verbist, K.C., Tedrick, P.E., Tillman, H., Picarsic, J., Bassett, R., and Nichols, K.E. 2019. Mechanisms of action of ruxolitinib in murine models of hemophagocytic lymphohistiocytosis. Blood **134**(2): 147–159. doi:10.1182/blood.2019000761.

Almeida, M.M.A. de, Watson, A.E.S., Bibi, S., Dittmann, N.L., Goodkey, K., Sharafodinzadeh, P., Galleguillos, D., Nakhaei-Nejad, M., Kosaraju, J., Steinberg, N., Wang, B.S., Footz, T., Giuliani, F., Wang, J., Sipione, S., Edgar, J.M., and Voronova, A. 2023. Fractalkine enhances oligodendrocyte regeneration and remyelination in a demyelination mouse model. Stem Cell Rep. **18**(2): 519–533. doi:10.1016/j.stemcr.2022.12.001.

Alzheimer Society of Canada. 2016. Report summary prevalence and monetary costs of dementia in Canada: a report by the Alzheimer Society of Canada. Health Promot. Chronic Dis. Prev. Can. Res. Policy Pract. **36**(10): 231–232.

Ashton, J.C., and Glass, M. 2007. The cannabinoid CB_2 receptor as a target for inflammation-dependent neurodegeneration. Curr. Neuropharmacol. **5**(2): 73–80. doi:10.2174/157015907780866884.

Askari, V.R., and Shafiee-Nick, R. 2019. The protective effects of β-caryophyllene on LPS-induced primary microglia M1/M2 imbalance: A mechanistic evaluation. Life Sci. **219**: 40–73. doi:10.1016/j.lfs.2018.12.059.

Aso, E., Juvés, S., Maldonado, R., and Ferrer, I. 2013. CB_2 cannabinoid receptor agonist ameliorates Alzheimer-like phenotype in AβPP/PS1 mice. J. Alzheimers Dis. **35**(4): 847–858. doi:10.3233/JAD-130137.

d'Avila, J.C., Siqueira, L.D., Mazeraud, A., Azevedo, E.P., Foguel, D., Castro-Faria-Neto, H.C., Sharshar, T., Chrétien, F., and Bozza, F.A. 2018. Age-related cognitive impairment is associated with long-term neuroinflammation and oxidative stress in a mouse model of episodic systemic inflammation. J. Neuroinflammation **15**(1): 28. doi:10.1186/s12974-018-1059-y.

Bachiller, S., Jiménez-Ferrer, I., Paulus, A., Yang, Y., Swanberg, M., Deierborg, T., and Boza-Serrano, A. 2018. Microglia in neurological diseases: A road map to brain-disease dependent-inflammatory response. Front. Cell. Neurosci. **12**. Frontiers. doi:10.3389/fncel.2018.00488.

Bachstetter, A.D., Xing, B., de Almeida, L., Dimayuga, E.R., Watterson, D.M., and Van Eldik, L.J. 2011. Microglial p38α MAPK is a key regulator of proinflammatory cytokine up-regulation induced by toll-like receptor (TLR) ligands or beta-amyloid (Aβ). J. Neuroinflammation **8**(1): 79. doi:10.1186/1742-2094-8-79.

Badimon, A., Strasburger, H.J., Ayata, P., Chen, X., Nair, A., Ikegami, A., Hwang, P., Chan, A.T., Graves, S.M., Uweru, J.O., Ledderose, C., Kutlu, M.G., Wheeler, M.A., Kahan, A., Ishikawa, M., Wang, Y.-C., Loh, Y.-H.E., Jiang, J.X., Surmeier, D.J., Robson, S.C., Junger, W.G., Sebra, R., Calipari, E.S., Kenny, P.J., Eyo, U.B., Colonna, M., Quintana, F.J., Wake, H., Gradinaru, V., and Schaefer, A. 2020. Negative feedback control of neuronal activity by microglia. Nature **586**(7829): 417–423. doi:10.1038/s41586-020-2777-8.

Bagher, A.M., Laprairie, R.B., Kelly, M.E.M., and Denovan-Wright, E.M. 2016. Antagonism of dopamine receptor 2 long affects cannabinoid receptor 1 signaling in a cell culture model of striatal medium spiny projection neurons. Mol. Pharmacol. **89**(6): 652–666. doi:10.1124/mol.116.103465.

Bagher, A.M., Laprairie, R.B., Toguri, J.T., Kelly, M.E.M., and Denovan-Wright, E.M. 2017. Bidirectional allosteric interactions between cannabinoid receptor 1 (CB_1) and dopamine receptor 2 long (D_{2L}) heterotetramers. Eur. J. Pharmacol. **813**: 66–83. doi:10.1016/j.ejphar.2017.07.034.

Bagher, A.M., Young, A.P., Laprairie, R.B., Toguri, J.T., Kelly, M.E.M., and Denovan-Wright, E.M. 2020. Heteromer formation between cannabinoid type 1 and dopamine type 2 receptors is altered by combination cannabinoid and antipsychotic treatments. J. Neurosci. Res. **98**(12): 2496–2509. doi:https://doi.org/10.1002/jnr.24716.

Bai, X., Wey, M.C.-Y., Fernandez, E., Hart, M.J., Gelfond, J., Bokov, A.F., Rani, S., and Strong, R. 2015. Rapamycin improves motor function, reduces 4-hydroxynonenal adducted protein in brain, and attenuates synaptic injury in a mouse model of synucleinopathy. Pathobiol. Aging Age Relat. Dis. **5**: 28743. doi:10.3402/pba.v5.28743.

Baker, M. 2015. Reproducibility crisis: Blame it on the antibodies. Nature **521**(7552): 274–276. doi:10.1038/521274a.

Bal-Price, A., and Brown, G.C. 2001. Inflammatory neurodegeneration mediated by nitric oxide from activated glia-inhibiting neuronal respiration, causing glutamate release and excitotoxicity. J. Neurosci. **21**(17): 6480–6491. doi:10.1523/JNEUROSCI.21-17-06480.2001.

Bandrés, E., Merino, J., Vázquez, B., Inogés, S., Moreno, C., Subirá, M.L., and Sánchez-Ibarrola, A. 2000. The increase of IFN-gamma production through aging correlates with the expanded CD8(+high)CD28(-)CD57(+) subpopulation. Clin. Immunol. Orlando Fla **96**(3): 230–235. doi:10.1006/clim.2000.4894.

Banks, W.A., Gray, A.M., Erickson, M.A., Salameh, T.S., Damodarasamy, M., Sheibani, N., Meabon, J.S., Wing, E.E., Morofuji, Y., Cook, D.G., and Reed, M.J. 2015. Lipopolysaccharide-induced blood-brain barrier disruption: roles of cyclooxygenase, oxidative stress, neuroinflammation, and elements of the neurovascular unit. J. Neuroinflammation **12**: 223. doi:10.1186/s12974-015-0434-1.

Barbiellini Amidei, C., Fayosse, A., Dumurgier, J., Machado-Fragua, M.D., Tabak, A.G., van Sloten, T., Kivimäki, M., Dugravot, A., Sabia, S., and Singh-Manoux, A. 2021. Association between age at diabetes onset and subsequent risk of dementia. JAMA **325**(16): 1640–1649. doi:10.1001/jama.2021.4001.

Barcia, C., Ros, C.M., Annese, V., Gómez, A., Ros-Bernal, F., Aguado-Yera, D., Martínez-Pagán, M.E., de Pablos, V., Fernandez-Villalba, E., and Herrero, M.T. 2011. IFN-γ signaling, with the synergistic contribution of TNF-α, mediates cell specific microglial and astroglial activation in experimental models of Parkinson's disease. Cell Death Dis. **2**(4): e142. doi:10.1038/cddis.2011.17.

Baruch, K., Deczkowska, A., Rosenzweig, N., Tsitsou-Kampeli, A., Sharif, A.M., Matcovitch-Natan, O., Kertser, A., David, E., Amit, I., and Schwartz, M. 2016. PD-1 immune checkpoint blockade reduces pathology and improves memory in mouse models of Alzheimer's disease. Nat. Med. **22**(2): 135–137. doi:10.1038/nm.4022.

Batista, C.R.A., Gomes, G.F., Candelario-Jalil, E., Fiebich, B.L., and de Oliveira, A.C.P. 2019. Lipopolysaccharide-induced neuroinflammation as a bridge to understand neurodegeneration. Int. J. Mol. Sci. **20**(9): 2293. doi:10.3390/ijms20092293.

Baughman, J.M., Perocchi, F., Girgis, H.S., Plovanich, M., Belcher-Timme, C.A., Sancak, Y., Bao, X.R., Strittmatter, L., Goldberger, O., Bogorad, R.L., Koteliansky, V., and Mootha, V.K. 2011. Integrative genomics identifies MCU as an essential component of the mitochondrial calcium uniporter. Nature **476**(7360): 341–345. doi:10.1038/nature10234.

Beattie, E.C., Stellwagen, D., Morishita, W., Bresnahan, J.C., Ha, B.K., Von Zastrow, M., Beattie, M.S., and Malenka, R.C. 2002. Control of synaptic strength by glial TNFalpha. Science **295**(5563): 2282–2285. doi:10.1126/science.1067859.

Beers, D.R., Henkel, J.S., Zhao, W., Wang, J., and Appel, S.H. 2008. CD4+ T cells support glial neuroprotection, slow disease progression, and modify glial morphology in an animal model of inherited ALS. Proc. Natl. Acad. Sci. **105**(40): 15558–15563. Proceedings of the National Academy of Sciences. doi:10.1073/pnas.0807419105.

Benito, C., Núñez, E., Tolón, R.M., Carrier, E.J., Rábano, A., Hillard, C.J., and Romero, J. 2003. Cannabinoid CB_2 receptors and fatty acid amide hydrolase are selectively overexpressed in neuritic plaque-associated glia in Alzheimer's disease brains. J. Neurosci. **23**(35): 11136–11141. doi:10.1523/JNEUROSCI.23-35-11136.2003.

Berghe, T.V., Linkermann, A., Jouan-Lanhouet, S., Walczak, H., and Vandenabeele, P. 2014. Regulated necrosis: the expanding network of non-apoptotic cell death pathways. Nat. Rev. Mol. Cell Biol. **15**(2): 135–147. doi:10.1038/nrm3737.

Bettcher, B.M., Tansey, M.G., Dorothée, G., and Heneka, M.T. 2021. Peripheral and central immune system crosstalk in Alzheimer disease - a research prospectus. Nat. Rev. Neurol. **17**(11): 689–701. doi:10.1038/s41582-021-00549-x.

Bhattacherjee, A., Daskhan, G.C., Bains, A., Watson, A.E.S., Eskandari-Sedighi, G., St. Laurent, C.D., Voronova, A., and Macauley, M.S. 2021. Increasing phagocytosis of microglia by targeting CD33 with liposomes displaying glycan ligands. J. Controlled Release **338**: 680–693. doi:10.1016/j.jconrel.2021.09.010.

Biber, K., Neumann, H., Inoue, K., and Boddeke, H.W.G.M. 2007. Neuronal "On" and "Off" signals control microglia. Trends Neurosci. **30**(11): 596–602. doi:10.1016/j.tins.2007.08.007.

Biber, K., Pinto-Duarte, A., Wittendorp, M.C., Dolga, A.M., Fernandes, C.C., Von Frijtag Drabbe Künzel, J., Keijser, J.N., de Vries, R., Ijzerman, A.P., Ribeiro, J.A., Eisel, U., Sebastião, A.M., and Boddeke, H.W.G.M. 2008. Interleukin-6 Upregulates Neuronal Adenosine A1 Receptors: Implications for Neuromodulation and Neuroprotection. Neuropsychopharmacology **33**(9): 2237–2250. doi:10.1038/sj.npp.1301612.

Bilimoria, P.M., and Stevens, B. 2015. Microglia function during brain development: New insights from animal models. Brain Res. **1617**: 7–17. doi:10.1016/j.brainres.2014.11.032.

Björkqvist, M., Wild, E.J., Thiele, J., Silvestroni, A., Andre, R., Lahiri, N., Raibon, E., Lee, R.V., Benn, C.L., Soulet, D., Magnusson, A., Woodman, B., Landles, C., Pouladi, M.A., Hayden, M.R., Khalili-Shirazi, A., Lowdell, M.W., Brundin, P., Bates, G.P., Leavitt, B.R., Möller, T., and Tabrizi, S.J. 2008. A novel pathogenic pathway of immune activation detectable before clinical onset in Huntington's disease. J. Exp. Med. **205**(8): 1869–1877. doi:10.1084/jem.20080178.

Blacher, E., Bashiardes, S., Shapiro, H., Rothschild, D., Mor, U., Dori-Bachash, M., Kleimeyer, C., Moresi, C., Harnik, Y., Zur, M., Zabari, M., Brik, R.B.-Z., Kviatcovsky, D., Zmora, N., Cohen, Y., Bar, N., Levi, I., Amar, N., Mehlman, T., Brandis, A., Biton, I., Kuperman, Y., Tsoory, M., Alfahel, L., Harmelin, A., Schwartz, M., Israelson, A., Arike, L., Johansson, M.E.V., Hansson, G.C., Gotkine, M., Segal, E., and Elinav, E. 2019. Potential roles of gut microbiome and metabolites in modulating ALS in mice. Nature **572**(7770): 474–480. doi:10.1038/s41586-019-1443-5.

Blasi, E., Barluzzi, R., Bocchini, V., Mazzolla, R., and Bistoni, F. 1990. Immortalization of murine microglial cells by a v-raf/v-myc carrying retrovirus. J. Neuroimmunol. **27**(2–3): 229–237. doi:10.1016/0165-5728(90)90073-v.

Boddy, S.L., Giovannelli, I., Sassani, M., Cooper-Knock, J., Snyder, M.P., Segal, E., Elinav, E., Barker, L.A., Shaw, P.J., and McDermott, C.J. 2021. The gut microbiome: a key player in the complexity of amyotrophic lateral sclerosis (ALS). BMC Med. **19**(1): 13. doi:10.1186/s12916-020-01885-3.

Boudakov, I., Liu, J., Fan, N., Gulay, P., Wong, K., and Gorczynski, R.M. 2007. Mice lacking CD200R1 show absence of suppression of lipopolysaccharide-induced tumor necrosis factor-alpha and mixed leukocyte culture responses by CD200. Transplantation **84**(2): 251–257. doi:10.1097/01.tp.0000269795.04592.cc.

Bradley, D., Smith, A.J., Blaszczak, A., Shantaram, D., Bergin, S.M., Jalilvand, A., Wright, V., Wyne, K.L., Dewal, R.S., Baer, L.A., Wright, K.R., Stanford, K.I., Needleman, B., Brethauer, S., Noria, S., Renton, D., Joseph, J.J., Lovett-Racke, A., Liu, J., and Hsueh, W.A. 2022. Interferon gamma mediates the reduction of adipose tissue regulatory T cells in human obesity. Nat. Commun. **13**(1): 5606. doi:10.1038/s41467-022-33067-5.

Brakedal, B., Tzoulis, C., Tysnes, O.-B., and Haugarvoll, K. 2021. NSAID use is not associated with Parkinson's disease incidence: A Norwegian Prescription Database study. PLoS ONE **16**(9): e0256602. doi:10.1371/journal.pone.0256602.

Brenchley, J.M., Price, D.A., Schacker, T.W., Asher, T.E., Silvestri, G., Rao, S., Kazzaz, Z., Bornstein, E., Lambotte, O., Altmann, D., Blazar, B.R., Rodriguez, B., Teixeira-Johnson, L., Landay, A., Martin, J.N., Hecht, F.M., Picker, L.J., Lederman, M.M., Deeks, S.G., and Douek, D.C. 2006. Microbial translocation is a cause of systemic immune activation in chronic HIV infection. Nat. Med. **12**(12): 1365–1371. doi:10.1038/nm1511.

Bright, F., Chan, G., van Hummel, A., Ittner, L.M., and Ke, Y.D. 2021. TDP-43 and Inflammation: Implications for amyotrophic lateral sclerosis and frontotemporal dementia. Int. J. Mol. Sci. **22**(15): 7781. doi:10.3390/ijms22157781.

Brinkman, R.R., Mezei, M.M., Theilmann, J., Almqvist, E., and Hayden, M.R. 1997. The likelihood of being affected with Huntington disease by a particular age, for a specific CAG size. Am. J. Hum. Genet. **60**(5): 1202–1210.

Brombacher, T.M., Nono, J.K., De Gouveia, K.S., Makena, N., Darby, M., Womersley, J., Tamgue, O., and Brombacher, F. 2017. IL-13-mediated regulation of learning and memory. J. Immunol. **198**(7): 2681–2688. doi:10.4049/jimmunol.1601546.

Brown, G.C. 2019. The endotoxin hypothesis of neurodegeneration. J. Neuroinflammation **16**: 180. doi:10.1186/s12974-019-1564-7.

Brown, G.C., and Vilalta, A. 2015. How microglia kill neurons. Brain Res. **1628**(Pt B): 288–297. doi:10.1016/j.brainres.2015.08.031.

Brown, K.T., Levis, S.C., O'Neill, C.E., Levy, C., Rice, K.C., Watkins, L.R., and Bachtell, R.K. 2023. Toll-like receptor 4 antagonists reduce cocaine-primed reinstatement of drug seeking. Psychopharmacology. **240**(7): 1587–1600. doi:10.1007/s00213-023-06392-w.

Brynskikh, A., Warren, T., Zhu, J., and Kipnis, J. 2008. Adaptive immunity affects learning behavior in mice. Brain. Behav. Immun. **22**(6): 861–869. doi:10.1016/j.bbi.2007.12.008.

Cabral, G.A., Raborn, E.S., Griffin, L., Dennis, J., and Marciano-Cabral, F. 2008. CB2 receptors in the brain: role in central immune function. Br. J. Pharmacol. **153**(2): 240–251. doi:10.1038/sj.bjp.0707584.

Caccamo, A., Majumder, S., Richardson, A., Strong, R., and Oddo, S. 2010. Molecular interplay between mammalian target of rapamycin (mTOR), amyloid-beta, and Tau: effects on cognitive impairments. J. Biol. Chem. **285**(17): 13107–13120. doi:10.1074/jbc.M110.100420.

Calderón, F.H., Bonnefont, A., Muñoz, F.J., Fernández, V., Videla, L.A., and Inestrosa, N.C. 1999. PC12 and neuro 2a cells have different susceptibilities to acetylcholinesterase-amyloid complexes, amyloid25-35 fragment, glutamate, and hydrogen peroxide. J. Neurosci. Res. **56**(6): 620–631. doi:10.1002/(SICI)1097-4547(19990615)56:6<620::AID-JNR8>3.0.CO;2-F.

Calfee, D.P. 2017. Recent advances in the understanding and management of *Klebsiella pneumoniae*. F1000Research **6**: 1760. doi:10.12688/f1000research.11532.1.

Callén, L., Moreno, E., Barroso-Chinea, P., Moreno-Delgado, D., Cortés, A., Mallol, J., Casadó, V., Lanciego, J.L., Franco, R., Lluis, C., Canela, E.I., and McCormick, P.J. 2012. Cannabinoid receptors CB_1 and CB_2 form functional heteromers in brain. J. Biol. Chem. **287**(25): 20851–20865. doi:10.1074/jbc.M111.335273.

Cardona, A.E., Pioro, E.P., Sasse, M.E., Kostenko, V., Cardona, S.M., Dijkstra, I.M., Huang, D., Kidd, G., Dombrowski, S., Dutta, R., Lee, J.-C., Cook, D.N., Jung, S., Lira, S.A., Littman, D.R., and Ransohoff, R.M. 2006. Control of microglial neurotoxicity by the fractalkine receptor. Nat. Neurosci. **9**(7): 917–924. doi:10.1038/nn1715.

Carl, V.S., Gautam, J.K., Comeau, L.D., and Smith, M.F. 2004. Role of endogenous IL-10 in LPS-induced STAT3 activation and IL-1 receptor antagonist gene expression. J. Leukoc. Biol. **76**(3): 735–742. doi:10.1189/jlb.1003526.

Carlisle, S.J., Marciano-Cabral, F., Staab, A., Ludwick, C., and Cabral, G.A. 2002. Differential expression of the CB_2 cannabinoid receptor by rodent macrophages and macrophage-like cells in relation to cell activation. Int. Immunopharmacol. **2**(1): 69–82. doi:10.1016/S1567-5769(01)00147-3.

Caron, N.S., Wright, G.E., and Hayden, M.R. 1993. Huntington Disease. *In* GeneReviews®. *Edited by* M.P. Adam, G.M. Mirzaa, R.A. Pagon, S.E. Wallace, L.J. Bean, K.W. Gripp, and A. Amemiya. University of Washington, Seattle, Seattle (WA). Available from http://www.ncbi.nlm.nih.gov/books/NBK1305/ [accessed 3 July 2023].

Cassano, T., Calcagnini, S., Pace, L., De Marco, F., Romano, A., and Gaetani, S. 2017. Cannabinoid receptor 2 signaling in neurodegenerative disorders: From pathogenesis to a promising therapeutic target. Front. Neurosci. **11**. doi:10.3389/fnins.2017.00030.

Cassatella, M.A., Meda, L., Bonora, S., Ceska, M., and Constantin, G. 1993. Interleukin 10 (IL-10) inhibits the release of proinflammatory cytokines from human polymorphonuclear leukocytes. Evidence for an autocrine role of tumor necrosis factor and IL-1 beta in mediating the production of IL-8 triggered by lipopolysaccharide. J. Exp. Med. **178**(6): 2207–2211. doi:10.1084/jem.178.6.2207.

Castro-Sánchez, S., García-Yagüe, Á.J., López-Royo, T., Casarejos, M., Lanciego, J.L., and Lastres-Becker, I. 2018. Cx3cr1-deficiency exacerbates alpha-synuclein-A53T induced neuroinflammation and neurodegeneration in a mouse model of Parkinson's disease. Glia **66**(8): 1752–1762. doi:10.1002/glia.23338.

Cattaneo, A., Cattane, N., Galluzzi, S., Provasi, S., Lopizzo, N., Festari, C., Ferrari, C., Guerra, U.P., Paghera, B., Muscio, C., Bianchetti, A., Volta, G.D., Turla, M., Cotelli, M.S., Gennuso, M., Prelle, A., Zanetti, O., Lussignoli, G., Mirabile, D., Bellandi, D., Gentile, S., Belotti, G., Villani, D., Harach, T., Bolmont, T., Padovani, A., Boccardi, M., and Frisoni, G.B. 2017. Association of brain amyloidosis with pro-inflammatory gut bacterial taxa and peripheral inflammation markers in cognitively impaired elderly. Neurobiol. Aging **49**: 60–68. doi:10.1016/j.neurobiolaging.2016.08.019.

Cepeda, C., Colwell, C.S., Itri, J.N., Chandler, S.H., and Levine, M.S. 1998. Dopaminergic modulation of NMDA-induced whole cell currents in neostriatal neurons in slices: contribution of calcium conductances. J. Neurophysiol. **79**(1): 82–94. doi:10.1152/jn.1998.79.1.82.

Cepeda, C., Murphy, K.P.S., Parent, M., and Levine, M.S. 2014. The role of dopamine in Huntington's Disease. Prog. Brain Res. **211**: 235–254. doi:10.1016/B978-0-444-63425-2.00010-6.

Céspedes Rubio, Á.E., Pérez-Alvarez, M.J., Lapuente Chala, C., and Wandosell, F. 2018. Sex steroid hormones as neuroprotective elements in ischemia models. J. Endocrinol. **237**(2): R65–R81. doi:10.1530/JOE-18-0129.

Chai, Q., He, W.Q., Zhou, M., Lu, H., and Fu, Z.F. 2014. Enhancement of blood-brain barrier permeability and reduction of tight junction protein expression are modulated by chemokines/cytokines induced by rabies virus infection. J. Virol. **88**(9): 4698–4710. doi:10.1128/JVI.03149-13.

Chambers-Richards, T., Chireh, B., and D'Arcy, C. 2022. Trends in prevalence of self-reports of Alzheimer's disease/dementia among non-institutionalized individuals 45+ in Canada, 1994–2014. J. Public Health Res. **11**(4): 22799036221135220. doi:10.1177/22799036221135221.

Chandra, S., Sisodia, S.S., and Vassar, R.J. 2023. The gut microbiome in Alzheimer's disease: what we know and what remains to be explored. Mol. Neurodegener. **18**(1): 9. doi:10.1186/s13024-023-00595-7.

Chang, R., Yee, K.-L., and Sumbria, R.K. 2017. Tumor necrosis factor α inhibition for Alzheimer's Disease. J. Cent. Nerv. Syst. Dis. **9**: 1179573517709278. doi:10.1177/1179573517709278.

Chang, Y.-Y., Juhász, G., Goraksha-Hicks, P., Arsham, A.M., Mallin, D.R., Muller, L.K., and Neufeld, T.P. 2009. Nutrient-dependent regulation of autophagy through the target of rapamycin pathway. Biochem. Soc. Trans. **37**(Pt 1): 232–236. doi:10.1042/BST0370232.

Chao, C.C., Hu, S.X., Ehrlich, L., and Peterson, P.K. 1995. Interleukin-1 and tumor necrosis factor-α synergistically mediate neurotoxicity: Involvement of nitric oxide and of n-methyl-d-aspartate receptors. Brain. Behav. Immun. **9**(4): 355–365. doi:10.1006/brbi.1995.1033.

Chen, D., Gao, M., Gao, F., Su, Q., and Wu, J. 2017. Brain cannabinoid receptor 2: expression, function and modulation. Acta Pharmacol. Sin. **38**(3): 312–316. doi:10.1038/aps.2016.149.

Chen, J.Y., Wang, E.A., Cepeda, C., and Levine, M.S. 2013. Dopamine imbalance in Huntington's disease: a mechanism for the lack of behavioral flexibility. Front. Neurosci. **7**: 114. doi:10.3389/fnins.2013.00114.

Chen, M.J., Ramesha, S., Weinstock, L.D., Gao, T., Ping, L., Xiao, H., Dammer, E.B., Duong, D.D., Levey, A.I., Lah, J.J., Seyfried, N.T., Wood, L.B., and Rangaraju, S. 2021. Extracellular signal-regulated kinase regulates microglial immune responses in Alzheimer's disease. J. Neurosci. Res. **99**(6): 1704–1721. doi:10.1002/jnr.24829.

Chen, W.-N.U., Woodbury, R.L., Kathmann, L.E., Opresko, L.K., Zangar, R.C., Wiley, H.S., and Thrall, B.D. 2004. Induced autocrine signaling through the epidermal growth factor receptor contributes to the response of mammary epithelial cells to tumor necrosis factor alpha. J. Biol. Chem. **279**(18): 18488–18496. doi:10.1074/jbc.M310874200.

Chen, X., Firulyova, M., Manis, M., Herz, J., Smirnov, I., Aladyeva, E., Wang, C., Bao, X., Finn, M.B., Hu, H., Shchukina, I., Kim, M.W., Yuede, C.M., Kipnis, J., Artyomov, M.N., Ulrich, J.D., and Holtzman, D.M. 2023. Microglia-mediated T cell infiltration drives neurodegeneration in tauopathy. Nature **615**(7953): 668–677. doi:10.1038/s41586-023-05788-0.

Chen, X., Hu, Y., Cao, Z., Liu, Q., and Cheng, Y. 2018. Cerebrospinal fluid inflammatory cytokine aberrations in Alzheimer's Disease, Parkinson's Disease and Amyotrophic Lateral Sclerosis: A systematic review and meta-analysis. Front. Immunol. **9**: 2122. doi:10.3389/fimmu.2018.02122.

Chen, Z., Jalabi, W., Shpargel, K.B., Farabaugh, K.T., Dutta, R., Yin, X., Kidd, G.J., Bergmann, C.C., Stohlman, S.A., and Trapp, B.D. 2012. Lipopolysaccharide-induced microglial activation and neuroprotection against experimental brain injury is independent of hematogenous TLR4. J. Neurosci. **32**(34): 11706–11715. doi:10.1523/JNEUROSCI.0730-12.2012.

Cherry, J.D., Olschowka, J.A., and O'Banion, M.K. 2014. Neuroinflammation and M2 microglia: the good, the bad, and the inflamed. J. Neuroinflammation **11**: 98. doi:10.1186/1742-2094-11-98.

Chevalier, C., Stojanović, O., Colin, D.J., Suarez-Zamorano, N., Tarallo, V., Veyrat-Durebex, C., Rigo, D., Fabbiano, S., Stevanović, A., Hagemann, S., Montet, X., Seimbille, Y., Zamboni, N., Hapfelmeier, S., and Trajkovski, M. 2015. Gut microbiota orchestrates energy homeostasis during cold. Cell **163**(6): 1360–1374. doi:10.1016/j.cell.2015.11.004.

Chhor, V., Le Charpentier, T., Lebon, S., Oré, M.-V., Celador, I.L., Josserand, J., Degos, V., Jacotot, E., Hagberg, H., Sävman, K., Mallard, C., Gressens, P., and Fleiss, B. 2013. Characterization of phenotype markers and neuronotoxic potential of polarised primary microglia *in vitro*. Brain. Behav. Immun. **32**: 70–85. doi:10.1016/j.bbi.2013.02.005.

Chitnis, T., Imitola, J., Wang, Y., Elyaman, W., Chawla, P., Sharuk, M., Raddassi, K., Bronson, R.T., and Khoury, S.J. 2007. Elevated neuronal expression of CD200 protects wlds mice from inflammation-mediated neurodegeneration. Am. J. Pathol. **170**(5): 1695–1712. doi:10.2353/ajpath.2007.060677.

Cho, Y., Challa, S., Moquin, D., Genga, R., Ray, T.D., Guildford, M., and Chan, F.K.-M. 2009. Phosphorylation-driven assembly of the RIP1-RIP3 complex regulates programmed necrosis and virus-induced inflammation. Cell **137**(6): 1112–1123. doi:10.1016/j.cell.2009.05.037.

Choi, I., Zhang, Y., Seegobin, S.P., Pruvost, M., Wang, Q., Purtell, K., Zhang, B., and Yue, Z. 2020. Microglia clear neuron-released α-synuclein via selective autophagy and prevent neurodegeneration. Nat. Commun. **11**(1): 1386. doi:10.1038/s41467-020-15119-w.

Chou, T.-C. 2006. Theoretical basis, experimental design, and computerized simulation of synergism and antagonism in drug combination studies. Pharmacol. Rev. **58**(3): 621–681. doi:10.1124/pr.58.3.10.

Chou, T.-C. 2018. The combination index (CI < 1) as the definition of synergism and of synergy claims. Synergy **7**: 49–50. doi:10.1016/j.synres.2018.04.001.

Chou, T.C., and Talalay, P. 1984. Quantitative analysis of dose-effect relationships: the combined effects of multiple drugs or enzyme inhibitors. Adv. Enzyme Regul. **22**: 27–55. doi:10.1016/0065-2571(84)90007-4.

Christofferson, D.E., Li, Y., and Yuan, J. 2014. Control of life-or-death decisions by RIP1 kinase. Annu. Rev. Physiol. **76**: 129–150. doi:10.1146/annurev-physiol-021113-170259.

Chung, Y.C., Shin, W.-H., Baek, J.Y., Cho, E.J., Baik, H.H., Kim, S.R., Won, S.-Y., and Jin, B.K. 2016. CB_2 receptor activation prevents glial-derived neurotoxic mediator production, BBB leakage and peripheral immune cell infiltration and rescues dopamine neurons in the MPTP model of Parkinson's disease. Exp. Mol. Med. **48**(1): e205–e205. doi:10.1038/emm.2015.100.

Cinar, R., Gochuico, B.R., Iyer, M.R., Jourdan, T., Yokoyama, T., Park, J.K., Coffey, N.J., Pri-Chen, H., Szanda, G., Liu, Z., Mackie, K., Gahl, W.A., and Kunos, G. 2017. Cannabinoid CB_1 receptor overactivity contributes to the pathogenesis of idiopathic pulmonary fibrosis. JCI Insight **2**(8). doi:10.1172/jci.insight.92281.

Cocks, G., Romanyuk, N., Amemori, T., Jendelova, P., Forostyak, O., Jeffries, A.R., Perfect, L., Thuret, S., Dayanithi, G., Sykova, E., and Price, J. 2013. Conditionally immortalized stem cell lines from human spinal cord retain regional identity and generate functional V2a interneurons and motorneurons. Stem Cell Res. Ther. **4**(3): 69. doi:10.1186/scrt220.

Correa, F., Hernangómez, M., Mestre, L., Loría, F., Spagnolo, A., Docagne, F., Di Marzo, V., and Guaza, C. 2010. Anandamide enhances IL-10 production in activated microglia by targeting CB_2 receptors: Roles of ERK1/2, JNK, and NF-κB. Glia **58**(2): 135–147. doi:10.1002/glia.20907.

Correa, F., Hernangómez-Herrero, M., Mestre, L., Loría, F., Docagne, F., and Guaza, C. 2011. The endocannabinoid anandamide downregulates IL-23 and IL-12 subunits in a viral model of multiple sclerosis: evidence for a cross-talk between IL-12p70/IL-23 axis and IL-10 in microglial cells. Brain. Behav. Immun. **25**(4): 736–749. doi:10.1016/j.bbi.2011.01.020.

Cox, F.F., Carney, D., Miller, A.-M., and Lynch, M.A. 2012. CD200 fusion protein decreases microglial activation in the hippocampus of aged rats. Brain. Behav. Immun. **26**(5): 789–796. doi:10.1016/j.bbi.2011.10.004.

Crapser, J.D., Arreola, M.A., Tsourmas, K.I., and Green, K.N. 2021. Microglia as hackers of the matrix: sculpting synapses and the extracellular space. Cell. Mol. Immunol. **18**(11): 2472–2488. doi:10.1038/s41423-021-00751-3.

Crapser, J.D., Ochaba, J., Soni, N., Reidling, J.C., Thompson, L.M., and Green, K.N. 2020. Microglial depletion prevents extracellular matrix changes and striatal volume reduction in a model of Huntington's disease. Brain **143**(1): 266–288. doi:10.1093/brain/awz363.

Crimmins, E.M. 2015. Lifespan and Healthspan: Past, Present, and Promise. The Gerontologist **55**(6): 901–911. doi:10.1093/geront/gnv130.

Crotti, A., Benner, C., Kerman, B.E., Gosselin, D., Lagier-Tourenne, C., Zuccato, C., Cattaneo, E., Gage, F.H., Cleveland, D.W., and Glass, C.K. 2014. Mutant Huntingtin promotes autonomous microglia activation via myeloid lineage-determining factors. Nat. Neurosci. **17**(4): 513–521. doi:10.1038/nn.3668.

Crotti, A., and Glass, C.K. 2015. The choreography of neuroinflammation in Huntington's disease. Trends Immunol. **36**(6): 364–373. doi:10.1016/j.it.2015.04.007.

Dai, L., and Shen, Y. 2021. Insights into T-cell dysfunction in Alzheimer's disease. Aging Cell **20**(12): e13511. doi:10.1111/acel.13511.

Dai, X., Li, N., Yu, L., Chen, Z., Hua, R., Qin, X., and Zhang, Y.-M. 2015. Activation of BV2 microglia by lipopolysaccharide triggers an inflammatory reaction in PC12 cell apoptosis through a toll-like receptor 4-dependent pathway. Cell Stress Chaperones **20**(2): 321–331. doi:10.1007/s12192-014-0552-1.

Dalvi, P.S., Nazarians-Armavil, A., Tung, S., and Belsham, D.D. 2011. Immortalized neurons for the study of hypothalamic function. Am. J. Physiol.-Regul. Integr. Comp. Physiol. **300**(5): R1030–R1052. doi:10.1152/ajpregu.00649.2010.

Darnell, J.E., Kerr, I.M., and Stark, G.R. 1994. Jak-STAT pathways and transcriptional activation in response to IFNs and other extracellular signaling proteins. Science **264**(5164): 1415–1421. doi:10.1126/science.8197455.

Davalos, D., Grutzendler, J., Yang, G., Kim, J.V., Zuo, Y., Jung, S., Littman, D.R., Dustin, M.L., and Gan, W.-B. 2005. ATP mediates rapid microglial response to local brain injury in vivo. Nat. Neurosci. **8**(6): 752–758. doi:10.1038/nn1472.

De, S., Wirthensohn, D.C., Flagmeier, P., Hughes, C., Aprile, F.A., Ruggeri, F.S., Whiten, D.R., Emin, D., Xia, Z., Varela, J.A., Sormanni, P., Kundel, F., Knowles, T.P.J., Dobson, C.M., Bryant, C., Vendruscolo, M., and Klenerman, D. 2019. Different soluble aggregates of Aβ42 can give rise to cellular toxicity through different mechanisms. Nat. Commun. **10**(1): 1541. doi:10.1038/s41467-019-09477-3.

Decourt, B., Boumelhem, F., Pope, E.D., Shi, J., Mari, Z., and Sabbagh, M.N. 2021. Critical appraisal of amyloid lowering agents in AD. Curr. Neurol. Neurosci. Rep. **21**(8): 39. doi:10.1007/s11910-021-01125-y.

Degterev, A., Huang, Z., Boyce, M., Li, Y., Jagtap, P., Mizushima, N., Cuny, G.D., Mitchison, T.J., Moskowitz, M.A., and Yuan, J. 2005. Chemical inhibitor of nonapoptotic cell death with therapeutic potential for ischemic brain injury. Nat. Chem. Biol. **1**(2): 112–119. doi:10.1038/nchembio711.

Derecki, N.C., Cardani, A.N., Yang, C.H., Quinnies, K.M., Crihfield, A., Lynch, K.R., and Kipnis, J. 2010. Regulation of learning and memory by meningeal immunity: a key role for IL-4. J. Exp. Med. **207**(5): 1067–1080. doi:10.1084/jem.20091419.

Desai, R.J., Varma, V.R., Gerhard, T., Segal, J., Mahesri, M., Chin, K., Horton, D.B., Kim, S.C., Schneeweiss, S., and Thambisetty, M. 2022. Comparative risk of Alzheimer disease and related dementia among medicare beneficiaries with rheumatoid arthritis treated with targeted disease-modifying antirheumatic agents. JAMA Netw. Open **5**(4): e226567. doi:10.1001/jamanetworkopen.2022.6567.

Dhuriya, Y.K., and Sharma, D. 2018. Necroptosis: a regulated inflammatory mode of cell death. J. Neuroinflammation **15**(1): 199. doi:10.1186/s12974-018-1235-0.

DiSabato, D., Quan, N., and Godbout, J.P. 2016. Neuroinflammation: The devil is in the details. J. Neurochem. **139**(Suppl 2): 136–153. doi:10.1111/jnc.13607.

Doody, R.S., Thomas, R.G., Farlow, M., Iwatsubo, T., Vellas, B., Joffe, S., Kieburtz, K., Raman, R., Sun, X., Aisen, P.S., Siemers, E., Liu-Seifert, H., Mohs, R., Alzheimer's disease cooperative study steering committee, and solanezumab study group. 2014. Phase 3 trials of solanezumab for mild-to-moderate Alzheimer's disease. N. Engl. J. Med. **370**(4): 311–321. doi:10.1056/NEJMoa1312889.

Doyle, H.H., Eidson, L.N., Sinkiewicz, D.M., and Murphy, A.Z. 2017. Sex differences in microglia activity within the periaqueductal gray of the Rat: A potential mechanism driving the dimorphic effects of morphine. J. Neurosci. Off. J. Soc. Neurosci. **37**(12): 3202–3214. doi:10.1523/JNEUROSCI.2906-16.2017.

Dubbelaar, M.L., Kracht, L., Eggen, B.J.L., and Boddeke, E.W.G.M. 2018. The kaleidoscope of microglial phenotypes. Front. Immunol. **9**: 1753. doi:10.3389/fimmu.2018.01753.

Dudiki, T., Meller, J., Mahajan, G., Liu, H., Zhevlakova, I., Stefl, S., Witherow, C., Podrez, E., Kothapalli, C.R., and Byzova, T.V. 2020. Microglia control vascular architecture via a TGFβ1 dependent paracrine mechanism linked to tissue mechanics. Nat. Commun. **11**(1): 986. doi:10.1038/s41467-020-14787-y.

Dudvarski Stankovic, N., Teodorczyk, M., Ploen, R., Zipp, F., and Schmidt, M.H.H. 2016. Microglia–blood vessel interactions: a double-edged sword in brain pathologies. Acta Neuropathol. **131**(3): 347–363. doi:10.1007/s00401-015-1524-y.

Dumont, M., Kipiani, K., Yu, F., Wille, E., Katz, M., Calingasan, N.Y., Gouras, G.K., Lin, M.T., and Beal, M.F. 2011. Coenzyme Q10 decreases amyloid pathology and improves behavior in a transgenic mouse model of Alzheimer's disease. J. Alzheimers Dis. **27**(1): 211–223. doi:10.3233/JAD-2011-110209.

Duncan, K.A., and Saldanha, C.J. 2011. Neuroinflammation induces glial aromatase expression in the uninjured songbird brain. J. Neuroinflammation **8**: 81. doi:10.1186/1742-2094-8-81.

Dundee, J.M., Puigdellívol, M., Butler, R., Cockram, T.O.J., and Brown, G.C. 2023. P2Y6 receptor-dependent microglial phagocytosis of synapses mediates synaptic and memory loss in aging. Aging Cell **22**(2): e13761. doi:10.1111/acel.13761.

Dunkelberger, J.R., and Song, W.-C. 2010. Complement and its role in innate and adaptive immune responses. Cell Res. **20**(1): 34–50. doi:10.1038/cr.2009.139.

van Dyck, C.H. 2018. Anti-amyloid-β monoclonal antibodies for Alzheimer's disease: pitfalls and promise. Biol. Psychiatry **83**(4): 311–319. doi:10.1016/j.biopsych.2017.08.010.

Edison, P., Archer, H.A., Gerhard, A., Hinz, R., Pavese, N., Turkheimer, F.E., Hammers, A., Tai, Y.F., Fox, N., Kennedy, A., Rossor, M., and Brooks, D.J. 2008. Microglia, amyloid, and cognition in Alzheimer's disease: An [11C](R)PK11195-PET and [11C]PIB-PET study. Neurobiol. Dis. **32**(3): 412–419. doi:10.1016/j.nbd.2008.08.001.

Edwards, M.A., Loxley, R.A., Williams, A.J., Connor, M., and Phillips, J.K. 2007. Lack of functional expression of NMDA receptors in PC12 cells. Neurotoxicology **28**(4): 876–885. doi:10.1016/j.neuro.2007.04.006.

Efthymiou, A.G., and Goate, A.M. 2017. Late onset Alzheimer's disease genetics implicates microglial pathways in disease risk. Mol. Neurodegener. **12**: 43. doi:10.1186/s13024-017-0184-x.

Ehrhart, J., Obregon, D., Mori, T., Hou, H., Sun, N., Bai, Y., Klein, T., Fernandez, F., Tan, J., and Shytle, R.D. 2005. Stimulation of cannabinoid receptor 2 (CB_2) suppresses microglial activation. J. Neuroinflammation **2**: 29. doi:10.1186/1742-2094-2-29.

Eljaschewitsch, E., Witting, A., Mawrin, C., Lee, T., Schmidt, P.M., Wolf, S., Hoertnagl, H., Raine, C.S., Schneider-Stock, R., Nitsch, R., and Ullrich, O. 2006. The Endocannabinoid Anandamide Protects Neurons during CNS inflammation by induction of MKP-1 in microglial cells. Neuron **49**(1): 67–79. doi:10.1016/j.neuron.2005.11.027.

Ellul, M., and Solomon, T. 2018. Acute encephalitis – diagnosis and management. Clin. Med. **18**(2): 155–159. doi:10.7861/clinmedicine.18-2-155.

Elmore, M.R.P., Najafi, A.R., Koike, M.A., Dagher, N.N., Spangenberg, E.E., Rice, R.A., Kitazawa, M., Matusow, B., Nguyen, H., West, B.L., and Green, K.N. 2014. CSF1 receptor signaling is necessary for microglia viability, which unmasks a cell that rapidly repopulates the microglia-depleted adult brain. Neuron **82**(2): 380–397. doi:10.1016/j.neuron.2014.02.040.

Engelhart, M.J., Geerlings, M.I., Meijer, J., Kiliaan, A., Ruitenberg, A., van Swieten, J.C., Stijnen, T., Hofman, A., Witteman, J.C.M., and Breteler, M.M.B. 2004. Inflammatory proteins in plasma and the risk of dementia: the rotterdam study. Arch. Neurol. **61**(5): 668–672. doi:10.1001/archneur.61.5.668.

Erblich, B., Zhu, L., Etgen, A.M., Dobrenis, K., and Pollard, J.W. 2011. Absence of colony stimulation factor-1 receptor results in loss of microglia, disrupted brain development and olfactory deficits. PloS One **6**(10): e26317. doi:10.1371/journal.pone.0026317.

Erkkinen, M.G., Kim, M.-O., and Geschwind, M.D. 2018. Clinical neurology and epidemiology of the major neurodegenerative diseases. Cold Spring Harb. Perspect. Biol. **10**(4): a033118. doi:10.1101/cshperspect.a033118.

Estus, S., Shaw, B.C., Devanney, N., Katsumata, Y., Press, E.E., and Fardo, D.W. 2019. Evaluation of CD33 as a genetic risk factor for Alzheimer's disease. Acta Neuropathol. (Berl.) **138**(2): 187–199. doi:10.1007/s00401-019-02000-4.

Evans, M.E., and Pollack, M. 1993. Effect of antibiotic class and concentration on the release of lipopolysaccharide from *Escherichia coli*. J. Infect. Dis. **167**(6): 1336–1343. doi:10.1093/infdis/167.6.1336.

Everard, A., Belzer, C., Geurts, L., Ouwerkerk, J.P., Druart, C., Bindels, L.B., Guiot, Y., Derrien, M., Muccioli, G.G., Delzenne, N.M., de Vos, W.M., and Cani, P.D. 2013. Cross-talk between *Akkermansia muciniphila* and intestinal epithelium controls diet-induced obesity. Proc. Natl. Acad. Sci. U. S. A. **110**(22): 9066–9071. doi:10.1073/pnas.1219451110.

Eyo, U.B., and Wu, L.-J. 2013. Bidirectional microglia-neuron communication in the healthy brain. Neural Plast. **2013**: 456857. doi:10.1155/2013/456857.

Fakhfouri, G., Ahmadiani, A., Rahimian, R., Grolla, A.A., Moradi, F., and Haeri, A. 2012. WIN55212-2 attenuates amyloid-beta-induced neuroinflammation in rats through activation of cannabinoid receptors and PPAR-γ pathway. Neuropharmacology **63**(4): 653–666. doi:10.1016/j.neuropharm.2012.05.013.

Federici, S., Kredo-Russo, S., Valdés-Mas, R., Kviatcovsky, D., Weinstock, E., Matiuhin, Y., Silberberg, Y., Atarashi, K., Furuichi, M., Oka, A., Liu, B., Fibelman, M., Weiner, I.N., Khabra, E., Cullin, N., Ben-Yishai, N., Inbar, D., Ben-David, H., Nicenboim, J., Kowalsman, N., Lieb, W., Kario, E., Cohen, T., Geffen, Y.F., Zelcbuch, L., Cohen, A., Rappo, U., Gahali-Sass, I., Golembo, M., Lev, V., Dori-Bachash, M., Shapiro, H., Moresi, C., Cuevas-Sierra, A., Mohapatra, G., Kern, L., Zheng, D., Nobs, S.P., Suez, J., Stettner, N., Harmelin, A., Zak, N., Puttagunta, S., Bassan, M., Honda, K., Sokol, H., Bang, C., Franke, A., Schramm, C., Maharshak, N., Sartor, R.B., Sorek, R., and Elinav, E. 2022. Targeted suppression of human IBD-associated gut microbiota commensals by phage consortia for treatment of intestinal inflammation. Cell **185**(16): 2879-2898.e24. doi:10.1016/j.cell.2022.07.003.

Feinberg, P.A., Becker, S.C., Chung, L., Ferrari, L., Stellwagen, D., Anaclet, C., Durán-Laforet, V., Faust, T.E., Sumbria, R.K., and Schafer, D.P. 2022. Elevated TNF-α leads to neural circuit instability in the absence of interferon regulatory factor 8. J. Neurosci. **42**(32): 6171–6185. doi:10.1523/JNEUROSCI.0601-22.2022.

Fellner, L., Irschick, R., Schanda, K., Reindl, M., Klimaschewski, L., Poewe, W., Wenning, G.K., and Stefanova, N. 2013. Toll-like receptor 4 is required for α-synuclein dependent activation of microglia and astroglia. Glia **61**(3): 349–360. doi:10.1002/glia.22437.

Fernández-López, D., Martínez-Orgado, J., Nuñez, E., Romero, J., Lorenzo, P., Moro, M.A., and Lizasoain, I. 2006. Characterization of the neuroprotective effect of the cannabinoid agonist WIN-55212 in an in vitro model of hypoxic-ischemic brain damage in newborn rats. Pediatr. Res. **60**(2): 169–173. doi:10.1203/01.pdr.0000228839.00122.6c.

Ferré, S., Bonaventura, J., Tomasi, D., Navarro, G., Moreno, E., Cortés, A., Lluís, C., Casadó, V., and Volkow, N.D. 2016. Allosteric mechanisms within the adenosine A2A–dopamine D2 receptor heterotetramer. Neuropharmacology **104**: 154–160. doi:10.1016/j.neuropharm.2015.05.028.

Ferré, S., Lluís, C., Justinova, Z., Quiroz, C., Orru, M., Navarro, G., Canela, E.I., Franco, R., and Goldberg, S.R. 2010. Adenosine–cannabinoid receptor interactions. Implications for striatal function. Br. J. Pharmacol. **160**(3): 443–453. doi:10.1111/j.1476-5381.2010.00723.x.

Filiano, A.J., Xu, Y., Tustison, N.J., Marsh, R.L., Baker, W., Smirnov, I., Overall, C.C., Gadani, S.P., Turner, S.D., Weng, Z., Peerzade, S.N., Chen, H., Lee, K.S., Scott, M.M., Beenhakker, M.P., Litvak, V., and Kipnis, J. 2016. Unexpected role of interferon-γ in regulating neuronal connectivity and social behaviour. Nature **535**(7612): 425–429. doi:10.1038/nature18626.

Finlay, G.A., Hunter, D.S., Walker, C.L., Paulson, K.E., and Fanburg, B.L. 2003. Regulation of PDGF production and ERK activation by estrogen is associated with TSC2 gene expression. Am. J. Physiol.-Cell Physiol. **285**(2): C409–C418. American Physiological Society. doi:10.1152/ajpcell.00482.2002.

Fischer, R., Padutsch, T., Bracchi-Ricard, V., Murphy, K.L., Martinez, George.F., Delguercio, N., Elmer, N., Sendetski, M., Diem, R., Eisel, U.L.M., Smeyne, R.J., Kontermann, R.E., Pfizenmaier, K., and Bethea, J.R. 2019. Exogenous activation of tumor necrosis factor receptor 2 promotes recovery from sensory and motor disease in a model of multiple sclerosis. Brain. Behav. Immun. **81**: 247–259. doi:10.1016/j.bbi.2019.06.021.

Floden, A.M., Li, S., and Combs, C.K. 2005. β-amyloid-stimulated microglia induce neuron death via synergistic Stimulation of Tumor Necrosis Factor α and NMDA Receptors. J. Neurosci. **25**(10): 2566–2575. doi:10.1523/JNEUROSCI.4998-04.2005.

Fondell, E., O'Reilly, É.J., Fitzgerald, K.C., Falcone, G.J., McCullough, M.L., Thun, M.J., Park, Y., Kolonel, L.N., and Ascherio, A. 2012. Non-steroidal anti-inflammatory drugs and amyotrophic lateral sclerosis: Results from five prospective cohort studies. Amyotroph. Lateral Scler. **13**(6): 573–579. Taylor & Francis. doi:10.3109/17482968.2012.703209.

Forsyth, C.B., Shannon, K.M., Kordower, J.H., Voigt, R.M., Shaikh, M., Jaglin, J.A., Estes, J.D., Dodiya, H.B., and Keshavarzian, A. 2011. Increased intestinal permeability correlates with sigmoid mucosa alpha-synuclein staining and endotoxin exposure markers in early Parkinson's disease. PloS One **6**(12): e28032. doi:10.1371/journal.pone.0028032.

Frakes, A.E., Ferraiuolo, L., Haidet-Phillips, A.M., Schmelzer, L., Braun, L., Miranda, C.J., Ladner, K.J., Bevan, A.K., Foust, K.D., Godbout, J.P., Popovich, P.G., Guttridge, D.C., and Kaspar, B.K. 2014. Microglia induce motor neuron death via the classical NF-κB pathway in amyotrophic lateral sclerosis. Neuron **81**(5): 1009–1023. doi:10.1016/j.neuron.2014.01.013.

Fu, J., Chen, S., Liu, J., Yang, J., Ou, R., Zhang, L., Chen, X., and Shang, H. 2023. Serum inflammatory cytokines levels and the correlation analyses in Parkinson's disease. Front. Cell Dev. Biol. **11**: 1104393. doi:10.3389/fcell.2023.1104393.

Gaber, T., Strehl, C., and Buttgereit, F. 2017. Metabolic regulation of inflammation. Nat. Rev. Rheumatol. **13**(5): 267–279. Nature Publishing Group. doi:10.1038/nrrheum.2017.37.

Galea, I. 2021. The blood-brain barrier in systemic infection and inflammation. Cell. Mol. Immunol. **18**(11): 2489–2501. doi:10.1038/s41423-021-00757-x.

Galiègue, S., Mary, S., Marchand, J., Dussossoy, D., Carrière, D., Carayon, P., Bouaboula, M., Shire, D., LE Fur, G., and Casellas, P. 1995. Expression of central and peripheral cannabinoid receptors in human immune tissues and leukocyte subpopulations. Eur. J. Biochem. **232**(1): 54–61. doi:10.1111/j.1432-1033.1995.tb20780.x.

Galvan, L., André, V.M., Wang, E.A., Cepeda, C., and Levine, M.S. 2012. Functional differences between direct and indirect striatal output pathways in Huntington's disease. J. Huntingt. Dis. **1**(1): 17–25. doi:10.3233/JHD-2012-120009.

Garber, C., Soung, A., Vollmer, L.L., Kanmogne, M., Last, A., Brown, J., and Klein, R.S. 2019. T cells promote microglia-mediated synaptic elimination and cognitive dysfunction during recovery from neuropathogenic flaviviruses. Nat. Neurosci. **22**(8): 1276–1288. doi:10.1038/s41593-019-0427-y.

Garber, C., Vasek, M.J., Vollmer, L.L., Sun, T., Jiang, X., and Klein, R.S. 2018. Astrocytes decrease adult neurogenesis during virus-induced memory dysfunction via interleukin-1. Nat. Immunol. **19**(2): 151–161. doi:10.1038/s41590-017-0021-y.

García, C., Gómez-Cañas, M., Burgaz, S., Palomares, B., Gómez-Gálvez, Y., Palomo-Garo, C., Campo, S., Ferrer-Hernández, J., Pavicic, C., Navarrete, C., Luz Bellido, M., García-Arencibia, M., Ruth Pazos, M., Muñoz, E., and Fernández-Ruiz, J. 2018. Benefits of VCE-003.2, a cannabigerol quinone derivative, against inflammation-driven neuronal deterioration in experimental Parkinson's disease: possible involvement of different binding sites at the PPARγ receptor. J. Neuroinflammation **15**: 19. doi:10.1186/s12974-018-1060-5.

García-Ovejero, D., Veiga, S., García-Segura, L.M., and Doncarlos, L.L. 2002. Glial expression of estrogen and androgen receptors after rat brain injury. J. Comp. Neurol. **450**(3): 256–271. doi:10.1002/cne.10325.

Gardoni, F., and Bellone, C. 2015. Modulation of the glutamatergic transmission by Dopamine: a focus on Parkinson, Huntington and Addiction diseases. Front. Cell. Neurosci. **9**.

Garvey, E.P., Oplinger, J.A., Furfine, E.S., Kiff, R.J., Laszlo, F., Whittle, B.J.R., and Knowles, R.G. 1997. 1400W Is a slow, tight binding, and highly selective inhibitor of inducible nitric-oxide synthase *in vitro* and *in vivo*. J. Biol. Chem. **272**(8): 4959–4963. doi:10.1074/jbc.272.8.4959.

Gate, D., Saligrama, N., Leventhal, O., Yang, A.C., Unger, M.S., Middeldorp, J., Chen, K., Lehallier, B., Channappa, D., De Los Santos, M.B., McBride, A., Pluvinage, J., Elahi, F., Tam, G.K.-Y., Kim, Y., Greicius, M., Wagner, A.D., Aigner, L., Galasko, D.R., Davis, M.M., and Wyss-Coray, T. 2020. Clonally expanded CD8 T cells patrol the cerebrospinal fluid in Alzheimer's disease. Nature **577**(7790): 399–404. Nature Publishing Group. doi:10.1038/s41586-019-1895-7.

Gavegnano, C., Haile, W.B., Hurwitz, S., Tao, S., Jiang, Y., Schinazi, R.F., and Tyor, W.R. 2019. Baricitinib reverses HIV-associated neurocognitive disorders in a SCID mouse model and reservoir seeding in vitro. J. Neuroinflammation **16**(1): 182. doi:10.1186/s12974-019-1565-6.

Gerfen, C.R., Engber, T.M., Mahan, L.C., Susel, Z., Chase, T.N., Monsma, F.J., and Sibley, D.R. 1990. D_1 and D_2 dopamine receptor-regulated gene expression of striatonigral and striatopallidal neurons. Science **250**(4986): 1429–1432. doi:10.1126/science.2147780.

Gerritse, K., Laman, J.D., Noelle, R.J., Aruffo, A., Ledbetter, J.A., Boersma, W.J., and Claassen, E. 1996. CD40-CD40 ligand interactions in experimental allergic encephalomyelitis and multiple sclerosis. Proc. Natl. Acad. Sci. U. S. A. **93**(6): 2499–2504.

Ghosh, A., Chandran, K., Kalivendi, S.V., Joseph, J., Antholine, W.E., Hillard, C.J., Kanthasamy, A., Kanthasamy, A., and Kalyanaraman, B. 2010. Neuroprotection by a mitochondria-targeted drug in a Parkinson's disease model. Free Radic. Biol. Med. **49**(11): 1674–1684. doi:10.1016/j.freeradbiomed.2010.08.028.

Gillies, G.E., and McArthur, S. 2010. Estrogen actions in the brain and the basis for differential action in men and women: a case for sex-specific medicines. Pharmacol. Rev. **62**(2): 155–198. doi:10.1124/pr.109.002071.

Ginhoux, F., Greter, M., Leboeuf, M., Nandi, S., See, P., Gokhan, S., Mehler, M.F., Conway, S.J., Ng, L.G., Stanley, E.R., Samokhvalov, I.M., and Merad, M. 2010. Fate mapping analysis reveals that adult microglia derive from primitive macrophages. Science **330**(6005): 841–845. doi:10.1126/science.1194637.

Glass, M., Dragunow, M., and Faull, R.L.M. 2000. The pattern of neurodegeneration in Huntington's disease: a comparative study of cannabinoid, dopamine, adenosine and GABAA receptor alterations in the human basal ganglia in Huntington's disease. Neuroscience **97**(3): 505–519. doi:10.1016/S0306-4522(00)00008-7.

Glass, M., Faull, R.L., and Dragunow, M. 1993. Loss of cannabinoid receptors in the substantia nigra in Huntington's disease. Neuroscience **56**(3): 523–527. doi:10.1016/0306-4522(93)90352-g.

Gregersen, R., Lambertsen, K., and Finsen, B. 2000. Microglia and macrophages are the major source of tumor necrosis factor in permanent middle cerebral artery occlusion in mice. J. Cereb. Blood Flow Metab. **20**(1): 53–65. doi:10.1097/00004647-200001000-00009.

Grenier, P., Sunavsky, A., and Olmstead, M.C. 2021. Morphine induces upregulation of neuronally expressed CB_2 receptors in the spinal dorsal horn of rats. Cannabis Cannabinoid Res. **6**(2): 137–147. doi:10.1089/can.2020.0004.

Griffin, J. 2008. Changing life expectancy throughout history. J. R. Soc. Med. **101**(12): 577. doi:10.1258/jrsm.2008.08k037.

Group, T.L.M.S.S.G. and T.U. of B.C.M.A. 1999. TNF neutralization in MS: Results of a randomized, placebo-controlled multicenter study. Neurology **53**(3): 457–457. doi:10.1212/WNL.53.3.457.

Guindon, J., and Hohmann, A.G. 2008. Cannabinoid CB_2 receptors: a therapeutic target for the treatment of inflammatory and neuropathic pain. Br. J. Pharmacol. **153**(2): 319–334. doi:10.1038/sj.bjp.0707531.

Guneykaya, D., Ivanov, A., Hernandez, D.P., Haage, V., Wojtas, B., Meyer, N., Maricos, M., Jordan, P., Buonfiglioli, A., Gielniewski, B., Ochocka, N., Cömert, C., Friedrich, C., Artiles, L.S., Kaminska, B., Mertins, P., Beule, D., Kettenmann, H., and Wolf, S.A. 2018. Transcriptional and translational differences of microglia from male and female brains. Cell Rep. **24**(10): 2773-2783.e6. doi:10.1016/j.celrep.2018.08.001.

Guthrie, P.B., Knappenberger, J., Segal, M., Bennett, M.V.L., Charles, A.C., and Kater, S.B. 1999. ATP released from astrocytes mediates glial calcium waves. J. Neurosci. **19**(2): 520–528. doi:10.1523/JNEUROSCI.19-02-00520.1999.

Guttenplan, K.A., Stafford, B.K., El-Danaf, R.N., Adler, D.I., Münch, A.E., Weigel, M.K., Huberman, A.D., and Liddelow, S.A. 2020a. Neurotoxic reactive astrocytes drive neuronal death after retinal injury. Cell Rep. **31**(12): 107776. doi:10.1016/j.celrep.2020.107776.

Guttenplan, K.A., Weigel, M.K., Adler, D.I., Couthouis, J., Liddelow, S.A., Gitler, A.D., and Barres, B.A. 2020b. Knockout of reactive astrocyte activating factors slows disease progression in an ALS mouse model. Nat. Commun. **11**(1): 3753. doi:10.1038/s41467-020-17514-9.

Guttenplan, K.A., Weigel, M.K., Prakash, P., Wijewardhane, P.R., Hasel, P., Rufen-Blanchette, U., Münch, A.E., Blum, J.A., Fine, J., Neal, M.C., Bruce, K.D., Gitler, A.D., Chopra, G., Liddelow, S.A., and Barres, B.A. 2021. Neurotoxic reactive astrocytes induce cell death via saturated lipids. Nature **599**(7883): 102–107. doi:10.1038/s41586-021-03960-y.

Guzman-Martinez, L., Maccioni, R.B., Andrade, V., Navarrete, L.P., Pastor, M.G., and Ramos-Escobar, N. 2019. Neuroinflammation as a common feature of neurodegenerative disorders. Front. Pharmacol. **10**. doi:10.3389/fphar.2019.01008.

Hadi, T., Barrichon, M., Mourtialon, P., Wendremaire, M., Garrido, C., Sagot, P., Bardou, M., and Lirussi, F. 2013. Biphasic ERK1/2 activation sequentially involving Gs and Gi signaling is required in beta3-adrenergic receptor-induced primary smooth muscle cell proliferation. Biochim. Biophys. Acta. **1833**(5): 1041–1051. doi:10.1016/j.bbamcr.2013.01.019.

Haeberlein, S., Aisen, P.S., Barkhof, F., Chalkias, S., Chen, T., Cohen, S., Dent, G., Hansson, O., Harrison, K., von Hehn, C., Iwatsubo, T., Mallinckrodt, C., Mummery, C.J., Muralidharan, K.K., Nestorov, I., Nisenbaum, L., Rajagovindan, R., Skordos, L., Tian, Y., van Dyck, C.H., Vellas, B., Wu, S., Zhu, Y., and Sandrock, A. 2022. Two randomized phase 3 studies of aducanumab in early Alzheimer's disease. J. Prev. Alzheimers Dis. **9**(2): 197–210. doi:10.14283/jpad.2022.30.

Hagan, P., Poole, S., Bristow, A.F., Tilders, F., and Silverstein, F.S. 1996. Intracerebral NMDA injection stimulates production of interleukin-1 beta in perinatal rat brain. J. Neurochem. **67**(5): 2215–2218. doi:10.1046/j.1471-4159.1996.67052215.x.

Hammang, J.P., Baetge, E.E., Behringer, R.R., Brinster, R.L., Palmiter, R.D., and Messing, A. 1990. Immortalized retinal neurons derived from SV40 T-antigen-induced tumors in transgenic mice. Neuron **4**(5): 775–782. doi:10.1016/0896-6273(90)90204-s.

Hammond, T.R., Dufort, C., Dissing-Olesen, L., Giera, S., Young, A., Wysoker, A., Walker, A.J., Gergits, F., Segel, M., Nemesh, J., Marsh, S.E., Saunders, A., Macosko, E., Ginhoux, F., Chen, J., Franklin, R.J.M., Piao, X., McCarroll, S.A., and Stevens, B. 2019. Single-Cell RNA sequencing of microglia throughout the mouse lifespan and in the injured brain reveals complex cell-state changes. immunity **50**(1): 253-271.e6. doi:10.1016/j.immuni.2018.11.004.

Han, J., Fan, Y., Zhou, K., Blomgren, K., and Harris, R.A. 2021. Uncovering sex differences of rodent microglia. J. Neuroinflammation **18**(1): 74. doi:10.1186/s12974-021-02124-z.

Han, S., Thatte, J., Buzard, D.J., and Jones, R.M. 2013. Therapeutic utility of cannabinoid receptor type 2 (CB_2) selective agonists. J. Med. Chem. **56**(21): 8224–8256. American Chemical Society. doi:10.1021/jm4005626.

Hanus, L., Breuer, A., Tchilibon, S., Shiloah, S., Goldenberg, D., Horowitz, M., Pertwee, R.G., Ross, R.A., Mechoulam, R., and Fride, E. 1999. HU-308: a specific agonist for CB_2, a peripheral cannabinoid receptor. Proc. Natl. Acad. Sci. U. S. A. **96**(25): 14228–14233. doi:10.1073/pnas.96.25.14228.

Harris, K.L., Kuan, W.-L., Mason, S.L., and Barker, R.A. 2020. Antidopaminergic treatment is associated with reduced chorea and irritability but impaired cognition in Huntington's disease (Enroll-HD). J. Neurol. Neurosurg. Psychiatry **91**(6): 622–630. doi:10.1136/jnnp-2019-322038.

Harrison, D.E., Strong, R., Sharp, Z.D., Nelson, J.F., Astle, C.M., Flurkey, K., Nadon, N.L., Wilkinson, J.E., Frenkel, K., Carter, C.S., Pahor, M., Javors, M.A., Fernandez, E., and Miller, R.A. 2009. Rapamycin fed late in life extends lifespan in genetically heterogeneous mice. Nature **460**(7253): 392–395. doi:10.1038/nature08221.

Haruwaka, K., Ikegami, A., Tachibana, Y., Ohno, N., Konishi, H., Hashimoto, A., Matsumoto, M., Kato, D., Ono, R., Kiyama, H., Moorhouse, A.J., Nabekura, J., and Wake, H. 2019. Dual microglia effects on blood brain barrier permeability induced by systemic inflammation. Nat. Commun. **10**(1): 5816. doi:10.1038/s41467-019-13812-z.

Hauber, W. 1998. Involvement of basal ganglia transmitter systems in movement initiation. Prog. Neurobiol. **56**(5): 507–540. doi:10.1016/s0301-0082(98)00041-0.

Häusler, K.G., Prinz, M., Nolte, C., Weber, J.R., Schumann, R.R., Kettenmann, H., and Hanisch, U.-K. 2002. Interferon-γ differentially modulates the release of cytokines and chemokines in lipopolysaccharide- and pneumococcal cell wall-stimulated mouse microglia and macrophages. Eur. J. Neurosci. **16**(11): 2113–2122. doi:10.1046/j.1460-9568.2002.02287.x.

Hayes, M.P., Freeman, S.L., and Donnelly, R.P. 1995. IFN-gamma priming of monocytes enhances LPS-induced TNF production by augmenting both transcription and mRNA stability. Cytokine **7**(5): 427–435. doi:10.1006/cyto.1995.0058.

He, P., Liu, Q., Wu, J., and Shen, Y. 2012. Genetic deletion of TNF receptor suppresses excitatory synaptic transmission via reducing AMPA receptor synaptic localization in cortical neurons. FASEB J. **26**(1): 334–345. doi:10.1096/fj.11-192716.

He, X.-H., Zang, Y., Chen, X., Pang, R.-P., Xu, J.-T., Zhou, X., Wei, X.-H., Li, Y.-Y., Xin, W.-J., Qin, Z.-H., and Liu, X.-G. 2010. TNF-α contributes to up-regulation of Nav1.3 and Nav1.8 in DRG neurons following motor fiber injury. Pain **151**(2): 266–279. doi:10.1016/j.pain.2010.06.005.

Heifets, B.D., and Castillo, P.E. 2009. Endocannabinoid signaling and long-term synaptic plasticity. Annu. Rev. Physiol. **71**: 283–306. doi:10.1146/annurev.physiol.010908.163149.

Held, T.K., Weihua, X., Yuan, L., Kalvakolanu, D.V., and Cross, A.S. 1999. Gamma interferon augments macrophage activation by lipopolysaccharide by two distinct mechanisms, at the signal transduction level and via an autocrine mechanism involving tumor necrosis factor alpha and interleukin-1. Infect. Immun. **67**(1): 206–212. doi:10.1128/IAI.67.1.206-212.1999.

Hernangómez, M., Mestre, L., Correa, F.G., Loría, F., Mecha, M., Iñigo, P.M., Docagne, F., Williams, R.O., Borrell, J., and Guaza, C. 2012. CD200-CD200R1 interaction contributes to neuroprotective effects of anandamide on experimentally induced inflammation. Glia **60**(9): 1437–1450. doi:10.1002/glia.22366.

Hickman, S., Izzy, S., Sen, P., Morsett, L., and El Khoury, J. 2018. Microglia in neurodegeneration. Nat. Neurosci. **21**(10): 1359–1369. doi:10.1038/s41593-018-0242-x.

Hillard, C.J., Manna, S., Greenberg, M.J., DiCamelli, R., Ross, R.A., Stevenson, L.A., Murphy, V., Pertwee, R.G., and Campbell, W.B. 1999. Synthesis and characterization of potent and selective agonists of the neuronal cannabinoid receptor (CB_1). J. Pharmacol. Exp. Ther. **289**(3): 1427–1433.

Hoeffel, G., and Ginhoux, F. 2015. Ontogeny of tissue-resident macrophages. Front. Immunol. **6**. Frontiers. doi:10.3389/fimmu.2015.00486.

Hoek, R.M., Ruuls, S.R., Murphy, C.A., Wright, G.J., Goddard, R., Zurawski, S.M., Blom, B., Homola, M.E., Streit, W.J., Brown, M.H., Barclay, A.N., and Sedgwick, J.D. 2000. Down-regulation of the macrophage lineage through interaction with OX2 (CD200). Science **290**(5497): 1768–1771. doi:10.1126/science.290.5497.1768.

Holler, N., Zaru, R., Micheau, O., Thome, M., Attinger, A., Valitutti, S., Bodmer, J.-L., Schneider, P., Seed, B., and Tschopp, J. 2000. Fas triggers an alternative, caspase-8–independent cell death pathway using the kinase RIP as effector molecule. Nat. Immunol. **1**(6): 489–495. doi:10.1038/82732.

Holmes, C., Cunningham, C., Zotova, E., Woolford, J., Dean, C., Kerr, S., Culliford, D., and Perry, V.H. 2009. Systemic inflammation and disease progression in Alzheimer disease. Neurology **73**(10): 768–774. doi:10.1212/WNL.0b013e3181b6bb95.

Hong, S., Beja-Glasser, V.F., Nfonoyim, B.M., Frouin, A., Li, S., Ramakrishnan, S., Merry, K.M., Shi, Q., Rosenthal, A., Barres, B.A., Lemere, C.A., Selkoe, D.J., and Stevens, B. 2016. Complement and microglia mediate early synapse loss in Alzheimer mouse models. Science **352**(6286): 712–716. doi:10.1126/science.aad8373.

Honig, L.S., Vellas, B., Woodward, M., Boada, M., Bullock, R., Borrie, M., Hager, K., Andreasen, N., Scarpini, E., Liu-Seifert, H., Case, M., Dean, R.A., Hake, A., Sundell, K., Poole Hoffmann, V., Carlson, C., Khanna, R., Mintun, M., DeMattos, R., Selzler, K.J., and Siemers, E. 2018. Trial of solanezumab for mild dementia due to Alzheimer's disease. N. Engl. J. Med. **378**(4): 321–330. doi:10.1056/NEJMoa1705971.

Hoogland, I.C.M., Houbolt, C., van Westerloo, D.J., van Gool, W.A., and van de Beek, D. 2015. Systemic inflammation and microglial activation: systematic review of animal experiments. J. Neuroinflammation **12**: 114. doi:10.1186/s12974-015-0332-6.

Horvath, R.J., Nutile-McMenemy, N., Alkaitis, M.S., and De Leo, J.A. 2008. Differential migration, LPS-induced cytokine, chemokine and NO expression in immortalized BV-2 and HAPI cell lines and primary microglial cultures. J. Neurochem. **107**(2): 557–569. doi:10.1111/j.1471-4159.2008.05633.x.

Hou, Y., Dan, X., Babbar, M., Wei, Y., Hasselbalch, S.G., Croteau, D.L., and Bohr, V.A. 2019. Ageing as a risk factor for neurodegenerative disease. Nat. Rev. Neurol. **15**(10): 565–581. doi:10.1038/s41582-019-0244-7.

Howlett, A.C. 2002. The cannabinoid receptors. Prostaglandins Other Lipid Mediat. **68–69**: 619–631. doi:10.1016/S0090-6980(02)00060-6.

Howlett, A.C., Barth, F., Bonner, T.I., Cabral, G., Casellas, P., Devane, W.A., Felder, C.C., Herkenham, M., Mackie, K., Martin, B.R., Mechoulam, R., and Pertwee, R.G. 2002. International Union of Pharmacology. XXVII. Classification of Cannabinoid Receptors. Pharmacol. Rev. **54**(2): 161–202.

Hsiao, H.-Y., Chiu, F.-L., Chen, C.-M., Wu, Y.-R., Chen, H.-M., Chen, Y.-C., Kuo, H.-C., and Chern, Y. 2014. Inhibition of soluble tumor necrosis factor is therapeutic in Huntington's disease. Hum. Mol. Genet. **23**(16): 4328–4344. doi:10.1093/hmg/ddu151.

Hu, S., Peterson, P.K., and Chao, C.C. 1997. Cytokine-mediated neuronal apoptosis. Neurochem. Int. **30**(4–5): 427–431. doi:10.1016/s0197-0186(96)00078-2.

Huang, L., Pu, J., He, F., Liao, B., Hao, B., Hong, W., Ye, X., Chen, J., Zhao, J., Liu, S., Xu, J., Li, B., and Ran, P. 2017. Positive feedback of the amphiregulin-EGFR-ERK pathway mediates PM2.5 from wood smoke-induced MUC5AC expression in epithelial cells. Sci. Rep. **7**: 11084. doi:10.1038/s41598-017-11541-1.

Hughes, C., Choi, M.L., Yi, J.-H., Kim, S.-C., Drews, A., George-Hyslop, P.St., Bryant, C., Gandhi, S., Cho, K., and Klenerman, D. 2020. Beta amyloid aggregates induce sensitised TLR4 signalling causing long-term potentiation deficit and rat neuronal cell death. Commun. Biol. **3**: 79. doi:10.1038/s42003-020-0792-9.

Hussain, S., Johnson, C.G., Sciurba, J., Meng, X., Stober, V.P., Liu, C., Cyphert-Daly, J.M., Bulek, K., Qian, W., Solis, A., Sakamachi, Y., Trempus, C.S., Aloor, J.J., Gowdy, K.M., Foster, W.M., Hollingsworth, J.W., Tighe, R.M., Li, X., Fessler, M.B., and Garantziotis, S. 2020. TLR5 participates in the TLR4 receptor complex and promotes MyD88-dependent signaling in environmental lung injury. eLife **9**: e50458. eLife Sciences Publications, Ltd. doi:10.7554/eLife.50458.

Hutchinson, M.R., Northcutt, A.L., Hiranita, T., Wang, X., Lewis, S.S., Thomas, J., van Steeg, K., Kopajtic, T.A., Loram, L.C., Sfregola, C., Galer, E., Miles, N.E., Bland, S.T., Amat, J., Rozeske, R.R., Maslanik, T., Chapman, T.R., Strand, K.A., Fleshner, M., Bachtell, R.K., Somogyi, A.A., Yin, H., Katz, J.L., Rice, K.C., Maier, S.F., and Watkins, L.R. 2012. Opioid activation of toll-like receptor 4 contributes to drug reinforcement. J. Neurosci. **32**(33): 11187–11200. doi:10.1523/JNEUROSCI.0684-12.2012.

Imamura, K., Hishikawa, N., Sawada, M., Nagatsu, T., Yoshida, M., and Hashizume, Y. 2003. Distribution of major histocompatibility complex class II-positive microglia and cytokine profile of Parkinson's disease brains. Acta Neuropathol. **106**(6): 518–526. doi:10.1007/s00401-003-0766-2.

Imeri, L., and Opp, M.R. 2009. How (and why) the immune system makes us sleep. Nat. Rev. Neurosci. **10**(3): 199–210. doi:10.1038/nrn2576.

Jafari, M., Schumacher, A.-M., Snaidero, N., Ullrich Gavilanes, E.M., Neziraj, T., Kocsis-Jutka, V., Engels, D., Jürgens, T., Wagner, I., Weidinger, J.D.F., Schmidt, S.S., Beltrán, E., Hagan, N., Woodworth, L., Ofengeim, D., Gans, J., Wolf, F., Kreutzfeldt, M., Portugues, R., Merkler, D., Misgeld, T., and Kerschensteiner, M. 2021. Phagocyte-mediated synapse removal in cortical neuroinflammation is promoted by local calcium accumulation. Nat. Neurosci. **24**(3): 355–367. doi:10.1038/s41593-020-00780-7.

Jain, M., Singh, M.K., Shyam, H., Mishra, A., Kumar, S., Kumar, A., and Kushwaha, J. 2021. Role of JAK/STAT in the neuroinflammation and its association with neurological disorders. Ann. Neurosci. **28**(3–4): 191–200. doi:10.1177/09727531211070532.

Jakel, R.J., and Maragos, W.F. 2000. Neuronal cell death in Huntington's disease: a potential role for dopamine. Trends Neurosci. **23**(6): 239–245. doi:10.1016/s0166-2236(00)01568-x.

Janefjord, E., Mååg, J.L.V., Harvey, B.S., and Smid, S.D. 2014. Cannabinoid effects on β amyloid fibril and aggregate formation, neuronal and microglial-activated neurotoxicity *in vitro*. Cell. Mol. Neurobiol. **34**(1): 31–42. doi:10.1007/s10571-013-9984-x.

Jang, Y., Lee, W.-J., Lee, H.S., Chu, K., Lee, S.K., and Lee, S.-T. 2021. Tofacitinib treatment in refractory autoimmune encephalitis (2482). Neurology **96**(15 Supplement).

Jara, J.H., Singh, B.B., Floden, A.M., and Combs, C.K. 2007. Tumor necrosis factor alpha stimulates NMDA receptor activity in mouse cortical neurons resulting in ERK-dependent death. J. Neurochem. **100**(5): 1407–1420. doi:10.1111/j.1471-4159.2006.04330.x.

Jaturapatporn, D., Isaac, M.G.E.K.N., McCleery, J., and Tabet, N. 2012. Aspirin, steroidal and non-steroidal anti-inflammatory drugs for the treatment of Alzheimer's disease. Cochrane Database Syst. Rev. (2): CD006378. doi:10.1002/14651858.CD006378.pub2.

Javed, H., Azimullah, S., Haque, M.E., and Ojha, S.K. 2016. Cannabinoid type 2 (CB_2) receptors activation protects against oxidative stress and neuroinflammation associated dopaminergic neurodegeneration in rotenone model of Parkinson's Disease. Front. Neurosci. **10**: 321. doi:10.3389/fnins.2016.00321.

Jayaraman, A., Htike, T.T., James, R., Picon, C., and Reynolds, R. 2021. TNF-mediated neuroinflammation is linked to neuronal necroptosis in Alzheimer's disease hippocampus. Acta Neuropathol. Commun. **9**(1): 159. doi:10.1186/s40478-021-01264-w.

Jensen, P., Myhre, C.L., Lassen, P.S., Metaxas, A., Khan, A.M., Lambertsen, K.L., Babcock, A.A., Finsen, B., Larsen, M.R., and Kempf, S.J. 2017. TNFα affects CREB-mediated neuroprotective signaling pathways of synaptic plasticity in neurons as revealed by proteomics and phospho-proteomics. Oncotarget **8**(36): 60223–60242. doi:10.18632/oncotarget.19428.

Jin, Y., Kang, Y., Wang, M., Wu, B., Su, B., Yin, H., Tang, Y., Li, Q., Wei, W., Mei, Q., Hu, G., Lukacs-Kornek, V., Li, J., Wu, K., Yuan, X., and Wang, W. 2022. Targeting polarized phenotype of microglia via IL6/JAK2/STAT3 signaling to reduce NSCLC brain metastasis. Signal Transduct. Target. Ther. **7**: 52. doi:10.1038/s41392-022-00872-9.

Jones, R.S., Minogue, A.M., Fitzpatrick, O., and Lynch, M.A. 2015. Inhibition of JAK2 attenuates the increase in inflammatory markers in microglia from APP/PS1 mice. Neurobiol. Aging **36**(10): 2716–2724. doi:10.1016/j.neurobiolaging.2015.04.018.

Jordan, C.J., and Xi, Z.-X. 2019. Progress in brain cannabinoid CB_2 receptor research: from genes to behavior. Neurosci. Biobehav. Rev. **98**: 208–220. doi:10.1016/j.neubiorev.2018.12.026.

Kamal, H., Tan, G.C., Ibrahim, S.F., Shaikh, Mohd.F., Mohamed, I.N., Mohamed, R.M.P., Hamid, A.A., Ugusman, A., and Kumar, J. 2020. Alcohol use disorder, neurodegeneration, Alzheimer's and Parkinson's Disease: Interplay between oxidative stress, neuroimmune response and excitotoxicity. Front. Cell. Neurosci. **14**: 282. doi:10.3389/fncel.2020.00282.

Kang, J.-B., Park, D.-J., Shah, M.-A., Kim, M.-O., and Koh, P.-O. 2019. Lipopolysaccharide induces neuroglia activation and NF-κB activation in cerebral cortex of adult mice. Lab. Anim. Res. **35**(1): 19. doi:10.1186/s42826-019-0018-9.

Karki, R., Sharma, B.R., Tuladhar, S., Williams, E.P., Zalduondo, L., Samir, P., Zheng, M., Sundaram, B., Banoth, B., Malireddi, R.K.S., Schreiner, P., Neale, G., Vogel, P., Webby, R., Jonsson, C.B., and Kanneganti, T.-D. 2021. Synergism of TNF-α and IFN-γ triggers inflammatory cell death, tissue damage, and mortality in SARS-CoV-2 infection and cytokine shock syndromes. Cell **184**(1): 149-168.e17. doi:10.1016/j.cell.2020.11.025.

Kasahara, T., Hooks, J.J., Dougherty, S.F., and Oppenheim, J.J. 1983. Interleukin 2-mediated immune interferon (IFN-gamma) production by human T cells and T cell subsets. J. Immunol. Baltim. Md 1950 **130**(4): 1784–1789.

Katze, M.G., He, Y., and Gale, M. 2002. Viruses and interferon: a fight for supremacy. Nat. Rev. Immunol. **2**(9): 675–687. doi:10.1038/nri888.

Kaya, T., Mattugini, N., Liu, L., Ji, H., Cantuti-Castelvetri, L., Wu, J., Schifferer, M., Groh, J., Martini, R., Besson-Girard, S., Kaji, S., Liesz, A., Gokce, O., and Simons, M. 2022. CD8+ T cells induce interferon-responsive oligodendrocytes and microglia in white matter aging. Nat. Neurosci. **25**(11): 1446–1457. doi:10.1038/s41593-022-01183-6.

Kell, D., and Pretorius, E. 2015. On the translocation of bacteria and their lipopolysaccharides between blood and peripheral locations in chronic, inflammatory diseases: the central roles of LPS and LPS-induced cell death. Integr. Biol. **7**(11): 1339–1377. doi:10.1039/C5IB00158G.

Kenakin, T. 2007. Allosteric agonist modulators. J. Recept. Signal Transduct. Res. **27**(4): 247–259. doi:10.1080/10799890701509000.

Keren-Shaul, H., Spinrad, A., Weiner, A., Matcovitch-Natan, O., Dvir-Szternfeld, R., Ulland, T.K., David, E., Baruch, K., Lara-Astaiso, D., Toth, B., Itzkovitz, S., Colonna, M., Schwartz, M., and Amit, I. 2017. A unique microglia type associated with restricting development of Alzheimer's disease. Cell **169**(7): 1276-1290.e17. doi:10.1016/j.cell.2017.05.018.

Kern, D.M., Lovestone, S., and Cepeda, M.S. 2021. Treatment with TNF-α inhibitors versus methotrexate and the association with dementia and Alzheimer's disease. Alzheimers Dement. Transl. Res. Clin. Interv. **7**(1): e12163. doi:10.1002/trc2.12163.

Kettenmann, H., Hanisch, U.-K., Noda, M., and Verkhratsky, A. 2011. Physiology of microglia. Physiol. Rev. **91**(2): 461–553. doi:10.1152/physrev.00011.2010.

Keum, J.W., Shin, A., Gillis, T., Mysore, J.S., Abu Elneel, K., Lucente, D., Hadzi, T., Holmans, P., Jones, L., Orth, M., Kwak, S., MacDonald, M.E., Gusella, J.F., and Lee, J.-M. 2016. The HTT CAG-expansion mutation determines age at death but not disease duration in Huntington disease. Am. J. Hum. Genet. **98**(2): 287–298. doi:10.1016/j.ajhg.2015.12.018.

Khatchadourian, A., Bourque, S.D., Richard, V.R., Titorenko, V.I., and Maysinger, D. 2012. Dynamics and regulation of lipid droplet formation in lipopolysaccharide (LPS)-stimulated microglia. Biochim. Biophys. Acta BBA - Mol. Cell Biol. Lipids **1821**(4): 607–617. doi:10.1016/j.bbalip.2012.01.007.

Kim, A., García-García, E., Straccia, M., Comella-Bolla, A., Miguez, A., Masana, M., Alberch, J., Canals, J.M., and Rodríguez, M.J. 2020. Reduced fractalkine levels lead to striatal synaptic plasticity deficits in Huntington's disease. Front. Cell. Neurosci. **14**.

Kim, D.H., Choi, S.-M., Jho, J., Park, M.-S., Kang, J., Park, S.J., Ryu, J.H., Jo, J., Kim, H.H., and Kim, B.C. 2016. Infliximab ameliorates AD-associated object recognition memory impairment. Behav. Brain Res. **311**: 384–391. doi:10.1016/j.bbr.2016.06.001.

Kim, J., Kundu, M., Viollet, B., and Guan, K.-L. 2011. AMPK and mTOR regulate autophagy through direct phosphorylation of Ulk1. Nat. Cell Biol. **13**(2): 132–141. doi:10.1038/ncb2152.

Kim, S.H., Smith, C.J., and Van Eldik, L.J. 2004. Importance of MAPK pathways for microglial pro-inflammatory cytokine IL-1 beta production. Neurobiol. Aging **25**(4): 431–439. doi:10.1016/S0197-4580(03)00126-X.

Kim, Y., Zheng, X., Ansari, Z., Bunnell, M.C., Herdy, J.R., Traxler, L., Lee, H., Paquola, A.C.M., Blithikioti, C., Ku, M., Schlachetzki, J.C.M., Winkler, J., Edenhofer, F., Glass, C.K., Paucar, A.A., Jaeger, B.N., Pham, S., Boyer, L., Campbell, B.C., Hunter, T., Mertens, J., and Gage, F.H. 2018. Mitochondrial aging defects emerge in directly reprogrammed human neurons due to their metabolic profile. Cell Rep. **23**(9): 2550–2558. doi:10.1016/j.celrep.2018.04.105.

Kimura, A., Naka, T., Muta, T., Takeuchi, O., Akira, S., Kawase, I., and Kishimoto, T. 2005. Suppressor of cytokine signaling-1 selectively inhibits LPS-induced IL-6 production by regulating JAK–STAT. Proc. Natl. Acad. Sci. **102**(47): 17089–17094. doi:10.1073/pnas.0508517102.

Klawonn, A.M., Fritz, M., Castany, S., Pignatelli, M., Canal, C., Similä, F., Tejeda, H.A., Levinsson, J., Jaarola, M., Jakobsson, J., Hidalgo, J., Heilig, M., Bonci, A., and Engblom, D. 2021. Microglial activation elicits a negative affective state through prostaglandin-mediated modulation of striatal neurons. Immunity **54**(2): 225-234.e6. doi:10.1016/j.immuni.2020.12.016.

Kleine-Brueggeney, M., Greif, R., Brenneisen, R., Urwyler, N., Stueber, F., and Theiler, L.G. 2015. Intravenous delta-9-tetrahydrocannabinol to prevent postoperative nausea and vomiting: A randomized controlled trial. Anesth. Analg. **121**(5): 1157–1164. doi:10.1213/ANE.0000000000000877.

Knopman, D.S., Jones, D.T., and Greicius, M.D. 2021. Failure to demonstrate efficacy of aducanumab: An analysis of the EMERGE and ENGAGE trials as reported by Biogen, December 2019. Alzheimers Dement. **17**(4): 696–701. doi:10.1002/alz.12213.

Kodama, S., Davis, M., and Faustman, D.L. 2005. The therapeutic potential of tumor necrosis factor for autoimmune disease: a mechanistically based hypothesis. Cell. Mol. Life Sci. CMLS **62**(16): 1850–1862. doi:10.1007/s00018-005-5022-6.

Koizumi, S., Shigemoto-Mogami, Y., Nasu-Tada, K., Shinozaki, Y., Ohsawa, K., Tsuda, M., Joshi, B.V., Jacobson, K.A., Kohsaka, S., and Inoue, K. 2007. UDP acting at P2Y6 receptors is a mediator of microglial phagocytosis. Nature **446**(7139): 1091–1095. doi:10.1038/nature05704.

Kolosova, N.G., Tyumentsev, M.A., Muraleva, N.A., Kiseleva, E., Vitovtov, A.O., and Stefanova, N.A. 2017. Antioxidant SkQ1 alleviates signs of Alzheimer's disease-like pathology in old OXYS rats by reversing mitochondrial deterioration. Curr. Alzheimer Res. **14**(12): 1283–1292. doi:10.2174/1567205014666170621111033.

Komorowska-Müller, J.A., and Schmöle, A.-C. 2020. CB_2 receptor in microglia: The guardian of self-control. Int. J. Mol. Sci. **22**(1): 19. doi:10.3390/ijms22010019.

Koshiba, T., Detmer, S.A., Kaiser, J.T., Chen, H., McCaffery, J.M., and Chan, D.C. 2004. Structural basis of mitochondrial tethering by mitofusin complexes. Science **305**(5685): 858–862. doi:10.1126/science.1099793.

Koyama, A., O'Brien, J., Weuve, J., Blacker, D., Metti, A.L., and Yaffe, K. 2013. The role of peripheral inflammatory markers in dementia and Alzheimer's disease: A meta-analysis. J. Gerontol. A. Biol. Sci. Med. Sci. **68**(4): 433–440. doi:10.1093/gerona/gls187.

Krasnow, S.M., Knoll, J.G., Verghese, S.C., Levasseur, P.R., and Marks, D.L. 2017. Amplification and propagation of interleukin-1β signaling by murine brain endothelial and glial cells. J. Neuroinflammation **14**(1): 133. doi:10.1186/s12974-017-0908-4.

Kreutzberg, G.W. 1996. Microglia: a sensor for pathological events in the CNS. Trends Neurosci. **19**(8): 312–318. doi:10.1016/0166-2236(96)10049-7.

Kristian, T., Balan, I., Schuh, R., and Onken, M. 2011. Mitochondrial dysfunction and nicotinamide dinucleotide catabolism as mechanisms of cell death and promising targets for neuroprotection. J. Neurosci. Res. **89**(12): 1946–1955. doi:10.1002/jnr.22626.

Krstic, D., Madhusudan, A., Doehner, J., Vogel, P., Notter, T., Imhof, C., Manalastas, A., Hilfiker, M., Pfister, S., Schwerdel, C., Riether, C., Meyer, U., and Knuesel, I. 2012. Systemic immune challenges trigger and drive Alzheimer-like neuropathology in mice. J. Neuroinflammation **9**(1): 151. doi:10.1186/1742-2094-9-151.

Kumar, R. 2020. Understanding and managing acute encephalitis. F1000Research **9**: F1000. doi:10.12688/f1000research.20634.1.

Kumar, R., Claassen, D., Mongan, A., Hoehn, B., Lin, P., Cahir-Mcfarland, E., Guo, C., Volman, V., Taylor, L., Chandra, P., Yednock, T., and Kroon, H.-A. 2023. A phase 2 open-label study to assess the safety, tolerability, pharmacokinetics, and pharmacodynamics of intravenous ANX005 in patients with, or at risk of, manifest Huntington's disease (HD) (S32.009). Neurology **100**(17 Supplement 2). Wolters Kluwer Health, Inc. on behalf of the American Academy of Neurology. doi:10.1212/WNL.0000000000203217.

Kusakabe, K., Iso, Y., Tada, Y., Sakagami, M., Morioka, Y., Chomei, N., Shinonome, S., Kawamoto, K., Takenaka, H., Yasui, K., Hamana, H., and Hanasaki, K. 2013. Selective CB_2 agonists with anti-pruritic activity: discovery of potent and orally available bicyclic 2-pyridones. Bioorg. Med. Chem. **21**(11): 3154–3163. doi:10.1016/j.bmc.2013.03.030.

Lajqi, T., Lang, G.-P., Haas, F., Williams, D.L., Hudalla, H., Bauer, M., Groth, M., Wetzker, R., and Bauer, R. 2019. Memory-like inflammatory responses of microglia to rising doses of LPS: Key role of PI3Kγ. Front. Immunol. **10**.

Lajqi, T., Stojiljkovic, M., Williams, D.L., Hudalla, H., Bauer, M., Witte, O.W., Wetzker, R., Bauer, R., and Schmeer, C. 2020. Memory-like responses of brain microglia are controlled by developmental state and pathogen dose. Front. Immunol. **11**: 546415. doi:10.3389/fimmu.2020.546415.

Lambertsen, K.L., Meldgaard, M., Ladeby, R., and Finsen, B. 2005. A quantitative study of microglial-macrophage synthesis of tumor necrosis factor during acute and late focal cerebral ischemia in mice. J. Cereb. Blood Flow Metab. Off. J. Int. Soc. Cereb. Blood Flow Metab. **25**(1): 119–135. doi:10.1038/sj.jcbfm.9600014.

Lamigeon, C., Bellier, J.P., Sacchettoni, S., Rujano, M., and Jacquemont, B. 2001. Enhanced neuronal protection from oxidative stress by coculture with glutamic acid decarboxylase-expressing astrocytes. J. Neurochem. **77**(2): 598–606. doi:10.1046/j.1471-4159.2001.00278.x.

Lanciego, J.L., Barroso-Chinea, P., Rico, A.J., Conte-Perales, L., Callén, L., Roda, E., Gómez-Bautista, V., López, I.P., Lluis, C., Labandeira-García, J.L., and Franco, R. 2011. Expression of the mRNA coding the cannabinoid receptor 2 in the pallidal complex of Macaca fascicularis. J. Psychopharmacol. **25**(1): 97–104. doi:10.1177/0269881110367732.

van Langevelde, P., Kwappenberg, K.M.C., Groeneveld, P.H.P., Mattie, H., and van Dissel, J.T. 1998. Antibiotic-induced lipopolysaccharide (LPS) release from *Salmonella typhi*: Delay between killing by ceftazidime and imipenem and release of LPS. Antimicrob. Agents Chemother. **42**(4): 739–743.

Laprairie, R.B., Bagher, A.M., Rourke, J.L., Zrein, A., Cairns, E.A., Kelly, M.E.M., Sinal, C.J., Kulkarni, P.M., Thakur, G.A., and Denovan-Wright, E.M. 2019. Positive allosteric modulation of the type 1 cannabinoid receptor reduces the signs and symptoms of Huntington's disease in the R6/2 mouse model. Neuropharmacology **151**: 1–12. doi:10.1016/j.neuropharm.2019.03.033.

Laprairie, R.B., Kelly, M.E.M., and Denovan-Wright, E.M. 2013. Cannabinoids increase type 1 cannabinoid receptor expression in a cell culture model of striatal neurons: Implications for Huntington's disease. Neuropharmacology **72**: 47–57. doi:10.1016/j.neuropharm.2013.04.006.

Lashgari, N.-A., Roudsari, N.M., Momtaz, S., Sathyapalan, T., Abdolghaffari, A.H., and Sahebkar, A. 2021. The involvement of JAK/STAT signaling pathway in the treatment of Parkinson's disease. J. Neuroimmunol. **361**: 577758. doi:10.1016/j.jneuroim.2021.577758.

Lawson, L.J., Perry, V.H., and Gordon, S. 1992. Turnover of resident microglia in the normal adult mouse brain. Neuroscience **48**(2): 405–415. doi:10.1016/0306-4522(92)90500-2.

Lehnardt, S. 2010. Innate immunity and neuroinflammation in the CNS: The role of microglia in Toll-like receptor-mediated neuronal injury. Glia **58**(3): 253–263. doi:10.1002/glia.20928.

Lei, H., Crawford, M.S., and McCole, D.F. 2021. JAK-STAT pathway regulation of intestinal permeability: Pathogenic roles and therapeutic opportunities in inflammatory bowel disease. Pharmaceuticals **14**(9): 840. doi:10.3390/ph14090840.

Leicht, H., König, H.-H., Stuhldreher, N., Bachmann, C., Bickel, H., Fuchs, A., Heser, K., Jessen, F., Köhler, M., Luppa, M., Mösch, E., Pentzek, M., Riedel-Heller, S., Scherer, M., Werle, J., Weyerer, S., Wiese, B., Maier, W., and Group, for the A. study. 2013. Predictors of costs in dementia in a longitudinal perspective. PLOS ONE **8**(7): e70018. doi:10.1371/journal.pone.0070018.

LePage, K.T., Dickey, R.W., Gerwick, W.H., Jester, E.L., and Murray, T.F. 2005. On the use of neuro-2a neuroblastoma cells versus intact neurons in primary culture for neurotoxicity studies. Crit. Rev. Neurobiol. **17**(1): 27–50. doi:10.1615/critrevneurobiol.v17.i1.20.

Leweke, F.M. 2012. Anandamide dysfunction in prodromal and established psychosis. Curr. Pharm. Des. **18**(32): 5188–5193. doi:10.2174/138161212802884843.

Lewis, A.J., Seymour, C.W., and Rosengart, M.R. 2016. Current murine models of sepsis. Surg. Infect. **17**(4): 385–393. doi:10.1089/sur.2016.021.

Li, B., Vincent, A., Cates, J., Brantley-Sieders, D.M., Polk, D.B., and Young, P.P. 2009. Low levels of tumor necrosis factor alpha increase tumor growth by inducing an endothelial phenotype of monocytes recruited to the tumor site. Cancer Res. **69**(1): 338–348. doi:10.1158/0008-5472.CAN-08-1565.

Li, C., Shi, J., Wang, B., Li, J., and Jia, H. 2019a. CB_2 cannabinoid receptor agonist ameliorates novel object recognition but not spatial memory in transgenic APP/PS1 mice. Neurosci. Lett. **707**: 134286. doi:10.1016/j.neulet.2019.134286.

Li, H., Chen, C., Dou, Y., Wu, H., Liu, Y., Lou, H.-F., Zhang, J., Li, X., Wang, H., and Duan, S. 2013. $P2Y_4$ receptor-mediated pinocytosis contributes to amyloid beta-induced self-uptake by microglia. Mol. Cell. Biol. **33**(21): 4282–4293. doi:10.1128/MCB.00544-13.

Li, J., Lin, S., Vanhoutte, P.M., Woo, C.W., and Xu, A. 2016. *Akkermansia muciniphila* protects against atherosclerosis by preventing metabolic endotoxemia-induced inflammation in Apoe−/− mice. Circulation **133**(24): 2434–2446. doi:10.1161/CIRCULATIONAHA.115.019645.

Li, M., Zhang, D., Ge, X., Zhu, X., Zhou, Y., Zhang, Y., Peng, X., and Shen, A. 2019b. TRAF6-p38/JNK-ATF2 axis promotes microglial inflammatory activation. Exp. Cell Res. **376**(2): 133–148. doi:10.1016/j.yexcr.2019.02.005.

Li, X., Feng, X., Sun, X., Hou, N., Han, F., and Liu, Y. 2022. Global, regional, and national burden of Alzheimer's disease and other dementias, 1990–2019. Front. Aging Neurosci. **14**.

Li, Y., Yin, L., Fan, Z., Su, B., Chen, Y., Ma, Y., Zhong, Y., Hou, W., Fang, Z., and Zhang, X. 2020. Microglia: A potential therapeutic target for sepsis-associated encephalopathy and sepsis-associated chronic pain. Front. Pharmacol. **11**: 1923. doi:10.3389/fphar.2020.600421.

Liang, J., Shao, S.H., Xu, Z.-X., Hennessy, B., Ding, Z., Larrea, M., Kondo, S., Dumont, D.J., Gutterman, J.U., Walker, C.L., Slingerland, J.M., and Mills, G.B. 2007. The energy sensing LKB1-AMPK pathway regulates p27(kip1) phosphorylation mediating the decision to enter autophagy or apoptosis. Nat. Cell Biol. **9**(2): 218–224. doi:10.1038/ncb1537.

Liddelow, S.A., Guttenplan, K.A., Clarke, L.E., Bennett, F.C., Bohlen, C.J., Schirmer, L., Bennett, M.L., Münch, A.E., Chung, W.-S., Peterson, T.C., Wilton, D.K., Frouin, A., Napier, B.A., Panicker, N., Kumar, M., Buckwalter, M.S., Rowitch, D.H., Dawson, V.L., Dawson, T.M., Stevens, B., and Barres, B.A. 2017. Neurotoxic reactive astrocytes are induced by activated microglia. Nature **541**(7638): 481–487. doi:10.1038/nature21029.

Lin, H., Lee, E., Hestir, K., Leo, C., Huang, M., Bosch, E., Halenbeck, R., Wu, G., Zhou, A., Behrens, D., Hollenbaugh, D., Linnemann, T., Qin, M., Wong, J., Chu, K., Doberstein, S.K., and Williams, L.T. 2008. Discovery of a cytokine and its receptor by functional screening of the extracellular proteome. Science **320**(5877): 807–811. doi:10.1126/science.1154370.

Liu, H., Hu, X., Jiang, R., Cai, J., Lin, Q., Fan, Z., Zhao, P., Wang, S., Zou, C., Du, W., Dong, Z., and Liu, Y. 2021. CQMUH-011 inhibits LPS-induced microglia activation and ameliorates brain ischemic injury in mice. Inflammation **44**(4): 1345–1358. doi:10.1007/s10753-021-01420-3.

Liu, J., Li, Y., Xia, X., Yang, X., Zhao, R., Peer, J., Wang, H., Tong, Z., Gao, F., Lin, H., Wu, B., Huang, Y., and Zheng, J.C. 2019. Propofol reduces microglia activation and neurotoxicity through inhibition of extracellular vesicle release. J. Neuroimmunol. **333**: 476962. doi:10.1016/j.jneuroim.2019.05.003.

Liu, Q., Qiu, J., Liang, M., Golinski, J., van Leyen, K., Jung, J.E., You, Z., Lo, E.H., Degterev, A., and Whalen, M.J. 2014. Akt and mTOR mediate programmed necrosis in neurons. Cell Death Dis. **5**(2): e1084–e1084. doi:10.1038/cddis.2014.69.

Loiola, R.A., Wickstead, E.S., Solito, E., and McArthur, S. 2019. Estrogen promotes pro-resolving microglial behavior and phagocytic cell clearance through the actions of annexin A1. Front. Endocrinol. **10**: 420. doi:10.3389/fendo.2019.00420.

Lourbopoulos, A., Grigoriadis, N., Lagoudaki, R., Touloumi, O., Polyzoidou, E., Mavromatis, I., Tascos, N., Breuer, A., Ovadia, H., Karussis, D., Shohami, E., Mechoulam, R., and Simeonidou, C. 2011. Administration of 2-arachidonoylglycerol ameliorates both acute and chronic experimental autoimmune encephalomyelitis. Brain Res. **1390**: 126–141. doi:10.1016/j.brainres.2011.03.020.

Lowe, P.P., Morel, C., Ambade, A., Iracheta-Vellve, A., Kwiatkowski, E., Satishchandran, A., Furi, I., Cho, Y., Gyongyosi, B., Catalano, D., Lefebvre, E., Fischer, L., Seyedkazemi, S., Schafer, D.P., and Szabo, G. 2020. Chronic alcohol-induced neuroinflammation involves CCR2/5-dependent peripheral macrophage infiltration and microglia alterations. J. Neuroinflammation **17**(1): 296. doi:10.1186/s12974-020-01972-5.

Lu, H.-C., and Mackie, K. 2016. An introduction to the endogenous cannabinoid system. Biol. Psychiatry **79**(7): 516–525. doi:10.1016/j.biopsych.2015.07.028.

Lu, H.-C., and Mackie, K. 2021. Review of the endocannabinoid system. Biol. Psychiatry Cogn. Neurosci. Neuroimaging **6**(6): 607–615. doi:10.1016/j.bpsc.2020.07.016.

Lu, Y.-C., Yeh, W.-C., and Ohashi, P.S. 2008. LPS/TLR4 signal transduction pathway. Cytokine **42**(2): 145–151. doi:10.1016/j.cyto.2008.01.006.

Lu, Z., Liu, S., Lopes-Virella, M.F., and Wang, Z. 2021. LPS and palmitic acid co-upregulate microglia activation and neuroinflammatory response. Compr. Psychoneuroendocrinology **6**: 100048. doi:10.1016/j.cpnec.2021.100048.

Ma, L., Jia, J., Liu, X., Bai, F., Wang, Q., and Xiong, L. 2015. Activation of murine microglial N9 cells is attenuated through cannabinoid receptor CB_2 signaling. Biochem. Biophys. Res. Commun. **458**(1): 92–97. doi:10.1016/j.bbrc.2015.01.073.

Ma, L., Niu, W., Lv, J., Jia, J., Zhu, M., and Yang, S. 2018. PGC-1α-mediated mitochondrial biogenesis is involved in cannabinoid receptor 2 agonist AM1241-induced microglial phenotype amelioration. Cell. Mol. Neurobiol. **38**(8): 1529–1537. doi:10.1007/s10571-018-0628-z.

Ma, S.-H., Li, B., Huang, H.-W., Peng, Y.-P., and Qiu, Y.-H. 2012. Interleukin-6 inhibits L-type calcium channel activity of cultured cerebellar granule neurons. J. Physiol. Sci. JPS **62**(5): 385–392. doi:10.1007/s12576-012-0215-x.

Ma, Z., Gao, F., Larsen, B., Gao, M., Luo, Z., Chen, D., Ma, X., Qiu, S., Zhou, Y., Xie, J., Xi, Z.-X., and Wu, J. 2019. Mechanisms of cannabinoid CB_2 receptor-mediated reduction of dopamine neuronal excitability in mouse ventral tegmental area. EBioMedicine **42**: 225–237. doi:10.1016/j.ebiom.2019.03.040.

MacDonald, M.E., Gines, S., Gusella, J.F., and Wheeler, V.C. 2003. Huntington's disease. Neuromolecular Med. **4**(1–2): 7–20. doi:10.1385/NMM:4:1-2:7.

Magaki, S., Mueller, C., Dickson, C., and Kirsch, W. 2007. Increased production of inflammatory cytokines in mild cognitive impairment. Exp. Gerontol. **42**(3): 233–240. doi:10.1016/j.exger.2006.09.015.

Magliozzi, R., Pezzini, F., Pucci, M., Rossi, S., Facchiano, F., Marastoni, D., Montagnana, M., Lippi, G., Reynolds, R., and Calabrese, M. 2021. Changes in cerebrospinal fluid balance of TNF and TNF receptors in naïve multiple sclerosis patients: Early involvement in compartmentalised intrathecal inflammation. Cells **10**(7): 1712. doi:10.3390/cells10071712.

Malagelada, C., Jin, Z.H., Jackson-Lewis, V., Przedborski, S., and Greene, L.A. 2010. Rapamycin protects against neuron death in in vitro and in vivo models of Parkinson's disease. J. Neurosci. **30**(3): 1166–1175. doi:10.1523/JNEUROSCI.3944-09.2010.

Malek, N., Popiolek-Barczyk, K., Mika, J., Przewlocka, B., and Starowicz, K. 2015. Anandamide, acting via CB_2 receptors, alleviates LPS-induced neuroinflammation in rat primary microglial cultures. Neural Plast. **2015**: e130639. doi:10.1155/2015/130639.

Mamuladze, T., and Kipnis, J. 2023. Type 2 immunity in the brain and brain borders. Cell. Mol. Immunol.: 1–10. doi:10.1038/s41423-023-01043-8.

Mantov, N., Zrounba, M., Brollo, M., Grassin-Delyle, S., Glorion, M., David, M., Naline, E., Devillier, P., and Salvator, H. 2022. Ruxolitinib inhibits cytokine production by human lung macrophages without impairing phagocytic ability. Front. Pharmacol. **13**.

Maresz, K., Carrier, E.J., Ponomarev, E.D., Hillard, C.J., and Dittel, B.N. 2005. Modulation of the cannabinoid CB_2 receptor in microglial cells in response to inflammatory stimuli. J. Neurochem. **95**(2): 437–445. doi:10.1111/j.1471-4159.2005.03380.x.

Maresz, K., Pryce, G., Ponomarev, E.D., Marsicano, G., Croxford, J.L., Shriver, L.P., Ledent, C., Cheng, X., Carrier, E.J., Mann, M.K., Giovannoni, G., Pertwee, R.G., Yamamura, T., Buckley, N.E., Hillard, C.J., Lutz, B., Baker, D., and Dittel, B.N. 2007. Direct suppression of CNS autoimmune inflammation via the cannabinoid receptor CB_1 on neurons and CB_2 on autoreactive T cells. Nat. Med. **13**(4): 492–497. doi:10.1038/nm1561.

Marquart, S., Zerr, P., Akhmetshina, A., Palumbo, K., Reich, N., Tomcik, M., Horn, A., Dees, C., Engel, M., Zwerina, J., Distler, O., Schett, G., and Distler, J.H.W. 2010. Inactivation of the cannabinoid receptor CB_1 prevents leukocyte infiltration and experimental fibrosis. Arthritis Rheum. **62**(11): 3467–3476. doi:10.1002/art.27642.

Marsicano, G., and Lafenêtre, P. 2009. Roles of the endocannabinoid system in learning and memory. Curr. Top. Behav. Neurosci. **1**: 201–230. doi:10.1007/978-3-540-88955-7_8.

Marsicano, G., and Lutz, B. 1999. Expression of the cannabinoid receptor CB_1 in distinct neuronal subpopulations in the adult mouse forebrain. Eur. J. Neurosci. **11**(12): 4213–4225. doi:10.1046/j.1460-9568.1999.00847.x.

Marsicano, G., Wotjak, C.T., Azad, S.C., Bisogno, T., Rammes, G., Cascio, M.G., Hermann, H., Tang, J., Hofmann, C., Zieglgänsberger, W., Di Marzo, V., and Lutz, B. 2002. The endogenous cannabinoid system controls extinction of aversive memories. Nature **418**(6897): 530–534. doi:10.1038/nature00839.

Martín-Moreno, A.M., Brera, B., Spuch, C., Carro, E., García-García, L., Delgado, M., Pozo, M.A., Innamorato, N.G., Cuadrado, A., and de Ceballos, M.L. 2012. Prolonged oral cannabinoid administration prevents neuroinflammation, lowers β-amyloid levels and improves cognitive performance in Tg APP 2576 mice. J. Neuroinflammation **9**: 8. doi:10.1186/1742-2094-9-8.

Masuda, T., and Prinz, M. 2016. Microglia: A unique versatile cell in the central nervous system. ACS Chem. Neurosci. **7**(4): 428–434. doi:10.1021/acschemneuro.5b00317.

Masuda, T., Sankowski, R., Staszewski, O., Böttcher, C., Amann, L., Sagar, null, Scheiwe, C., Nessler, S., Kunz, P., van Loo, G., Coenen, V.A., Reinacher, P.C., Michel, A., Sure, U., Gold, R., Grün, D., Priller, J., Stadelmann, C., and Prinz, M. 2019. Spatial and temporal heterogeneity of mouse and human microglia at single-cell resolution. Nature **566**(7744): 388–392. doi:10.1038/s41586-019-0924-x.

Matsunaga, N., Tsuchimori, N., Matsumoto, T., and Ii, M. 2011. TAK-242 (resatorvid), a small-molecule inhibitor of toll-like receptor (TLR) 4 signaling, binds selectively to TLR4 and interferes with interactions between TLR4 and its adaptor molecules. Mol. Pharmacol. **79**(1): 34–41. doi:10.1124/mol.110.068064.

Mazon, J.N., de Mello, A.H., Ferreira, G.K., and Rezin, G.T. 2017. The impact of obesity on neurodegenerative diseases. Life Sci. **182**: 22–28. doi:10.1016/j.lfs.2017.06.002.

McCoy, M.K., Martinez, T.N., Ruhn, K.A., Szymkowski, D.E., Smith, C.G., Botterman, B.R., Tansey, K.E., and Tansey, M.G. 2006. Blocking soluble tumor necrosis factor signaling with dominant-negative tumor necrosis factor inhibitor attenuates loss of dopaminergic neurons in models of Parkinson's disease. J. Neurosci. **26**(37): 9365–9375. doi:10.1523/JNEUROSCI.1504-06.2006.

McGarry, T., Orr, C., Wade, S., Biniecka, M., Wade, S., Gallagher, L., Low, C., Veale, D.J., and Fearon, U. 2018. JAK/STAT blockade alters synovial bioenergetics, mitochondrial function, and proinflammatory mediators in rheumatoid arthritis. Arthritis Rheumatol. **70**(12): 1959–1970. doi:10.1002/art.40569.

McGeer, P.L., Itagaki, S., Boyes, B.E., and McGeer, E.G. 1988. Reactive microglia are positive for HLA-DR in the substantia nigra of Parkinson's and Alzheimer's disease brains. Neurology **38**(8): 1285–1285. doi:10.1212/WNL.38.8.1285.

McGrath, M.S., Zhang, R., Bracci, P.M., Azhir, A., and Forrest, B.D. 2023. Regulation of the innate immune system as a therapeutic approach to supporting respiratory function in ALS. Cells **12**(7): 1031. doi:10.3390/cells12071031.

McHugh, D., Hu, S.S.J., Rimmerman, N., Juknat, A., Vogel, Z., Walker, J.M., and Bradshaw, H.B. 2010. N-arachidonoyl glycine, an abundant endogenous lipid, potently drives directed cellular migration through GPR18, the putative abnormal cannabidiol receptor. BMC Neurosci. **11**: 44. doi:10.1186/1471-2202-11-44.

McKenna, M., and McDougall, J.J. 2020. Cannabinoid control of neurogenic inflammation. Br. J. Pharmacol. **177**(19): 4386–4399. doi:10.1111/bph.15208.

McManus, M.J., Murphy, M.P., and Franklin, J.L. 2011. The mitochondria-targeted antioxidant MitoQ prevents loss of spatial memory retention and early neuropathology in a transgenic mouse model of Alzheimer's disease. J. Neurosci. **31**(44): 15703–15715. doi:10.1523/JNEUROSCI.0552-11.2011.

Mecha, M., Feliú, A., Carrillo-Salinas, F.J., Rueda-Zubiaurre, A., Ortega-Gutiérrez, S., de Sola, R.G., and Guaza, C. 2015. Endocannabinoids drive the acquisition of an alternative phenotype in microglia. Brain. Behav. Immun. **49**: 233–245. doi:10.1016/j.bbi.2015.06.002.

Mechoulam, R., and Parker, L.A. 2013. The endocannabinoid system and the brain. Annu. Rev. Psychol. **64**(1): 21–47. doi:10.1146/annurev-psych-113011-143739.

Medawar, P.B. 1948. Immunity to Homologous Grafted Skin. III. The fate of skin homographs transplanted to the brain, to subcutaneous tissue, and to the anterior chamber of the eye. Br. J. Exp. Pathol. **29**(1): 58–69.

Meier, F.M., Frerix, M., Hermann, W., and Müller-Ladner, U. 2013. Current immunotherapy in rheumatoid arthritis. Immunotherapy **5**(9): 955–974. doi:10.2217/imt.13.94.

Meroni, P.L., Valentini, G., Ayala, F., Cattaneo, A., and Valesini, G. 2015. New strategies to address the pharmacodynamics and pharmacokinetics of tumor necrosis factor (TNF) inhibitors: A systematic analysis. Autoimmun. Rev. **14**(9): 812–829. doi:10.1016/j.autrev.2015.05.001.

Miller, R.G., Block, G., Katz, J.S., Barohn, R.J., Gopalakrishnan, V., Cudkowicz, M., Zhang, J.R., McGrath, M.S., Ludington, E., Appel, S.H., and Azhir, A. 2015. Randomized phase 2 trial of NP001, a novel immune regulator: Safety and early efficacy in ALS. Neurol. - Neuroimmunol. Neuroinflammation **2**(3). doi:10.1212/NXI.0000000000000100.

Miller, R.G., Zhang, R., Block, G., Katz, J., Barohn, R.J., KASARSKIS, E., FORSHEW, D., GOPALAKRISHNAN, V., and MCGRATH, M.S. 2014. NP001 regulation of macrophage activation markers in ALS: A phase I clinical and biomarker study. Amyotroph. Lateral Scler. Front. Degener. **15**(7–8): 601–609. doi:10.3109/21678421.2014.951940.

Miller, R.G., Zhang, R., Bracci, P.M., Azhir, A., Barohn, R., Bedlack, R., Benatar, M., Berry, J.D., Cudkowicz, M., Kasarskis, E.J., Mitsumoto, H., Manousakis, G., Walk, D., Oskarsson, B., Shefner, J., and McGrath, M.S. 2022. Phase 2B randomized controlled trial of NP001 in amyotrophic lateral sclerosis: Pre-specified and post hoc analyses. Muscle Nerve **66**(1): 39–49. doi:10.1002/mus.27511.

Minogue, A.M., Barrett, J.P., and Lynch, M.A. 2012. LPS-induced release of IL-6 from glia modulates production of IL-1β in a JAK2-dependent manner. J. Neuroinflammation **9**(1): 126. doi:10.1186/1742-2094-9-126.

Mishra, M., Kane, A.E., Young, A.P., and Howlett, S.E. 2023. Age, sex, and frailty modify the expression of common reference genes in skeletal muscle from ageing mice. Mech. Ageing Dev. **210**: 111762. doi:10.1016/j.mad.2022.111762.

Moalem, G., Leibowitz–Amit, R., Yoles, E., Mor, F., Cohen, I.R., and Schwartz, M. 1999. Autoimmune T cells protect neurons from secondary degeneration after central nervous system axotomy. Nat. Med. **5**(1): 49–55. doi:10.1038/4734.

Moe, A., Rayasam, A., Sauber, G., Shah, R., Yuan, C.Y., Szabo, A., Moore, B., Colonna, M., Cui, W., Romero, J., Zamora, A., Hillard, C., and Drobyski, W. 2023. Microglial cell expression of the type 2 cannabinoid receptor regulates immune-mediated neuroinflammation. bioRxiv. doi:10.1101/2023.08.10.552854.

Mohr, A.E., Crawford, M., Jasbi, P., Fessler, S., and Sweazea, K.L. 2022. Lipopolysaccharide and the gut microbiota: considering structural variation. FEBS Lett. **596**(7): 849–875. doi:10.1002/1873-3468.14328.

Monteiro, S., Roque, S., Marques, F., Correia-Neves, M., and Cerqueira, J.J. 2017. Brain interference: Revisiting the role of IFNγ in the central nervous system. Prog. Neurobiol. **156**: 149–163. doi:10.1016/j.pneurobio.2017.05.003.

Mount, M.P., Lira, A., Grimes, D., Smith, P.D., Faucher, S., Slack, R., Anisman, H., Hayley, S., and Park, D.S. 2007. Involvement of interferon-γ in microglial-mediated loss of dopaminergic neurons. J. Neurosci. **27**(12): 3328–3337. doi:10.1523/JNEUROSCI.5321-06.2007.

Mulder, J., Zilberter, M., Pasquaré, S.J., Alpár, A., Schulte, G., Ferreira, S.G., Köfalvi, A., Martín-Moreno, A.M., Keimpema, E., Tanila, H., Watanabe, M., Mackie, K., Hortobágyi, T., de Ceballos, M.L., and Harkany, T. 2011. Molecular reorganization of endocannabinoid signalling in Alzheimer's disease. Brain **134**(4): 1041–1060. doi:10.1093/brain/awr046.

Munro, S., Thomas, K.L., and Abu-Shaar, M. 1993. Molecular characterization of a peripheral receptor for cannabinoids. Nature **365**(6441): 61–65. doi:10.1038/365061a0.

Murphy, J.B., and Sturm, E. 1923. Conditions determining the transplantability of tissues in the brain. J. Exp. Med. **38**(2): 183–197. doi:10.1084/jem.38.2.183.

Murray, C.L., Skelly, D.T., and Cunningham, C. 2011. Exacerbation of CNS inflammation and neurodegeneration by systemic LPS treatment is independent of circulating IL-1β and IL-6. J. Neuroinflammation **8**: 50. doi:10.1186/1742-2094-8-50.

Murtaj, V., Belloli, S., Di Grigoli, G., Pannese, M., Ballarini, E., Rodriguez-Menendez, V., Marmiroli, P., Cappelli, A., Masiello, V., Monterisi, C., Bellelli, G., Panina-Bordignon, P., and Moresco, R.M. 2019. Age and sex influence the neuro-inflammatory response to a peripheral acute LPS challenge. Front. Aging Neurosci. **11**: 299. doi:10.3389/fnagi.2019.00299.

Nagai, M., Re, D.B., Nagata, T., Chalazonitis, A., Jessell, T.M., Wichterle, H., and Przedborski, S. 2007. Astrocytes expressing ALS-linked mutated SOD1 release factors selectively toxic to motor neurons. Nat. Neurosci. **10**(5): 615–622. doi:10.1038/nn1876.

Nagamoto-Combs, K., Kulas, J., and Combs, C.K. 2014. A novel cell line from spontaneously immortalized murine microglia. J. Neurosci. Methods **233**: 187–198. doi:10.1016/j.jneumeth.2014.05.021.

Nakagawa, T., Shimizu, S., Watanabe, T., Yamaguchi, O., Otsu, K., Yamagata, H., Inohara, H., Kubo, T., and Tsujimoto, Y. 2005. Cyclophilin D-dependent mitochondrial permeability transition regulates some necrotic but not apoptotic cell death. Nature **434**(7033): 652–658. doi:10.1038/nature03317.

Nandi, A., Counts, N., Chen, S., Seligman, B., Tortorice, D., Vigo, D., and Bloom, D.E. 2022. Global and regional projections of the economic burden of Alzheimer's disease and related dementias from 2019 to 2050: A value of statistical life approach. eClinicalMedicine **51**. Elsevier. doi:10.1016/j.eclinm.2022.101580.

Nandi, S., Gokhan, S., Dai, X.-M., Wei, S., Enikolopov, G., Lin, H., Mehler, M.F., and Stanley, E.R. 2012. The CSF-1 receptor ligands IL-34 and CSF-1 exhibit distinct developmental brain expression patterns and regulate neural progenitor cell maintenance and maturation. Dev. Biol. **367**(2): 100–113. doi:10.1016/j.ydbio.2012.03.026.

Navarro, G., Borroto-Escuela, D., Angelats, E., Etayo, Í., Reyes-Resina, I., Pulido-Salgado, M., Rodríguez-Pérez, A.I., Canela, E.I., Saura, J., Lanciego, J.L., Labandeira-García, J.L., Saura, C.A., Fuxe, K., and Franco, R. 2018a. Receptor-heteromer mediated regulation of endocannabinoid signaling in activated microglia. Role of CB_1 and CB_2 receptors and relevance for Alzheimer's disease and levodopa-induced dyskinesia. Brain. Behav. Immun. **67**: 139–151. doi:10.1016/j.bbi.2017.08.015.

Navarro, G., Morales, P., Rodríguez-Cueto, C., Fernández-Ruiz, J., Jagerovic, N., and Franco, R. 2016. Targeting cannabinoid CB_2 receptors in the central nervous

system. medicinal chemistry approaches with focus on neurodegenerative disorders. Front. Neurosci. **10**: 406. doi:10.3389/fnins.2016.00406.

Navarro, G., Varani, K., Reyes-Resina, I., Sánchez de Medina, V., Rivas-Santisteban, R., Sánchez-Carnerero Callado, C., Vincenzi, F., Casano, S., Ferreiro-Vera, C., Canela, E.I., Borea, P.A., Nadal, X., and Franco, R. 2018b. Cannabigerol action at cannabinoid CB_1 and CB_2 receptors and at CB_1–CB_2 heteroreceptor complexes. Front. Pharmacol. **9**: 632. doi:10.3389/fphar.2018.00632.

Nehmé, R., Carpenter, B., Singhal, A., Strege, A., Edwards, P.C., White, C.F., Du, H., Grisshammer, R., and Tate, C.G. 2017. Mini-G proteins: Novel tools for studying GPCRs in their active conformation. PLOS ONE **12**(4): e0175642. doi:10.1371/journal.pone.0175642.

Neniskyte, U., Vilalta, A., and Brown, G.C. 2014. Tumour necrosis factor alpha-induced neuronal loss is mediated by microglial phagocytosis. FEBS Lett. **588**(17): 2952–2956. doi:10.1016/j.febslet.2014.05.046.

Neumann, H., Kotter, M.R., and Franklin, R.J.M. 2009. Debris clearance by microglia: an essential link between degeneration and regeneration. Brain **132**(2): 288–295. doi:10.1093/brain/awn109.

Neumann, H., Schweigreiter, R., Yamashita, T., Rosenkranz, K., Wekerle, H., and Barde, Y.-A. 2002. Tumor necrosis factor inhibits neurite outgrowth and branching of hippocampal neurons by a rho-dependent mechanism. J. Neurosci. **22**(3): 854–862. doi:10.1523/JNEUROSCI.22-03-00854.2002.

Nguyen, P.T., Dorman, L.C., Pan, S., Vainchtein, I.D., Han, R.T., Nakao-Inoue, H., Taloma, S.E., Barron, J.J., Molofsky, A.B., Kheirbek, M.A., and Molofsky, A.V. 2020. Microglial remodeling of the extracellular matrix promotes synapse plasticity. Cell **182**(2): 388-403.e15. doi:10.1016/j.cell.2020.05.050.

Nicolas, C.S., Amici, M., Bortolotto, Z.A., Doherty, A., Csaba, Z., Fafouri, A., Dournaud, P., Gressens, P., Collingridge, G.L., and Peineau, S. 2013. The role of JAK-STAT signaling within the CNS. JAK-STAT **2**(1): e22925. doi:10.4161/jkst.22925.

Nie, X., Kitaoka, S., Tanaka, K., Segi-Nishida, E., Imoto, Y., Ogawa, A., Nakano, F., Tomohiro, A., Nakayama, K., Taniguchi, M., Mimori-Kiyosue, Y., Kakizuka, A.,

Narumiya, S., and Furuyashiki, T. 2018. The innate immune receptors TLR2/4 mediate repeated social defeat stress-induced social avoidance through prefrontal microglial activation. Neuron **99**(3): 464-479.e7. doi:10.1016/j.neuron.2018.06.035.

Nimmerjahn, A., Kirchhoff, F., and Helmchen, F. 2005. Resting microglial cells are highly dynamic surveillants of brain parenchyma *in vivo*. Science **308**(5726): 1314–1318. doi:10.1126/science.1110647.

Nomura, D.K., Morrison, B.E., Blankman, J.L., Long, J.Z., Kinsey, S.G., Marcondes, M.C.G., Ward, A.M., Lichtman, A.H., Conti, B., and Cravatt, B.F. 2011. Endocannabinoid hydrolysis generates brain prostaglandins that promote neuroinflammation. Science **334**(6057): 809–813. doi:10.1126/science.1209200.

Norris, G.T., Smirnov, I., Filiano, A.J., Shadowen, H.M., Cody, K.R., Thompson, J.A., Harris, T.H., Gaultier, A., Overall, C.C., and Kipnis, J. 2018. Neuronal integrity and complement control synaptic material clearance by microglia after CNS injury. J. Exp. Med. **215**(7): 1789–1801. doi:10.1084/jem.20172244.

Novorolsky, R.J., Nichols, M., Kim, J.S., Pavlov, E.V., J Woods, J., Wilson, J.J., and Robertson, G.S. 2020. The cell-permeable mitochondrial calcium uniporter inhibitor Ru265 preserves cortical neuron respiration after lethal oxygen glucose deprivation and reduces hypoxic/ischemic brain injury. J. Cereb. Blood Flow Metab. **40**(6): 1172–1181. doi:10.1177/0271678X20908523.

O'Brien, A., Hanlon, M.M., Marzaioli, V., Wade, S.C., Flynn, K., Fearon, U., and Veale, D.J. 2021. Targeting JAK-STAT signalling alters psa synovial fibroblast pro-inflammatory and metabolic function. Front. Immunol. **12**: 672461. doi:10.3389/fimmu.2021.672461.

Ofengeim, D., Ito, Y., Najafov, A., Zhang, Y., Shan, B., DeWitt, J.P., Ye, J., Zhang, X., Chang, A., Vakifahmetoglu-Norberg, H., Geng, J., Py, B., Zhou, W., Amin, P., Lima, J.B., Qi, C., Yu, Q., Trapp, B., and Yuan, J. 2015. Activation of necroptosis in multiple sclerosis. Cell Rep. **10**(11): 1836–1849. doi:10.1016/j.celrep.2015.02.051.

Ofengeim, D., and Yuan, J. 2013. Regulation of RIP1 kinase signalling at the crossroads of inflammation and cell death. Nat. Rev. Mol. Cell Biol. **14**(11): 727–736. doi:10.1038/nrm3683.

Oh, S.J., Ahn, H., Jung, K.-H., Han, S.J., Nam, K.R., Kang, K.J., Park, J.-A., Lee, K.C., Lee, Y.J., and Choi, J.Y. 2020. Evaluation of the neuroprotective effect of microglial depletion by CSF-1R inhibition in a Parkinson's animal model. Mol. Imaging Biol. **22**(4): 1031–1042. doi:10.1007/s11307-020-01485-w.

Oka, S., Wakui, J., Ikeda, S., Yanagimoto, S., Kishimoto, S., Gokoh, M., Nasui, M., and Sugiura, T. 2006. Involvement of the cannabinoid CB_2 receptor and its endogenous ligand 2-arachidonoylglycerol in oxazolone-induced contact dermatitis in mice. J. Immunol. **177**(12): 8796–8805. doi:10.4049/jimmunol.177.12.8796.

Oka, S., Yanagimoto, S., Ikeda, S., Gokoh, M., Kishimoto, S., Waku, K., Ishima, Y., and Sugiura, T. 2005. Evidence for the involvement of the cannabinoid CB_2 receptor and its endogenous ligand 2-arachidonoylglycerol in 12-O-tetradecanoylphorbol-13-acetate-induced acute inflammation in mouse ear. J. Biol. Chem. **280**(18): 18488–18497. doi:10.1074/jbc.M413260200.

Okugawa, S., Ota, Y., Kitazawa, T., Nakayama, K., Yanagimoto, S., Tsukada, K., Kawada, M., and Kimura, S. 2003. Janus kinase 2 is involved in lipopolysaccharide-induced activation of macrophages. Am. J. Physiol.-Cell Physiol. **285**(2): C399–C408. doi:10.1152/ajpcell.00026.2003.

O'Regan, G.C., Farag, S.H., Casey, C.S., Wood-Kaczmar, A., Pocock, J.M., Tabrizi, S.J., and Andre, R. 2021. Human Huntington's disease pluripotent stem cell-derived microglia develop normally but are abnormally hyper-reactive and release elevated levels of reactive oxygen species. J. Neuroinflammation **18**(1): 94. doi:10.1186/s12974-021-02147-6.

Orihuela, R., McPherson, C.A., and Harry, G.J. 2016. Microglial M1/M2 polarization and metabolic states. Br. J. Pharmacol. **173**(4): 649–665. doi:10.1111/bph.13139.

Ortí-Casañ, N., Zuhorn, I.S., Naudé, P.J.W., De Deyn, P.P., van Schaik, P.E.M., Wajant, H., and Eisel, U.L.M. 2022. A TNF receptor 2 agonist ameliorates neuropathology and improves cognition in an Alzheimer's disease mouse model. Proc. Natl. Acad. Sci. **119**(37): e2201137119. doi:10.1073/pnas.2201137119.

Ou, W., Yang, J., Simanauskaite, J., Choi, M., Castellanos, D.M., Chang, R., Sun, J., Jagadeesan, N., Parfitt, K.D., Cribbs, D.H., and Sumbria, R.K. 2021. Biologic TNF-α inhibitors reduce microgliosis, neuronal loss, and tau phosphorylation in a transgenic mouse model of tauopathy. J. Neuroinflammation **18**(1): 312. doi:10.1186/s12974-021-02332-7.

Pabon, M.M., Bachstetter, A.D., Hudson, C.E., Gemma, C., and Bickford, P.C. 2011. CX3CL1 reduces neurotoxicity and microglial activation in a rat model of Parkinson's disease. J. Neuroinflammation **8**: 9. doi:10.1186/1742-2094-8-9.

Pacher, P., Bátkai, S., and Kunos, G. 2006. The endocannabinoid system as an emerging target of pharmacotherapy. Pharmacol. Rev. **58**(3): 389–462. doi:10.1124/pr.58.3.2.

Pacifico, L., Renzo, L.D., Anania, C., Osborn, J.F., Ippoliti, F., Schiavo, E., and Chiesa, C. 2006. Increased T-helper interferon-γ-secreting cells in obese children. Eur. J. Endocrinol. **154**(5): 691–697. European Society of Endocrinology. doi:10.1530/eje.1.02138.

Palazuelos, J., Aguado, T., Pazos, M.R., Julien, B., Carrasco, C., Resel, E., Sagredo, O., Benito, C., Romero, J., Azcoitia, I., Fernández-Ruiz, J., Guzmán, M., and Galve-Roperh, I. 2009. Microglial CB_2 cannabinoid receptors are neuroprotective in Huntington's disease excitotoxicity. Brain **132**(11): 3152–3164. doi:10.1093/brain/awp239.

Pan, J., Ma, N., Zhong, J., Yu, B., Wan, J., and Zhang, W. 2021. Age-associated changes in microglia and astrocytes ameliorate blood-brain barrier dysfunction. Mol. Ther. - Nucleic Acids **26**: 970–986. doi:10.1016/j.omtn.2021.08.030.

Pandey, R., Mousawy, K., Nagarkatti, M., and Nagarkatti, P. 2009. Endocannabinoids and immune regulation. Pharmacol. Res. **60**(2): 85–92. doi:10.1016/j.phrs.2009.03.019.

Panikashvili, D., Shein, N.A., Mechoulam, R., Trembovler, V., Kohen, R., Alexandrovich, A., and Shohami, E. 2006. The endocannabinoid 2-AG protects the blood-brain barrier after closed head injury and inhibits mRNA expression of proinflammatory cytokines. Neurobiol. Dis. **22**(2): 257–264. doi:10.1016/j.nbd.2005.11.004.

Panza, F., Lozupone, M., Logroscino, G., and Imbimbo, B.P. 2019. A critical appraisal of amyloid-β-targeting therapies for Alzheimer disease. Nat. Rev. Neurol. **15**(2): 73–88. doi:10.1038/s41582-018-0116-6.

Paoletti, P., Vila, I., Rifé, M., Lizcano, J.M., Alberch, J., and Ginés, S. 2008. Dopaminergic and glutamatergic signaling crosstalk in Huntington's disease

neurodegeneration: The Role of p25/Cyclin-Dependent Kinase 5. J. Neurosci. **28**(40): 10090–10101. Society for Neuroscience. doi:10.1523/JNEUROSCI.3237-08.2008.

Papageorgiou, I.E., Lewen, A., Galow, L.V., Cesetti, T., Scheffel, J., Regen, T., Hanisch, U.-K., and Kann, O. 2016. TLR4-activated microglia require IFN-γ to induce severe neuronal dysfunction and death in situ. Proc. Natl. Acad. Sci. **113**(1): 212–217. doi:10.1073/pnas.1513853113.

Pasparakis, M., and Vandenabeele, P. 2015. Necroptosis and its role in inflammation. Nature **517**(7534): 311–320. doi:10.1038/nature14191.

Pattison, M.J., MacKenzie, K.F., and Arthur, J.S.C. 2012. Inhibition of JAKs in macrophages increases lipopolysaccharide-induced cytokine production by blocking IL-10–mediated feedback. J. Immunol. **189**(6): 2784–2792. doi:10.4049/jimmunol.1200310.

Pavese, N., Gerhard, A., Tai, Y.F., Ho, A.K., Turkheimer, F., Barker, R.A., Brooks, D.J., and Piccini, P. 2006. Microglial activation correlates with severity in Huntington disease: a clinical and PET study. Neurology **66**(11): 1638–1643. doi:10.1212/01.wnl.0000222734.56412.17.

Pavshintsev, V.V., Podshivalova, L.S., Frolova, O.Y., Belopolskaya, M.V., Averina, O.A., Kushnir, E.A., Marmiy, N.V., and Lovat, M.L. 2017. Effects of mitochondrial antioxidant SkQ1 on biochemical and behavioral parameters in a Parkinsonism model in mice. Biochem. **82**(12): 1513–1520. doi:10.1134/S0006297917120100.

Pawelec, P., Ziemka-Nalecz, M., Sypecka, J., and Zalewska, T. 2020. The impact of the CX3CL1/CX3CR1 axis in neurological disorders. Cells **9**(10): 2277. doi:10.3390/cells9102277.

Pegoretti, V., Bauer, J., Fischer, R., Paro, I., Douwenga, W., Kontermann, R.E., Pfizenmaier, K., Houben, E., Broux, B., Hellings, N., Baron, W., Laman, J.D., and Eisel, U.L.M. 2023. Sequential treatment with a TNFR2 agonist and a TNFR1 antagonist improves outcomes in a humanized mouse model for MS. J. Neuroinflammation **20**(1): 106. doi:10.1186/s12974-023-02785-y.

Pérez-Navarro, E., Canals, J.M., Ginés, S., and Alberch, J. 2006. Cellular and molecular mechanisms involved in the selective vulnerability of striatal projection neurons in Huntington's disease. Histol. Histopathol. **21**(11): 1217–1232. doi:10.14670/HH-21.1217.

Perry, V.H., and Holmes, C. 2014. Microglial priming in neurodegenerative disease. Nat. Rev. Neurol. **10**(4): 217–224. doi:10.1038/nrneurol.2014.38.

Perry, V.H., Nicoll, J.A.R., and Holmes, C. 2010. Microglia in neurodegenerative disease. Nat. Rev. Neurol. **6**(4): 193–201. doi:10.1038/nrneurol.2010.17.

Pertwee, R.G. 1997. Pharmacology of cannabinoid CB1 and CB2 receptors. Pharmacol. Ther. **74**(2): 129–180. doi:10.1016/s0163-7258(97)82001-3.

Peter, I., Dubinsky, M., Bressman, S., Park, A., Lu, C., Chen, N., and Wang, A. 2018. Anti-tumor necrosis factor therapy and incidence of Parkinson disease among patients with inflammatory bowel disease. JAMA Neurol. **75**(8): 939–946. doi:10.1001/jamaneurol.2018.0605.

Phuan, P.-W., Zhang, H., Asavapanumas, N., Leviten, M., Rosenthal, A., Tradtrantip, L., and Verkman, A.S. 2013. C1q-targeted monoclonal antibody prevents complement-dependent cytotoxicity and neuropathology in in vitro and mouse models of neuromyelitis optica. Acta Neuropathol. **125**(6): 829–840. doi:10.1007/s00401-013-1128-3.

Pickering, M., Cumiskey, D., and O'Connor, J.J. 2005. Actions of TNF-alpha on glutamatergic synaptic transmission in the central nervous system. Exp. Physiol. **90**(5): 663–670. doi:10.1113/expphysiol.2005.030734.

Piehl, N., Olst, L. van, Ramakrishnan, A., Teregulova, V., Simonton, B., Zhang, Z., Tapp, E., Channappa, D., Oh, H., Losada, P.M., Rutledge, J., Trelle, A.N., Mormino, E.C., Elahi, F., Galasko, D.R., Henderson, V.W., Wagner, A.D., Wyss-Coray, T., and Gate, D. 2022. Cerebrospinal fluid immune dysregulation during healthy brain aging and cognitive impairment. Cell **185**(26): 5028-5039.e13. doi:10.1016/j.cell.2022.11.019.

Politis, M., Lahiri, N., Niccolini, F., Su, P., Wu, K., Giannetti, P., Scahill, R.I., Turkheimer, F.E., Tabrizi, S.J., and Piccini, P. 2015. Increased central microglial activation associated with peripheral cytokine levels in premanifest Huntington's disease gene carriers. Neurobiol. Dis. **83**: 115–121. doi:10.1016/j.nbd.2015.08.011.

Politis, M., Pavese, N., Tai, Y.F., Kiferle, L., Mason, S.L., Brooks, D.J., Tabrizi, S.J., Barker, R.A., and Piccini, P. 2011. Microglial activation in regions related to cognitive function predicts disease onset in Huntington's disease: A multimodal imaging study. Hum. Brain Mapp. **32**(2): 258–270. doi:10.1002/hbm.21008.

Ponomarev, E.D., Shriver, L.P., and Dittel, B.N. 2006. CD40 expression by microglial cells is required for their completion of a two-step activation process during central nervous system autoimmune inflammation1. J. Immunol. **176**(3): 1402–1410. doi:10.4049/jimmunol.176.3.1402.

Price, D.A., Martinez, A.A., Seillier, A., Koek, W., Acosta, Y., Fernandez, E., Strong, R., Lutz, B., Marsicano, G., Roberts, J.L., and Giuffrida, A. 2009. WIN55,212-2, a cannabinoid receptor agonist, protects against nigrostriatal cell loss in the 1-methyl-4-phenyl-1,2,3,6-tetrahydropyridine mouse model of Parkinson's disease. Eur. J. Neurosci. **29**(11): 2177–2186. doi:10.1111/j.1460-9568.2009.06764.x.

Prinz, M., and Priller, J. 2017. The role of peripheral immune cells in the CNS in steady state and disease. Nat. Neurosci. **20**(2): 136–144. doi:10.1038/nn.4475.

Puigdellívol, M., Milde, S., Vilalta, A., Cockram, T.O.J., Allendorf, D.H., Lee, J.Y., Dundee, J.M., Pampuščenko, K., Borutaite, V., Nuthall, H.N., Brelstaff, J.H., Spillantini, M.G., and Brown, G.C. 2021. The microglial $P2Y_6$ receptor mediates neuronal loss and memory deficits in neurodegeneration. Cell Rep. **37**(13): 110148. doi:10.1016/j.celrep.2021.110148.

Qin, H., Buckley, J.A., Li, X., Liu, Y., Fox, T.H., Meares, G.P., Yu, H., Yan, Z., Harms, A.S., Li, Y., Standaert, D.G., and Benveniste, E.N. 2016. Inhibition of the JAK/STAT pathway protects against α-synuclein-induced neuroinflammation and dopaminergic neurodegeneration. J. Neurosci. **36**(18): 5144–5159. Society for Neuroscience. doi:10.1523/JNEUROSCI.4658-15.2016.

Qin, L., Wu, X., Block, M.L., Liu, Y., Breese, G.R., Hong, J.-S., Knapp, D.J., and Crews, F.T. 2007. Systemic LPS causes chronic neuroinflammation and progressive neurodegeneration. Glia **55**(5): 453–462. doi:10.1002/glia.20467.

Quan, N., Whiteside, M., and Herkenham, M. 1998. Time course and localization patterns of interleukin-1beta messenger RNA expression in brain and pituitary after peripheral administration of lipopolysaccharide. Neuroscience **83**(1): 281–293. doi:10.1016/s0306-4522(97)00350-3.

Quintás-Cardama, A., Vaddi, K., Liu, P., Manshouri, T., Li, J., Scherle, P.A., Caulder, E., Wen, X., Li, Y., Waeltz, P., Rupar, M., Burn, T., Lo, Y., Kelley, J., Covington, M., Shepard, S., Rodgers, J.D., Haley, P., Kantarjian, H., Fridman, J.S., and Verstovsek, S. 2010. Preclinical characterization of the selective JAK1/2 inhibitor INCB018424: therapeutic implications for the treatment of myeloproliferative neoplasms. Blood **115**(15): 3109–3117. doi:10.1182/blood-2009-04-214957.

Rabaneda-Lombarte, N., Serratosa, J., Bové, J., Vila, M., Saura, J., and Solà, C. 2021. The CD200R1 microglial inhibitory receptor as a therapeutic target in the MPTP model of Parkinson's disease. J. Neuroinflammation **18**(1): 88. doi:10.1186/s12974-021-02132-z.

Ramana, C.V., Gil, M.P., Schreiber, R.D., and Stark, G.R. 2002. STAT1-dependent and -independent pathways in IFN-gamma-dependent signaling. Trends Immunol. **23**(2): 96–101. doi:10.1016/s1471-4906(01)02118-4.

Ransohoff, R.M. 2016a. A polarizing question: do M1 and M2 microglia exist? Nat. Neurosci. **19**(8): 987–991. doi:10.1038/nn.4338.

Ransohoff, R.M. 2016b. How neuroinflammation contributes to neurodegeneration. Science **353**(6301): 777–783. doi:10.1126/science.aag2590.

Raparelli, V., Basili, S., Carnevale, R., Napoleone, L., Del Ben, M., Nocella, C., Bartimoccia, S., Lucidi, C., Talerico, G., Riggio, O., and Violi, F. 2017. Low-grade endotoxemia and platelet activation in cirrhosis. Hepatology **65**(2): 571–581. doi:10.1002/hep.28853.

Rashid, T., Ebringer, A., and Wilson, C. 2013. The role of *Klebsiella* in Crohn's disease with a potential for the use of antimicrobial measures. Int. J. Rheumatol. **2013**: 610393. doi:10.1155/2013/610393.

Ravikumar, B., Vacher, C., Berger, Z., Davies, J.E., Luo, S., Oroz, L.G., Scaravilli, F., Easton, D.F., Duden, R., O'Kane, C.J., and Rubinsztein, D.C. 2004. Inhibition of mTOR induces autophagy and reduces toxicity of polyglutamine expansions in fly and mouse models of Huntington disease. Nat. Genet. **36**(6): 585–595. doi:10.1038/ng1362.

Raymon, H.K., Thode, S., Zhou, J., Friedman, G.C., Pardinas, J.R., Barrere, C., Johnson, R.M., and Sah, D.W.Y. 1999. Immortalized human dorsal root ganglion cells differentiate into neurons with nociceptive properties. J. Neurosci. **19**(13): 5420–5428. doi:10.1523/JNEUROSCI.19-13-05420.1999.

Re, D.B., Le Verche, V., Yu, C., Amoroso, M.W., Politi, K.A., Phani, S., Ikiz, B., Hoffmann, L., Koolen, M., Nagata, T., Papadimitriou, D., Nagy, P., Mitsumoto, H., Kariya, S., Wichterle, H., Henderson, C.E., and Przedborski, S. 2014. Necroptosis drives motor neuron death in models of both sporadic and familial ALS. Neuron **81**(5): 1001–1008. doi:10.1016/j.neuron.2014.01.011.

Reed-Geaghan, E.G., Savage, J.C., Hise, A.G., and Landreth, G.E. 2009. CD14 and toll-like receptors 2 and 4 are required for fibrillar A{beta}-stimulated microglial activation. J. Neurosci. **29**(38): 11982–11992. doi:10.1523/JNEUROSCI.3158-09.2009.

Reines, S.A., Block, G.A., Morris, J.C., Liu, G., Nessly, M.L., Lines, C.R., Norman, B.A., Baranak, C.C., and Rofecoxib Protocol 091 Study Group. 2004. Rofecoxib: no effect on Alzheimer's disease in a 1-year, randomized, blinded, controlled study. Neurology **62**(1): 66–71. doi:10.1212/wnl.62.1.66.

Reish, H.E., and Standaert, D.G. 2015. Role of α-synuclein in inducing innate and adaptive immunity in Parkinson disease. J. Park. Dis. **5**(1): 1–19. doi:10.3233/JPD-140491.

Réu, P., Khosravi, A., Bernard, S., Mold, J.E., Salehpour, M., Alkass, K., Perl, S., Tisdale, J., Possnert, G., Druid, H., and Frisén, J. 2017. The lifespan and turnover of microglia in the human brain. Cell Rep. **20**(4): 779–784. doi:10.1016/j.celrep.2017.07.004.

Reusch, N., Ravichandran, K.A., Olabiyi, B.F., Komorowska-Müller, J.A., Hansen, J.N., Ulas, T., Beyer, M., Zimmer, A., and Schmöle, A.-C. 2022. Cannabinoid receptor 2 is necessary to induce toll-like receptor-mediated microglial activation. Glia **70**(1): 71–88. doi:10.1002/glia.24089.

Ribeiro, R., Wen, J., Li, S., and Zhang, Y. 2013. Involvement of ERK1/2, cPLA2 and NF-κB in microglia suppression by cannabinoid receptor agonists and antagonists. Prostaglandins Other Lipid Mediat. **100–101**: 1–14. doi:10.1016/j.prostaglandins.2012.11.003.

Richard, R., and Mousa, S. 2022. Necroptosis in Alzheimer's disease: Potential therapeutic target. Biomed. Pharmacother. **152**: 113203. doi:10.1016/j.biopha.2022.113203.

Richards, E.M., Zanotti-Fregonara, P., Fujita, M., Newman, L., Farmer, C., Ballard, E.D., Machado-Vieira, R., Yuan, P., Niciu, M.J., Lyoo, C.H., Henter, I.D., Salvadore, G., Drevets, W.C., Kolb, H., Innis, R.B., and Zarate Jr, C.A. 2018. PET radioligand binding to translocator protein (TSPO) is increased in unmedicated depressed subjects. EJNMMI Res. **8**: 57. doi:10.1186/s13550-018-0401-9.

Richfield, E.K., O'Brien, C.F., Eskin, T., and Shoulson, I. 1991. Heterogeneous dopamine receptor changes in early and late Huntington's disease. Neurosci. Lett. **132**(1): 121–126. doi:10.1016/0304-3940(91)90448-3.

Rietschel, E.T., Kirikae, T., Schade, F.U., Mamat, U., Schmidt, G., Loppnow, H., Ulmer, A.J., Zähringer, U., Seydel, U., Di Padova, F., Schreier, M., and Brade, H. 1994. Bacterial endotoxin: molecular relationships of structure to activity and function. FASEB J. **8**(2): 217–225. doi:10.1096/fasebj.8.2.8119492.

Rigamonti, D., Bauer, J.H., De-Fraja, C., Conti, L., Sipione, S., Sciorati, C., Clementi, E., Hackam, A., Hayden, M.R., Li, Y., Cooper, J.K., Ross, C.A., Govoni, S., Vincenz, C., and Cattaneo, E. 2000. Wild-Type Huntingtin Protects from Apoptosis Upstream of Caspase-3. J. Neurosci. **20**(10): 3705–3713. doi:10.1523/JNEUROSCI.20-10-03705.2000.

Righi, M., Mori, L., De Libero, G., Sironi, M., Biondi, A., Mantovani, A., Donini, S.D., and Ricciardi-Castagnoli, P. 1989. Monokine production by microglial cell clones. Eur. J. Immunol. **19**(8): 1443–1448. doi:10.1002/eji.1830190815.

Rinaldi-Carmona, M., Barth, F., Millan, J., Derocq, J.M., Casellas, P., Congy, C., Oustric, D., Sarran, M., Bouaboula, M., Calandra, B., Portier, M., Shire, D., Brelière, J.C., and Le Fur, G.L. 1998. SR 144528, the first potent and selective antagonist of the CB2 cannabinoid receptor. J. Pharmacol. Exp. Ther. **284**(2): 644–650.

Rocha, N.P., Ribeiro, F.M., Furr-Stimming, E., and Teixeira, A.L. 2016. Neuroimmunology of Huntington's Disease: Revisiting evidence from human studies. Mediators Inflamm. **2016**: 8653132. doi:10.1155/2016/8653132.

Rodems, S.M., and Spector, D.H. 1998. Extracellular signal-regulated kinase activity is sustained early during human cytomegalovirus infection. J. Virol. **72**(11): 9173–9180.

Rodriguez, S., Hug, C., Todorov, P., Moret, N., Boswell, S.A., Evans, K., Zhou, G., Johnson, N.T., Hyman, B.T., Sorger, P.K., Albers, M.W., and Sokolov, A. 2021. Machine learning identifies candidates for drug repurposing in Alzheimer's disease. Nat. Commun. **12**(1): 1033. doi:10.1038/s41467-021-21330-0.

Romano, S., Savva, G.M., Bedarf, J.R., Charles, I.G., Hildebrand, F., and Narbad, A. 2021. Meta-analysis of the Parkinson's disease gut microbiome suggests alterations linked to intestinal inflammation. Npj Park. Dis. **7**(1): 1–13. doi:10.1038/s41531-021-00156-z.

Rook, M.E., and Southwell, A.L. 2022. Antisense oligonucleotide Therapy: From design to the Huntington disease clinic. Biodrugs **36**(2): 105–119. doi:10.1007/s40259-022-00519-9.

Ross, R.A., Brockie, H.C., and Pertwee, R.G. 2000. Inhibition of nitric oxide production in RAW264.7 macrophages by cannabinoids and palmitoylethanolamide. Eur. J. Pharmacol. **401**(2): 121–130. doi:10.1016/S0014-2999(00)00437-4.

Ross, R.A., Brockie, H.C., Stevenson, L.A., Murphy, V.L., Templeton, F., Makriyannis, A., and Pertwee, R.G. 1999. Agonist-inverse agonist characterization at CB_1 and CB_2 cannabinoid receptors of L759633, L759656 and AM630. Br. J. Pharmacol. **126**(3): 665–672. doi:10.1038/sj.bjp.0702351.

Rossi, F., Tortora, C., Punzo, F., Bellini, G., Argenziano, M., Di Paola, A., Torella, M., and Perrotta, S. 2019. The endocannabinoid/endovanilloid system in bone: From osteoporosis to osteosarcoma. Int. J. Mol. Sci. **20**(8): 1919. doi:10.3390/ijms20081919.

Roy, E.R., Chiu, G., Li, S., Propson, N.E., Kanchi, R., Wang, B., Coarfa, C., Zheng, H., and Cao, W. 2022. Concerted type I interferon signaling in microglia and neural cells promotes memory impairment associated with amyloid β plaques. Immunity **55**(5): 879-894.e6. doi:10.1016/j.immuni.2022.03.018.

Roy, E.R., Wang, B., Wan, Y.-W., Chiu, G., Cole, A., Yin, Z., Propson, N.E., Xu, Y., Jankowsky, J.L., Liu, Z., Lee, V.M.-Y., Trojanowski, J.Q., Ginsberg, S.D.,

Butovsky, O., Zheng, H., and Cao, W. 2020. Type I interferon response drives neuroinflammation and synapse loss in Alzheimer disease. J. Clin. Invest. **130**(4): 1912–1930. doi:10.1172/JCI133737.

Rubinsztein, D.C., and Nixon, R.A. 2010. Rapamycin induces autophagic flux in neurons. Proc. Natl. Acad. Sci. **107**(49): E181–E181. doi:10.1073/pnas.1014633107.

Runne, H., Kuhn, A., Wild, E.J., Pratyaksha, W., Kristiansen, M., Isaacs, J.D., Régulier, E., Delorenzi, M., Tabrizi, S.J., and Luthi-Carter, R. 2007. Analysis of potential transcriptomic biomarkers for Huntington's disease in peripheral blood. Proc. Natl. Acad. Sci. U. S. A. **104**(36): 14424–14429. doi:10.1073/pnas.0703652104.

Rusek, M., Smith, J., El-Khatib, K., Aikins, K., Czuczwar, S.J., and Pluta, R. 2023. The role of the JAK/STAT signaling pathway in the pathogenesis of Alzheimer's disease: New potential treatment target. Int. J. Mol. Sci. **24**(1): 864. doi:10.3390/ijms24010864.

Rustenhoven, J., Drieu, A., Mamuladze, T., de Lima, K.A., Dykstra, T., Wall, M., Papadopoulos, Z., Kanamori, M., Salvador, A.F., Baker, W., Lemieux, M., Da Mesquita, S., Cugurra, A., Fitzpatrick, J., Sviben, S., Kossina, R., Bayguinov, P., Townsend, R.R., Zhang, Q., Erdmann-Gilmore, P., Smirnov, I., Lopes, M.-B., Herz, J., and Kipnis, J. 2021. Functional characterization of the dural sinuses as a neuroimmune interface. Cell **184**(4): 1000-1016.e27. doi:10.1016/j.cell.2020.12.040.

Sagredo, O., González, S., Aroyo, I., Pazos, M.R., Benito, C., Lastres-Becker, I., Romero, J.P., Tolón, R.M., Mechoulam, R., Brouillet, E., Romero, J., and Fernández-Ruiz, J. 2009. Cannabinoid CB_2 receptor agonists protect the striatum against malonate toxicity: Relevance for Huntington's disease. Glia **57**(11): 1154–1167. doi:10.1002/glia.20838.

Saha, R.N., Ghosh, A., Palencia, C.A., Fung, Y.K., Dudek, S.M., and Pahan, K. 2009. TNF-alpha preconditioning protects neurons via neuron-specific up-regulation of CREB-binding protein. J. Immunol. **183**(3): 2068–2078. doi:10.4049/jimmunol.0801892.

Sánchez, I., Xu, C.J., Juo, P., Kakizaka, A., Blenis, J., and Yuan, J. 1999. Caspase-8 is required for cell death induced by expanded polyglutamine repeats. Neuron **22**(3): 623–633. doi:10.1016/s0896-6273(00)80716-3.

Sandiego, C.M., Gallezot, J.-D., Pittman, B., Nabulsi, N., Lim, K., Lin, S.-F., Matuskey, D., Lee, J.-Y., O'Connor, K.C., Huang, Y., Carson, R.E., Hannestad, J., and Cosgrove, K.P. 2015. Imaging robust microglial activation after lipopolysaccharide administration in humans with PET. Proc. Natl. Acad. Sci. U. S. A. **112**(40): 12468–12473. doi:10.1073/pnas.1511003112.

Sangha, P.S., Thakur, M., Akhtar, Z., Ramani, S., and Gyamfi, R.S. 2020. The link between rheumatoid arthritis and dementia: A review. Cureus **12**(4): e7855. doi:10.7759/cureus.7855.

Sankowski, R., Mader, S., and Valdés-Ferrer, S.I. 2015. Systemic inflammation and the brain: novel roles of genetic, molecular, and environmental cues as drivers of neurodegeneration. Front. Cell. Neurosci. **9**: 28. doi:10.3389/fncel.2015.00028.

Sano, E., Kazaana, A., Tadakuma, H., Takei, T., Yoshimura, S., Hanashima, Y., Ozawa, Y., Yoshino, A., Suzuki, Y., and Ueda, T. 2021. Interleukin-6 sensitizes TNF-α and TRAIL/Apo2L dependent cell death through upregulation of death receptors in human cancer cells. Biochim. Biophys. Acta Mol. Cell Res. **1868**(7): 119037. doi:10.1016/j.bbamcr.2021.119037.

Sapp, E., Kegel, K.B., Aronin, N., Hashikawa, T., Uchiyama, Y., Tohyama, K., Bhide, P.G., Vonsattel, J.P., and DiFiglia, M. 2001. Early and progressive accumulation of reactive microglia in the Huntington disease brain. J. Neuropathol. Exp. Neurol. **60**(2): 161–172. doi:10.1093/jnen/60.2.161.

Sarkar, S., Ravikumar, B., Floto, R.A., and Rubinsztein, D.C. 2009. Rapamycin and mTOR-independent autophagy inducers ameliorate toxicity of polyglutamine-expanded huntingtin and related proteinopathies. Cell Death Differ. **16**(1): 46–56. doi:10.1038/cdd.2008.110.

Sattler, R., and Tymianski, M. 2001. Molecular mechanisms of glutamate receptor-mediated excitotoxic neuronal cell death. Mol. Neurobiol. **24**(1): 107–129. doi:10.1385/MN:24:1-3:107.

Sayoc-Becerra, A., Krishnan, M., Fan, S., Jimenez, J., Hernandez, R., Gibson, K., Preciado, R., Butt, G., and McCole, D.F. 2020. The JAK-Inhibitor tofacitinib rescues human intestinal epithelial cells and colonoids from cytokine-induced

barrier dysfunction. Inflamm. Bowel Dis. **26**(3): 407–422. doi:10.1093/ibd/izz266.

Schafer, D.P., Lehrman, E.K., Kautzman, A.G., Koyama, R., Mardinly, A.R., Yamasaki, R., Ransohoff, R.M., Greenberg, M.E., Barres, B.A., and Stevens, B. 2012. Microglia sculpt postnatal neural circuits in an activity and complement-dependent manner. Neuron **74**(4): 691–705. doi:10.1016/j.neuron.2012.03.026.

Schafer, D.P., and Stevens, B. 2015. Microglia function in central nervous system development and plasticity. Cold Spring Harb. Perspect. Biol. **7**(10). doi:10.1101/cshperspect.a020545.

Scharf, S., Mander, A., Ugoni, A., Vajda, F., and Christophidis, N. 1999. A double-blind, placebo-controlled trial of diclofenac/misoprostol in Alzheimer's disease. Neurology **53**(1): 197–201. doi:10.1212/wnl.53.1.197.

Schiltz, J.C., and Sawchenko, P.E. 2002. Distinct brain vascular cell types manifest inducible cyclooxygenase expression as a function of the strength and nature of immune insults. J. Neurosci. **22**(13): 5606–5618. doi:10.1523/JNEUROSCI.22-13-05606.2002.

Schmöle, A.-C., Lundt, R., Ternes, S., Albayram, Ö., Ulas, T., Schultze, J.L., Bano, D., Nicotera, P., Alferink, J., and Zimmer, A. 2015. Cannabinoid receptor 2 deficiency results in reduced neuroinflammation in an Alzheimer's disease mouse model. Neurobiol. Aging **36**(2): 710–719. doi:10.1016/j.neurobiolaging.2014.09.019.

Schroder, K., Hertzog, P.J., Ravasi, T., and Hume, D.A. 2004. Interferon-γ: an overview of signals, mechanisms and functions. J. Leukoc. Biol. **75**(2): 163–189. doi:10.1189/jlb.0603252.

Schroder, K., Sweet, M.J., and Hume, D.A. 2006. Signal integration between IFNγ and TLR signalling pathways in macrophages. Immunobiology **211**(6): 511–524. doi:10.1016/j.imbio.2006.05.007.

Schwartz, D.M., Bonelli, M., Gadina, M., and O'Shea, J.J. 2016. Type I/II cytokines, JAKs, and new strategies for treating autoimmune diseases. Nat. Rev. Rheumatol. **12**(1): 25–36. doi:10.1038/nrrheum.2015.167.

Schwartz, D.M., Kanno, Y., Villarino, A., Ward, M., Gadina, M., and O'Shea, J.J. 2017. JAK inhibition as a therapeutic strategy for immune and inflammatory diseases. Nat. Rev. Drug Discov. **17**(1): 78. doi:10.1038/nrd.2017.267.

Sekar, A., Bialas, A.R., de Rivera, H., Davis, A., Hammond, T.R., Kamitaki, N., Tooley, K., Presumey, J., Baum, M., Van Doren, V., Genovese, G., Rose, S.A., Handsaker, R.E., Daly, M.J., Carroll, M.C., Stevens, B., and McCarroll, S.A. 2016. Schizophrenia risk from complex variation of complement component 4. Nature **530**(7589): 177–183. doi:10.1038/nature16549.

Selkoe, D.J., and Hardy, J. 2016. The amyloid hypothesis of Alzheimer's disease at 25 years. EMBO Mol. Med. **8**(6): 595–608. doi:10.15252/emmm.201606210.

Sellgren, C.M., Gracias, J., Watmuff, B., Biag, J.D., Thanos, J.M., Whittredge, P.B., Fu, T., Worringer, K., Brown, H.E., Wang, J., Kaykas, A., Karmacharya, R., Goold, C.P., Sheridan, S.D., and Perlis, R.H. 2019. Increased synapse elimination by microglia in schizophrenia patient-derived models of synaptic pruning. Nat. Neurosci. **22**(3): 374–385. doi:10.1038/s41593-018-0334-7.

Setiawan, E., Wilson, A.A., Mizrahi, R., Rusjan, P.M., Miler, L., Rajkowska, G., Suridjan, I., Kennedy, J.L., Rekkas, P.V., Houle, S., and Meyer, J.H. 2015. Role of Translocator Protein Density, a Marker of Neuroinflammation, in the Brain During Major Depressive Episodes. JAMA Psychiatry **72**(3): 268–275. doi:10.1001/jamapsychiatry.2014.2427.

Shi, J.-Q., Shen, W., Chen, J., Wang, B.-R., Zhong, L.-L., Zhu, Y.-W., Zhu, H.-Q., Zhang, Q.-Q., Zhang, Y.-D., and Xu, J. 2011. Anti-TNF-α reduces amyloid plaques and tau phosphorylation and induces CD11c-positive dendritic-like cell in the APP/PS1 transgenic mouse brains. Brain Res. **1368**: 239–247. doi:10.1016/j.brainres.2010.10.053.

Shirai, Y. 1921. On the transplantation of the rat sarcoma in adult heterogenous animals. Jap Med World **1**: 14–15.

Sicotte, N.L., and Voskuhl, R.R. 2001. Onset of multiple sclerosis associated with anti-TNF therapy. Neurology **57**(10): 1885–1888. doi:10.1212/WNL.57.10.1885.

Siegel, R.M. 2006. Caspases at the crossroads of immune-cell life and death. Nat. Rev. Immunol. **6**(4): 308–317. doi:10.1038/nri1809.

Sieradzan, K.A., and Mann, D.M. 2001. The selective vulnerability of nerve cells in Huntington's disease. Neuropathol. Appl. Neurobiol. **27**(1): 1–21. doi:10.1046/j.0305-1846.2001.00299.x.

Sipieter, F., Cappe, B., Leray, A., De Schutter, E., Bridelance, J., Hulpiau, P., Van Camp, G., Declercq, W., Héliot, L., Vincent, P., Vandenabeele, P., and Riquet, F.B. 2021. Characteristic ERK1/2 signaling dynamics distinguishes necroptosis from apoptosis. iScience **24**(9): 103074. doi:10.1016/j.isci.2021.103074.

Sipilä, P.N., Heikkilä, N., Lindbohm, J.V., Hakulinen, C., Vahtera, J., Elovainio, M., Suominen, S., Väänänen, A., Koskinen, A., Nyberg, S.T., Pentti, J., Strandberg, T.E., and Kivimäki, M. 2021. Hospital-treated infectious diseases and the risk of dementia: a large, multicohort, observational study with a replication cohort. Lancet Infect. Dis. **21**(11): 1557–1567. doi:10.1016/S1473-3099(21)00144-4.

Skrzypczak-Wiercioch, A., and Sałat, K. 2022. Lipopolysaccharide-induced model of neuroinflammation: Mechanisms of action, research application and future directions for its use. Molecules **27**(17): 5481. doi:10.3390/molecules27175481.

Smoum, R., Baraghithy, S., Chourasia, M., Breuer, A., Mussai, N., Attar-Namdar, M., Kogan, N.M., Raphael, B., Bolognini, D., Cascio, M.G., Marini, P., Pertwee, R.G., Shurki, A., Mechoulam, R., and Bab, I. 2015. CB_2 cannabinoid receptor agonist enantiomers HU-433 and HU-308: An inverse relationship between binding affinity and biological potency. Proc. Natl. Acad. Sci. **112**(28): 8774–8779. doi:10.1073/pnas.1503395112.

Soethoudt, M., Grether, U., Fingerle, J., Grim, T.W., Fezza, F., de Petrocellis, L., Ullmer, C., Rothenhäusler, B., Perret, C., van Gils, N., Finlay, D., MacDonald, C., Chicca, A., Gens, M.D., Stuart, J., de Vries, H., Mastrangelo, N., Xia, L., Alachouzos, G., Baggelaar, M.P., Martella, A., Mock, E.D., Deng, H., Heitman, L.H., Connor, M., Di Marzo, V., Gertsch, J., Lichtman, A.H., Maccarrone, M., Pacher, P., Glass, M., and van der Stelt, M. 2017. Cannabinoid CB_2 receptor ligand profiling reveals biased signalling and off-target activity. Nat. Commun. **8**: 13958. doi:10.1038/ncomms13958.

Sominsky, L., Walker, A.K., Ong, L.K., Tynan, R.J., Walker, F.R., and Hodgson, D.M. 2012. Increased microglial activation in the rat brain following neonatal exposure to a bacterial mimetic. Behav. Brain Res. **226**(1): 351–356. doi:10.1016/j.bbr.2011.08.038.

Spangenberg, E., Severson, P.L., Hohsfield, L.A., Crapser, J., Zhang, J., Burton, E.A., Zhang, Y., Spevak, W., Lin, J., Phan, N.Y., Habets, G., Rymar, A., Tsang, G., Walters, J., Nespi, M., Singh, P., Broome, S., Ibrahim, P., Zhang, C., Bollag, G., West, B.L., and Green, K.N. 2019. Sustained microglial depletion with CSF1R inhibitor impairs parenchymal plaque development in an Alzheimer's disease model. Nat. Commun. **10**(1): 3758. doi:10.1038/s41467-019-11674-z.

Spangenberg, E.E., Lee, R.J., Najafi, A.R., Rice, R.A., Elmore, M.R.P., Blurton-Jones, M., West, B.L., and Green, K.N. 2016. Eliminating microglia in Alzheimer's mice prevents neuronal loss without modulating amyloid-β pathology. Brain **139**(4): 1265–1281. doi:10.1093/brain/aww016.

Spilman, P., Podlutskaya, N., Hart, M.J., Debnath, J., Gorostiza, O., Bredesen, D., Richardson, A., Strong, R., and Galvan, V. 2010. Inhibition of mTOR by rapamycin abolishes cognitive deficits and reduces amyloid-beta levels in a mouse model of Alzheimer's disease. PloS One **5**(4): e9979. doi:10.1371/journal.pone.0009979.

Staiano, R.I., Loffredo, S., Borriello, F., Iannotti, F.A., Piscitelli, F., Orlando, P., Secondo, A., Granata, F., Lepore, M.T., Fiorelli, A., Varricchi, G., Santini, M., Triggiani, M., Di Marzo, V., and Marone, G. 2016. Human lung-resident macrophages express CB_1 and CB_2 receptors whose activation inhibits the release of angiogenic and lymphangiogenic factors. J. Leukoc. Biol. **99**(4): 531–540. doi:10.1189/jlb.3HI1214-584R.

Stefanova, N.A., Muraleva, N.A., Maksimova, K.Y., Rudnitskaya, E.A., Kiseleva, E., Telegina, D.V., and Kolosova, N.G. 2016. An antioxidant specifically targeting mitochondria delays progression of Alzheimer's disease-like pathology. Aging **8**(11): 2713–2733. doi:10.18632/aging.101054.

Steiner, J., Bielau, H., Brisch, R., Danos, P., Ullrich, O., Mawrin, C., Bernstein, H.-G., and Bogerts, B. 2008. Immunological aspects in the neurobiology of suicide: elevated microglial density in schizophrenia and depression is associated with suicide. J. Psychiatr. Res. **42**(2): 151–157. doi:10.1016/j.jpsychires.2006.10.013.

Stella, N. 2009. Endocannabinoid signaling in microglial cells. Neuropharmacology **56**(Suppl 1): 244–253. doi:10.1016/j.neuropharm.2008.07.037.

Stella, N. 2010. Cannabinoid and cannabinoid-like receptors in microglia, astrocytes and astrocytomas. Glia **58**(9): 1017–1030. doi:10.1002/glia.20983.

Stellwagen, D., and Malenka, R.C. 2006. Synaptic scaling mediated by glial TNF-alpha. Nature **440**(7087): 1054–1059. doi:10.1038/nature04671.

Stempel, A.V., Stumpf, A., Zhang, H.-Y., Özdoğan, T., Pannasch, U., Theis, A.-K., Otte, D.-M., Wojtalla, A., Rácz, I., Ponomarenko, A., Xi, Z.-X., Zimmer, A., and Schmitz, D. 2016. Cannabinoid type 2 receptors mediate a cell type-specific plasticity in the hippocampus. Neuron **90**(4): 795–809. doi:10.1016/j.neuron.2016.03.034.

Stevens, B., Allen, N.J., Vazquez, L.E., Howell, G.R., Christopherson, K.S., Nouri, N., Micheva, K.D., Mehalow, A.K., Huberman, A.D., Stafford, B., Sher, A., Litke, A.M., Lambris, J.D., Smith, S.J., John, S.W.M., and Barres, B.A. 2007. The classical complement cascade mediates CNS synapse elimination. Cell **131**(6): 1164–1178. doi:10.1016/j.cell.2007.10.036.

Stevens, B., and Johnson, M.B. 2021. The complement cascade repurposed in the brain. Nat. Rev. Immunol. **21**(10): 624–625. doi:10.1038/s41577-021-00621-z.

Subedi, L., Kwon, O.W., Pak, C., Lee, G., Lee, K., Kim, H., and Kim, S.Y. 2017. N,N-disubstituted azines attenuate LPS-mediated neuroinflammation in microglia and neuronal apoptosis via inhibiting MAPK signaling pathways. BMC Neurosci. **18**: 82. doi:10.1186/s12868-017-0399-3.

Suk, K., Chang, I., Kim, Y.-H., Kim, S., Kim, J.Y., Kim, H., and Lee, M.-S. 2001. Interferon γ (IFNγ) and tumor necrosis factor α synergism in me-180 cervical cancer cell apoptosis and necrosis: ifnγ inhibits cytoprotective nf-κb through stat1/irf-1 pathways. J. Biol. Chem. **276**(16): 13153–13159. doi:10.1074/jbc.M007646200.

Sun, J., Ludvigsson, J.F., Ingre, C., Piehl, F., Wirdefeldt, K., Zagai, U., Ye, W., and Fang, F. 2022. Hospital-treated infections in early- and mid-life and risk of Alzheimer's disease, Parkinson's disease, and amyotrophic lateral sclerosis: A nationwide nested case-control study in Sweden. PLoS Med. **19**(9). PLOS. doi:10.1371/journal.pmed.1004092.

Sun, L., Wang, H., Wang, Z., He, S., Chen, S., Liao, D., Wang, L., Yan, J., Liu, W., Lei, X., and Wang, X. 2012. Mixed lineage kinase domain-like protein mediates necrosis signaling downstream of RIP3 kinase. Cell **148**(1–2): 213–227. doi:10.1016/j.cell.2011.11.031.

Sun, X., Lee, J., Navas, T., Baldwin, D.T., Stewart, T.A., and Dixit, V.M. 1999. RIP3, a novel apoptosis-inducing kinase. J. Biol. Chem. **274**(24): 16871–16875. doi:10.1074/jbc.274.24.16871.

Sun, X., Yin, J., Starovasnik, M.A., Fairbrother, W.J., and Dixit, V.M. 2002. Identification of a novel homotypic interaction motif required for the phosphorylation of receptor-interacting Protein (RIP) by RIP3. J. Biol. Chem. **277**(11): 9505–9511. doi:10.1074/jbc.M109488200.

Swardfager, W., Lanctôt, K., Rothenburg, L., Wong, A., Cappell, J., and Herrmann, N. 2010. A meta-analysis of cytokines in Alzheimer's disease. Biol. Psychiatry **68**(10): 930–941. Elsevier. doi:10.1016/j.biopsych.2010.06.012.

Szepesi, Z., Manouchehrian, O., Bachiller, S., and Deierborg, T. 2018. Bidirectional microglia–neuron communication in health and disease. Front. Cell. Neurosci. **12**.

Tabrizi, M.A., Baraldi, P.G., Borea, P.A., and Varani, K. 2016. medicinal chemistry, pharmacology, and potential therapeutic benefits of cannabinoid CB_2 receptor agonists. Chem. Rev. **116**(2): 519–560. doi:10.1021/acs.chemrev.5b00411.

Tai, Y.F., Pavese, N., Gerhard, A., Tabrizi, S.J., Barker, R.A., Brooks, D.J., and Piccini, P. 2007. Microglial activation in presymptomatic Huntington's disease gene carriers. Brain **130**(Pt 7): 1759–1766. doi:10.1093/brain/awm044.

Takashima, K., Matsunaga, N., Yoshimatsu, M., Hazeki, K., Kaisho, T., Uekata, M., Hazeki, O., Akira, S., Iizawa, Y., and Ii, M. 2009. Analysis of binding site for the novel small-molecule TLR4 signal transduction inhibitor TAK-242 and its therapeutic effect on mouse sepsis model. Br. J. Pharmacol. **157**(7): 1250–1262. doi:10.1111/j.1476-5381.2009.00297.x.

Takeuchi, H., Jin, S., Wang, J., Zhang, G., Kawanokuchi, J., Kuno, R., Sonobe, Y., Mizuno, T., and Suzumura, A. 2006. Tumor necrosis factor-α induces neurotoxicity via glutamate release from hemichannels of activated microglia in an autocrine manner. J. Biol. Chem. **281**(30): 21362–21368. doi:10.1074/jbc.M600504200.

Tan, Z.S., Beiser, A.S., Vasan, R.S., Roubenoff, R., Dinarello, C.A., Harris, T.B., Benjamin, E.J., Au, R., Kiel, D.P., Wolf, P.A., and Seshadri, S. 2007. Inflammatory markers and the risk of Alzheimer disease: the Framingham Study. Neurology **68**(22): 1902–1908. doi:10.1212/01.wnl.0000263217.36439.da.

Tanaka, M., Sackett, S., and Zhang, Y. 2020. Endocannabinoid modulation of microglial phenotypes in neuropathology. Front. Neurol. **11**: 87. doi:10.3389/fneur.2020.00087.

Tang, T.-S., Slow, E., Lupu, V., Stavrovskaya, I.G., Sugimori, M., Llinás, R., Kristal, B.S., Hayden, M.R., and Bezprozvanny, I. 2005. Disturbed Ca2+ signaling and apoptosis of medium spiny neurons in Huntington's disease. Proc. Natl. Acad. Sci. **102**(7): 2602–2607. doi:10.1073/pnas.0409402102.

Tang, T.-S., Tu, H., Chan, E.Y.W., Maximov, A., Wang, Z., Wellington, C.L., Hayden, M.R., and Bezprozvanny, I. 2003. Huntingtin and Huntingtin-associated protein 1 influence neuronal calcium signaling mediated by inositol-(1,4,5) triphosphate receptor type 1. Neuron **39**(2): 227–239. doi:10.1016/S0896-6273(03)00366-0.

Tarkowski, E., Liljeroth, A.M., Minthon, L., Tarkowski, A., Wallin, A., and Blennow, K. 2003. Cerebral pattern of pro- and anti-inflammatory cytokines in dementias. Brain Res. Bull. **61**(3): 255–260. doi:10.1016/s0361-9230(03)00088-1.

Tau, G., and Rothman, P. 1999. Biologic functions of the IFN-γ receptors. Allergy **54**(12): 1233–1251. doi:10.1034/j.1398-9995.1999.00099.x.

Taylor, D.L., Jones, F., Kubota, E.S.F.C.S., and Pocock, J.M. 2005. Stimulation of microglial metabotropic glutamate receptor mGlu2 triggers tumor necrosis factor α-induced neurotoxicity in concert with microglial-derived Fas ligand. J. Neurosci. **25**(11): 2952–2964. doi:10.1523/JNEUROSCI.4456-04.2005.

Taylor, J.M., Moore, Z., Minter, M.R., and Crack, P.J. 2018. Type-I interferon pathway in neuroinflammation and neurodegeneration: focus on Alzheimer's disease. J. Neural Transm. **125**(5): 797–807. doi:10.1007/s00702-017-1745-4.

Thapa, D., Cairns, E.A., Szczesniak, A.-M., Toguri, J.T., Caldwell, M.D., and Kelly, M.E.M. 2018. The cannabinoids Δ8THC, CBD, and HU-308 act via distinct receptors to reduce corneal pain and inflammation. Cannabis Cannabinoid Res. **3**(1): 11–20. doi:10.1089/can.2017.0041.

Toguri, J.T., Lehmann, C., Laprairie, R.B., Szczesniak, A.M., Zhou, J., Denovan-Wright, E.M., and Kelly, M.E.M. 2014. Anti-inflammatory effects of cannabinoid CB_2 receptor activation in endotoxin-induced uveitis. Br. J. Pharmacol. **171**(6): 1448–1461. doi:10.1111/bph.12545.

Too, L.K., Ball, H.J., McGregor, I.S., and Hunt, N.H. 2014. The pro-inflammatory cytokine interferon-gamma is an important driver of neuropathology and behavioural sequelae in experimental pneumococcal meningitis. Brain. Behav. Immun. **40**: 252–268. doi:10.1016/j.bbi.2014.02.020.

Torres-Acosta, N., O'Keefe, J.H., O'Keefe, E.L., Isaacson, R., and Small, G. 2020. Therapeutic potential of TNF-α inhibition for Alzheimer's disease prevention. J. Alzheimers Dis. **78**(2): 619–626. doi:10.3233/JAD-200711.

Torres-Platas, S.G., Cruceanu, C., Chen, G.G., Turecki, G., and Mechawar, N. 2014. Evidence for increased microglial priming and macrophage recruitment in the dorsal anterior cingulate white matter of depressed suicides. Brain. Behav. Immun. **42**: 50–59. doi:10.1016/j.bbi.2014.05.007.

Town, T., Tan, J., Flavell, R.A., and Mullan, M. 2005. T-cells in Alzheimer's disease. Neuromolecular Med. **7**(3): 255–264. doi:10.1385/NMM:7:3:255.

Träger, U., Andre, R., Lahiri, N., Magnusson-Lind, A., Weiss, A., Grueninger, S., McKinnon, C., Sirinathsinghji, E., Kahlon, S., Pfister, E.L., Moser, R., Hummerich, H., Antoniou, M., Bates, G.P., Luthi-Carter, R., Lowdell, M.W., Björkqvist, M., Ostroff, G.R., Aronin, N., and Tabrizi, S.J. 2014. HTT-lowering reverses Huntington's disease immune dysfunction caused by NFκB pathway dysregulation. Brain **137**(3): 819–833. doi:10.1093/brain/awt355.

Trettel, F., Rigamonti, D., Hilditch-Maguire, P., Wheeler, V.C., Sharp, A.H., Persichetti, F., Cattaneo, E., and MacDonald, M.E. 2000. Dominant phenotypes produced by the HD mutation in STHdh(Q111) striatal cells. Hum. Mol. Genet. **9**(19): 2799–2809. doi:10.1093/hmg/9.19.2799.

Tsiavou, A., Hatziagelaki, E., Chaidaroglou, A., Koniavitou, K., Degiannis, D., and Raptis, S.A. 2005. Correlation between intracellular interferon-gamma (IFN-gamma) production by CD4+ and CD8+ lymphocytes and IFN-gamma gene polymorphism in patients with type 2 diabetes mellitus and latent autoimmune diabetes of adults (LADA). Cytokine **31**(2): 135–141. doi:10.1016/j.cyto.2005.02.011.

Tuazon Kels, Ma.J., Ng, E., Al Rumaih, Z., Pandey, P., Ruuls, S.R., Korner, H., Newsome, T.P., Chaudhri, G., and Karupiah, G. 2020. TNF deficiency dysregulates inflammatory cytokine production, leading to lung pathology and death during respiratory poxvirus infection. Proc. Natl. Acad. Sci. **117**(27): 15935–15946. doi:10.1073/pnas.2004615117.

Turcotte, C., Blanchet, M.-R., Laviolette, M., and Flamand, N. 2016. The CB_2 receptor and its role as a regulator of inflammation. Cell. Mol. Life Sci. **73**(23): 4449–4470. doi:10.1007/s00018-016-2300-4.

Ueno, M., Fujita, Y., Tanaka, T., Nakamura, Y., Kikuta, J., Ishii, M., and Yamashita, T. 2013. Layer V cortical neurons require microglial support for survival during postnatal development. Nat. Neurosci. **16**(5): 543–551. doi:10.1038/nn.3358.

Valadão, P.A.C., Santos, K.B.S., Ferreira e Vieira, T.H., Macedo e Cordeiro, T., Teixeira, A.L., Guatimosim, C., and de Miranda, A.S. 2020. Inflammation in Huntington's disease: A few new twists on an old tale. J. Neuroimmunol. **348**: 577380. doi:10.1016/j.jneuroim.2020.577380.

Vargas-Caraveo, A., Sayd, A., Maus, S.R., Caso, J.R., Madrigal, J.L.M., García-Bueno, B., and Leza, J.C. 2017. Lipopolysaccharide enters the rat brain by a lipoprotein-mediated transport mechanism in physiological conditions. Sci. Rep. **7**(1): 13113. doi:10.1038/s41598-017-13302-6.

Vatanen, T., Kostic, A.D., d'Hennezel, E., Siljander, H., Franzosa, E.A., Yassour, M., Kolde, R., Vlamakis, H., Arthur, T.D., Hämäläinen, A.-M., Peet, A., Tillmann, V., Uibo, R., Mokurov, S., Dorshakova, N., Ilonen, J., Virtanen, S.M., Szabo, S.J., Porter, J.A., Lähdesmäki, H., Huttenhower, C., Gevers, D., Cullen, T.W., Knip, M., and Xavier, R.J. 2016. Variation in microbiome LPS immunogenicity contributes to autoimmunity in humans. Cell **165**(4): 842–853. doi:10.1016/j.cell.2016.04.007.

Vaux, D.L., and Korsmeyer, S.J. 1999. Cell death in development. Cell **96**(2): 245–254. doi:10.1016/S0092-8674(00)80564-4.

in t' Veld, B.A., Ruitenberg, A., Hofman, A., Launer, L.J., van Duijn, C.M., Stijnen, T., Breteler, M.M., and Stricker, B.H. 2001. Nonsteroidal antiinflammatory drugs and the risk of Alzheimer's disease. N. Engl. J. Med. **345**(21): 1515–1521. doi:10.1056/NEJMoa010178.

Villa, A., Gelosa, P., Castiglioni, L., Cimino, M., Rizzi, N., Pepe, G., Lolli, F., Marcello, E., Sironi, L., Vegeto, E., and Maggi, A. 2018. Sex-specific features of microglia from adult mice. Cell Rep. **23**(12): 3501–3511. doi:10.1016/j.celrep.2018.05.048.

Villarino, A.V., Kanno, Y., and O'Shea, J.J. 2017. Mechanisms and consequences of Jak–STAT signaling in the immune system. Nat. Immunol. **18**(4): 374–384. Nature Publishing Group. doi:10.1038/ni.3691.

Viviani, B., Bartesaghi, S., Gardoni, F., Vezzani, A., Behrens, M.M., Bartfai, T., Binaglia, M., Corsini, E., Di Luca, M., Galli, C.L., and Marinovich, M. 2003. Interleukin-1β enhances NMDA receptor-mediated intracellular calcium increase through activation of the Src family of kinases. J. Neurosci. **23**(25): 8692–8700. doi:10.1523/JNEUROSCI.23-25-08692.2003.

Vlad, S.C., Miller, D.R., Kowall, N.W., and Felson, D.T. 2008. Protective effects of NSAIDs on the development of Alzheimer disease. Neurology **70**(19): 1672–1677. doi:10.1212/01.wnl.0000311269.57716.63.

Vogel, S.N., Fitzgerald, K.A., and Fenton, M.J. 2003. TLRs: differential adapter utilization by toll-like receptors mediates TLR-specific patterns of gene expression. Mol. Interv. **3**(8): 466–477. doi:10.1124/mi.3.8.466.

Vogt, N.M., Kerby, R.L., Dill-McFarland, K.A., Harding, S.J., Merluzzi, A.P., Johnson, S.C., Carlsson, C.M., Asthana, S., Zetterberg, H., Blennow, K., Bendlin, B.B., and Rey, F.E. 2017. Gut microbiome alterations in Alzheimer's disease. Sci. Rep. **7**(1): 13537. doi:10.1038/s41598-017-13601-y.

Volkow, N.D., Baler, R.D., Compton, W.M., and Weiss, S.R.B. 2014. Adverse health effects of marijuana use. N. Engl. J. Med. **370**(23): 2219–2227. doi:10.1056/NEJMra1402309.

Vonkeman, H.E., and van de Laar, M.A.F.J. 2010. Nonsteroidal anti-inflammatory drugs: adverse effects and their prevention. Semin. Arthritis Rheum. **39**(4): 294–312. doi:10.1016/j.semarthrit.2008.08.001.

Waetzig, V., Czeloth, K., Hidding, U., Mielke, K., Kanzow, M., Brecht, S., Goetz, M., Lucius, R., Herdegen, T., and Hanisch, U.-K. 2005. c-Jun N-terminal kinases (JNKs) mediate pro-inflammatory actions of microglia. Glia **50**(3): 235–246. doi:10.1002/glia.20173.

Waksman, Y., Olson, J.M., Carlisle, S.J., and Cabral, G.A. 1999. The central cannabinoid receptor (CB1) mediates inhibition of nitric oxide production by rat microglial cells. J. Pharmacol. Exp. Ther. **288**(3): 1357–1366.

Walker, D.G., Dalsing-Hernandez, J.E., Campbell, N.A., and Lue, L.-F. 2009. Decreased expression of CD200 and CD200 receptor in Alzheimer's disease: A potential mechanism leading to chronic inflammation. Exp. Neurol. **215**(1): 5–19. doi:10.1016/j.expneurol.2008.09.003.

Walsh, J.T., Watson, N., and Kipnis, J. 2014. T cells in the central nervous system: messengers of destruction or purveyors of protection? Immunology **141**(3): 340–344. doi:10.1111/imm.12187.

Walter, L., Franklin, A., Witting, A., Wade, C., Xie, Y., Kunos, G., Mackie, K., and Stella, N. 2003. Nonpsychotropic cannabinoid receptors regulate microglial cell migration. J. Neurosci. **23**(4): 1398–1405.

Wang, H.-M., Zhang, T., Huang, J.-K., Xiang, J.-Y., Chen, J.-J., Fu, J.-L., and Zhao, Y.-W. 2017. Edaravone attenuates the proinflammatory response in amyloid-β-treated microglia by inhibiting NLRP3 inflammasome-mediated IL-1β Secretion. Cell. Physiol. Biochem. **43**(3): 1113–1125. doi:10.1159/000481753.

Wang, K.-C., Fan, L.-W., Kaizaki, A., Pang, Y., Cai, Z., and Tien, L.-T. 2013. Neonatal lipopolysaccharide exposure induces long-lasting learning impairment, less anxiety-like response and hippocampal injury in adult rats. Neuroscience **234**: 146–157. doi:10.1016/j.neuroscience.2012.12.049.

Wang, L., Du, F., and Wang, X. 2008. TNF-α induces two distinct caspase-8 activation pathways. Cell **133**(4): 693–703. doi:10.1016/j.cell.2008.03.036.

Wang, W.-Y., Tan, M.-S., Yu, J.-T., and Tan, L. 2015. Role of pro-inflammatory cytokines released from microglia in Alzheimer's disease. Ann. Transl. Med. **3**(10): 136. doi:10.3978/j.issn.2305-5839.2015.03.49.

Wang, X., Su, B., Lee, H., Li, X., Perry, G., Smith, M.A., and Zhu, X. 2009. Impaired balance of mitochondrial fission and fusion in Alzheimer's disease. J. Neurosci. **29**(28): 9090–9103. doi:10.1523/JNEUROSCI.1357-09.2009.

Watad, A., McGonagle, D., Anis, S., Carmeli, R., Cohen, A.D., Tsur, A.M., Ben-Shabat, N., Luigi Bragazzi, N., Lidar, M., and Amital, H. 2022. TNF inhibitors have a protective role in the risk of dementia in patients with ankylosing spondylitis: Results from a nationwide study. Pharmacol. Res. **182**: 106325. doi:10.1016/j.phrs.2022.106325.

Webster, J.D., and Vucic, D. 2020. The balance of TNF mediated pathways regulates inflammatory cell death signaling in healthy and diseased tissues. Front. Cell Dev. Biol. **8**.

Wen, A.Y., Sakamoto, K.M., and Miller, L.S. 2010. The role of the transcription factor CREB in immune function. J. Immunol. **185**(11): 6413–6419. doi:10.4049/jimmunol.1001829.

Wenger, T., and Moldrich, G. 2002. The role of endocannabinoids in the hypothalamic regulation of visceral function. Prostaglandins Leukot. Essent. Fat. Acids **66**(2): 301–307. doi:10.1054/plef.2001.0353.

Whiting, Z.M., Yin, J., de la Harpe, S.M., Vernall, A.J., and Grimsey, N.L. 2022. Developing the cannabinoid receptor 2 (CB_2) pharmacopoeia: past, present, and future. Trends Pharmacol. Sci. **43**(9): 754–771. doi:10.1016/j.tips.2022.06.010.

Widmann, C.N., and Heneka, M.T. 2014. Long-term cerebral consequences of sepsis. Lancet Neurol. **13**(6): 630–636. Elsevier. doi:10.1016/S1474-4422(14)70017-1.

Widner, H., and Brundin, P. 1988. Immunological aspects of grafting in the mammalian central nervous system. A review and speculative synthesis. Brain Res. Rev. **13**(3): 287–324. doi:10.1016/0165-0173(88)90010-0.

Williams, S.K., Fairless, R., Maier, O., Liermann, P.C., Pichi, K., Fischer, R., Eisel, U.L.M., Kontermann, R., Herrmann, A., Weksler, B., Romero, N., Couraud, P.-O., Pfizenmaier, K., and Diem, R. 2018. Anti-TNFR1 targeting in humanized mice ameliorates disease in a model of multiple sclerosis. Sci. Rep. **8**(1): 13628. Nature Publishing Group. doi:10.1038/s41598-018-31957-7.

Wilton, D.K., Mastro, K., Heller, M.D., Gergits, F.W., Willing, C.R., Frouin, A., Daggett, A., Gu, X., Kim, A.Y., Faull, R., Jayadev, S., Yednock, T., Yang, X.W., and Stevens, B. 2021, December 4. Microglia mediate early corticostriatal synapse loss and cognitive dysfunction in Huntington's disease through complement-dependent mechanisms. bioRxiv. doi:10.1101/2021.12.03.471180.

Witcher, K.G., Bray, C.E., Chunchai, T., Zhao, F., O'Neil, S.M., Gordillo, A.J., Campbell, W.A., McKim, D.B., Liu, X., Dziabis, J.E., Quan, N., Eiferman, D.S., Fischer, A.J., Kokiko-Cochran, O.N., Askwith, C., and Godbout, J.P. 2021. Traumatic brain injury causes chronic cortical inflammation and neuronal

dysfunction mediated by microglia. J. Neurosci. **41**(7): 1597–1616. doi:10.1523/JNEUROSCI.2469-20.2020.

Witting, A., Chen, L., Cudaback, E., Straiker, A., Walter, L., Rickman, B., Möller, T., Brosnan, C., and Stella, N. 2006. Experimental autoimmune encephalomyelitis disrupts endocannabinoid-mediated neuroprotection. Proc. Natl. Acad. Sci. U. S. A. **103**(16): 6362–6367. doi:10.1073/pnas.0510418103.

Witting, A., Walter, L., Wacker, J., Möller, T., and Stella, N. 2004. $P2X_7$ receptors control 2-arachidonoylglycerol production by microglial cells. Proc. Natl. Acad. Sci. U. S. A. **101**(9): 3214–3219. doi:10.1073/pnas.0306707101.

Woodhams, S.G., Sagar, D.R., Burston, J.J., and Chapman, V. 2015. The role of the endocannabinoid system in pain. Handb. Exp. Pharmacol. **227**: 119–143. doi:10.1007/978-3-662-46450-2_7.

Woods, J.J., Novorolsky, R.J., Bigham, N.P., Robertson, G.S., and Wilson, J.J. 2023. Dinuclear nitrido-bridged osmium complexes inhibit the mitochondrial calcium uniporter and protect cortical neurons against lethal oxygen–glucose deprivation. RSC Chem. Biol. **4**(1): 84–93. doi:10.1039/d2cb00189f.

Wotherspoon, G., Fox, A., McIntyre, P., Colley, S., Bevan, S., and Winter, J. 2005. Peripheral nerve injury induces cannabinoid receptor 2 protein expression in rat sensory neurons. Neuroscience **135**(1): 235–245. doi:10.1016/j.neuroscience.2005.06.009.

Wright, C.L., Hoffman, J.H., and McCarthy, M.M. 2019. Evidence that inflammation promotes estradiol synthesis in human cerebellum during early childhood. Transl. Psychiatry **9**(1): 58. doi:10.1038/s41398-018-0363-8.

Wright, S.D., Ramos, R.A., Tobias, P.S., Ulevitch, R.J., and Mathison, J.C. 1990. CD14, a receptor for complexes of lipopolysaccharide (LPS) and LPS binding protein. science **249**(4975): 1431–1433. doi:10.1126/science.1698311.

Wu, J., Shih, H.-P., Vigont, V., Hrdlicka, L., Diggins, L., Singh, C., Mahoney, M., Chesworth, R., Shapiro, G., Zimina, O., Chen, X., Wu, Q., Glushankova, L., Ahlijanian, M., Koenig, G., Mozhayeva, G.N., Kaznacheyeva, E., and Bezprozvanny, I. 2011. Neuronal store-operated calcium entry pathway as a novel

therapeutic target for Huntington's disease treatment. Chem. Biol. **18**(6): 777–793. doi:10.1016/j.chembiol.2011.04.012.

Wu, J., Wang, J., Zhou, S., Yang, L., Yin, J., Cao, J., and Cheng, Y. 2015. Necrostatin-1 protection of dopaminergic neurons. Neural Regen. Res. **10**(7): 1120–1124. doi:10.4103/1673-5374.160108.

Wynne, A.M., Henry, C.J., Huang, Y., Cleland, A., and Godbout, J.P. 2010. Protracted downregulation of CX3CR1 on microglia of aged mice after lipopolysaccharide challenge. Brain. Behav. Immun. **24**(7): 1190–1201. doi:10.1016/j.bbi.2010.05.011.

Xie, L., Zhang, N., Zhang, Q., Li, C., Sandhu, A.F., III, G.W., Lin, S., Lv, P., Liu, Y., Wu, Q., and Yu, S. 2020. Inflammatory factors and amyloid β-induced microglial polarization promote inflammatory crosstalk with astrocytes. Aging **12**(22): 22538–22549. doi:10.18632/aging.103663.

Xu, C., Wu, J., Wu, Y., Ren, Z., Yao, Y., Chen, G., Fang, E.F., Noh, J.H., Liu, Y.U., Wei, L., Chen, X., and Sima, J. 2021. TNF-α-dependent neuronal necroptosis regulated in Alzheimer's disease by coordination of RIPK1-p62 complex with autophagic UVRAG. Theranostics **11**(19): 9452–9469. doi:10.7150/thno.62376.

Yadav, E., Yadav, P., Khan, M.M.U., Singh, H., and Verma, A. 2022. Resveratrol: A potential therapeutic natural polyphenol for neurodegenerative diseases associated with mitochondrial dysfunction. Front. Pharmacol. **13**: 922232. doi:10.3389/fphar.2022.922232.

Yan, Z., Gibson, S.A., Buckley, J.A., Qin, H., and Benveniste, E.N. 2018. Role of the JAK/STAT signaling pathway in regulation of innate immunity in neuroinflammatory diseases. Clin. Immunol. Orlando Fla **189**: 4–13. doi:10.1016/j.clim.2016.09.014.

Yang, S., Qin, C., Hu, Z.-W., Zhou, L.-Q., Yu, H.-H., Chen, M., Bosco, D.B., Wang, W., Wu, L.-J., and Tian, D.-S. 2021. Microglia reprogram metabolic profiles for phenotype and function changes in central nervous system. Neurobiol. Dis. **152**: 105290. doi:10.1016/j.nbd.2021.105290.

Yang, Y., Coleman, M., Zhang, L., Zheng, X., and Yue, Z. 2013. Autophagy in axonal and dendritic degeneration. Trends Neurosci. **36**(7): 418–428. doi:10.1016/j.tins.2013.04.001.

Ye, J., Ortaldo, J.R., Conlon, K., Winkler-Pickett, R., and Young, H.A. 1995. Cellular and molecular mechanisms of IFN-gamma production induced by IL-2 and IL-12 in a human NK cell line. J. Leukoc. Biol. **58**(2): 225–233. doi:10.1002/jlb.58.2.225.

Ye, X., Zhu, M., Che, X., Wang, H., Liang, X.-J., Wu, C., Xue, X., and Yang, J. 2020. Lipopolysaccharide induces neuroinflammation in microglia by activating the MTOR pathway and downregulating Vps34 to inhibit autophagosome formation. J. Neuroinflammation **17**(1): 18. doi:10.1186/s12974-019-1644-8.

Ye, Z.C., and Sontheimer, H. 1998. Astrocytes protect neurons from neurotoxic injury by serum glutamate. Glia **22**(3): 237–248. doi:10.1002/(sici)1098-1136(199803)22:3<237::aid-glia3>3.0.co;2-2.

Young, A.P., Adderley, S.J., Bagher, A.M., and Denovan-Wright, E.M. 2022. Protein-protein allosteric effects on cannabinoid receptor heteromer signaling. *In* Allosteric Modulation of G Protein-Coupled Receptors. *Edited by* R.B. Laprairie. Academic Press. pp. 71–96. doi:10.1016/B978-0-12-819771-4.00001-4.

Young, A.P., and Denovan-Wright, E.M. 2022a. The dynamic role of microglia and the endocannabinoid system in neuroinflammation. Front. Pharmacol. **12**.

Young, A.P., and Denovan-Wright, E.M. 2022b. Synthetic cannabinoids reduce the inflammatory activity of microglia and subsequently improve neuronal survival *in vitro*. Brain. Behav. Immun. **105**: 29–43. doi:10.1016/j.bbi.2022.06.011.

Young, A.P., and Denovan-Wright, E.M. 2022c. The microglial endocannabinoid system is similarly regulated by lipopolysaccharide and interferon gamma. J. Neuroimmunol. **372**: 577971. doi:10.1016/j.jneuroim.2022.577971.

Young, A.P., Landry, C.F., Jackson, D.J., and Wyeth, R.C. 2019. Tissue-specific evaluation of suitable reference genes for RT-qPCR in the pond snail, Lymnaea stagnalis. PeerJ **7**: e7888. doi:10.7717/peerj.7888.

Yu, C.-H., Davidson, S., Harapas, C.R., Hilton, J.B., Mlodzianoski, M.J., Laohamonthonkul, P., Louis, C., Low, R.R.J., Moecking, J., De Nardo, D., Balka, K.R., Calleja, D.J., Moghaddas, F., Ni, E., McLean, C.A., Samson, A.L., Tyebji, S., Tonkin, C.J., Bye, C.R., Turner, B.J., Pepin, G., Gantier, M.P., Rogers, K.L., McArthur, K., Crouch, P.J., and Masters, S.L. 2020. TDP-43 triggers mitochondrial DNA release via MPTP to activate cGAS/STING in ALS. Cell **183**(3): 636-649.e18. doi:10.1016/j.cell.2020.09.020.

Yuan, J., Amin, P., and Ofengeim, D. 2019. Necroptosis and RIPK1-mediated neuroinflammation in CNS diseases. Nat. Rev. Neurosci. **20**(1): 19–33. doi:10.1038/s41583-018-0093-1.

Zelek, W.M., and Morgan, B.P. 2022. Targeting complement in neurodegeneration: challenges, risks, and strategies. Trends Pharmacol. Sci. **43**(8): 615–628. doi:10.1016/j.tips.2022.02.006.

Zhang, D., Li, S., Hou, L., Jing, L., Ruan, Z., Peng, B., Zhang, X., Hong, J.-S., Zhao, J., and Wang, Q. 2021a. Microglial activation contributes to cognitive impairments in rotenone-induced mouse Parkinson's disease model. J. Neuroinflammation **18**(1): 4. doi:10.1186/s12974-020-02065-z.

Zhang, D.-W., Shao, J., Lin, J., Zhang, N., Lu, B.-J., Lin, S.-C., Dong, M.-Q., and Han, J. 2009a. RIP3, an energy metabolism regulator that switches TNF-induced cell death from apoptosis to necrosis. Science **325**(5938): 332–336. doi:10.1126/science.1172308.

Zhang, F., Wei, K., Slowikowski, K., Fonseka, C.Y., Rao, D.A., Kelly, S., Goodman, S.M., Tabechian, D., Hughes, L.B., Salomon-Escoto, K., Watts, G.F.M., Jonsson, A.H., Rangel-Moreno, J., Pellett, N.M., Rozo, C., Apruzzese, W., Eisenhaure, T.M., Lieb, D.J., Boyle, D.L., Mandelin, A.M., Boyce, B.F., DiCarlo, E., Gravallese, E.M., Gregersen, P.K., Moreland, L., Firestein, G.S., Hacohen, N., Nusbaum, C., Lederer, J.A., Perlman, H., Pitzalis, C., Filer, A., Holers, V.M., Bykerk, V.P., Donlin, L.T., Anolik, J.H., Brenner, M.B., Raychaudhuri, S., Albrecht, J., Bridges, S.L., Buckley, C.D., Buckner, J.H., Dolan, J., Guthridge, J.M., Gutierrez-Arcelus, M., Ivashkiv, L.B., James, E.A., James, J.A., Keegan, J., Lee, Y.C., McGeachy, M.J., McNamara, M.A., Mears, J.R., Mizoguchi, F., Nguyen, J.P., Noma, A., Orange, D.E., Rohani-Pichavant, M., Ritchlin, C., Robinson, W.H., Seshadri, A., Sutherby, D., Seifert, J., Turner, J.D., and Utz, P.J. 2019a. Defining inflammatory cell states in rheumatoid arthritis joint synovial tissues by integrating single-cell transcriptomics and mass cytometry. Nat. Immunol. **20**(7): 928–942. doi:10.1038/s41590-019-0378-1.

Zhang, H., Shen, H., Jordan, C.J., Liu, Q., Gardner, E.L., Bonci, A., and Xi, Z. 2019b. CB_2 receptor antibody signal specificity: correlations with the use of partial CB2-knockout mice and anti-rat CB_2 receptor antibodies. Acta Pharmacol. Sin. **40**(3): 398–409. doi:10.1038/s41401-018-0037-3.

Zhang, H.-Y., Gao, M., Liu, Q.-R., Bi, G.-H., Li, X., Yang, H.-J., Gardner, E.L., Wu, J., and Xi, Z.-X. 2014. Cannabinoid CB_2 receptors modulate midbrain dopamine neuronal activity and dopamine-related behavior in mice. Proc. Natl. Acad. Sci. **111**(46): E5007–E5015. doi:10.1073/pnas.1413210111.

Zhang, H.-Y., Shen, H., Gao, M., Ma, Z., Hempel, B., Bi, G.-H., Gardner, E.L., Wu, J., and Xi, Z.-X. 2021b. Cannabinoid CB_2 receptors are expressed in glutamate neurons in the red nucleus and functionally modulate motor behavior in mice. Neuropharmacology **189**: 108538. doi:10.1016/j.neuropharm.2021.108538.

Zhang, J., An, S., Hu, W., Teng, M., Wang, X., Qu, Y., Liu, Y., Yuan, Y., and Wang, D. 2016. The neuroprotective properties of *Hericium erinaceus* in glutamate-damaged differentiated PC12 cells and an Alzheimer's disease mouse model. Int. J. Mol. Sci. **17**(11): 1810. doi:10.3390/ijms17111810.

Zhang, L., Xu, J., Gao, J., Wu, Y., Yin, M., and Zhao, W. 2018. CD200-, CX3CL1-, and TREM2-mediated neuron-microglia interactions and their involvements in Alzheimer's disease. Rev. Neurosci. **29**(8): 837–848. doi:10.1515/revneuro-2017-0084.

Zhang, M., Li, J., Geng, R., Ge, W., Zhou, Y., Zhang, C., Cheng, Y., and Geng, D. 2013. The inhibition of ERK activation mediates the protection of necrostatin-1 on glutamate toxicity in HT-22 cells. Neurotox. Res. **24**(1): 64–70. doi:10.1007/s12640-012-9361-4.

Zhang, P., Kong, L., Huang, H., Pan, Y., Zhang, D., Jiang, J., Shen, Y., Xi, C., Lai, J., Ng, C.H., and Hu, S. 2022a. Gut microbiota – A potential contributor in the pathogenesis of bipolar disorder. Front. Neurosci. **16**.

Zhang, Q., Su, X., Zhang, C., Chen, W., Wang, Y., Yang, X., Liu, D., Zhang, Y., and Yang, R. 2022b. *Klebsiella pneumoniae* induces inflammatory bowel disease through caspase-11-mediated IL18 in the gut epithelial cells. Cell. Mol. Gastroenterol. Hepatol.: S2352-345X(22)00238–7. doi:10.1016/j.jcmgh.2022.11.005.

Zhang, R., Bracci, P.M., Azhir, A., Forrest, B.D., and McGrath, M.S. 2022c. Macrophage-targeted sodium chlorite (NP001) slows progression of amyotrophic lateral sclerosis (ALS) through regulation of microbial translocation. Biomedicines **10**(11): 2907. doi:10.3390/biomedicines10112907.

Zhang, R., Miller, R.G., Gascon, R., Champion, S., Katz, J., Lancero, M., Narvaez, A., Honrada, R., Ruvalcaba, D., and McGrath, M.S. 2009b. Circulating endotoxin and systemic immune activation in sporadic Amyotrophic Lateral Sclerosis (sALS). J. Neuroimmunol. **206**(1–2): 121–124. doi:10.1016/j.jneuroim.2008.09.017.

Zhang, W., Zhao, J., Wang, R., Jiang, M., Ye, Q., Smith, A.D., Chen, J., and Shi, Y. 2019c. Macrophages reprogram after ischemic stroke and promote efferocytosis and inflammation resolution in the mouse brain. CNS Neurosci. Ther. **25**(12): 1329–1342. doi:10.1111/cns.13256.

Zhao, J., Bi, W., Xiao, S., Lan, X., Cheng, X., Zhang, J., Lu, D., Wei, W., Wang, Y., Li, H., Fu, Y., and Zhu, L. 2019. Neuroinflammation induced by lipopolysaccharide causes cognitive impairment in mice. Sci. Rep. **9**(1): 5790. doi:10.1038/s41598-019-42286-8.

Zhao, J., Kong, H.J., Li, H., Huang, B., Yang, M., Zhu, C., Bogunovic, M., Zheng, F., Mayer, L., Ozato, K., Unkeless, J., and Xiong, H. 2006. IRF-8/interferon (IFN) consensus sequence-binding protein is involved in Toll-like receptor (TLR) signaling and contributes to the cross-talk between TLR and IFN-gamma signaling pathways. J. Biol. Chem. **281**(15): 10073–10080. doi:10.1074/jbc.M507788200.

Zhao, X., Bausano, B., Pike, B.R., Newcomb-Fernandez, J.K., Wang, K.K., Shohami, E., Ringger, N.C., DeFord, S.M., Anderson, D.K., and Hayes, R.L. 2001. TNF-alpha stimulates caspase-3 activation and apoptotic cell death in primary septo-hippocampal cultures. J. Neurosci. Res. **64**(2): 121–131. doi:10.1002/jnr.1059.

Zhelev, Z., Bakalova, R., Aoki, I., Lazarova, D., and Saga, T. 2013. Imaging of superoxide generation in the dopaminergic area of the brain in Parkinson's disease, using mito-TEMPO. ACS Chem. Neurosci. **4**(11): 1439–1445. doi:10.1021/cn400159h.

Zheng, Z.-H., Tu, J.-L., Li, X.-H., Hua, Q., Liu, W.-Z., Liu, Y., Pan, B.-X., Hu, P., and Zhang, W.-H. 2021. Neuroinflammation induces anxiety- and depressive-like behavior by modulating neuronal plasticity in the basolateral amygdala. Brain. Behav. Immun. **91**: 505–518. doi:10.1016/j.bbi.2020.11.007.

Zhong, Y.H., Dhawan, J., Kovoor, J.A., Sullivan, J., Zhang, W.X., Choi, D., and Biegon, A. 2017. Aromatase and neuroinflammation in rat focal brain ischemia. J. Steroid Biochem. Mol. Biol. **174**: 225–233. doi:10.1016/j.jsbmb.2017.09.019.

Zhou, K. 2017. Strategies to promote abundance of *Akkermansia muciniphila*, an emerging probiotics in the gut, evidence from dietary intervention studies. J. Funct. Foods **33**: 194–201. doi:10.1016/j.jff.2017.03.045.

Zhou, M., Xu, R., Kaelber, D.C., and Gurney, M.E. 2020. Tumor necrosis factor (TNF) blocking agents are associated with lower risk for Alzheimer's disease in patients with rheumatoid arthritis and psoriasis. PLoS ONE **15**(3): e0229819. doi:10.1371/journal.pone.0229819.

Zrein, A., Bagher, A.M., Young, A.P., Denovan-Wright, E.M., and Kelly, M.E.M. 2020. Endothelin receptor heteromerization inhibits β-arrestin function in HEK293 cells. Can. J. Physiol. Pharmacol. **98**(8): 531–540. doi:10.1139/cjpp-2019-0620.

Zrzavy, T., Hametner, S., Wimmer, I., Butovsky, O., Weiner, H.L., and Lassmann, H. 2017. Loss of 'homeostatic' microglia and patterns of their activation in active multiple sclerosis. Brain **140**(7): 1900–1913. doi:10.1093/brain/awx113.

Zujovic, V., Schussler, N., Jourdain, D., Duverger, D., and Taupin, V. 2001. *In vivo* neutralization of endogenous brain fractalkine increases hippocampal TNFalpha and 8-isoprostane production induced by intracerebroventricular injection of LPS. J. Neuroimmunol. **115**(1–2): 135–143. doi:10.1016/s0165-5728(01)00259-4.